STRATEGIES TOWARDS IMPROVED DEVELOPMENT OF SEMISOLID VAGINAL MICROBICIDE GELS FOR THE PREVENTION OF HETEROSEXUAL TRANSMISSION OF HIV-1

by

Alamelu Mahalingam

A dissertation submitted to the faculty of
The University of Utah
in partial fulfillment of the requirements for the degree of

Doctor of Philosophy

Department of Pharmaceutics and Pharmaceutical Chemistry

The University of Utah

December 2011

The University of Utah Graduate School

STATEMENT OF DISSERTATION APPROVAL

The dissertation of **Alamelu Mahalingam**

has been approved by the following supervisory committee members:

Patrick F. Kiser	, Chair	**28th June, 2011** Date Approved
John Mauger	, Member	**28th June, 2011** Date Approved
Hamid Ghandehari	, Member	**28th June, 2011** Date Approved
Steven Kern	, Member	**28th June, 2011** Date Approved
Margit Janat-Amsbury	, Member	**28th June, 2011** Date Approved

and by **David Grainger**, Chair of the Department of **Pharmaceutics and Pharmaceutical Chemistry**

and by Charles A. Wight, Dean of The Graduate School.

ABSTRACT

The work described in this dissertation attempts to advance the science of developing semisolid microbicide products through (a) application-oriented design of drug delivery vehicles and (b) selection of HIV-specific active ingredients that yield advantage over the current antiretroviral strategies, particularly in regards to the mechanism of action through inhibition of HIV entry.

Two approaches that exploit the underlying composition-structure-property-performance relationship in polymeric systems to improve semisolid gels for the prevention of sexual transmission of HIV were explored. Firstly, an algorithm that allows *de novo* engineering of a delivery vehicle was developed, optimizing the composition and consequently the properties of the material to meet a predefined set of performance criteria for vaginal drug delivery. Secondly, a pH-responsive mucus-like material with the ability to attenuate the transport of virus and immune cells was engineered. Inhibition of viral transport was observed at pH above 4.8, with minimal signs of toxicity to vaginal tissue.

Second part of this dissertation describes the assessment of two potent antiretroviral agents that inhibit HIV entry. The ingenuity of these agents lies in (a) the dual mechanism of HIV inhibition associated with the small molecule pyrimidinedione analogs, and (b) the design of a gp120 targeted macromolecular therapeutic that is synthetic in nature and shows activity comparable to that of

the protein-based lectins. Hydroxyethyl cellulose gels formulated with 0.25 w% pyrimidinedione analog showed activity at ~ 14 ug/mL in an *in vitro* antiviral assay. In the design of gp120 targeted synthetic lectins, benzoboroxole showed weak affinity for nonreducing sugars; however, it demonstrated antiviral activity at nanomolar concentrations when incorporated into high molecular weight polymers. Activity increased with increasing degree of functionalization and molecular weight of the polymer. Supplementing the polymer backbone with sulfonic acid increased its aqueous solubility in addition to a synergistic increase in antiviral activity.

These strategies support the paradigm shift from use of generic semisolid drug delivery systems to a performance-based design of polymeric materials for vaginal drug delivery. Furthermore, formulating semisolid systems to deliver antiretroviral agents, such as the pyrimidinediones or the synthetic lectins, may provide a versatile microbicide candidate that is potent, affordable and nontoxic.

I would like to dedicate this dissertation to my parents,

S. Mahalingam and M. Lakshmi

for their unconditional support and encouragement.

TABLE OF CONTENTS

LIST OF TABLES

Table **Page**

LIST OF FIGURES

Figure **Page**

PREFACE

Work in this dissertation attempts to address two major challenges in the field of microbicides: (a) develop rational design of semisolid delivery vehicles for preventing the sexual transmission of HIV-1 and (b) synthesize and/or formulate new antiretroviral agents that inhibit HIV-1 entry. The work presented in this dissertation provides multiple strategies in regards to developing methods and materials towards improved design of semisolid vaginal microbicide gels, Chapter 2 and 3, pertain to the drug delivery vehicle, whereas Chapter 4 and 5 focus on the active ingredient.

Semisolid gels constitute a major class of dosage forms developed for vaginal delivery. Although there are over 50 vaginal products in the market, the knowledge regarding the criteria for selecting a gel for a predetermined application is still lacking. Most vaginal gels in the past have been designed to either mimic physical properties of commercially available gels, or alternately mimic the composition of gels that have been developed for other applications, such as contraceptive delivery, vaginal moisturizers or ocular delivery. The major problem with the traditional approach is that it confines the choice of gelling agents and composition of the gel. The effectiveness of a topical vaginal delivery system is, to a large extent, determined by the ability of the vehicle to deploy in the vaginal lumen immediately after application as well as it’s retention at the

target site, both of which depend on the mechanical properties of the delivery vehicle. Therefore, it is conceivable that inadequate understanding of the impact that mechanical properties of a gel may have on drug release, coating and retention, could limit our ability to develop vaginal gels for microbicide delivery.

Chapter 2 summarizes the work on the development of a semi-empirical approach that would enable optimization of a vaginal gel specifically tailored for use as a microbicide, prior to *in vivo* clinical evaluations. In doing so, an *in vitro* preclinical algorithm that elucidates the relationship between composition, mechanical properties and performance was designed. Until now, there have been no thorough explorations of the composition-performance relationship of vaginal gels and the work presented in this thesis is pioneering with respect to developing methods that empirically relate the composition of commonly used gel excipients to their performance by using deterministic flow calculations.

The second approach developed as a part of this study focuses on the design of a semisolid polymer system that impedes movement of HIV-1 by physically entrapping the virions in the polymer network. Barrier technologies, such as condoms, have been used for over 400 years as means to physically trap and contain the seminal fluid, thereby preventing pregnancy and transmission of STIs. Coitally dependent use of condoms in addition to the necessity of male consent outweighs the effectiveness of male condoms at preventing both conception and STIs. As a result, the usage of male condoms exhibits alarmingly low rates (~ 19%), especially in low-income drug abusing populations. In spite of the limited usage of male-condoms, they remain the most

popular method of contraception across the globe. Thus, in attempt to cater the growing need for women-controlled barrier modalities, several technologies such as the cervical caps, diaphragms and female condoms have been developed and approved for use. Although the female condom demonstrated efficacy in reducing HIV-1 transmission, its limited availability, low acceptability, non-covert usage and cost hindered the overall success of the device. Thus, other effective and acceptable, noncoitally dependent women-controlled methods need to be developed to prevent heterosexual HIV-1 transmission.

Chapter 3 presents the work on a bioresponsive crosslinked polymer system designed to trap and inhibit the migration of virions from semen to the genital tissue. The ingenuity of this system lays in the fact that it embodies the inherit advantages of a physical barrier technology whilst, unlike the existing barrier modalities, obviating application right before intercourse. The challenge with this work lies in designing the mechanical properties of the material that would allow complete vaginal tissue coating and, at the same time, serve as a barrier to viral transport. To tackle this mechanical tradeoff, the approach adopted in this work is the use of *in-situ* bioresponsive gelation. This particular approach allows the weakly crosslinked viscoelastic fluid to flow and coat the vaginal tissue on application. Soon after exposure to the semen that may carry infectious virions, the polymer network becomes densely crosslinked to form an impermeable solid-like barrier, capable of inhibiting viral transport. This system relies on a covalently-crosslinked polymer network between phenylboronic acid and salicylhydroxamic acid.

Focusing on the second challenge—as the spread of HIV-1 continues and the emergence of tolerant mutants to existing regimens escalates, the need for new drug candidates has become increasingly important. Pyrimidinediones represent a unique class of compounds that inhibit HIV-1 entry by targeting a conformational epitope that forms prior to fusion of the viral envelope with the cellular membrane. In addition, pyrimidinedione analogs also act as non-nucleoside reverse transcriptase inhibitor, exhibiting activity at nanomolar concentrations against clinical strains of HIV-1 and HIV-2.

Chapter 4 describes the work on preformulation of pyrimidinedione analogs and developing a semisolid gel dosage for the delivery of the lead drug molecule. It is a well known fact that, given the increasing number of hydrophobic and poorly permeable drugs being evaluated as microbicide candidates, it is critical to develop a drug delivery system that is not only cost-effective, biocompatible and stable, but also capable of delivering the drug to vaginal tissue at a concentration high enough to prevent viral replication. Thus, as a part of the present study, in order to examine the applicability of the gel as a microbicide, chemical stability of the drug candidate and physical stability of the gel, *in vitro* and *ex vivo* release, safety and antiviral activity was assayed.

In attempt to address the growing need for lumen active antiretroviral agents that target initial steps in the viral entry, work on polymeric synthetic lectins that target the gp120 and inhibit HIV-1 entry was initiated. Lectin based entry inhibitors present a promising class of antiretroviral agents that inactivate HIV-1 in the vaginal lumen even before they reach the susceptible CD4+ cells.

Moreover, lumen active agents offer several advantages over antiretroviral agents that require delivery to the cervicovaginal tissue, which include lower systemic levels of drugs, lower probability of developing resistant mutants and alleviated issues, with respect to permeability and biodistribution of the active ingredient. The viral envelope protein plays a critical role in HIV-1 entry into cells. The surface unit, gp120 initiates the binding between HIV-1 and the susceptible cells containing CD4 receptors. Carbohydrate-binding proteins capable of binding to the multiple glycans on the N-linked glycosylated regions of gp120 represent a promising class of entry inhibitors. Of these, cyanovirin-N, which binds specifically to α(1,2)mannose glycans, has shown consistent suppression of HIV-1 and HIV-2 replication irrespective of the virus, the cell type, or the coreceptor tropism of the viral strain. However, production, formulation and stability of protein-based lectins may economically impede their use by women in resource-deprived pandemic regions, such as sub-Saharan Africa.

Finally, Chapter 5 discusses the work on developing multivalent polymer based synthetic lectins that show activity comparable to the protein based lectins, without the associated issues with protein-based therapeutics, such as cost of isolation, purification, chemical and structural stability.

This dissertation personifies the four wonderful years of my graduate experience in the Microbicide delivery lab. I would like to express my deepest gratitude to Dr Patrick F. Kiser for his exemplary mentorship and unceasing motivation. My growth as a scientist and a person has been greatly influenced by what I have learnt from Dr Kiser. My gratitude also goes to the former and current

members of the Microbicide Delivery Lab, who were always there to offer their friendship and help when I needed it the most. I would like to thank all the coauthors on my manuscripts for their scientific contributions and valuable collaboration. I am incredibly grateful to my family, especially my dad, S. Mahalingam, my mom, M. Lakshmi, my sister and brother-in-law, S. Abhirami and T. Shanmuhanathan, and my nephew Shaan, for their unconditional support, patience and belief in me. Finally, I would like to thank my fiancé, Harsha Banda, for, without his support, this would not have been nearly as enjoyable of a journey.

CHAPTER 1

BACKGROUND AND INTRODUCTION

1.1 HIV Pandemic

AIDS is an opportunistic infection caused by HIV, leading to progressive failure of the immune system. With over 33 million individuals infected with HIV living globally, AIDS continues to be the most destructive pandemics known to date. The recent advent of highly active antiretroviral therapy (HAART) and rising awareness on the transmission methods has successfully curbed the spread of the AIDS pandemic in some parts of the world.[1] However, countries in the Sub-Saharan Africa remain the most heavily affected regions by the AIDS pandemic, accounting for 67% of the total HIV infected individuals and 72% of the total deaths due to HIV in the year of 2009.[1]

1.2 Impact of HIV on Women's Health

Over the last two decades, women have represented the fastest growing demographic of the HIV/AIDS pandemic, especially in the developing nations (Figure 1.1).[2] In some parts of Africa, where heterosexual transmission is the dominant mode of infection, women aged 15-24 are three times more likely to become infected than their male counterparts.[3]

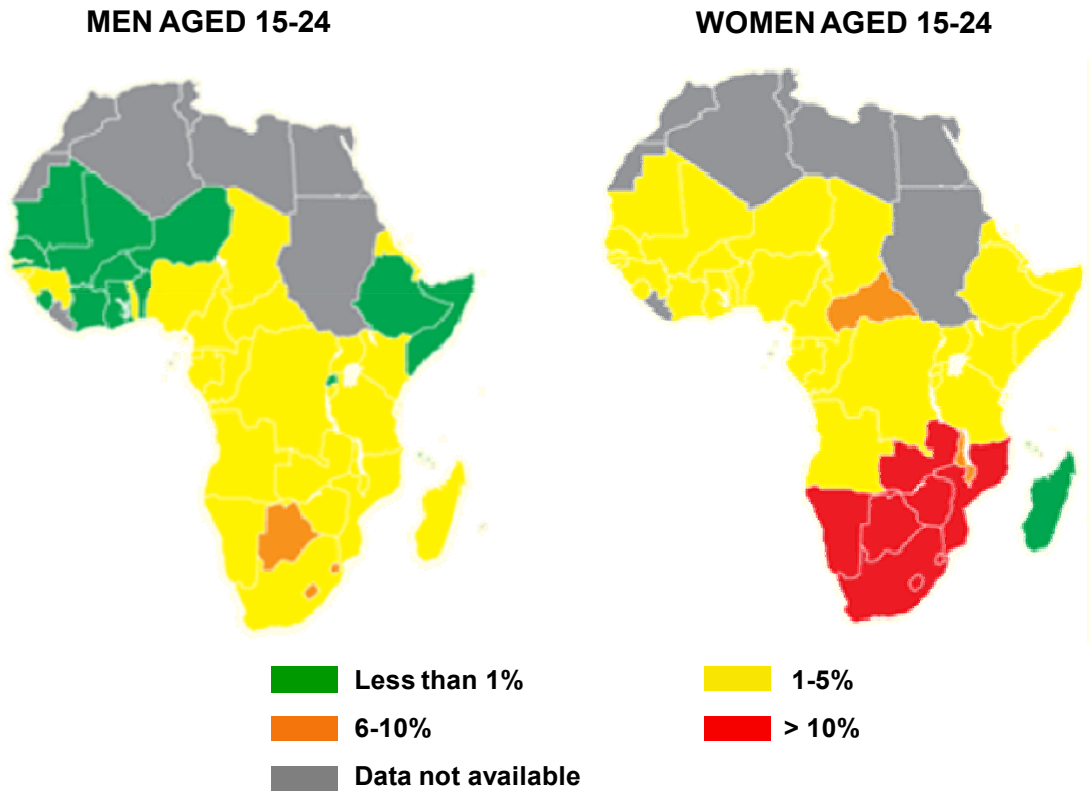

Figure 1.1 Illustration of the HIV prevalence rate among adult men and women in Africa. The high incidence rate in Sub-Saharan Africa underscores the disproportionate burden of the pandemic on women health, evident in the developing countries. Reprinted from www.unicef.org.

Furthermore, women in the childbearing age who are at high risk of HIV infection raise concerns related to mother to child transmission, which, in turn, increases the infant population infected with HIV and responsibility towards escalation in orphan population due to the HIV-related death toll.[2, 4] Both clinical and observational data suggest that the biological and socio-economical vulnerability makes women at higher risk for HIV.[5, 6] In addition, woman's susceptibility also stems from the fact that current methods of preventing HIV infection—abstinence, condoms, and monogamy—are ineffective and often

outside a woman's control.[7] Limitations of the existing prevention approaches and the fast spread of the infection rates signify the urgent need for prevention strategies, particularly those that women can control.[8]

Whilst the urgent need for continuing efforts on developing a preventive vaccine is unarguable, providing a women-controlled modality that prevents heterosexual transmission of HIV, such as a vaginally delivered microbicide, will likely prove to be crucial in containing the pandemic.[9-11] Vaginal microbicides are prophylactic strategies developed to be applied topically, to protect women against male to female sexual transmission of HIV.[10-15] Microbicides may function as a physical barrier[12] or deliver antiviral agents as a single agent or in combination.[16-18] The success of 1.0 wt% tenofovir (TFV) gel in the CAPRISA 004 microbicide trial is an historic milestone in the field of microbicides which reinforces the hope for preventive strategies in the fight against HIV.[15]

1.3 Vaginal Physiology

1.3.1 Anatomical considerations of the female genital tract

The vagina is a thin-walled, collapsed fibromuscular tube extending from the cervix to the vulva.[19, 20] The length of the vaginal canal and consequently the surface area varies considerably across populations.[21] Average length of the vaginal lumen has been estimated to range from 6.0 to 9.0 cm.[22] As shown in Figure 1.2, the genital mucosa can be subdivided into three major sections—the vaginal mucosa, endocervix and ectocervix.[20, 22]

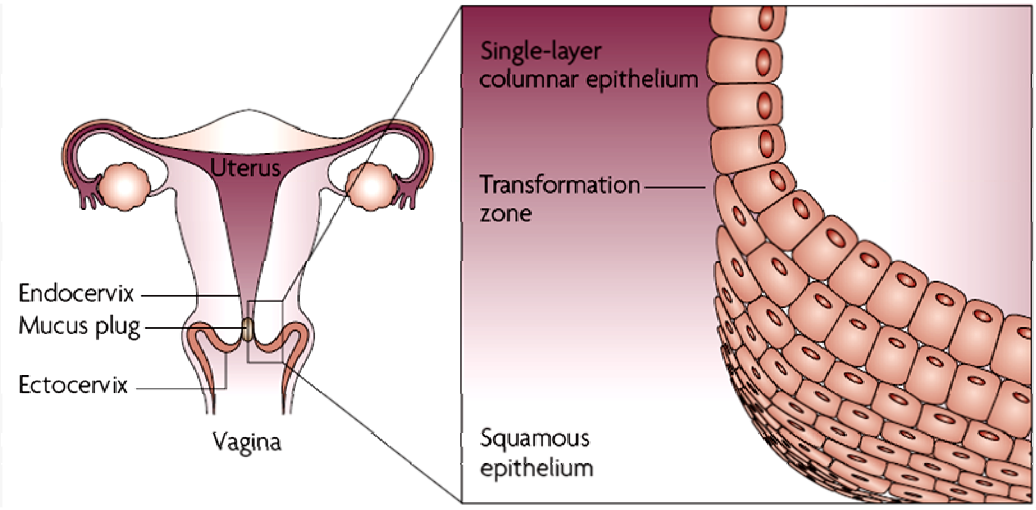

Figure 1.2 Schematic illustration of the female genital tract.[1] Viral infection was believed to occur readily through the endocervix; however, recent evidence suggests that infection may also occur through the squamous epithelium, in particular since the large surface area of these tissues may increase the susceptibility of infection in the vaginal lumen. Mucus provides a reasonable barrier to pathogen transport; however, neutralization of mucus by semen decreases its barrier function.

Although considered a mucosal tissue, the vaginal tissue is void of goblet cells. Mucin found in the vaginal tract is by virtue of the gravity-induced seeping of mucus secreted by goblet cells present in the endocervix.[22] Structurally, the ectocervix and the vaginal mucosa consist of multilayered nonkeratinized stratified squamous epithelium, whereas the endocervical canal is constructed of single layered columnar epithelium.[23] The squamous epithelium thickness varies

---

[1]Adapted with kind permission from Macmillan Publishers Ltd: Nature Review Immunology, Setting the stage: host invasion by HIV, Volume 8, 2008, 447-57, Florian Hladik & M. Juliana McElrath.

across population and more so with age.[21, 24-26] In women that have undergone menopause, the squamous epithelium becomes atrophic, consisting of fewer layers.[24, 27]

1.3.2 Natural defense mechanisms in the female genital tract

In addition to the protective multilayered squamous epithelium covering most of the female genital tract, innate immunity provides defense against invading pathogens.[26, 28] Mucin—a high molecular weight glycoprotein embellished with immunoglobulin, antimicrobial peptides and enzymes—may trap and curb the growth of pathogenic organisms.[29-33] Furthermore, the endogenous lactobacillus flora present in the vaginal lumen secretes hydrogen peroxide and maintains a nonconducive acidic environment to pathogen outgrowth.[34, 35] Ideally, the combination of these factors should provide sufficient defense against the invading pathogens and prevent occurrence of new infections.[33, 36] However, certain pathogens, including HIV, have evolved to bypass these natural defense mechanisms and pave way to gain entry into the human immune system.[29, 33, 37]

1.4 Heterosexual Transmission of HIV

Even though sexual contact transmits HIV in less than one in every 200-2000 events, it accounts for ~80% of the total HIV infections to date.[38] The risk of acquiring HIV from a single sexual contact may vary with the infectiousness of the HIV and susceptibility of the sexual partner towards HIV. The low probability of HIV transmission through sexual contact is counterbalanced by the high viral

load in the semen and the frequency of the event, making sexual transmission the largest contributor and the most concerning causative route of new infections.[37] Recognizing the factors that play a critical role in the sexual transmission of HIV may provide a valuable insight into developing effective prophylactic strategies against acquisition of HIV.[13, 37] Whilst the exact sequence of events occurring between introduction of semen-borne virus and establishment of productive infection is unclear,[37, 39] several mechanisms have been implicated in this initial process.

1.4.1 Sites in the female genital tract for HIV invasion

The relative susceptibility and contribution of the vagina, endocervix and ectocervix towards HIV infection is yet to be elucidated; reports suggest that dissemination of infection can occur at all three sites.[33, 38] The vaginal mucosa consists of the epithelium on the apical side and the lamina propia on the basal side. In the sexual transmission of HIV, the virions rely on the genital mucosa as the port of entry,[39] whereby the pathogen must diffuse across the epithelial barrier for a productive infection to occur,[33, 40] in particular since the vaginal epithelium is void of target cells or the traditional HIV receptors. On the contrary, the tissue underneath the epithelium contains a rich pool of multiple target cells for the virus to infect.[37]

The single layered endocervix epithelium is susceptible to microabrasions and is a vulnerable target for HIV invasion.[33] Until recently, the prevalent belief was that transmission of HIV primary occurred via breach in the vaginal epithelial.[38] Recent evidence corroborates that as, despite the robust mechanical

barrier provided by the multilayered squamous epithelium that covers the vagina and ectocervix, virions may undergo transcytosis and migrate efficiently across intact epithelium.[12, 33, 37, 39-42] Subsequently, the virions may be uptaken by the underlying rich network of macrophages, dendritic cells and memory lymphocytes in the squamous epithelium, eventually infecting intraepithelial Langerhan cells and CD4+ T lymphocytes.[29, 33, 43] Given that the total surface area contributed by the vagina and the ectocervical canal is 15 times greater than that of the endocervix, it is conceivable that the transcellular migration of HIV across intact epithelium could play a critical role in the dissemination of the infection.[37] Suggested mechanisms of effective migration of HIV across the epithelium are shown in Figure 1.3, including (a) microabrasions and lesions in the stratified vaginal epithelium and/or the monolayer (columnar) cervical epithelium due to sexual trauma or other genital infections;[33, 34, 43, 44] (b) infection of the epithelial cells;[12] (c) transcellular migration of virus;[40, 42, 45] or (d) uptake by immune cells, such as the macrophages residing in the vaginal canal.[34, 38]

1.4.2 Gaining cellular entry and dissemination of infection

Of the various mechanisms described above, *ex vivo* studies indicate that simultaneous infection of immune cells in the lamina propria (CD+ T-cell, macrophages) and active transport through antigen-processing cells to lymph nodes may propagate both local as well as systemic dissemination of productive infection.[41, 45-47] HIV binds to host cells via a cascade of binding events between the viral envelope and cell-surface moieties, such as the negatively charged heparan sulfate proteoglycans or lectins.

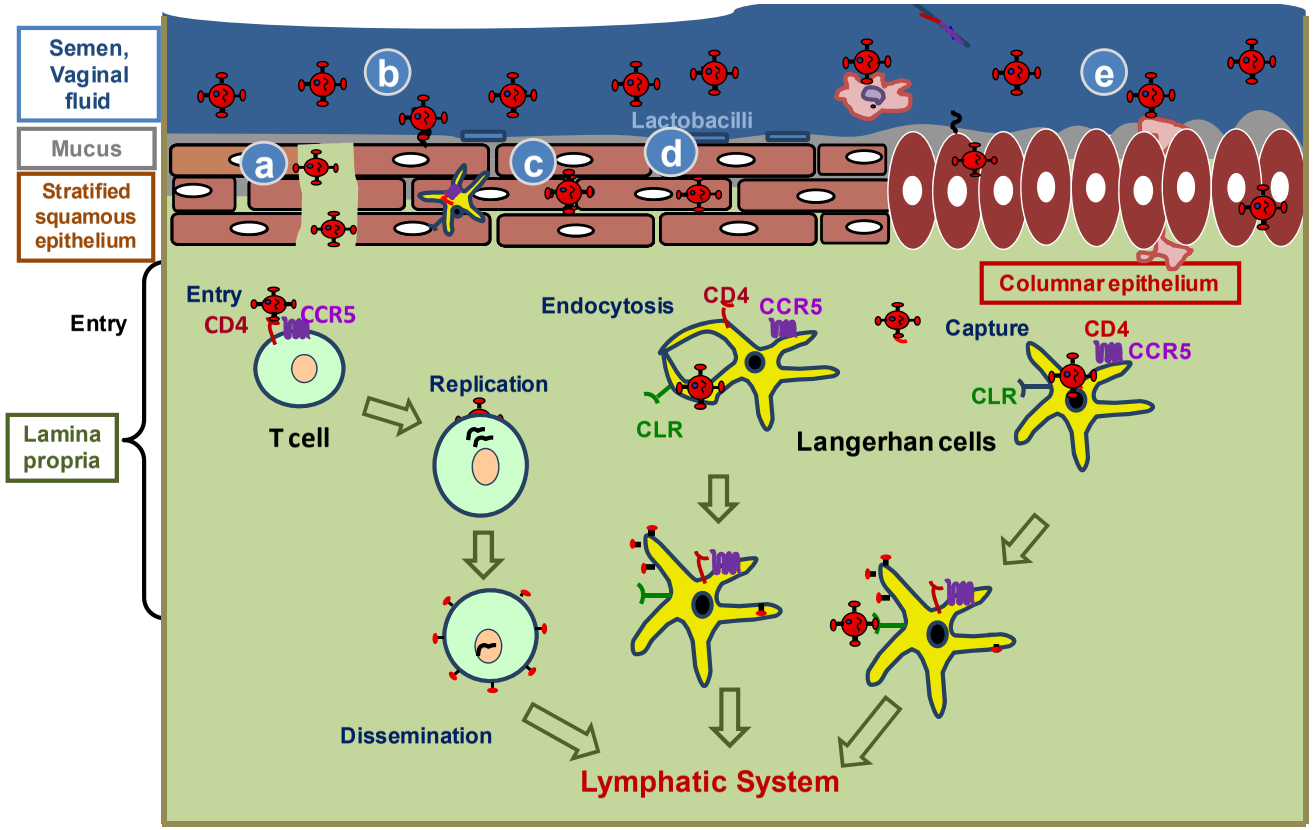

Figure 1.3 Schematic summarizing the plausible pathways of male-to-female sexual transmission of HIV. **(a)** Microabrasions in the stratified vaginal epithelium from sexual trauma or other genital infections in addition to thinning of the epithelium during changes associated with the menstrual cycle may allow HIV to migrate through the epithelium to the target cells. **(b)** HIV can fuse with epithelial cells and be endocytozed by immune cells that migrate into the epithelium to reach out to the virions. **(c)** Virions may also migrate through the transcellular route, paving its way through the multilayered squamous epithelium. **(d)** Once the virions move into the stroma, they can be uptaken by immune cells, such as the macrophages or the dendritic cells residing in the vaginal canal, establishing a productive infection. **(e)** Cell-associated virions may migrate across the single layered columnar epithelium, transporting the virions to the lymphatic system.

These binding events result in a structural change that facilitates secondary interactions with the chemokine coreceptors—CXCR4 and CCR5.[47, 48] Following the viral binding, the viral envelope protein gp120 and the transmembrane protein gp41 initiate envelope fusion and viral entry.[37, 49] The genomic RNA, enzymes (reverse transcriptase (RT), protease and integrase), and regulatory proteins (TAT and Rev) are transported into the host-cell. Replication of virus in the host cell is subsequently initiated by reverse transcription of the genomic RNA to produce proviral DNA that integrates into the host genome and subsequently results in establishment of HIV infection.[50]

1.4.3 Contributions of seminal plasma

The presence of semen-borne infectious virions in the vaginal lumen mediates the first step in the onset of the HIV infection.[47, 51] By virtue of the higher buffering capacity and volume of seminal fluid, the protective acidic environment maintained by lactic-acid producing micro flora is neutralized, thus creating a hospitable milieu for viral entry, binding and outgrowth.[52-54] The pathogens that exploit semen as the carrier, similar to the spermatozoa, benefit from the protective role of a large number of factors in the seminal fluid.[51, 54] For example, amines, such as spermine and spermidine, guard the virions from the threat of acid inactivation.[51] In addition, seminal fluid also triggers a cascade of signaling pathways that recruit chemokines, proinflammatory cytokines and neutrophils in the cervical epithelium.[29, 51] This, in turn, results in accumulation of susceptible target cells right at the site of viral inoculums. Thus, the adapted mechanisms of HIV transmission evade the inhibitory effect of the vaginal pH and

the innate ecosystem, while exploiting the protective role of semen and interspersed CD4+ T cells, dendritic cells and macrophages—all of which are initial cellular target of HIV.[33, 51]

1.5 Challenges with Vaginal Route of Microbicide Delivery

The complex geometry of the vaginal canal poses several difficulties for vaginal delivery of microbicides using semisolid dosage forms.[20, 33, 55] Firstly, the collapsed vaginal lumen and surfaces between the vaginal rugae present anatomical challenges towards homogenous application and distribution of a semisolid vaginal product. Secondly, seeping of the gel under gravity may result in considerable leakage of the product, resulting in suboptimum delivery and product acceptability.[21] Thirdly, the shearing forces experienced during intercourse can disrupt the gel layer.[23] Finally, dilution of formulation with vaginal fluid and semen prior to and during intercourse can compromise retention of the gel.[56] Thus, an array of issues related to gel deployment and retention can compromise efficacy and acceptability of vaginal gels.[57] In addition to the above mentioned anatomical challenges, the female genital tract intensifies the barrier to successful drug delivery and biological activity of microbicide candidates through several mechanisms, including changing epithelial barrier,[58] constant cell turnover, presence of biological fluids at the surface of the tissue varying from vaginal fluid, cervical mucus to seminal fluid[25] after the intercourse, activity of enzymes such as protease, hydrolases and lyases,[52, 57] as well as oxidative and acidic stress from hydrogen peroxide produced by the vaginal flora.[52, 59]

1.6 Microbicides – Past, Present and Future

Almost three decades ago, Zena Stein was the first scientist to propose the concept of a topical 'virucide or microbicide', analogous to the topical 'spermicides' to block HIV transmission.[36] Since then, several microbicide candidates have been pursued in clinical studies.[9, 13, 60-64] However, none of the developed microbicides, with the exception of the most recent Tenofovir gel, yielded safe and effective inhibition of HIV.[65, 66] With the expanding knowledge delineating the mechanisms and biological factors involved in the male-female sexual transmission of HIV and the lessons learnt from the unsuccessful clinical trials, there is increasing hope and optimism entrusted into the next generation microbicide candidates.[10] The likelihood of the first tier of microbicide products to embody all the characteristics of an ideal product is seemingly low. Thus, it is imperative that the immediate global priority remains the development of a safe, effective and affordable microbicide, which provides protection if used consistently and can appeal to those who need it most.[67]

1.6.1 Microbicides in the past

The first generation microbicide relied on nonspecific inhibition of HIV. The primary mechanism of action included disruption of viral membrane using nonionic surfactants (Nonxynol-9, C31G, Sodium lauryl sulfate), electrostatic interactions between high molecular weight anionic polymers and negatively charged viral envelope to block receptor binding (PRO2000, Carraguard, Cellulose sulfate, Dextrin sulfate) and systems that enhanced the innate vaginal defense through maintenance of vaginal acidity (Buffergel, AcidForm).[10, 13, 68] The

first generation microbicide candidates, starting with the failure of nonoxynol-9, have shown disappointing results in terms of interrupting transmission[68-70] and/or safety, thereby increasing user's susceptibility to HIV transmission.[70, 71] their failure most likely resulted from a combination of factors, including suboptimal efficacy especially in the presence of biological fluids, coital use of products leading to poor user compliance and potential toxicity.[72]

1.6.2 Microbicides pipeline in the changing landscape

In the past, development of a safe and effective microbicide may have been delayed by limited identification of targets and models of HIV transmission.[43, 67] As a result, candidates in the earlier generation were poorly designed and minimally surveyed for safety and efficacy prior to clinical failure.[15, 70, 73-75] Driven by the overwhelming emphasis and global prioritization of the need for HIV prophylactics, such as microbicides, there has been a tremendous growth in our scientific understanding of the events and pathways involved in HIV dissemination.[40, 41, 47, 76] This phenomenon is becoming increasingly evident with the recent emergence of new generation of antiviral agents, designed to target specific transmission events or enzymatic machinery engaged in the HIV lifecycle.[15, 18, 45, 77] With the advances in the mechanistic understanding of the HIV infection, microbicide candidates are being put through rigorous and robust safety and efficacy profiling.[11, 75, 78-80]

Antiviral agents that target several steps in HIV transmission, such as the viral fusion (Fuzeon that binds to gp41),[81] attachment driven by nonspecific interactions between gp120 and receptors on the cell surface (Cyanovirin that

binds to gp120),[82, 83] binding to the coreceptors on the cell surface (Maraviroc is a CCR5 inhibitor),[84] reverse transcription,[85] integration (Elvitegravir, MK-2048) and protease (saquinavir, ritonavir, indinavir) have been identified.[78] Of these, the two most popular categories of drugs being actively pursued for microbicide development are the entry and reverse transcriptase inhibitors.[1, 15, 73, 86, 87]

In the past decade, reverse transcriptase inhibitors (RTI) have set a milestone in the advancement of antiretroviral regimens.[77] Currently, the microbicide preclinical pipeline represents an assortment of candidates, which include 35 fusion and entry inhibitors, 11 reverse transcriptase inhibitors, 1 immunomodulator, 4 with unknown and 23 with multiple mechanisms of action.[85] In spite the diversity amongst the candidates currently in the preclinical stage, majority of those already in clinical trials include only RTI, such as tenofovir, dapivirine and UC781.[88] The two main issues that remain unaddressed by the current microbicide pipeline pertain to (a) unified approach of developing RTI-based microbicides instead of progressing candidates that target other less explored steps in the HIV cycle, and (b) preferential emergence of drug-resistant isolates of HIV, in which case RTI-based monotherapies may show suboptimal or no effect against resistant mutants, proving to be less effective in subsequent clinical management of infection.[13, 18, 77, 89, 90]

1.6.3 Lessons learnt from the past and approaches towards developing microbicides in the future

Based on the inadequacies learnt from the clinical trials on the first generation microbicide candidates, current research efforts have focused on

developing longer-duration systems that allow application of the product hours prior to intercourse and employ highly active and HIV-specific antiretroviral agents.[13, 73, 91] Significant resources have been invested in developing improved models for preclinical safety and efficacy testing of microbicide candidates.[15, 81]

Compared to efficacy and safety evaluations, issues related to formulation are often regarded as being of secondary importance.[75] Although formulation may not seem directly relevant and as critical in the earliest stages of the microbicide development process, formulation science plays a vital role in governing the overall effectiveness and user acceptability of the final product.[92] An example of this trend is evident in the negligent design of microbicide drug delivery vehicles (DDVs). Majority of the semisolid DDVs employed for vaginal microbicide delivery thus far, have been formulated by mimicking compositions of other commercially available vaginal care products, such as lubricants, moisturizers and contraceptives. As a result, all of the first generation microbicide candidates had short retention times and were coitally dependent; much like other over-the-counter (OTC) vaginal care products. However, meeting the distinct requirements of a women-controlled microbicide product, which include longer retention time, noncoitally dependent application and therefore ability to withstand dilution with biological fluids, inevitably requires engineering approaches that are specifically targeted for that purpose.[55]

Although RTIs present a promising class of antiviral agents, concerns in regards to emergence of drug-resistant strains of HIV underscores the need for combination therapies, in particular, including agents that may target other steps

in the HIV life cycle.[90, 92, 93] Furthermore, based on the outcomes from treatments with the HAART regimen, there is a prevailing consensus in the field of HIV therapeutics that an effective microbicide formulation would most likely employ multiple ARV agents to delay and mitigate the development of resistant HIV mutant strains.[73] Of the various classes of compounds under development, entry inhibitors that impede HIV from entering target cells represent an attractive class of molecules. They are of particular interest, given that, inactivating the virus right at the port of entry[17, 86] by using high molecular weight agents attenuates issues related to systemic exposure, development of drug-resistant mutants systemically, and tissue level biodistribution.

Based on the knowledge acquired from the clinical evaluation of microbicides and the current understanding of the HIV transmission events, as a part of the present study, a systemic methodology was developed, with the aim to facilitate vaginal product design and development of lumen active-systems that may aid future design of microbicides. Four areas of research were covered: (a) rational approach to design and optimize DDV for microbicide delivery; (b) developing a mucin-like physical barrier technology that inhibits viral transport from semen to target tissue; (c) formulation of a small-molecule antiretroviral agent with dual mechanism of action against HIV; and (d) evaluation of a novel class of synthetic lectin-based polymeric entry inhibitor.

1.7 Semisolid Gels - Overview and Classifications

Dosage forms can be subdivided either based on the route of delivery or the physical state of the system. Among the three most common physical

states—solid, semisolid and liquid—we have been especially interested in semisolid drug delivery systems (DDS). Semisolid DDS constitute a significant proportion of the products developed for topical drug delivery, as they allow (a) direct delivery of the drug to the accessible mucous membranes, (b) delivery of a wide variety of drug molecules, and (c) rapid formulation.[94-97]

In a semisolid gel, the solvent is trapped in the three dimensional polymer network formed by either physical or chemical crosslinks.[98, 99] The polymer forms an extended network capable of resisting flow and small deformations.[98] Given the long-standing history and thorough understanding of the solid and liquid states of material, characterization of these physical states is fairly well defined. In contrast, the structural complexity and uncertainty in regards to time scale associated with semisolid state of materials leaves room for ambiguity and further work.[98-100] Whilst there is no perfect definition of a ‘gel’, the persistent misuse of the terminology to represent materials with high viscosity has complicated the situation further.[98, 99] Despite significant work by several prominent authors, such as Flory, the true meaning of a ‘gel’ remains elusive.[101] The commonly accepted definition of a ‘gel’ is a crosslinked macroscopic material in a dilute dilution that exhibits no flow.[98, 101] However, observations made based on the above definition as a comprehensive representation of ‘gel’ may lead to distorted conclusions, as variables, such as the time scale of observation, amount of material and method used to determine flow play a crucial role.[98] Therefore, characterization of a semisolid gel requires a predefined time scale of measurement as well as consistent experimental methods and

conditions.[98, 100] The present study focuses on the exploration of semisolid gels for the prevention of sexual transmission of HIV through vaginal delivery of antiretroviral agents or by serving as a physical barrier. In attempt to examine the composition-structure-property relationships that affect the end performance of the semisolid microbicide gels, it is imperative to first identity these relationships and explore how these relationships, can be exploited to develop effective DDSs. The rest of this chapter focuses on understanding the relationship between composition, structure, property and performance (CSPP) of semisolid gels, as examining this complex relationship in polymeric systems might provide a framework to rationally design semisolid gels for drug delivery. It has to be noted that the scope of this section is rather specific, as it focuses only on the factors directly relevant to this dissertation, and therefore, should not be mistaken for an exhaustive review on factors that may play into the CSPP relationship of gels.

In the absence of crosslinking, substantially diluted polymer solutions display Newtonian flow behavior.[102] However, as concentration of the polymer increases, network crosslink points in the linear polymer chain may be introduced through crosslinks (physical or chemical) and chain entanglements, resulting in formation of a large macroscopic polymer networks that exhibit viscoelastic or even pure elastic behavior.[99, 101-103] The most common classification of gels is based on the nature of bonds that form the 3D network as transient networks formed by reversible crosslinks and permanent networks formed by irreversible crosslinks (Table 1.1).[101] Transient networks give rise to viscoelastic behavior, whereas permanent networks display properties similar to those of elastic solids.

Table 1.1 Comparative evaluation of the characteristics of reversible and irreversible network forming crosslinks.

Crosslinks	Reversible			Irreversible
Types of crosslinks	Noncovalent, Polymer chain entanglement	Noncovalent, physical crosslinks	Reversible covalent crosslinks	Permanent covalent crosslinks
Bond energy	Low	Low	Moderate	High
Crosslink lifetime	-	Finite	Finite	Infinite
Nature of the interaction	 Topological	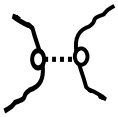 Physical	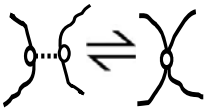 Reversible chemical	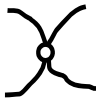 Permanent chemical
Polymer chains that participate in the crosslink	Free polymer chains at high concentration	Free and dangling polymer chains	Free, dangling and elastically active	Mainly elastically active polymer chains
Resistance to dilution	Very low	Low	Moderate	High

Gels may also be classified based on the ionic charge (anionic, cationic, neutral or ampholytic), source of the monomer or polymer (natural or synthetic), method of preparation (homopolymer, copolymer or multipolymer) and physical structure (amorphous, semicrystalline or H-bonded complexes).[104, 105]

1.7.1 Composition of polymeric gels and its relationship to gel structure and properties

Figure 1.4 shows a concept map outlining the relationships between composition of a semisolid gel and the structure and properties of the resulting polymer network. Variables associated with the composition of a polymeric gel

include chemical and physical nature of the building blocks (charge, hydrophilicity), interactions between the building blocks (covalent, ionic etc.) and concentration (w/w, mole functionalization).[101, 106, 107]

Hydrophilicity of the building blocks is determined by the presence of molecular groups that are capable of forming hydrogen bonds with water: -OH, -COOH,-$CONH_2$, -SO_3H, etc.[101, 107] Introduction of ionizable pendant groups in the polymer chain causes localization of charges and osmotic effects, whereby—at low salt concentration—repulsion between these identically charged domains may potentially force extended conformation of polymer chains in solution, resulting in altered flow properties.[103, 104, 107, 108] In the presence of high concentrations of salt, counter-ions from the salt shield the fixed charges on the polymer chain, thereby creating high osmotic pressure within the polymer network, which, in turn, causes polyelectrolyte gels to swell.

Polyacrylic acid (PAA) gels are a classic example of this phenomenon.[109] In an aqueous dispersion of PAA at pH < pKa (of the terminal carboxylic acid), the polymer chains stage a condensed globular structure whereas at pH > pKa, the ionized carboxylate groups repel each other and compel an rigid elongated polymer chain conformation, which results in reduced gel viscosity.[109] The polymer chain length is critical in defining the state and properties of the system.[107, 110] As the number of carbons in the polymer chain increases from 10 to 1000, the physical state transitions from liquid to waxy, and finally to solid, due to increase in the total interaction potential between polymeric molecules.

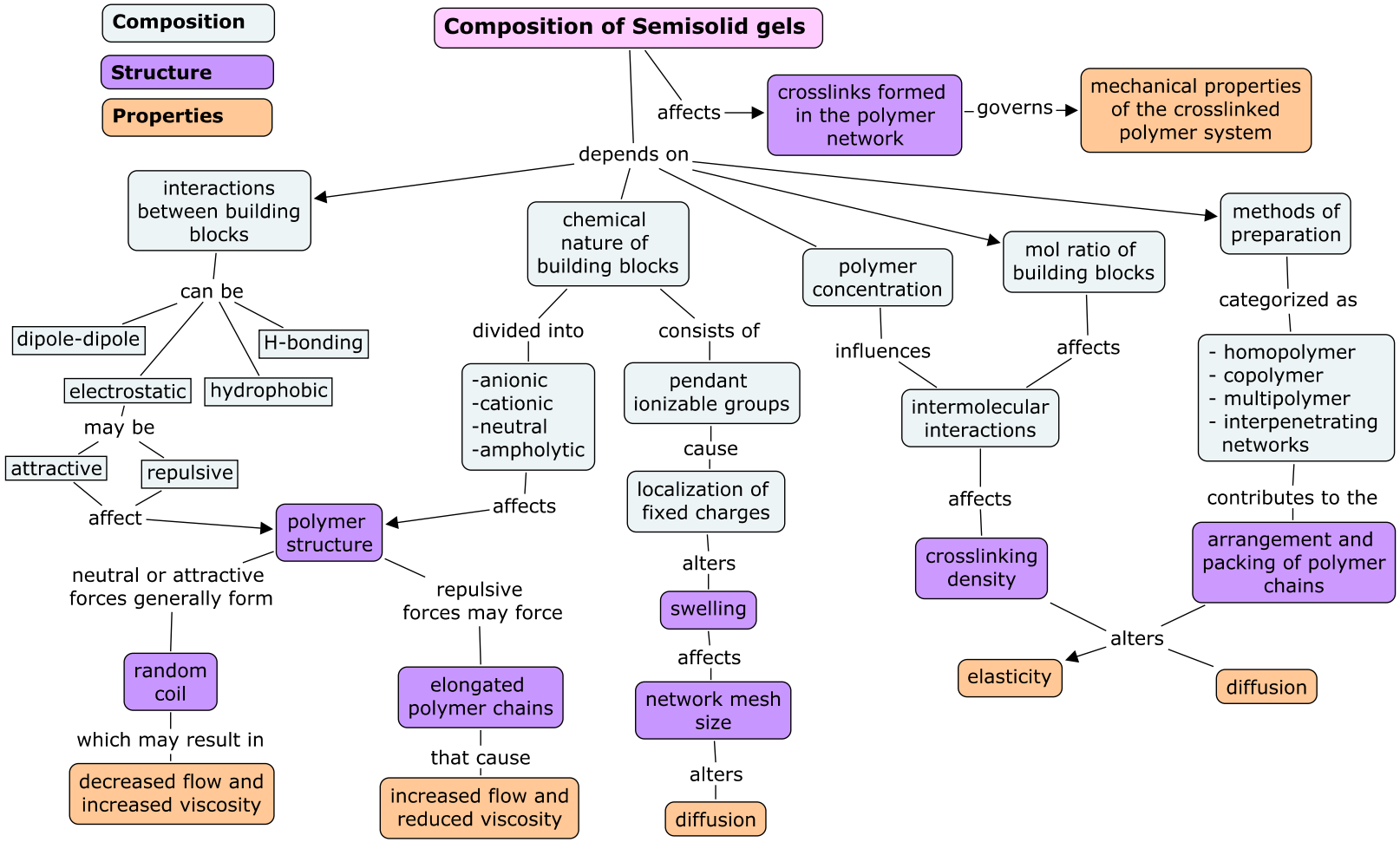

Figure 1.4 Concept map outlining the relationships between a semisolid gel composition and the structure and properties of the resulting polymer network.

Examples of the effect of secondary valence interactions between polymers strands on mechanical properties are H-bonding in Nylon and cellulose that form flexible fibers, van der Waal's interactions in polyethylene that form waxy materials, as well as electrostatic and dipole interactions in polyvinyl chlorides that form tough plastic materials.[101] Although the above discussion takes into account only the forces with major contribution, it is likely that several forces act simultaneously.[110] Polar substituents arrange symmetrically on the C-atom, increasing the polymer chain length.[106] Incorporation of bulky groups or increasing the number of stacked polar groups may decrease chain flexibility.[101]

1.7.2 Structure of polymeric gels and its relationship to gel properties

Polymer structure in a gel is comprised of three major structural components—the polymer chain, crosslinks and the solvent (Figure 1.5).[103, 105] Solvent entrapped in a polymer network could either be aqueous or an organic solvent.

Crosslinks tie the polymer chains together to form a macroscopic matter called a 'gel' of high molecular weight.[111] Since, crosslinks are what structurally differentiates network polymers from linear polymer, most gel material properties can be delineated by examining network-forming crosslinks.[103] The concept map depicted in Figure 1.6 outlines the relationships between the network structure of a semisolid gel and the properties of the resulting semisolid gel.

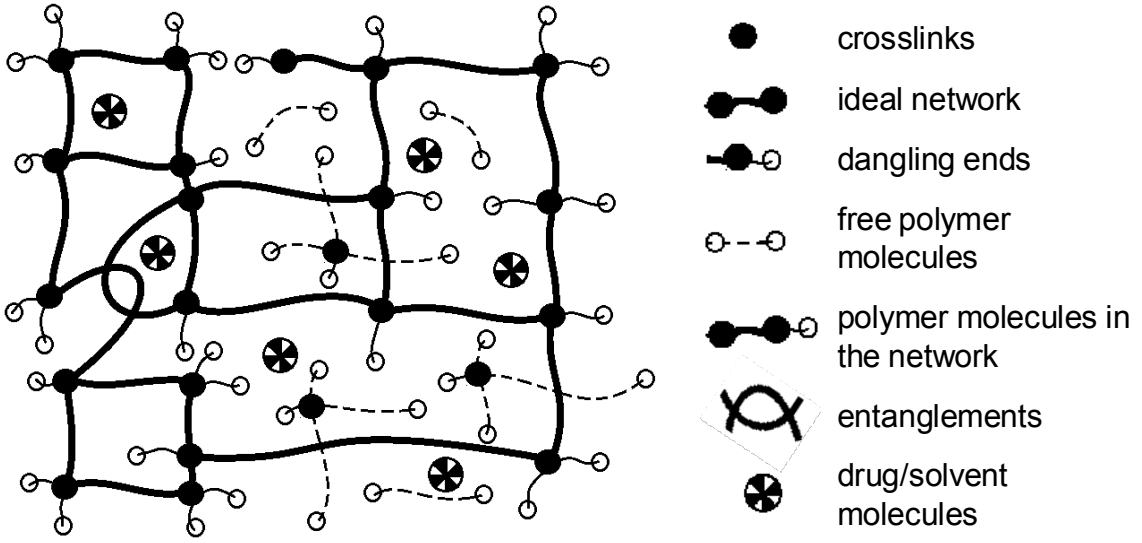

Figure 1.5 Schematic representation of a typical crosslinked polymer network.

Linear polymer chains typically dissolve when placed in a solvent due to the favorable entropy of mixing and enthalpic interactions with solvent molecules.[103, 104] On the other hand, crosslinked polymers imbibe solvent within the polymer network, and as a result swell.[102, 104] The minimum volume of solvent trapped in a polymer network is limited by the polymer-solvent interactions described by the Hildebrand's solubility parameter (δ) (Equation 1.1),[112, 113] which is the geometric mean of the cohesive energy density (c). ΔH_{vap} is the heat of vaporization and V_m is the molar volume. Difference in the solubility parameter of the polymer and the solvent ($\Delta\delta$) when is less than or equal to one, suggests that the systems are alike and would mix.

$$\delta = c^{1/2} = \left(\frac{\Delta H_{vap}}{V_m} \right)^{1/2} \qquad (1.1)$$

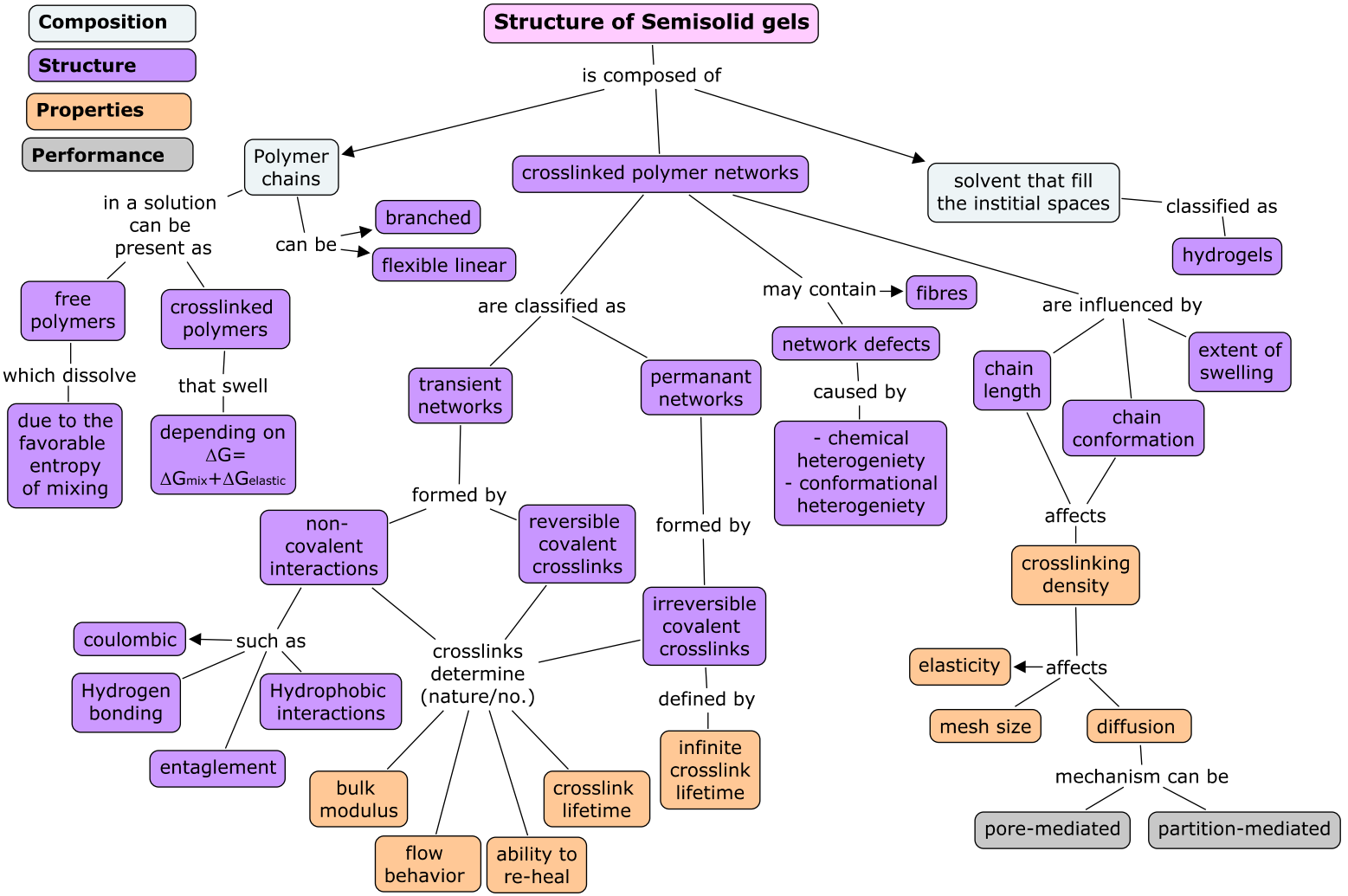

Figure 1.6 Concept map outlining the relationships between structure of a semisolid gel and the resulting semisolid gel properties.

Values of $\Delta\delta > 1$ indicates that the system would not mix. The maximum volume of a swollen gel is controlled by the elasticity of the polymer network.[103, 105] As described by Flory and Rehner (Equation 1.2),[113, 114] swelling reaches equilibrium ($\Delta G_T = 0$) when decrease in the solution free energy (ΔG_{mixing}) due to dilution is balanced by the increase in elastic free energy ($\Delta G_{elastic}$).

$$\left.\begin{aligned} \Delta G_T &= \Delta G_{mixing} + \Delta G_{elastic} = 0 \\ \Delta G_{mixing} &= kT\left(n_1 \ln \upsilon_1 + \chi_1 n_1 \upsilon_2\right) \\ \Delta G_{elastic} &= \frac{3kT\nu_e}{2}\left(\alpha_s^2 - 1 - \ln \alpha_s\right) \end{aligned}\right\} \quad (1.2)$$

where n is the moles of solvent and polymer, ϑ is the corresponding volume fractions, χ is the Flory polymer-solvent interaction parameter, k is the gas constant, T stands for the temperature, α_s is the expansion factor and ν_e is the number of elastically active chains.

As shown in Table 1.1, crosslinked polymer networks can be formed through physical entanglement of polymer chains, association via cohesive forces and/or covalent interactions.[103-105] The resulting networks can further be subdivided into two major functional classes—reversible and irreversible polymer networks (Table 1.1).[104] As shown in Figure 1.7, noncovalent physical interactions or a selected number of reversible covalent interactions (disulphide, polyol-borate) can form polymer networks consisting of reversible crosslinks.

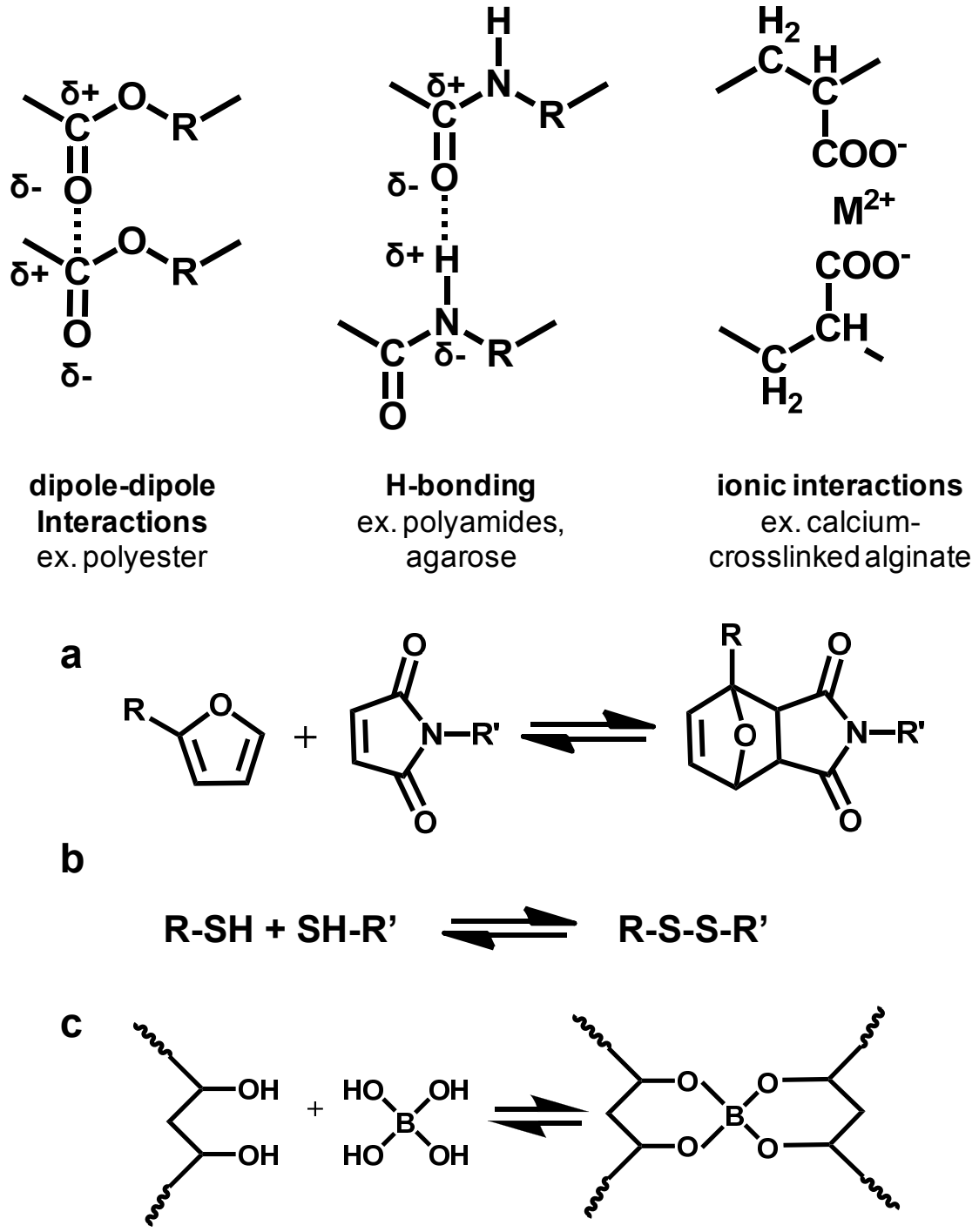

Figure 1.7 Illustration of plausible network forming interactions in a reversibly crosslinked polymer gel. Physical interactions (Top panel) and reversible covalent crosslinks formed by (a) Diels-Alder cycloaddition reaction, (b) disulfide bond formation and (c) borate-polyol crosslinking (bottom panel).

Entangled polymer networks formed by topological interactions between polymer chains form ‘pseudo gels’. As given by Equation 1.3, the plateau modulus (G_N) of an entangled polymer network depends on the critical molecular weight for entanglement (M_e), polymer concentration (W_2), and density (ρ) .Unlike physical and chemical networks, entangled polymer networks often dissolve on dilution.[100, 103]

$$G_N = \frac{4W_2\rho RT}{5M_e} \tag{1.3}$$

Physical polymer networks comprise of a continuous disordered arrangement of crosslinks formed through cohesion forces, which include H-bonding, van der Waals, electrostatic interactions as well as forces that arise from hydrophobic interactions.[104] Bonds formed through short-range noncovalent interactions are usually weak (bond energy ~ 5 kcal/mol) when compared to a covalent bond (bond energy ~ 90–100 kcal/mole) and require close proximity of the interacting groups (0.4 nm or less). Therefore, to attain network strengths comparable those obtained from covalent interactions, a large number of associations must occur simultaneously. In addition, formation of physical crosslinks shows profound dependence on the thermodynamic factors, such as temperature, pH, ionic strength and others.[104]

Chemical polymer networks formed through covalent interactions, which are most often irreversible in nature, are often considered permanent

networks.[104, 111] Unlike linear polymer chains, the macroscopic networks formed by covalent interactions between polymer chains do not dissolve on dilution unless the covalent crosslinks or the polymer chains are cleaved.[104, 111] Alternatively, a small fraction of covalent interactions that are reversible in nature form transient networks.

Polymer networks formed predominantly by chain entanglements are constructed on bonds with low bond energies and exhibit properties similar to a viscous fluid.[102] Whereas, networks formed by irreversible covalent interactions form extended macroscopic networks with infinite lifetime and high bond energies, exhibiting properties similar to an elastic solid.[100] Intermediate to these two network categories are those formed by noncovalent physical interactions. Networks formed by physical interactions or reversible covalent crosslinks have small but finite bond energy and crosslink lifetime. Consequently, these networks exhibit viscoelastic properties.[99]

Materials that completely abide to the Hooke's law of deformation given by $\sigma = G\gamma$, where stress (σ) equals product of the elastic modulus (G) and deformation (γ), are termed ideal elastic solids. In contrast, materials that obey the Newton's law of deformation given by $\sigma = \eta(d\gamma/dt)$, where η is viscosity and $d\gamma/dt$ is velocity gradient, are considered viscous fluids. It was not until the 19th century, that scientist found materials such as silk threads, that did not fully obey either the Hooke's law of elasticity or the Newton's law of viscosity. Deborah was the first to suggest that, "seemingly solid materials could behave like liquids", which Reiner described through Equation 1.4.[113, 114]

$$D_e = \frac{\tau}{t} \tag{1.4}$$

where τ is a characteristic lifetime of the crosslink and t is the time of the deformation. D_e = 0 for a viscous liquid; D_e = ∞ for a elastic solid and 0 < D_e < ∞ represents a viscoelastic material. Structural evaluations of polymer networks reveal that ideal network structures are rarely observed.[101, 104] Network defects may occur due to presence of unreacted groups, intermolecular loops or chain entanglements.[104] Additionally, non uniform distribution of crosslinks or phase separation during crosslinking may introduce inhomogeniety in networks.[101]

Material deformation can be studied using rheology by measuring the change in the deformation with time under externally applied force or under steady state flow or through application of small perturbations (shown in Table 1.2). Networks comprised of reversible crosslinks demonstrate time-dependent changes in crosslink association and dissociation states, yielding dynamic-mechanical and viscoelastic properties. When subjected to an external force of deformation, randomly coiled polymer chains rapidly consume the energy to facilitate relaxation of molecules through bond rotation, causing permanent deformation in the form of viscous flow of the polymer.[110] In contrast, in the presence of permanent covalent crosslinks flow and relaxation of stress is either delayed or in some cases prevented due to lower entropy of the polymer chains and a higher retractive force.[115]

Table 1.2 Mechanical and rheological characterization of semisolid gels.

	Viscous Fluid	Viscoelastic	Elastic Solid
Law of deformation	Obeys Newton's law of deformation	Neither the Hook's law or the Newton's law completely	Obeys Hook's law of deformation
Mechanical model	 $\tau = \eta\,\dot{\gamma}$ Spring	 Maxwell Model	 $\tau = G\,\gamma$ Dashpot
Creep (constant stress)	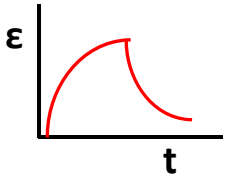	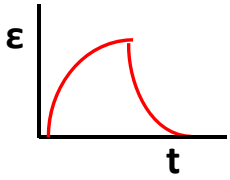	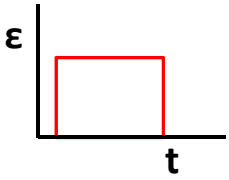
Stress relaxation (constant strain)	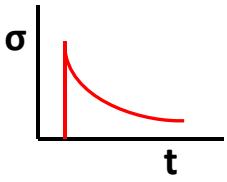	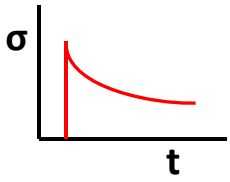	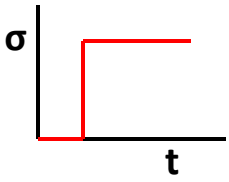
On deformation	Flows and looses form	Network breaks, deforms and reforms	Retains/recovers form
Energy	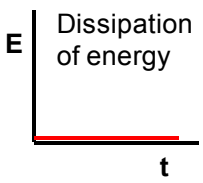	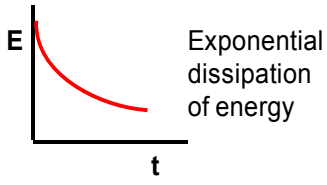	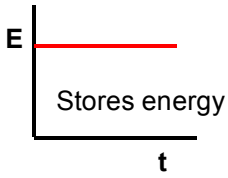
Oscillatory response	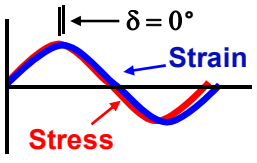	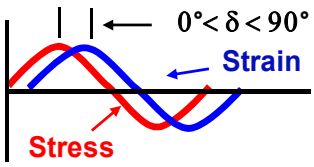	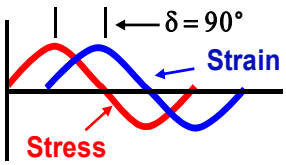
Modulus	Loss/viscous modulus $G'' = \frac{\gamma_0 \cos(\omega t)}{\sigma(t)}$	Dynamic complex modulus $G = G' + G''$ $= \frac{\gamma_0 \left[\sin(\omega t) + i\cos(\omega t)\right]}{\sigma(t)}$	Storage/elastic modulus $G' = \frac{\gamma_0 \sin(\omega t)}{\sigma(t)}$
Crosslink lifetime	Low	Finite, Moderate	Infinite

Transient networks formed through reversible covalent crosslinks, display viscoelastic properties at varying timescales that can be monitored and studied using techniques such as dynamic rheology.[98]

1.7.3 Polymer network properties and its effect on the performance of semisolid gels

Figure 1.8 shows a concept map outlining the relationships between properties of a polymer network and its performance as a semisolid gel for microbicide applications. Some of the most important characteristics of an anti-HIV microbicide semisolid gel include (a) deployment, (b) activity that, depending on the method of action, may be through drug delivery or physical entrapment, (c) bioadhesion, (d) ability to withstand dilution with biofluids, and (e) safety. Each of these performance criteria are discussed below.

In engineering a semisolid gel, it is imperative to control its mechanical properties for ease of application, coating and retention of the system.[98, 116, 117] Application and coating necessitates low network viscosity that can easily flow over tissue.[117, 118] However, low viscosity materials suffer from an inherent difficulty in being retained in the vaginal lumen, and may not have the capacity to inhibit viral transport to tissue, especially if applied hours prior to intercourse. Therefore, being mindful of this property-performance tradeoff—both low and higher viscosity—is critical.[117, 118]

Alternately, stimuli-responsive gels (pH, temperature etc.) have been employed as means to create formulations that can be applied as a liquid ensued by *in situ* gelation to potentially improve coating and retention.[118-121]

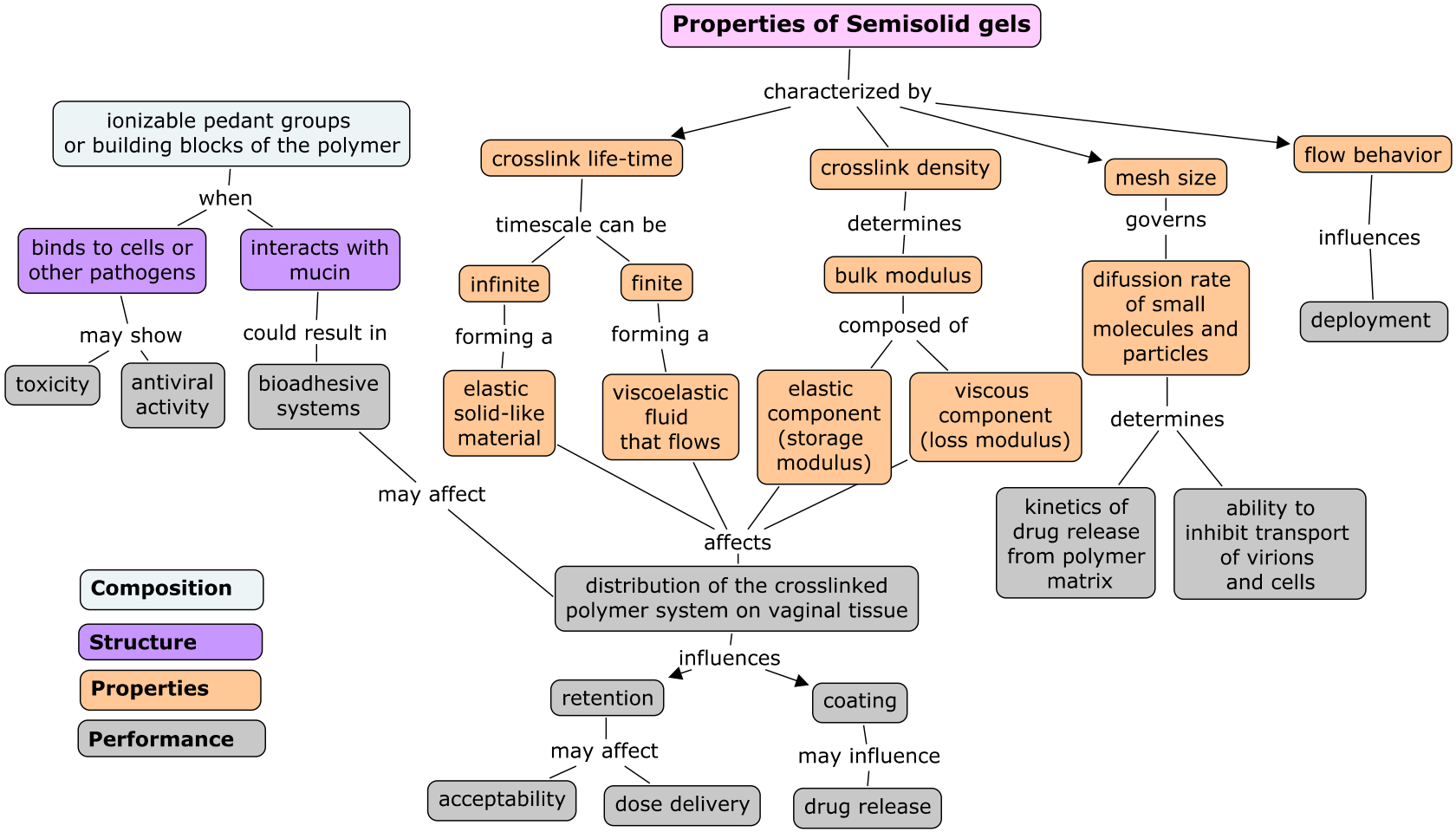

Figure 1.8 Concept map outlining the relationships between the properties of a polymer network and its performance as a semisolid gel for microbicide applications.

A semisolid gel may prevent sexual transmission of HIV by either acting as a chemical barrier by delivering inhibitory concentrations of antiretroviral agents to the tissue[14, 122] or by acting as a physical barrier and prevent the viral transport from semen to the susceptible genital tissue.[66, 120] In both cases, understanding and modulating the diffusion of either drug molecules or virions through the polymer network is imperative.

Permeability of drug molecules and particles through polymer networks depends on the structure of the polymer that, in turn, depends on the polymer hydrophilicity and crystallinity, extent of hydration, chemical and physical nature of the releasing agent and crosslinking density.[123] Permeation of the releasing agent in the polymer matrix may occur via diffusion through solvent-filled pores or partitioning of dissolved drug through the different layers of the polymer matrix.[104] In pore-mediated diffusion, the molecular size of the diffusing molecule has an important effect on the diffusion coefficient, whereas in partition-mediated diffusion, size of the particle plays a lesser role.

The diffusion process is explained by three prominent theories—free volume theory, hydrodynamic theory and the obstruction theory of diffusion. Often, a combination of mechanisms collectively govern diffusion rate of molecules through polymer networks.[104] The free volume theory of diffusion developed by Yasuda and modified by Peppas and Cohen-Turnbull, proposes that the molecules diffusing through a polymer network are required to find a sufficiently large free volume of solvent, in addition to an opening between the polymer chains that is large enough to allow the passage of molecules (Equation

1.5). The size of diffusing molecule becomes very critical in regards to the openings between the polymer chains, the chain mobility and the presence of functional groups on the polymer chain that may bind to the solute and impede its transport. In the free volume theory, diffusion coefficient in the gel (D_{gel}) is given by Equation 1.5.[124, 125]

$$\frac{D_{gel}}{D_o} = P_o \exp\left[-\frac{Ba^*}{V_{f,w}}\left(\frac{\phi}{1-\phi}\right)\right] \tag{1.5}$$

where D_o is diffusion coefficient of solute in an infinitely dilute solution, P_o is the probability of finding a opening large enough for diffusion of solute, B is the constant of proportionality, a^* is the cross-sectional area of the solute, $V_{f,,w}$ is the free volume occupied in water and Φ is the volume fraction of polymer in the gel.

Stoke-Einstein's theory assumes that the diffusing molecules moving at a constant velocity in a continuum of solvent are resisted by the frictional/hydrodynamic drag imposed by the bulk solvent, given by the relationship shown in Equation 1.6.[125]

$$D_o = \frac{k_B T}{f} = \frac{k_B T}{6\pi\eta r} \tag{1.6}$$

where k_B is the Boltzmann constant, T is the absolute temperature, f is the coefficient of frictional drag, η is the viscosity of medium and r is the radius of the

spherical particle. Ogston's obstruction theory (Equation 1.7) assumes that the diffusive transport of molecules through the tortuous polymer chains increases the path length and thereby obstructs diffusitivity.[125]

$$\frac{D_{gel}}{D_o} = \exp\left[-\frac{\pi}{4}\left(\frac{r_s + r_f}{\bar{r} + r_f} \right)^2 \right] \tag{1.7}$$

where r_s, r_f and $\bar{r}$ are the radius of the solute, length of the polymer fiber and average opening between polymer chains, respectively. Based on the above three theories, diffusion coefficient can be expected to decrease with increase in solute size, tortousity of the polymer chains and crystallizability of the polymer network.[104, 105]

Whilst above discussed theories aid a mechanistic understanding of the diffusion process, simple power law expression shown in Equation 1.8 may suffice to describe fractional release of drug from gels.[124]

$$\frac{m_t}{m_\infty} = kt^n \tag{1.8}$$

where m_t/m_∞ is the fraction released at time t; k is the factor dependent on the polymer network and n is indicative of the type of release mechanism (Table 1.3).

Table 1.3 Types of transport mechanisms described by the Power law for fractional drug release.[124]

Exponent	Types of transport	Diffusion
0.5	Fickian diffusion	$f(t^{0.5})$
$0.5 < n < 1.0$	Non-Fickian diffusion	$f(t^{n-1})$
1.0	Case-II transport	Time dependent
$n > 1$	Super time dependent	$f(t^{n-1})$

Higuchi developed relationships that describe the rate of drug release from a semisolid matrix. Equation 1.9[124] is applicable when the drug in the polymer matrix is completely dissolved. *M* (amount of drug released per unit area) is directly proportional to C_o (concentration of drug in the matrix) and $\sqrt{t}$ (time).

$$M = 2C_o\sqrt{\frac{Dt}{\pi}} \tag{1.9}$$

In contrast, Equation 1.10[126] is suitable for a system where the amount of drug present in the polymeric vehicle exceeds its solubility and, therefore, the drug is dispersed in the gel.

$$M = \sqrt{2 \times Q \times D \times C_s \times t} \tag{1.10}$$

where D is the diffusion coefficient of drug in the matrix; Q is the total amount of drug in the matrix and C_s stands for the solubility of drug in the semisolid vehicle.

As bioadhesion is an important beneficial characteristic required of most topical drug delivery systems, designing polymeric systems that exhibit bioadhesion may yield longer retention of the semisolid gel at the site of delivery and decreased leakage.[106, 116] Mechanism of bioadhesion can occur through mechanical bond formation facilitated by penetration of the gel into the tissue cracks and crevices.

In addition, acylating and alkylating agents in the polymeric gel can react with amines and hydroxyl groups on the serine or tyrosine, forming a covalent bond or interactions, such as H-bonding, van der Waal attractions, giving rise to strong bioadhesion.[106, 127] Factors that may affect bioadhesion include functional groups capable of interacting with the epithelium, turnover rate and hydration.[106] Furthermore, steric effect of substituents, charge density and molecular weight of the polymer affect chain flexibility, which is critical in defining the permissible conformations of the polymer to adhere to the tissue.[106, 110]

When developing materials for vaginal delivery, one essential aspect that needs to be considered is the dilution of the semisolid gel with biofluids, such as seminal fluid and cervical mucus, as well as the effect of sugars, ions and proteins inherently present in the vaginal canal. In particular, polymeric networks formed through noncovalent interactions may show marked variations in network properties, depending on environmental factors (pH, ionic strength etc). It is vital that the gels bear the ability to withstand dilution and retain their viscoelastic

network properties, as loss in viscosity on dilution could result in leakage, lower user compliance, compromised barrier properties and rapid drug release.

It is well known that incorporation of negatively charged groups in the polymer matrix results in nonspecific interactions between the polymer and positively charged cell or pathogen surface. These interactions have implications on both the antiviral activity of the end formulation as well as the gel toxicity to the genital tissue and the vaginal flora.

Polymer composition and the solvent in the polymer matrix affect the gel osmolarity that, in turn, may cause toxicity due to hyper- or hypo-osmolarity. The common issue inherent in synthetic polymeric systems is toxicity associated with unreacted monomers, residual organic solvent and toxic initiators that may leach out during application. Therefore, careful selection of monomers and a thorough understanding of the toxicity of the various building blocks of the polymer are very important.

.

CHAPTER 2

DESIGN OF A SEMISOLID VAGINAL MICROBICIDE GEL BY RELATING COMPOSITION TO PROPERTIES AND PERFORMANCE[2]

2.1 Introduction

To date, most vaginal semisolid gels have been designed empirically, with mechanical properties mimicking those of other commercial semisolid products. For drug delivery products, this approach may have originated, in part, due to inadequate recognition of the roles of delivery vehicles in the overall effectivenesses and acceptabilities of the products.[55, 127-129] Given the nature of the historical approach, we have limited appreciation for the extent to which these existing vaginal products achieve their designated functions. We therefore posit that there is a need for methodologies to help formulation scientists to objectively and intelligently select gel compositions for target applications.

[2]Adapted from Design of a Semisolid Vaginal Microbicide Gel by Relating Composition to Properties and Performance, Pharmaceutical Research, Volume 27, 2010, 2478-91, Alamelu Mahalingam, Eric Smith, Judit Fabian, Festo R. Damian, Jennifer J. Peters, Meredith R. Clark, David R. Friend, David F. Katz, Patrick F. Kiser.

Performance criteria will nonetheless vary based on the use of the vaginal product and the drug(s) it contains. Therefore, it is inevitable that pharmaceutical scientists will need to vary the properties of gel formulations to satisfy desired performance criteria. For this reason, it is important to understand the underlying composition-property-performance relationships (CPPR) of the gels, so that their compositions can be rationally varied to achieve given sets of properties and performance standards.

Vaginal gels are a primary dosage form for microbicides, which are topically applied products for the delivery of antiviral agents, intended to provide protection against the sexual transmission of HIV and other sexually transmitted pathogens.[10, 67, 92] The performance of a vaginal microbicide gel is both biological (i.e., drug delivery) and behavioral (i.e., user acceptability). Performance can be measured with respect to a number of functions, including the gel's ability to spread along the vaginal canal and coat the vaginal epithelium. This function governs delivery of active ingredient(s) to the target tissue; it also can lead to leakage outside the vagina, which adversely influences the acceptability of the product.[55, 67, 130] Gel performance in relation to the above criteria is strongly influenced by the administered volume, an often neglected parameter in gel design. Careful selection of the gel volume is crucial, since it has a causal relationship to the dynamics of gel coating[131] and the potential for leakage. That is, an ideal microbicide gel must provide desired coating with minimal leakage for a given volume of administration. To address this tradeoff between coating and leakage, an objective, quantitative method relating gel composition to both those

performance attributes is needed. An initial set of biomechanical flow models has been created, that relate gel rheological properties, gel volume, vaginal forces acting on a gel, and vaginal geometry to measures of gel spreading along the vaginal canal.[56, 118, 132] These fluid flow models enable us to predict the coating and leakage of a gel for a given volume and set of properties. However such information, alone, is of limited value to pharmaceutical scientists: the performance of a gel, and the properties that give rise to it, are multivariate; they depend on the composition-property relationships of the polymers and excipients within the formulation. Given the complexity of the relationships amongst composition, properties and performance, it is not surprising that most vaginal gel compositions were selected empirically with little effort devoted to quantitatively relate composition to properties and performance.[133]

To address this critical gap in the field of vaginal drug delivery from gels, a set of tools was developed to quantitatively explore composition-property-performance relationships in semisolid gels. A multivariate objective function constructed from gel properties, computations of flow behavior of the gel, and performance criteria for that flow behavior, is described herein. Analogous multivariate optimization approaches have previously been used in many fields, including computational biology, bioinformatics, drug discovery and molecular optimization for ligand binding.[92, 134, 135] As shown in Figure 2.1, Mixture Design of Experiments (MDOE) methodology[136-138] was used to establish a semi-empirical relationship between composition-property and property-performance relationships; this approach enabled us to obtain a local optimum within a given

composition space. Considerable work has been done on the development of hydrogels composed of PAA, cellulose and hyaluronic acid for ocular, buccal, vaginal and intestinal delivery.[97] Among these, cellulose and PAA based polymers have received increasing interest for cervical and vaginal drug delivery.[97] The major attributes of these polymeric carriers that make them attractive candidates for vaginal drug delivery are the GRAS status,[130] low cost and bioadhesion.[97] On the basis of the extensive literature available on the use of these polymers for vaginal drug delivery, we chose Carbopol 974P and hydroxyethylcellulose (HEC) as the two polymeric carriers to be evaluated;[55, 92, 97, 130, 131] however the general methodology we present can be used in any semisolid design space. The antiretroviral drugs used in development of the models were the HIV-1 reverse transcriptase inhibitors UC781[75, 97, 139] and TFV.[140-142]

2.2 Materials and Methods

2.2.1 Materials

Micronized UC781 and TFV were obtained from the CONRAD Program (Arlington, VA, USA). Carbopol 974P NF was purchased from Lubrizol (Wickliffe, OH, USA). HEC 250 HX PHARM was purchased from Hercules (Wilmington, DE, USA). Glycerin NF was purchased from J.T.Baker (Phillipsburg, NJ, USA). Methylparaben and propylparaben were purchased from Fluka (Milwaukee, WI, USA).

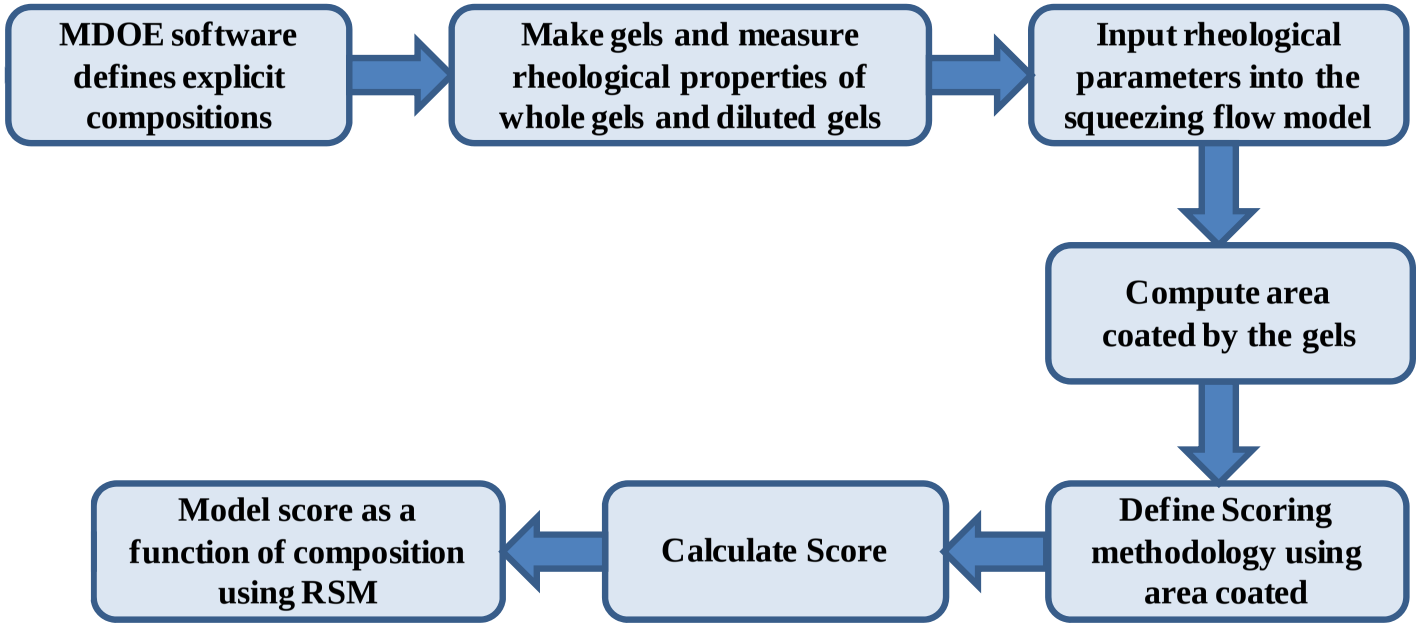

Figure 2.1 Algorithm developed to optimize gels based on performance of gels *in vivo* driving the selection of potential gels for future clinical evaluations. MDOE – Mixture Design of Experiments; RSM- Response surface methodology.

The following commercial gels, Replens® (lot # RD01015), K-Y Jelly® (lot # 0385C), Advantage-S™ (lot # A05101), Conceptrol® (lot # 8MM6346), and RepHresh® (lot # F09142) were purchased from a local pharmacy store. Methyl cellulose placebo gel (lot # 100306) and Carraguard (lot # 23175) were obtained from the Population Council (New York, NY, USA). The HEC clinical placebo gel (GMID #70018699), 6% Cellulose Sulfate microbicide gel (lot # C1564A001), TFV 1% microbicide gel from the CAPRISA trial (GMID #70018698) and UC781 microbicide gel (lot # 1061) were obtained from the CONRAD Program (Arlington, VA).

2.2.2 Experimental design

This work was part of our development of semisolid vaginal microbicide gels for the delivery of two highly potent antiretroviral drugs – TFV[143] and UC781[141], and these drugs were included in all formulations. To elucidate the relationship between composition-property and property-performance, a statistical tool - Mixture Design of Experiments (MDOE) was used. The fractions of the two polymers, X_1 (Carbopol 974P) and X_2 (HEC) were selected as two independent variables, which were varied simultaneously. Selection of model compositions and the optimization were performed using Design Expert® 7.1 (Stat-Ease, Inc., Minneapolis, MN) software.

In order to determine maximum concentrations of gelling agents, viscosity measurements was obtained on a series of gels with varying concentrations of Carbopol 974P and HEC. For initial comparison of these gels based on viscosity, a shear rate of 50 s^{-1} representing an intermediate physiologically relevant (1-100

s^{-1}) value was chosen.[139] Upper limits on the concentrations of the gelling agents were chosen such that each polymer at its highest concentration would create a gel with viscosity comparable to that for commercially available gels at 50 s^{-1}. Based on these preliminary investigations, 2.5 wt% and 3.0 wt% were chosen as the maximum concentrations to be tested for Carbopol 974P and HEC, respectively (Table 2.1). Fixed gel components consisted of 5 wt% glycerin, 0.1 wt% UC781, 1.0 wt% TFV, 0.15 wt% methylparaben and 0.05 wt% propylparaben (preservatives), totaling 6.3 wt% of the gel. DI water was used to make up the weight of the gel to 100 wt%.

Design space for an 'n' component mixture is represented by a surface in 'n-1' dimensions. Thus, an equilateral triangle in two-dimensional space represents the mixture design space for a three-component system. In this work, not all factors varied over the same range; the design space was represented by a fraction of the equilateral triangle, as shown in Figure 2.2. A design matrix comprising of 19 model compositions was constructed (Table 2.2). This included: three vertices of the triangular space (X_1, X_2, X_3) to determine the effect of the pure components; three binary blends (X_1X_2, X_2X_3, X_3X_1) to determine the effect of combinations of gelling agents; and one centroid point ($X_1X_2X_3$) and represents a center point with each ingredient at one third the maximum concentration. The order in which the gels were made and tested was randomized to counteract any differences due to aging or time-related effect (Table 2.2).

Table 2.1 Variables and constraints for the MDOE.

Components	Minimum (wt%)	Maximum (wt%)
X_1 : Carbopol	0.0	2.5
X_2 : HEC	0.0	3.0
X_3 : Water	78.2	83.7
$X_1 + X_2 + X_3$	83.7	83.7

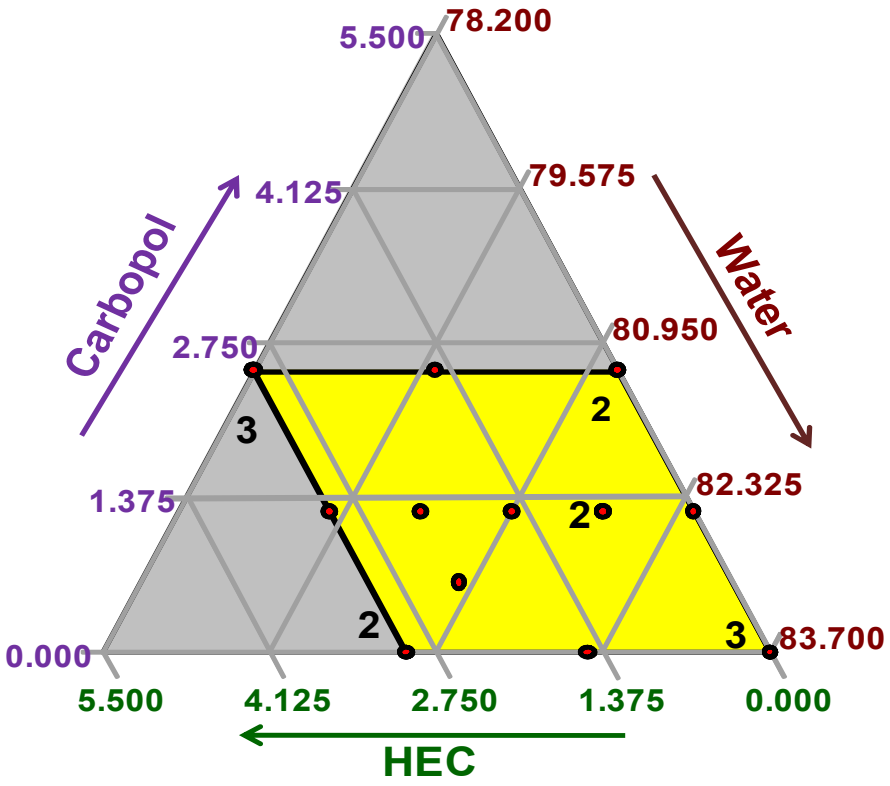

Figure 2.2 12 point mixture design for a three component mixture. The constraints on the model are Carbopol 974P (0 ≤ X1 ≤ 2.5 wt%); HEC (0 ≤ X2 ≤ 3.0 wt%) and Water (78.2 ≤ X3 ≤ 83.7 wt%). Red points in the design space indicate the 19 model compositions. The numbers next to the point indicate number of repeats of each composition.

Table 2.2 Composition matrix with 19 model compositions. The constraints on the model are Carbopol ($0 \leq X_1 \leq 2.5$ wt%); HEC ($0 \leq X_2 \leq 3.0$ wt%) and Water ($78.2 \leq X_3 \leq 83.7$ wt%)

Gel ID	Point type	X_1 (wt%)	X_2 (wt%)	X_3 (wt%)
1	Vertex	2.50	0.00	81.20
2	Vertex	2.50	3.00	78.20
3	Blend check	1.25	0.75	81.70
4	Axial midpoint	1.25	3.00	79.45
5	Centroid	1.25	1.50	80.95
6	Blend check	0.63	2.25	80.83
7	Vertex	0.00	0.00	83.70
8	Vertex	2.50	3.00	78.20
9	Axial midpoint	1.25	0.00	82.45
10	Blend check	1.25	0.75	81.70
11	Vertex	0.00	0.00	83.70
12	Axial midpoint	0.00	1.50	82.20
13	Vertex	0.00	3.00	80.70
14	Vertex	0.00	0.00	83.70
15	Vertex	0.00	3.00	80.70
16	Vertex	2.50	3.00	78.20
17	Axial midpoint	2.50	1.50	79.70
18	Vertex	2.50	0.00	81.20
19	Blend check	1.25	2.25	80.20

Design space for an ‘n’ component mixture is represented by a surface in ‘n-1’ dimensions. Thus, an equilateral triangle in two-dimensional space represents the mixture design space for a three-component system. In this work, not all factors varied over the same range; the design space was represented by a fraction of the equilateral triangle, as shown in Figure 2.2. A design matrix comprising of 19 model compositions was constructed (Table 2.2). This included:

three vertices of the triangular space (X_1, X_2, X_3) to determine the effect of the pure components; three binary blends (X_1X_2, X_2X_3, X_3X_1) to determine the effect of combinations of gelling agents; and one centroid point ($X_1X_2X_3$) and represents a center point with each ingredient at one third the maximum concentration. The order in which the gels were made and tested was randomized to counteract any differences due to aging or time-related effects (Table 2.2).

2.2.3 Model selection

The cubic model was chosen to model the responses because it provides a reasonable approximation of actual response surface for a three component mixture design. The Scheffé polynomial was used to eliminate redundant coefficients introduced by the constraints imposed by the mixture design.[57] In addition, to obtain a good response surface, extra points were augmented in the model to evaluate goodness of fit and pure error. Equation 2.1 gives the polynomial for the nonlinear cubic model.[144]

$$y = \sum_{i=1}^{q} \beta_i X_i + \sum_{i<j} \sum_{j=2}^{q} \beta_{ij} X_i X_j + \sum_{i<j} \sum_{j=2}^{q} \delta_{ij} X_i X_j (X_i - X_j) + \sum_{i<j} \sum_{j<k} \sum_{k=3}^{q} \beta_{ijk} X_i X_j X_k \quad (2.1)$$

Here y is the response; X_i, X_j, X_k represent the three components of the mixture; β_i, β_j, β_k represent the linear coefficients; β_{ij}, β_{jk}, β_{ik} represent the nonlinear blending model coefficients; and β_{ijk}, δ_{ij} represent the model coefficient for higher order nonlinear blending.

2.2.4 Preparation of the Carbopol 974P and HEC gels

UC781 (0.1 wt%) was dispersed in glycerin (3.5 wt%) to form a homogenous paste which was then added to 1 wt% TFV solution in water. Required amounts of Carbopol 974P were added to the above solution, and stirred with a paddle mixer at 350 rpm for 45 m to ensure complete hydration of the polymer. Stainless steel paddles (passivated 316L) and USP grade water should be used to avoid introduction of trace amounts of metal into the gel during preparation. Methylparaben (0.15 wt%) and propylparben (0.05 wt%) were weighed and mixed with preheated glycerin (1.5 wt%) at 65°C until all solids dissolved. Required amount of HEC was added to the glycerin paste after cooling to room temperature. The glycerin paste was then added to the Carbopol 974P dispersion with constant stirring. The pH of the gel was adjusted to 5.2 ± 0.2 with 10 wt% NaOH. Finally, the overall weight of the gel was adjusted to 100g with 18 mΩ DI water.

2.2.5 pH and osmolality measurements

The pH of the gels was recorded at room temperature using a 423 microprobe electrode (Mettler Toledo Instruments, Germany) prior to rheological measurements. Osmolality of gels was measured using a Vapro 5220 osmometer (Wescor Inc., UT, USA), with the goal of constraining hyperosmolality. Ten µL of gel was loaded on solvent free disc and placed in the precalibrated osmometer for osmolality measurements. Averages of five measurements were taken. The pH of the gels were 5.2 ± 0.2, and all osmolality values were < 1000 mOsm/kg.

2.2.6 Dilution of gels with vaginal fluid simulant (VFS)

To study the effect of dilution of gels with vaginal fluid, we performed a complete rheological characterization on gels mechanically mixed with VFS at a biologically relevant ratio (1:4 dilution; VFS: gel).[145] The VFS was prepared as previously reported.[57] One g of the VFS was mechanically mixed with 4 g of gel. Diluted gels were allowed to equilibrate for 24 h before measurements.

2.2.7 Determination of rheological properties

Viscosities of gel formulations (undiluted, diluted) were measured using a stress controlled AR 550 rheometer (TA Instruments, DE, USA) equipped with a 20 mm 4° steel cone geometry. One hundred and fifty µL of the gel was loaded using a positive displacement pipette and allowed to equilibrate for 2 m on the Peltier plate at 37°C, after which a steady state shear was applied. Shear rates experienced *in vivo* range from < 0.1 s^{-1} during passive seeping between epithelial surfaces to the order of ~ 100 s^{-1} during coitus.[146] Thus, viscosity was determined over the range of 10^{-4}-1000 s^{-1} to simulate physiological conditions.[57]

2.2.8 Stress growth and relaxation measurements

The yield and residual stresses in a gel influence its initial flow and also its sustained retention within the vaginal canal. We performed stress growth and relaxation studies to measure residual stresses, on both undiluted and diluted gels. For most gels, we used a Brookfield model 5HBDV-III Ultra rheometer equipped with a CPE40 cone at a shear rate of 10 s^{-1}. Gels (7, 11 and 14) had low viscosities and failed to produce measurable torque on this instrument;

therefore, a Brookfield model LVDV-III rheometer equipped with a CP40 cone at a shear rate of 300 s^{-1} was used for those gels.

2.2.9 Fitting rheological data to constitutive models

Data obtained from the steady state rheological studies and the stress growth and relaxation studies were fitted to the Power law and Herschel-Bulkley models (Table 2.3). The latter was used when a nonzero residual stress was measured, and the residual stress value was used to approximate the yield stress. Logarithmic values of shear stress or viscosity as a function of shear rate (over the range of 10^{-4} to 100 s^{-1}) were averaged over the replicate experiments, and fitted to the models using a Matlab function to minimize the residuals.

2.2.10 Squeezing flow model

Estimates of the vaginal area coated by the gel (*A*) were made, using a biomechanical fluid flow model of the coating process.[56, 57] This model utilizes the concept of constant-force squeezing of fluid between two plates, simulating the elastic forces from the posterior and anterior walls of the vagina. Inputs to the squeezing flow model were the rheological parameters from the constitutive model, initial height of the bolus (0.2 cm), volume of the gel, vaginal dimensions, and forces exerted by the vaginal muscles on the gel (1-10 N).[118] The output from the flow model is the area coated as a function of time. We focused upon that area at 120 s after the onset of gel flow, which serves as a measure of the deployment of the viscoelastic gel.[56]

Table 2.3 Constitutive equations to model the non-Newtonian rheological behavior of gels.

Model	Constitutive equation	
Power Law	$\tau = m\gamma^n$	τ - shear stress m - consistency index γ - shear rate n - shear thinning index
Herschel-Bulkley	$\tau = \tau_0 + m\gamma^n$	τ_0 - yield stress

2.2.11 Confirmation of the squeezing flow model

The results of the squeezing flow model were confirmed through calculation of area coated and *in vivo* MRI measurements of gel coating on four commercial over-the-counter products – K-Y Jelly®, Replens®, Conceptrol® and Advantage-S™.[118, 147]

2.2.12 Development of the objective function

An objective function was designed to serve as a DOE response factor, which was constructed as a piecewise continuous function of A: it has different analytical forms for $A \leq A_{max}$ and for $A > A_{max}$, which give equal results at $A = A_{max}$. The domain of the function is defined from zero to unity such that when its value, termed the score (S), equals 1, the gel fully meets the performance requirements (Figure 2.3).

If we assume that the amount of drug delivered by a gel is derived from drug diffusion within the gel, and that the process is quasi-state, then drug flux is inversely proportional to gel thickness, (h).

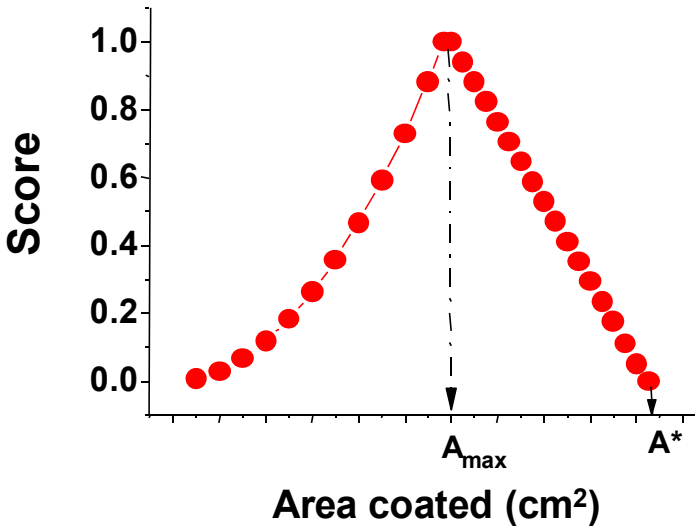

Figure 2.3 Schematic representation of the objective function as a function of area coated.

$$\text{Since, } J = -D\frac{\partial \phi}{\partial x} \tag{2.2}$$

$$J \propto \frac{1}{h} \tag{2.3}$$

where, J - diffusion flux, Φ - concentration and x - length or thickness. Volume of the gel (V) can be expressed as,

$$V = Ah \tag{2.4}$$

For constant value of V, h is inversely proportional to A.

$$h \propto \frac{1}{A} \tag{2.5}$$

Since, the amount of drug delivered (*Q*) depends on the flux and the surface area, *Q* is proportional to A^2.

$$Q \propto JA \tag{2.6}$$

$$\text{Since, } J \propto A \tag{2.7}$$

$$Q \propto A^2 \tag{2.8}$$

We chose a simple form of the objective function based upon this result, and the criterion that its value $S = 1$ when $A = A_{max}$.

$$S = \left(\frac{A}{A_{\max}} \right)^2 \text{ for } 0 < A \leq A_{\max} \tag{2.9}$$

This expression is evaluated at a fixed time, 120 s, and does not, of course, include the time course of the increase in area coated with time. As such, it represents an upper bound on drug delivery over this time interval. When the area coated exceeds A_{max}, the gel is predicted to leak from the vagina. Thus its merit would decrease in relation to the amount of predicted leakage. Letting V_L

be the volume of gel that has leaked, Equation 2.10 relates V_L to A^* which is the value of A at which the score becomes zero. A simple linear function was used to model the decline of the score from unity to zero, as area coated increases above A_{max}. Our expression inputs a maximum value of V_L at which the value of the objective function has declined to zero.

$$A^* = \frac{A_{\max}}{\left(1 - \frac{V_L}{V}\right)} \text{ for } A > A_{\max} \tag{2.10}$$

$$S = \frac{V - \left[(V - V_L)\left(\frac{A}{A_{\max}}\right)\right]}{V_L} \text{ for } A > A_{\max} \tag{2.11}$$

Separate computations were performed for undiluted ($S_{undiluted}$) and diluted ($S_{diluted}$) gels. These scores served as responses to create response surface modeling (RSM). In this algorithm, there are four key inputs: V, A_{max} and V_L and the mathematical form of the objective function. V was chosen to be 3.5 mL for the initial set of studies because this value is a common dose volume of microbicide gels. Maximum volume of the gel leaked after application was taken as V_L = 1.5 mL, at which the score declined to zero (Figure 2.3). This volume was based upon inputs from clinical investigators evaluating acceptability of gels in microbicide trials. Choosing the value A_{max}, which is a specified target area for optimal coating, requires information about the relationship between the

squeezing model predictions of area coated and actual values of areas coated in women. In the present study, we used values of area coated computed for the methylcellulose (MC) placebo gel from the Carraguard® trials as a reference.[148]

2.3 Results

2.3.1 Rheological measurements

Viscosity values vs. shear rate for different combinations of HEC and Carbopol 974P are presented in Figure 2.4. Shear rates are shown from 1 - 100 s^{-1} for undiluted gels (Figure 2.4A) and 1 - 1000 s^{-1} for gels diluted with VFS (Figure 2.4B). Combinations of Carbopol 974P and HEC were investigated in relation to any synergistic effect between the two polymers on gel viscosity. Similar observations for combinations of Carbopol 974P and HPMC have previously been reported.[149] At low shear rates (~ 1 s^{-1}) the viscosities of gels with both gelling agents, were approximately an order of magnitude higher than the sums of the viscosities for gels with the individual polymers. However, at higher shear rates (~100 s^{-1}) such differences became marginal. This result indicates that the shear rate dependent viscosity profile is critical, and that simply comparing viscosities at specific shear rates is insufficient in understanding and comparing rheological behavior of gels. When gels were diluted with VFS, those consisting of both HEC and Carbopol 974P exhibited > 50% loss in viscosity vs. undiluted values. The maximum impact of dilution was observed with gels consisting of 2.5 wt% Carbopol 974P and 3.0 wt% HEC (Figure 2.4B).

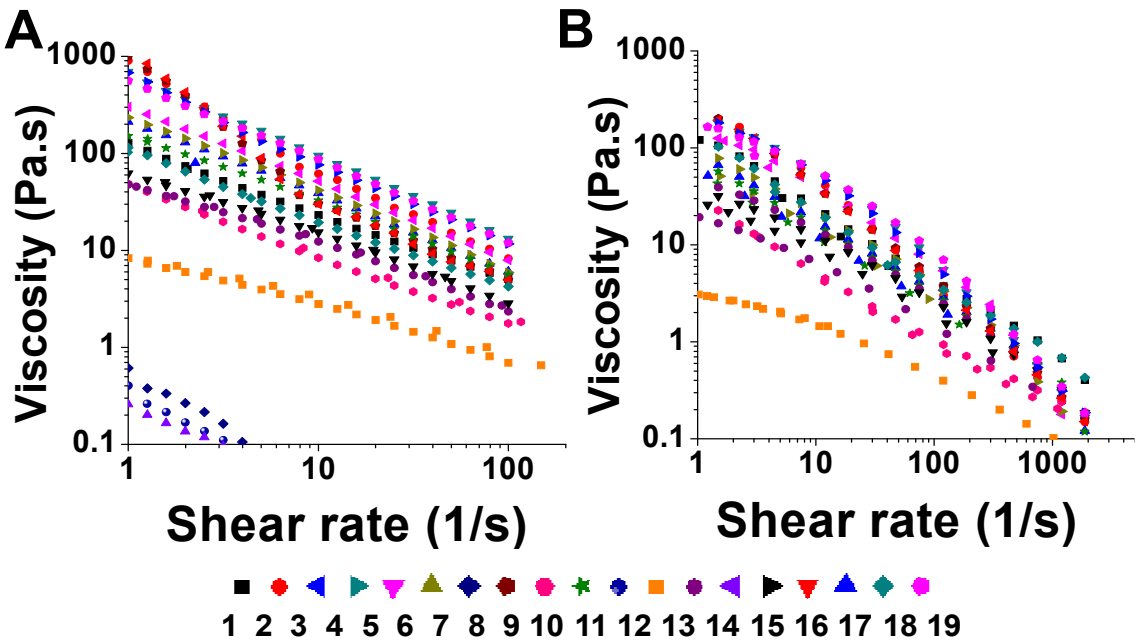

Figure 2.4 Results of the steady state flow experiments on undiluted gels **(A)** and gels after 20% dilution with VFS **(B)**.

2.3.2 Fitting rheological data to constitutive models

Table 2.4 summarizes the composition-property relationship in the gels. In general, the consistency index decreased on dilution with VFS, whereas the shear thinning coefficient increased, i.e., the degree of shear thinning decreased.

2.3.3 Stress growth and relaxation measurements

As expected, gels with HEC alone did not demonstrate measurable residual stresses.[150] Gels consisting of Carbopol 974P alone or in combination with HEC exhibited measurable residual stress. Carbopol 974P gels demonstrated a concentration dependent increase in measured residual stress. For all gels diluted with VFS (Figure 2.5B), there was a significant decrease in the residual stress.

Table 2.4 Power law parameters for gels undiluted and diluted 20% with VFS.

Gel ID	$m_{undiluted}$	$m_{diluted}$	$n_{undiluted}$	$n_{diluted}$	$r^2_{undiluted}$	$r^2_{diluted}$
1	1189	743	0.30	0.30	0.99	0.99
2	6157	1288	0.08	0.29	0.96	0.71
3	2253	785	0.22	0.31	0.99	1.00
4	6587	1554	0.16	0.42	0.99	0.75
5	3117	1482	0.21	0.35	0.99	0.93
6	2488	1054	0.21	0.30	0.97	0.99
7	4.07	0.00	0.14	1.47	0.91	-
8	2720	1362	0.25	0.23	0.90	0.70
9	454	129	0.28	0.42	0.99	1.00
10	1628	675	0.28	0.32	0.99	1.00
11	2.92	0.17	0.22	0.34	0.95	0.97
12	89.2	2.40	0.47	2.48	0.98	-
13	516	535	0.35	0.40	0.98	0.97
14	2.43	0.00	0.22	1.52	0.99	-
15	669	420	0.33	0.44	0.98	0.97
16	2517	1453	0.29	0.18	0.87	0.64
17	5923	1233	0.14	0.39	0.95	0.65
18	1051	884	0.29	0.27	0.99	0.99
19	5648	1352	0.17	0.48	0.99	0.83

n - shear thinning index, *m* - consistency index , r^2 - goodness of model fit and τ_r- residual stress from the stress relaxation experiments.

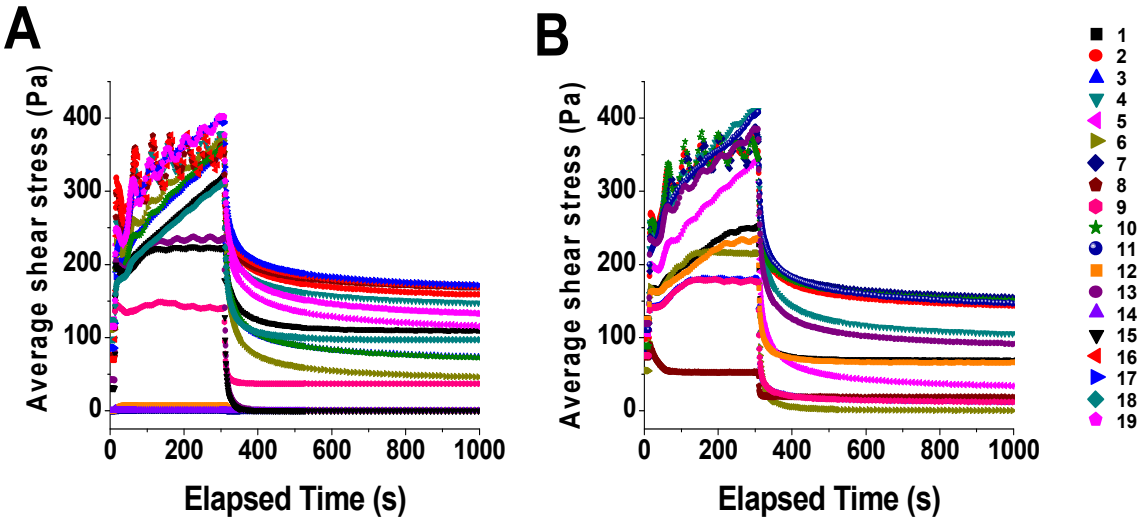

Figure 2.5 Comparisons of the stress growth and relaxation curves for gels from the MDOE. Plots **A** and **B** show the stress growth and the relaxation curve for the undiluted and diluted gels.

Carbopol 974P gels, in the absence of HEC, showed ~ 50% loss in residual stress on dilution; in contrast, gels containing both Carbopol 974P and HEC showed significant but less dramatic losses in residual stress compared to pure Carbopol 974P gels. Gels with Carbopol 974P at its highest concentration, in the presence of HEC, demonstrated the highest residual stress (~ 150 Pa).

2.3.4 Squeezing flow model

The MC placebo gel from the Carraguard® clinical trial[56, 65] has been previously reported to provide near complete coating of the vaginal epithelium *in vivo*, immediately after application with insignificant leakage post application.[149] For this gel we obtained an area coated of 117 cm^2 at 120 s for a 3.5 mL volume. This value is close to the actual value of human vaginal surface area.[56, 128] To compensate for the overestimations of area coated by the flow model, we renormalized all data with respect to MC placebo. Thus, A_{max} for both undiluted and diluted gels was set at 117 cm^2, for a volume of administration of 3.5 mL.

2.3.5 *In vivo* confirmation of the squeezing flow model

To validate the predictions of area coated obtained from the squeezing flow model; model data were compared to the percentage *A* obtained from *in vivo* imaging studies for four over the counter (OTC) gels – K-Y Jelly®, Replens®, Conceptrol® and Advantage-S™. The values of *A* predicted by the squeezing flow model showed good agreement (< 25% difference) with the results from imaging studies reported in literature, with a consistent but small overestimation of the *in vivo* values (Table 2.5).[22]

Table 2.5 Summary of the percentage surface area coated, obtained from the squeezing flow calculations and from *in vivo* MRI studies in women.

Gel	Percentage Area coated using MRI	Percentage A coated from the Squeezing flow model[c]
Conceptrol®[a]	59	72
K-Y Jelly®[b]	63	76
Replens®[b]	68	84
Advantage-S™[a]	96	104

[a]Reference[147], [b]Reference[147], [c]Using renormalized A_{max}

2.3.6 Area coated from squeezing flow model

Figure 2.6 summarizes the results of the squeezing flow computations on the gels. Upon dilution with VFS, gels with highest concentration of HEC and/or Carbopol 974P displayed 15-20% increase in the predicted area coated, whereas, at lower concentrations, there was a more pronounced effect of dilution (30-50%). At fixed concentrations of one gelling agent and increasing concentrations of the other agent, spreading of gels decreased significantly. These results are consistent with the trends observed in the viscosity vs. shear rate curves (Figure 2.4).

2.3.7 Fitting responses to model

$S_{undiluted}$ and $S_{diluted}$ computed for the model gels were simultaneously fitted to linear, quadratic, cubic and higher order special cubic models.

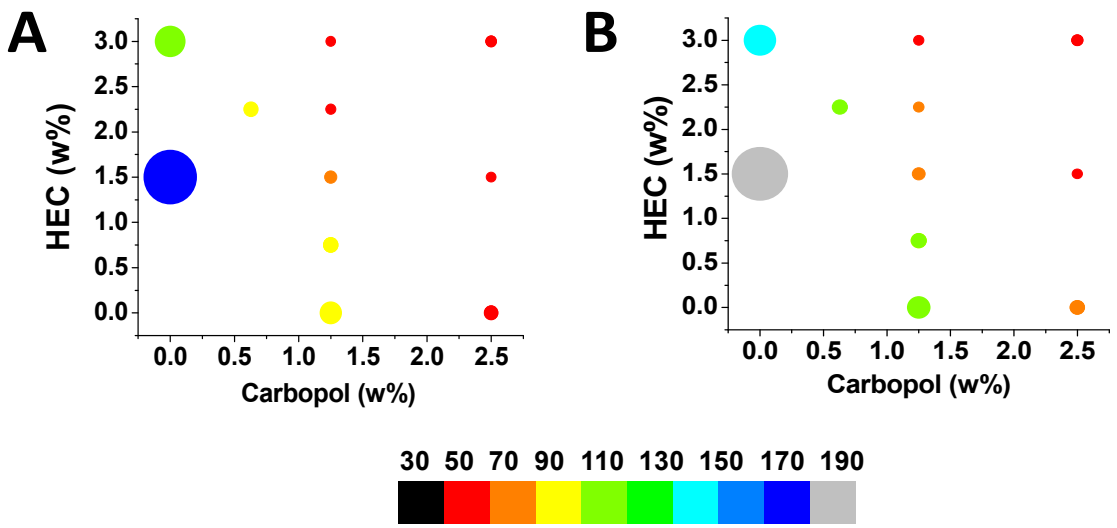

Figure 2.6 Predicted vaginal surface area covered after 120 s of constant-volume squeezing, using the squeezing flow model. Gel volume = 3.5 mL. **(A)** Undiluted gels and **(B)** gels diluted 20% with VFS. Increasing size of the bubble and color gradations from black to gray represents increasing values of area coated. 1.5 w% HEC gave the highest area coated followed by 3.0 w% HEC gel.

The cubic model provided the best estimation of coefficients for both responses. Comparative values of model fits are summarized in Table 2.6 along with the regression equation generated for each response. The fits indicated that a significant model did exist ($p < 0.05$), with insignificant lack of fit ($p > 0.10$) and an adequate signal-to-noise ratio (precision > 4). Using the backward elimination function in the program, only statistically significant ($p < 0.05$) coefficients were included in the regression equations. In general, positive values of model coefficients (β_i, β_j, β_k; Equation 2.1) indicate that the selected effect favors optimization of the response, whereas negative values suggest an inverse relationship.

Table 2.6 Results of the regression analysis for the responses – $S_{undiluted}$ and $S_{diluted}$, by fitting the responses to a cubic model. Only statistically significant terms included. X_1, X_2 and X_3 is Carbopol 974P, HEC and water, respectively after lower bound pseudo coding.

	Adjusted R^2	**Predicted R^2**	**Model p value**	**Lack of fit p value**
Undiluted V = 3.5 mL	0.9895	0.9812	< 0.0001	0.8954
Diluted V = 3.5 mL	0.9887	0.9773	< 0.0001	0.3214

$$S_{undiluted} = -3.38\,X_1 + 1.64\,X_2 + 4.08E^{-04}\,X_3 + 4.3\,X_1X_2 + 7.0\,X_1X_3 - 0.53\,X_2X_3 - 13.9\,X_1X_2X_3 + 13.6\,X_1X_2\,(X_1 - X_2) + 1.96\,X_2X_3\,(X_2 - X_3)$$

$$S_{diluted} = 42.2\,X_1 + 6.56\,X_2 - 5.9E^{-03}\,X_3 - 94.1\,X_1X_2 - 81.5\,X_1X_3 - 10.8\,X_2X_3 + 113.7\,X_1X_2X_3 - 31.8\,X_1X_2\,(X_1 - X_2) - 58.2\,X_1X_3\,(X_1 - X_3) - 4.4\,X_2X_3\,(X_2 - X_3)$$

From the linear coefficients for the pure component, it is evident that Carbopol 974P (X_1) with a negative β_i has an adverse effect on $S_{undiluted}$. This can be interpreted as being due to the yield stress acting to diminish spreading. The linear coefficient for HEC (X_2) is positive and indicates that HEC favors $S_{undiluted}$. The effect of variation in X_3 was ~ 3 orders of magnitude lower on both the responses, which can be considered negligible. The coefficients in the regression equations (Table 2.6) are large, which is due to the L-pseudo transformation that converts the compositions on a scale of 0 to 1. Unlike the case of $S_{undiluted}$, both X_1 and X_2 favor the optimization of the $S_{diluted}$, and the two-component nonlinear blending coefficients show an antagonistic effect on $S_{diluted}$. The surface for the response $S_{diluted}$ is more complex, due to the constant interplay between the linear and the nonlinear blending coefficients, as shown in the regression equation. In summary, based on the regression equations, it is evident that the

factors X_1 and X_2 play an important role in the optimization process. HEC (X_2) has a favorable effect on both responses whereas Carbopol (X_1) favors only the optimization of $S_{diluted}$.

2.3.8 Validation of the cubic model and RSM

To evaluate the ability of the model and RSM to predict the score, we chose four checkpoints within the design space. Rheological characterization of these gels was performed in the same manner as on all other gels in the study. Table 2.7 shows the composition of the checkpoints, their predicted and experimental values of the score, and the percentage error in predictions.

2.3.9 Response surface methodology (RSM)

Response surfaces provide visual depiction of the relationship between composition and scores. The score is suggestive of the relative performance of the gels. Figure 2.7 and 2.8 shows the surface plots for the score of the gels under undiluted and diluted conditions. All the responses exhibited nonlinear relationships with composition. Figure 2.7B&D show the 2D contour plots, while Figure 2.7A&C are 3D surface plots depicting effects of change in composition on gel score. $S_{undiluted}$ increases with increasing concentrations of HEC as shown in Figure 2.7A. The response surface peaks at the highest concentration of HEC in the absence of Carbopol 974P, whereas the surface that fits $S_{diluted}$ is more complex. The surface exhibits curvature at the intermediate concentrations of HEC (2.25 – 3.0 wt%) and Carbopol 974P (1.25 wt%). However, further increase in Carbopol 974P concentration results in a dip in the surface (Figure 2.7C).

Table 2.7 Composition of the checkpoints, their predicted and experimental values of the scores (*S*) and the percentage error in the predictions. X_1 and X_2 is Carbopol 974P and HEC concentration, respectively.

Composition	Response	Experimental value	Predicted value
X_1 - 1.6; X_2 - 0.0	$S_{undiluted}$	0.3669	0.3582
	$S_{diluted}$	0.5866	0.5250
X_1 - 2.0; X_2 - 1.8	$S_{undiluted}$	0.1197	0.1096
	$S_{diluted}$	0.1569	0.1751
X_1 - 1.0; X_2 - 0.9	$S_{undiluted}$	0.1449	0.1587
	$S_{diluted}$	0.2704	0.2526
X_1 - 0.0; X_2 - 2.5	$S_{undiluted}$	0.5582	0.5310
	$S_{diluted}$	0.1211	0.1346

2.3.10 Vehicle optimization using RSM

Individual response surfaces for the undiluted and diluted gels at 3.5 mL volume were generated. A multiple response optimization methodology was used to maximize $S_{undiluted}$ and $S_{diluted}$ simultaneously, with the constraints of Carbopol 974P (0-2.5 wt%), HEC (0-3.0 wt%) and score (0-1). Responses $S_{undiluted}$ and $S_{diluted}$ varied in the range of 0 - 0.876 and 0 - 0.830, respectively. The response surface for $S_{diluted}$ exhibited a curvature at the intermediate concentrations of HEC (2.25 – 3.0 wt%) and Carbopol 974P (1.25 wt%) and further increase in Carbopol 974P concentration resulted in a dip in the surface. For multiple response optimizations, the software utilizes a function that converts multiple responses into a univariate function – 'desirability', which ranges from 0-1. From the desirability plot, 0.0 wt% Carbopol 974P and 3.0 wt% HEC was identified as the optimum composition for 3.5 mL volume and A_{max} of 117 cm^2 (Figure 2.8).

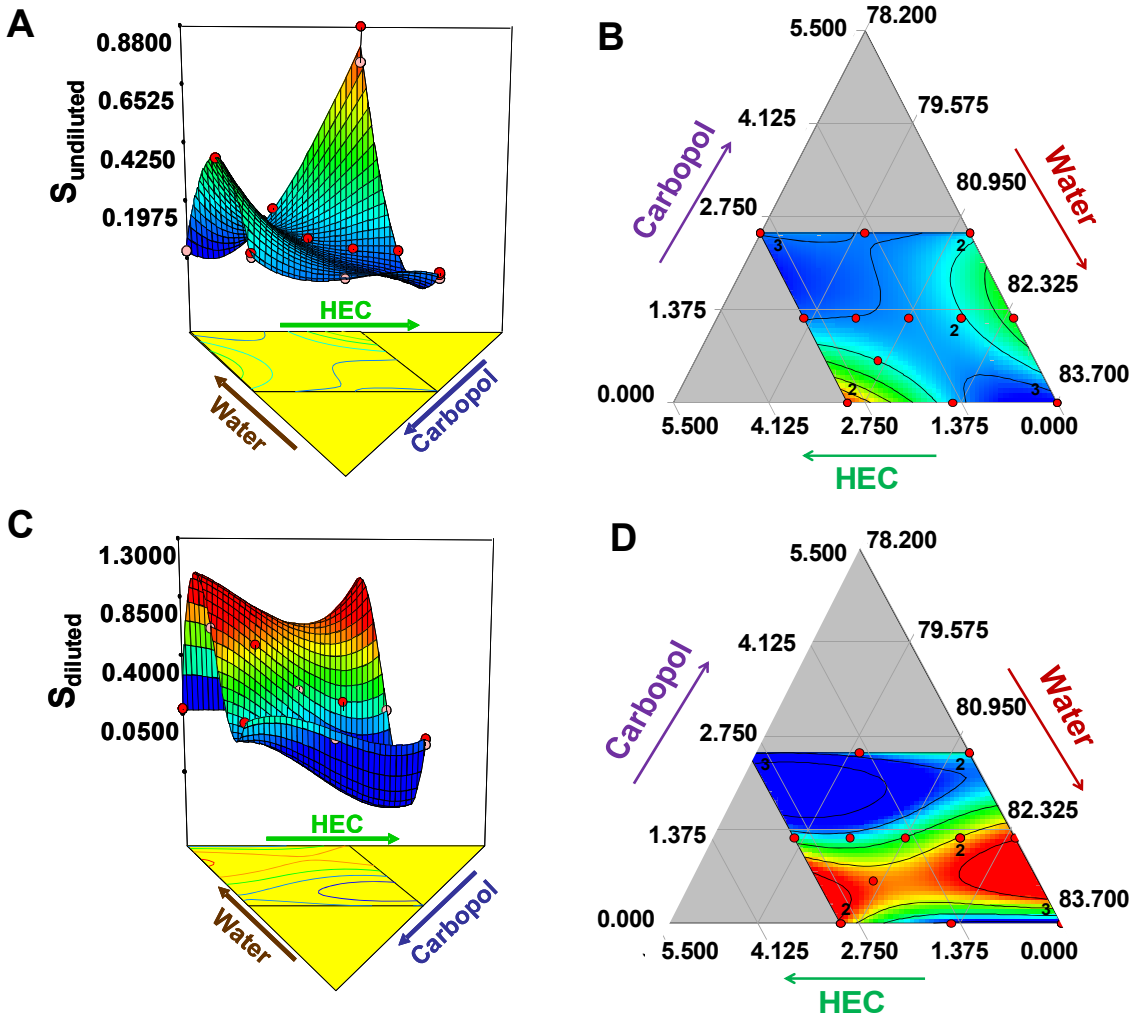

Figure 2.7 3D and 2D response surface plot showing the effect of concentration of Carbopol 974P (X_1) and HEC (X_2) on the responses. **(A)** and **(B)** 3D and 2D response surface plot of $S_{undiluted}$; **(C)** and **(D)** 3D and 2D response surface plot of $S_{diluted}$, respectively.

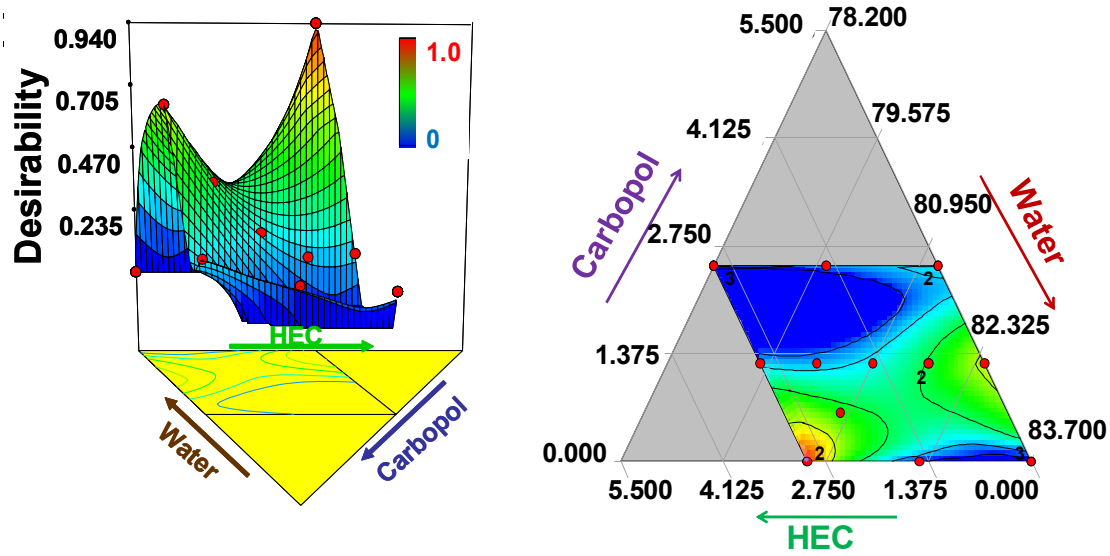

Figure 2.8 3D and 2D response surface showing the plot of desirability as a function of gel composition.

2.4 Discussion

The prophylactic capabilities of a vaginal microbicide depends on the potency of the Active Pharmaceutical Ingredients (API) and the capability of the vehicle to deliver it appropriately to the vaginal lumen.[148] For microbicide gels, the latter derives directly from the time course of gel deployment within the lumen. In general, an effective microbicide gel should achieve maximum coating of the vaginal epithelium; a coating that is retained for the desired duration of action.[92, 95] Thus, the deployment potential of microbicide gels should be a key component in product design. Only when this potential is understood, and can be related to gel composition during development, can rational design and optimization of vaginal gel carriers be realized.

Rheological behavior governs the ability of a gel to initially flow and coat the vaginal epithelial surfaces after insertion, as well as to resist further flow, facilitating retention.[95, 128] The most commonly used parameter to characterize the rheological behavior of vaginal gels is viscosity.[95] However, because majority of these gels are non-Newtonian, there is no single value of viscosity that characterizes spreading behavior. In general, it is the shear rate dependence of viscosity (which requires specification of at least two parameters), and also the value of the yield stress (an additional parameter; should a yield stress exist) governing the gel spreading process. The presence of Carbopol 974P in gels (but not HEC alone) gave rise to a nonzero yield stress. We evaluated the dependence of gel rheological behavior across jointly varying concentrations of Carbopol 974P and HEC. Consistent with results of other studies, viscosities of these gels increased as functions of concentration of the gelling agent.[95] All gels exhibited shear thinning behavior, with viscosity decreasing by approximately one order of magnitude as shear rate increased from 1 to 100 s^{-1}.

When a gel is inserted into the vagina using an applicator, it is delivered as a bolus near the fornix. *In situ*, the bolus experiences a continuous squeezing force from the vaginal musculature, initiating spreading.[56, 150] Therefore, in addition to the measurement of rheological properties of gels and its incorporation in constitutive models, *in vitro* methodologies have been developed to simulate gel flow and changes in gel properties *in vivo.*[118, 151] Once the gel begins to spread, it undergoes dilution with the vaginal secretions, likely further enhancing the spreading.[57] The rate and extent of dilution of the formulation in

the vagina may not be homogenous. This behavior may be due to several factors, including: a) the highly heterogeneous vaginal epithelium[10, 57]; b) variability between women;[57] c) cyclic changes in vaginal epithelium with changes in menstrual cycle;[10, 22, 25] and d) variability in the local dilution of the gels with vaginal secretions.[22] In order to study the effect of dilution of gels with vaginal fluid, we performed rheological characterization on gels diluted with VFS (1:4 VFS:gel).[57] This single ratio and the one time mechanical mixing do not mimic the kinetics of dilution *in vivo*, but they do provide an extreme case of dilution, which is relevant in understanding the potential effect of dilution on the deployment of gels. The degree of shear thinning decreased (i.e., *n* increased) and the consistency index (*m*) decreased after dilution with VFS. That is, the gels became less non-Newtonian. In addition, yield stress decreased on dilution. Consequently, there was a significant increase in the predicted area coated for the diluted gels as compared to the undiluted gels (Figure 2.6). Details of the response to dilution with VFS differed amongst gels with varying composition, with a greater sensitivity to dilution when Carbopol 974P was present.

Overall, computation of coated area and consequent computation of the score derived from interactions amongst the multiple rheological properties of the gels, whole and diluted. This methodology points to a 3.0 wt% HEC gel as the optimal candidate for a vaginal microbicide gel capable of quickly spreading throughout the vagina across the HEC-Carbopol 974P mixture space analyzed in this study. However, TFV, one of the two active ingredients incorporated in the gel is a sodium salt. Since, Carbopol is an ionic polymer; viscosity of Carbopol

974P gels was significantly affected by the presence of TFV. Therefore, the gels optimized in the work herein are specific to the delivery of 1 wt% TFV and will need to be reoptimized for other drugs or gelling agents.

To study the impact of gel volume on the score, we calculated scores for the 3.0 wt% HEC gel at varying volumes. $S_{undiluted}$ increased as volume increased (up to 4.0 mL) whereas $S_{diluted}$ exhibited a maximum at 3.5 mL. $S_{combined}$, was calculated from the arithmetic average of $S_{undiluted}$ and $S_{diluted}$. The use of the arithmetic average of $S_{undiluted}$ and $S_{diluted}$ is a first approximation, accounting for the complex process of progressive gel dilution during spreading *in vivo*. The 4:1 gel dilution with vaginal fluid (gel:vaginal fluid) is an upper bound on what is believed to be the extent of gel dilution with vaginal fluid *in vivo*. The arithmetic average for S equally weights the spreading of undiluted and fully diluted gel, and effectively assumes that net gel performance (i.e. the value of *S*) can be represented as the simple average of the lower (undiluted) and upper (diluted) bounds to the extent of gel spreading. $S_{combined}$ showed a maximum score at 3.5 mL (Figure 2.9). This supports our selection of 3.0 wt% HEC as the optimum spreading gel at an administered volume of 3.5 mL.

Since the optimized gel lies towards the extreme corner of the tested design space, additional studies were performed to ensure optimization was not compromised or limited by the design space. In order to evaluate the effect of increasing concentrations of HEC, we prepared gels with increasing HEC concentrations over the range 2.5 wt% - 5.0 wt%.

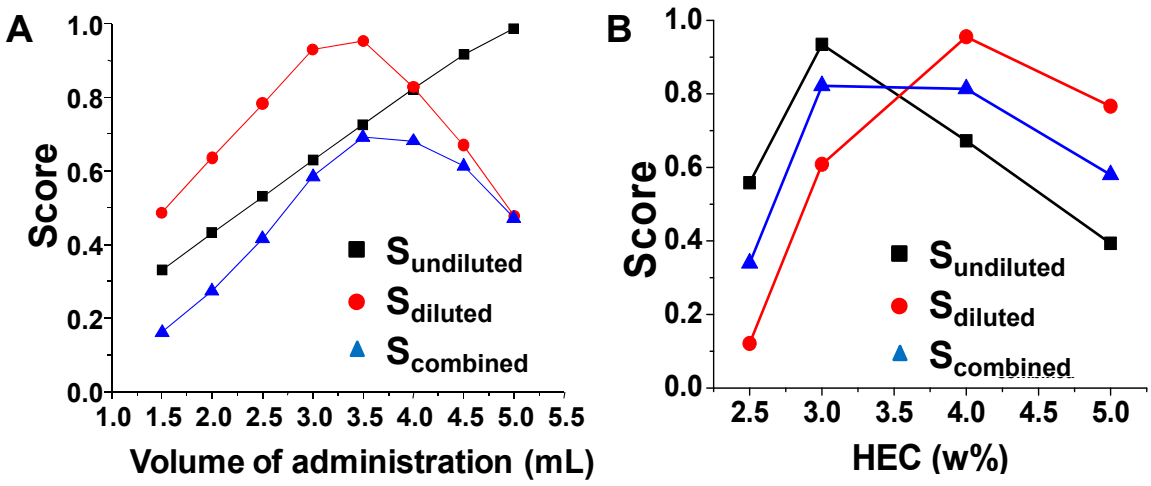

Figure 2.9 Variations in the score (S) for both undiluted and gels diluted with VFS with (A) increasing volume of administration and (B) concentrations of HEC in the gel. Highest value of $S_{combined}$ was achieved with 3.0 w% HEC gel at 3.5 mL volume.

As shown in Figure 2.9, the maximum for $S_{undiluted}$ was around 3.0 wt% HEC, and for $S_{diluted}$ it was around 4.0 wt% HEC. Since we optimized the scores for both undiluted and diluted gels – using the $S_{combined}$ – the 3.0 wt% HEC gel proved to be the optimum gel followed by the 4.0 wt% HEC gel. The squeezing flow model has been found to predict spreading reasonably well, compared to data from *in vivo* imaging studies (Table 2.5), for four polyacrylic acid or cellulose-based gels. Further improvements to the model are underway[57] to improve its accuracy and extends its applicability across different gels. Of course, all such modeling should be compared and validated against imaging studies whenever sufficient *in vivo* data are available. In addition to the above analysis, we compared the values of the score (undiluted, diluted) for the 3.0 wt% HEC gel created here with values for other microbicide gels and placebos, as well as for commercial over-the-counter vaginal gels used for lubrication.

Table 2.8 summarizes these results. In general, all undiluted gels exhibited spreading that did not exceed the target A_{max} = 117 cm^2. Upon dilution, spreading increased for all gels: for some, *A* still did not exceed A_{max}, and thus *S* increased. However, for others, *A* exceeded A_{max}; for all gels evaluated here, this resulted in a lower score after dilution. We note that the HEC Universal Placebo gel is a 2.7 wt% HEC gel,[133] and it has score values (0.77, 0.90; 0.84 undiluted, diluted; average) very close to those of the optimal HEC gel created here (0.73, 0.94; 0.84). Comparisons with the other gels vary. TFV 1% microbicide gel from the CAPRISA 004 trial (0.92, 0.80; 0.86) and Carraguard (0.88, 0.51; 0.70) have good scores. In contrast, the 6% cellulose sulfate (0.58, 0.03; 0.31) and UC781 clinical gel (0.44, 0.00; 0.22) have low scores when diluted, because their significant reductions in viscosity cause them to be prone to leakage. The contrasts across these results exemplify the uncertainty about gel coating performance inherent to traditional, empirical vaginal gel design. The three commercial gels exhibit contrasting behavior. Two have higher scores after dilution: RepHresh® (0.24, 0.85; 0.55) and K-Y Jelly® (0.59, 0.82; 0.71). The other gel, Replens®, exhibits the opposite trend (0.81, 0.56; 0.69).

Our work is the first to relate gel composition – comprised of two commonly used gelling agents – to gel performance as predicted using a deterministic vaginal squeezing flow model. The methodology described herein offers a quick empirically derived mathematical method that can be used to select composition of vaginal semisolid gels based on performance predictions.

Table 2.8 Values of score (*S*) for 3.0 wt % HEC gel and other commercial vaginal gels, clinical microbicide gels and placebos.

Gel	Score		
	Undiluted	**Diluted**	**Combined**
3.0 wt% HEC gel[a]	0.73	0.94	0.84
Universal placebo gel[b*]	0.77	0.90	0.84
6% Celluose sulfate[c*]	0.58	0.03	0.31
TFV 1% gel from CAPRISA 004 trial[d*]	0.92	0.80	0.86
UC781 clinical microbicide gel[e*]	0.44	0.00	0.22
Carragaurd[f*]	0.88	0.51	0.70
RepHresh[e]**	0.24	0.85	0.55
Replens[e]**	0.81	0.56	0.69
K-Y Jelly[d]**	0.59	0.82	0.71

[a] Optimized gel from this work; [b] HEC placebo gel (2.7% HEC); [c] Carboxymethylcellulose-based gel; [d] Cellulose-based gel; [e] Carbopol-based gel; [f] Carrageenan-based gel; [*] Obtained from the CONRAD Program; [**] Over the counter products

Furthermore, use of the objective function establishes an analytical and biologically relevant method for gel evaluation that can easily be modified to incorporate a range of desired performance parameters. Application of this model could enable expedited characterization and prediction of performances of the next generation of microbicide gels. This approach is flexible, and by knowing the volume of the gel and the predicted area coated one can create objective predictions about gel performance *in vivo* prior to human trials. Our methodology here includes only the pre and post dilution rheological properties and deployment predictions. However, this DOE approach can be diversified to

account for additional critical parameters of the formulation such as other gelling agents and excipients, drug release rate, drug stability, bioadhesion, toxicity, and dilution with other ambient vaginal fluids such as semen. Indeed, this approach could potentially be applied to a diverse range of vaginal delivery products used for artificial insemination, antifungal delivery, vaginal moisturization and hormone delivery. Furthermore, use of such an approach circumvents the problems associated with traditional methods of gel optimization and composition selection, which contain many subjective elements; and can lead to the reassessment of gel compositions to meet specific clinical applications, beyond microbicides.

2.5 Conclusion

This study is the first to describe the composition-property-performance relationship of vaginal semisolid drug delivery gels consisting of HEC and Carbopol 974P. The multivariate optimization approach introduced here, used in conjunction with rheological characterizations, fluid flow models and statistical tools, offers an integrated multitier approach for the optimization and selection of vaginal microbicide gels prior to *in vivo* investigations.

2.6 Acknowledgments

This work was generously supported by CONRAD under a Cooperative Agreement with USAID (HRN-A-00-98-00020-00). The views expressed by the authors do not necessarily reflect those of USAID.

CHAPTER 3

INHIBITION OF THE TRANSPORT OF HIV *IN VITRO* USING A PH-RESPONSIVE SYNTHETIC MUCIN-LIKE POLYMER SYSTEM[3]

3.1 Introduction

Recent advances in the dissection of the early events in the acquisition of sexually transmitted infections (STIs), and in particular HIV, tell a story of break down in barrier function at the level of transport of the virus and dissemination of infection.[152] It is believed that the doorway to the complicated, and not yet well understood acquisition process, is the movement of the semen-borne virus through the cervical mucus to the cervicovaginal epithelium.[45] Therefore, developing materials that prevent transport of the virus from semen to the vaginal tissue susceptible to infection, may constitute an important mechanism in preventing the heterosexual transmission of HIV. In fact biopolymers present in

---

[3]Adapted from Inhibition of the Transport of HIV-1 *In vitro* Using a pH-Responsive Synthetic Mucin-Like Polymer System, Biomaterials, Volume 32 (33), 2011, 8343-55, Alamelu Mahalingam, Julie I. Jay, Kristofer Langheinrich, Shetha Shukair, Mike McRaven, Lisa C. Rohan, Betsy C. Herold, Thomas J. Hope, Patrick F. Kiser.

the vaginal lumen are known to impede movement of viral particles and cells. Cervical mucus exhibits a flexible woven mesh molecular structure. The reversible nature of mucin crosslinks, promotes the formation of a transient polymer network that impedes the diffusion of HIV, which has been observed primarily at acidic pH.[38] Similarly, the highly viscous nature of semisolid vaginal formulations also interferes with viral transport.[31] However, neutralization of the cervical mucus with semen[53] and dilution of semisolid vaginal formulations with biological fluids (vaginal and seminal)[53] compromise the barrier properties of both systems.[153, 154] In addition, cell-associated virus within semen, which may be an important source of transmission,[54] may be less susceptible to the effects of biopolymers and cervical mucus.[31, 38, 54] Therefore, an effective physical barrier to the transmission of HIV should create a gel layer impermeable to both cell-free and cell-associated virions after dilution with seminal fluid of a neutral pH.

Given the burgeoning scope of materials in drug delivery applications, there is significant interest in materials that mimic the properties and the behavior of naturally occurring systems.[38, 155-158] We are interested in developing a synthetic mucin-like polymer system (SMP) (Figure 3.1), engineered to mimic certain characteristics of the cervical mucus that may be advantageous for a microbicide application. These include - (a) formation of a transient network at acidic pH (Figure 3.1-V), (b) bioadhesiveness (Figure 3.1-III) and (c) inhibition of transport of HIV from semen to the susceptible tissue (Figure 3.1-IV).

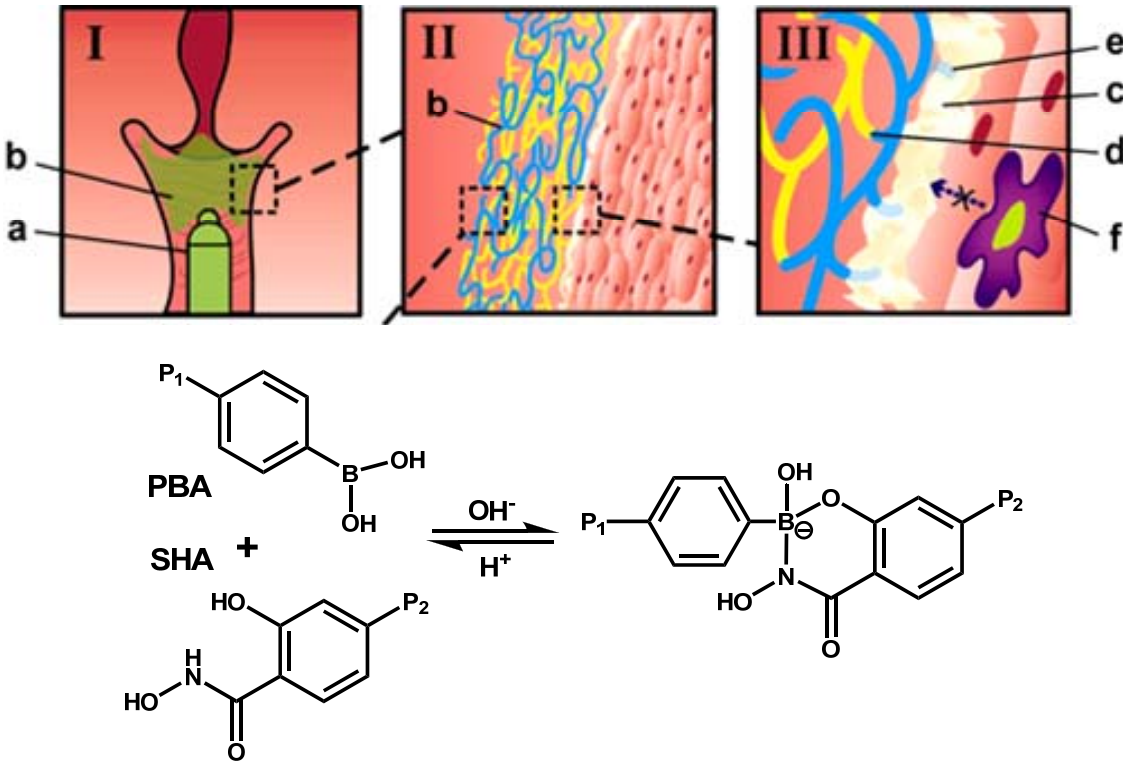

Figure 3.1 Schematic demonstrating the use of the phenylboronate salicylhydroxamate crosslinked polymer as a microbicide drug delivery system. **(I)** The two polymer solutions, pHPMAm$_{95}$-PBA$_5$ (PBA$_5$, blue) and pHPMAm$_{95}$-SHA$_5$ (SHA$_5$, yellow) on mixing form a weakly crosslinked viscoelastic fluid (**b**, green) which can be applied via an applicator **(a)**. **(II)** The crosslinked polymer solutions form a pH-sensitive polymeric network, which should flow and coat the cervicovaginal epithelium at vaginal pH. **(III)** On a molecular scale, the gel network is comprised of chemical crosslinks between the polymer bound PBA (blue) and SHA (yellow) **(d)** as well as bioadhesive interactions of PBA with diols present **(e)** within cervical mucus **(c)** and on the epithelial surface. The crosslinking chemistry utilizes the reversible covalent crosslinking between polymer-bound PBA and SHA, creating a pH-responsive network that is transient and viscoelastic at vaginal pH; and is elastic and solid-like at the seminal pH.

However, one aspect in which the SMP differ from cervical mucus is in regards to the sensitivity of the phenylboronic acid (PBA) and salicylhydroxamic acid (SHA) complexation to pH, where the crosslinking density, and thereby the barrier property, increases as pH increases from vaginal pH (~ 4.0-5.5) to seminal pH (~7.5). Owing to the decreased network mesh size, the SMP may perform better than the evolved barrier function of cervical mucus. This represents a viable and unprecedented approach to blocking the acquisition of HIV.

In engineering a semisolid system as a physical barrier to the transport of viral particles, it is imperative to understand and control the mechanical properties for ease of application, coating and retention of the system.[95, 118, 153, 159] Application and coating necessitate a comparatively low viscosity material that can easily flow over tissue.[58, 95] However, low viscosity materials have difficulty in being retained in the vaginal lumen,[58, 160] and therefore may not have the capacity to inhibit viral transport to tissue, especially if applied hours prior to intercourse. This biophysical property-performance tradeoff of needing both low and higher viscosity materials has been confirmed in optical imaging studies of human vaginal coating by semisolid gels.[160] Our group is interested in designing biomaterials that respond to cues in the female reproductive tract that can be used for vaginal drug delivery and HIV prevention. For example, we have investigated temperature responsive polymeric systems as a means to create formulations that can be applied as a liquid ensued by *in situ* gelation to potentially improve coating and retention.[164, 165]

In this work, we have designed a biologically inspired SMP to prevent transport of virions in the vagina that exploits the pH change from acidic (4.0-5.5) to near neutral pH induced by the presence of seminal fluid.[53] This pH change provides a physiological stimulus that could allow an environmentally responsive material to sense the presence of the semen and thus the potential presence of the infectious agent, HIV. The goal is then to design a material that can modulate its properties over its deployment lifetime: from a viscoelastic, weakly crosslinked transient network on application, to a more elastic, densely crosslinked network formed on interaction with semen. This then impedes the transport of virions from semen to the susceptible female genital tract tissue. This mechanism provides a physical barrier that is capable of augmenting the efficacy of any antiretroviral that is also locally delivered. This pH modulation of the material properties can be achieved by engineering the crosslinking interactions of polymer chains and thereby the network properties of the material. The reversible pH-dependent interaction between PBA and the diol SHA[53, 161] can be used to create pH-sensitive transient polymer networks[162, 163] that have properties similar to mucus but switch to a more densely crosslinked network in the presence of semen.

Boronic acids or the boronate species undergoes a well known condensation reaction with cis-diols to form cyclic boronate esters.[164] This condensation reaction is reversible and is influenced by the pH, chemical structure of the diols and/or the boronic acid.[165] The boronic acid undergoes conversion to the charged boronate tetrahedral conformation; a stable complex

that resists hydrolysis compared to its trigonal form, which is more readily reversible. We selected SHA as it has previously been reported that, even at slightly acidic pH, the complex formed between PBA-SHA exists in the tetrahedral boronate conformation[161, 165] and yields a viscoelastic crosslinked network at a pH as low as three units lower than the pKa of SHA.[162]

Our previous work investigated transient network gels, based on linear polymers composed of the water soluble, nontoxic polymer backbone poly(N-2-hydroxypropyl)methacrylamide (pHPMAm)[163] functionalized with five mole percent PBA or SHA.[163, 166] We investigated the structure-property relationship of materials created from the PBA-SHA crosslink as a function of pH[163, 164] and composition of the system.[163] Since our objective is to develop a microbicide that is semen-responsive, bioadhesive and safe, it is important to characterize the interactions between the PBA-SHA SMP and the biofluids in the vaginal milieu. Considering that the cervical mucus consists of high amounts of sialic acid;[164] and the seminal fluid, which is the carrier of the pathogen, is a rich source of fructose,[167] we are particularly interested in evaluating the effect these endogenous diols from the vaginal milieu may have on the complexation between PBA and SHA, and consequently on the mechanical properties of the SMP (Figure 3.1-V).

Herein, we assessed the kinetics of *in situ* gelation as well as the resulting material's viscosity under steady state flow. Gelation kinetics and modulation of the viscoelastic behavior of the PBA-SHA SMP in response to the addition of semen and mucus were examined to determine the SMP's potential to respond

to a changing vaginal milieu. Ability of the SMP to inhibit transport of macrophages and HIV virions across the crosslinked polymer network was deduced *in vitro* and *ex vivo* using a migration assay. Investigations also assayed the toxicity and irritation potential of the PBA-SHA SMP to human ectocervical tissue.

3.2 Materials and Methods

3.2.1 Materials

HPMA monomer was purchased from Polysciences, Inc. (Warrington, PA). 2,2'-azobisisobutyronitrile (AIBN) was purchased from Sigma-Aldrich, Inc. (St. Louis, MO) and was recrystallized from chloroform. With the exception of Dubelco's Modified Eagles Media (DMEM High Glucose) purchased from HyClone Laboratories (Logan, UT) all the media and supplements for the biological assay were purchased from Invitrogen (Carlsbad, CA). Succinimidyl-7-amino-4-methylcoumarin-3-acetate (AMCA-NHS) was purchased from Apollo Scientific Ltd. (Cheshire, UK). All other chemicals and reagents were purchased from Aldrich or Acros and were used without further purification unless otherwise noted. All ^{1}H NMR spectra were acquired on a Varian Mercury 400 MHz spectrometer. Polymer molecular weight distributions were determined in using gel permeation chromatography (GPC) (HPLC 1100, Agilent Technologies) equipped with an aqueous column (PLaquagel-OH mixed, Polymer Labs) or an organic column (PLgel mixed-B, Polymer Labs), a differential refractive index detector (BI-DNDC, Brookhaven Instruments) and a multiangle light scattering

detector (BI-MwA, Brookhaven Instruments). Human Semen was purchased from Lee BioSolutions, Inc (St. Louis, MO).

3.2.2 Monomer synthesis

Methylacryloylamino-propyl-4-amido phenylboronic acid (APMAmPBA), 4-[(2-Methyl-acryloylamino)-methyl]-salicylhydroxamic acid (MAAmSHA) and 2-hydroxypropylmethacrylamide (HPMAm) were synthesized according to the previously published protocols.[163, 168]

3.2.3 Polymer synthesis

APMAmPBA or MAAmSHA was copolymerized with HPMAm at 5-95 mol% feed ratio by free radical polymerization as previously described (Figure 3.2).[163] Briefly, polymerizations were performed in the presence of 0.7 mol% Azobisisobutyronitrile (AIBN) in anhydrous DMF at 65°C for 24 h under nitrogen atmosphere. Polymers were triturated twice in anhydrous ether. After the first trituration, PBA-containing polymers were deprotected by redissolving the polymer in methanol and acidifying with a 1:1 dilution of 1 M HCl for 30 mins at room temperature. Titurated polymers were then lyophilized, dissolved in 100 mM phosphate buffer at 30 mg/mL concentration and dialyzed across a 10 KDa MWCO membrane using a Vivaflow 50, a tangential flow through filtration system. Actual molar functionalization of PBA and SHA monomers in the copolymers was determined in ^{1}H NMR in D_2O.

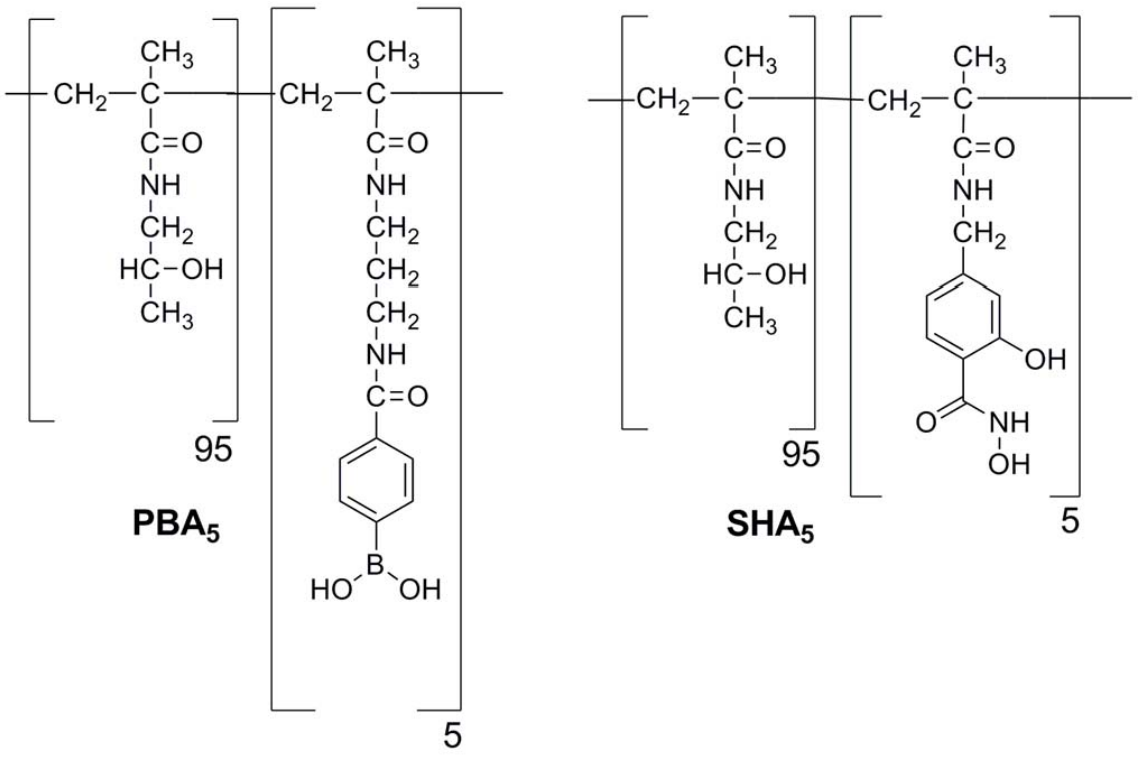

Figure 3.2 Chemical structure of the polymer bound PBA and SHA at 5 mol% functionalization. Both PBA_5 and SHA_5 were synthesized through free radical polymerization of APMAmPBA or MAAmSHA and mHPMA monomers in the presence of AIBN. Polymers were triturated twice in ether and were purified by dialysis across a 10,000 MWCO membrane.

3.2.4 Rheological assessment of the effect of seminal fluid on the PBA_5-SHA_5 crosslinked polymer network

The polymers were individually dissolved in buffer (100 mM acetate pH 4.8) at 75 mg/mL concentrations. Crosslinked polymer network was formed *in situ* by simultaneous pipetting of an equal volume of the polymer solutions directly onto the Peltier plate of the rheometer. A steel ring 48 mm in diameter and 10 mm in height was placed around the sample. Dynamic rheology was performed using methods previously described on an AR550 stress-controlled rheometer (TA Instruments, New Castle, DE).[163] Briefly, a flat steel 20 mm diameter plate

geometry was used for all experiments with a total sample volume of 170 µL. Six holes an eighth of an inch in diameter were drilled separated by 60° around the perimeter of the 20 mm geometry. A time sweep was initiated for 60 mins at a small amplitude oscillatory stress of 5 Pa and a small angular frequency of 10 rad/s. After approximately 25 mins, 500 µL of human semen was added into the trap on the top side of the steel geometry directly over the drilled holes. The effect of human semen on the network strength was then observed over the remainder of the time sweep.

To evaluate the effect of human semen on the viscoelastic properties of the SMP, time sweeps were performed until the networks' elastic modulus (*G'*) plateaued. Oscillatory frequency sweeps were then performed at a controlled stress of 5 Pa over a range of angular frequencies from 0.1-100 rad/s. After the initial time and frequency sweeps, a 5 m conditioning step allowed time for the human semen to be added to the sample. After addition of semen on the top side of the steel geometry with the drilled holes, time sweeps and oscillatory frequency sweeps were repeated using the parameters mentioned above. All experiments were done in triplicate unless otherwise noted.

3.2.5 Rheological assessment of the effect of mucin on the PBA_5-SHA_5 crosslinked polymer network

In general the rheological mucoadhesive interaction of materials with mucin has been described by calculating the rheological synergy parameter, *ΔG'*.[163] It is usually determined from Equation 3.1.

$$G'_{mix} = G'_{plateau} + G'_{mucin} + \Delta G' \quad (3.1)$$

where G'_{mix} is the plateau elastic modulus of the PBA-SHA SMP in the presence of mucin, $G'_{plateau}$ is the plateau elastic modulus of the PBA-SHA SMP alone, and G'_{mucin} is the elastic modulus of the mucin solution alone. The equation has been simplified in the literature due to negligible elastic modulus of mucin solutions[169] and therefore $\Delta G'$ was calculated from Equation 3.2.

$$G'_{mix} = G'_{plateau} + \Delta G' \quad (3.2)$$

Polymer solutions were prepared such that the final concentration of the polymers in the sample was 75 mg/mL with 1% w/w porcine gastric mucin. Dynamic rheology was performed using a cone-and-plate geometry.

3.2.6 Preparation of fluorescently tagged HIV_{BaL}

Gag Cherry labeled HIV virions were produced by transfection of 293T cells with proviral plasmids expressing BaL and a fluroscently labeled Gag protein using a previously described method.[170] The cell suspension was washed 24 h posttransfection. The supernatant solution containing the labeled virions was collected and concentrated by ultracentrifugation through a 30% sucrose cushion. The virions were then resuspended in Dubelco's modified eagles media (DMEM High Glucose, 4.0 mM L-Glutamine, 4500 mg/L Glucose, and no Sodium Pyruvate (0.1 μm sterile filtered) with 10% fetal bovine serum (FBS) and 50 μg/mL penicillin/streptomycin).

3.2.7 Tracking the fluorescently tagged HIV_{BaL} in PBA_5-SHA_5 crosslinked polymer network

Individual polymer solutions were prepared at 82.5 mg/mL in buffers at the required pH to account for dilution from the virus addition. After adjusting the pH of the solutions, Gag-cherry labeled HIV was added and vortexed for 30 s. Samples were prepared by mixing equal volumes of PBA_5 and SHA_5 polymer solutions containing 10% viral stock solution at the desired pH. The crosslinked polymer sample was placed in a 5 mm well on a Delta T4 culture dish at 37°C (Bioptechs Inc.). Five image stacks were collected using a 100x oil immersion objective (NA 1.4) on a DeltaVision Core microscope system with an EMCCD camera using SoftWorx software. Images were collected for 60 s with a 50 ms exposure and 85 ms time lapse. The mean squared displacement (MSD) of the virions was determined using an algorithm developed and kindly provided by John Crocker, David Grier, and Eric Weeks. Diffusion coefficients were computed as one-fourth of the slope of the line fitting the plot of $<\Delta r(t)^2>$ versus time.

3.2.8 Fluorescent labeling of macrophages

Fluorescent tagging was performed using a procedure provided by the suppliers. Briefly, a 0.05% solution of cell tracker dye (Molecular Probes, Invitrogen, Carlsbad, CA) was created in IMDM Serum Free Medium. The cells were counted using a hemocytometer and then the cells were spun down at 860 rpm for 5 mins. The cell medium was removed and the cells were resuspended in the working solution of the cell tracker dye (~ 2 mL). The cells were then incubated for 30 mins. The cells were then spun again at 860 rpm for 5 mins. The

medium was removed and the cells were resuspended in complete cell culture medium. The cells were incubated again for 30 mins. Lastly the cells were spun down at 860 rpm for 5 mins and resuspended in IMDM Serum Free Medium.

3.2.9 Z-Stack imaging to track macrophage migration in the PBA_5-SHA_5 crosslinked polymer network

A 10 mM solution of N-Formyl-Met-Leu-Phe (FMLP) (Sigma, St. Louis, MO) was made in DMSO and was diluted to 1 μM in IMDM Serum Free Medium. In a PCR tube 30 μL of the crosslinked polymer solution at pH 4.8 was mixed with 10 μL of chemo-attractant solution. Using a positive displacement pipette, 15 μL of the sample were pipetted into one of the wells on the culture dish. Following this, 30 μL of the sample was pipetted on top of the previous 15 μL of sample. The sample sat for 30 mins, to allow for diffusion of the chemo-attractant, covered with parafilm to prevent evaporation. Imaging was done using an Olympus FV1000-XY inverted microscope with a 40x water objective. The FluoView confocal operations software was used. A black mark was made on the bottom of the culture dish for ease in finding the bottom of the sample. After focusing on the black mark, the stage was moved up 150 μm (representing the approximate thickness of the dish). Using the software, this location was set as the bottom of the sample. To set the top of the sample and the z-stack location a simple calculation was done to determine approximate sample height:

$$h = \frac{V}{\Pi r^2}$$

where *r* is the radius of the PCR tube sections (approximately 2.75 mm) and *V* is the volume of sample used. For the above volume the thickness was approximately 1.8 mm. The stage was moved up ~1.8 mm and was set as the top of the polymer sample. The z-stack step size was set to 50 µm giving approximately 30-40 slices per z-stack. Imaging was initiated after placing 60 µL of cell suspension on top of the sample layer. Z-stacks were collected every hour from 0 - 4 h. The z-stacks were imported into Imaris and converted into a 3D image. A Gaussian filter of 1 µm was used to remove digital noise. Snapshots of all 3D images were taken and saved as tiff stacks.

3.2.10 *In vitro* safety evaluations using 3D ectocervical tissue model

Safety of the individual polymer solutions (PBA_5 and SHA_5) were evaluated on VK2/E6E7 cell line[171] after single exposure whereas safety of the PBA_5-SHA_5 crosslinked polymer after three repeated exposures was examined using VEC-100, a reconstructed human ectocervical tissue mode[171]. Polymer solutions (PBA_5 and SHA_5) were prepared at 150 mg/mL in keratintocyte serum-free media (KSF) and pasteurized at 70°C for 5 mins. Equal volumes of polymer solution and KSF containing 2X growth factors (supplemented with 0.2 ng/mL epidermal growth factor (EGF), 100 µg/mL bovine pituitary extract (BPE), 2% pen-strep (P/S), 0.8 mM $CaCl_2$) were mixed. The same dilution procedure was performed on all the samples. Cells were seeded at a density of 10^4 cells/100 µL of growth media. The cells were cultured for 24 h and were supplemented with additional 100 µL of growth medium containing PBA_5 and SHA_5. After an

additional 24 h of incubation, cell viability was quantified using MTS (3-(4,5-dimethylthiazol-2-yl)-5-(3-carboxymethoxyphenyl)-2-(4-sulfophenyl)- tetrazolium) cell proliferation assay (Promega, Madison, WI). Nonoxynol-9 (N-9, 0.0125 mg/mL) served as toxic control with ~ 40% cell viability. pHPMA served as the nontoxic control.[172]

Tissues were maintained as recommended by the suppliers.[166] The PBA_5-SHA_5 crosslinked polymer was placed in the insert on top of the VEC-100 tissue supported by a semiporous membrane at the bottom of the insert. pHPMA and N-9 were used as the nontoxic and toxic controls, respectively. After 24 h of incubation with the test sample, tissues were washed three times with PBS, and Trans Epithelial Electrical Resistance (TEER) was recorded for each tissue to ensure the integrity of the tissue during the study. Fresh samples were added to the tissue every 24 h, for 3 days and on day 3, tissues were evaluated for viability using MTT ((3-(4,5-Dimethylthiazol-2-yl)-2,5-diphenyltetrazolium bromide) assay. Meanwhile, culture medium was collected every 24 h for analysis of cytokine levels (IL-8, IL-1α, IL-6 and TNFα).

3.2.11 *Ex vivo* and *in vivo* safety evaluation using human ectocervical tissue and mouse model

Freshly excised human cervical tissue specimens were handled as previously described[75, 172] and were exposed to the SMP for a period of 4 h. Tissue culture media (DMEM) was used as the negative control. At the end of 4 h, tissue viability was determined using MTT assay (n=3). Tissues were also fixed in 10% neutral-buffered formalin solution, embedded in paraffin; sections

were cut and stained with hematoxylin and eosin (H&E). Tissue histology was compared between the SMP treated tissues and the control tissues to determine morphological changes (n=3).

Female BALB/c mice were used as an animal model to evaluate the *in vivo* safety of the SMP. The study consisted of six animals and two arms – the PBS (placebo) and SMP treated arm. On days 1 and 2, the mice were given a single dose (40 µL) of either the premixed PBA_5-SHA_5 crosslinked polymer or PBS. On day 3, the animals were sacrificed and the vaginal tract was dissected and fixed in 10% neutral-buffered formalin solution. Tissues were embedded in paraffin, sectioned and stained with H&E for histological analysis.

3.2.12 Aminomethylcoumarin Acetate (AMCA) conjugation to PBA polymer

The polymer was synthesized with a mole ratio of 94.5:5:0.5 by free radical polymerization using HPMAm, APMAmPBA, and APMA monomers respectively. Initiator concentration and reaction conditions were the same as described previously.[163, 173] Polymers were ultracentrifuged three times using Amicon Ultra-15 10K MWCO dialysis centrifuge tubes (Millipore) at a polymer concentration of 30 mg/mL. Samples were centrifuged at 3,000 rpm for 90 mins using 100 mM pH 7.5 PBS buffer once and using DDI water twice.

To conjugate AMCA-NHS ester to the free amines[164] on the polymer synthesized above, HPMA-APMAmPBA-APMA was massed to a 100 mL round bottom flask (115.8 mg). Anhydrous DMF (11 mL) was then added to the flask and the mixture was sonicated for 30 mins at 45°C to dissolve the polymer. A

stock of DIPEA (180 µL) was made in DMF (4.82 mL). DIPEA stock (50 µL) was added to the round bottom flask. While stirring, AMCA-NHS (5.6 mg) was added to the round bottom flask. The conjugation was performed at room temperature under nitrogen for 24 h. The reaction was then concentrated at 60°C and triturated into acetone. The polymers were ultracentrifuged seven times using an Amicon Ultra 10K MWCO dialysis tube to remove any unconjugated AMCA-NHS. Progress was determined by quantifying fluorescence in the dialysate.

3.2.13 Assessment of the ability of the PBA-SHA SMP to inhibit HIV_{BaL} transport using human cervical explants and PA-GFP-HIV

To determine the extent to which fluorescently labeled HIV penetrates intact human epithelial tissue in the presence or absence of the SMP, we utilized a cervical explant system. In this system, an explant was excised from a human cervix after a hysterectomy (obtained with IRB approval- Northwestern University IRB #STU00025456). The explant was then mounted in the top chamber of a transwell dish; SMP was added on top of the epithelial explant and allowed to rest for 10 mins. DMEM containing photoactivable (PA)-GFP-Vpr labeled HIV, harvested from transiently transfected 293T cells, was added to the epithelial side of the tissue explant. PAGFP-Vpr was created by replacing the GFP with PA-GFP in a well characterized GFP-Vpr.[174] With PAGFP-Vpr, a significant green signal is only achieved after photoactivation by exposure to 400-430 nm light (Carias et.al, manuscript in preperation). After 30 mins, 1 h or 2 h, media containing the virus was removed and the explant was mounted in tissue freezing medium (OCT) and quickly frozen at –80˚C. The OCT block was then sectioned

(10-12 μm), mounted on a slide, fixed (except in the cases of unfixed tissue), and stained with propidium iodide, and was visualized in red channel, to detect nuclei.

The sections were imaged using deconvolution microscopy. First, the tissue was scanned in the green channel to define any background. Then, the tissue was photoactivated by 413 nm light. After photoactivation, the tissue was scanned in the green channel again. The appearance of any green signal was a consequence of the photoactivation, revealing the location of any virions. The tissue was then scanned to visualize AMCA-labeled polymer and PI-labeled nuclei. To rule out the unlikely possibility that photoactivatable signals were present in tissues, we also conducted a blinded analysis of tissue that had not been exposed to virus.

3.2.14 Statistical Analysis

On all rheological plots, the mean of at least three replicates is provided. The standard deviation has been omitted to maintain clarity of the plots. A 2-tailed student's t-test was used to analyze the statistical difference between the G'_{mix} and $G'_{Plateau}$. Due to the variation in sample size for the pH 7.6 mucin samples, an unpaired t-test with equal variance was used. All other statistical analysis used single-factor ANOVA with Bonferroni correction for multiple comparisons. For all the analysis, a p-value of 0.05 was used.

3.3 Results and Discussion

3.3.1 Polymer characterization

Free radical polymerization of APMAmPBA or MAAmSHA with HPMA yielded polymers (Figure 3.2) with average M_w /M_n of 194/126 KDa and 212/115 KDa for PBA_5 and SHA_5, respectively. The average mole percent incorporation of PBA and SHA in the respective polymers was determined to be 4.6% and 4.8%. The SMP was prepared by mixing equal volumes of PBA_5 and SHA_5 polymer solutions prepared in 100 mM pH 4.8 acetate buffer solution.

3.3.2 Effect of semen on the viscoelasticity of the PBA_5-SHA_5 crosslinked polymer network

When developing materials for vaginal microbicide delivery, one essential aspect that needs to be accounted for is the dilution of the semisolid gel with biofluids such as seminal fluid and cervical mucus,[153, 175] as well as the effect of sugars, ions and proteins inherently present in the vaginal milieu.[154, 167] The presence of a high concentration of sugar in semen[52] and the cervical mucus[167] could result in competitive binding between SHA and the simple and/or complex sugars present in the vaginal milieu, thereby resulting in altered viscoelastic behavior of the PBA-SHA SMP.

Seminal fluid results in an approximately three unit change in pH,[53] one fold dilution and a high fructose environment in the vaginal lumen.[53] To assess the impact of these changes on the viscoelastic properties of the SMP, time sweeps and oscillatory frequency sweeps were collected at pH 4.8 before and after addition of seminal fluid. Time sweeps assess the gelation kinetics whereas

the oscillatory frequency sweeps provide an understanding of the overall network strength as well as to characterize the lifetime of the crosslinks.

We have previously shown the pH dependent change in viscoelastic behavior of the PBA-SHA crosslinked polymer in the pH range 4.0 - 7.5.[163, 168] However these studies were performed by dissolving the polymers in buffers and adjusting the pH. Although, these results testify to the pH-responsive behavior of this SMP, they fail to assess the effect of competitive binding induced by the presence of fructose in the semen on the PBA-SHA crosslinking. The assay reported herein has been designed to recapitulate the *in vivo* situation as much as possible by using seminal fluid instead of buffer solutions. The rheological behavior, which is a bulk property of the material, is expected to be consistent with the dynamic nature of the crosslinks between the boronic acid and diols. At acidic pH, the boronic acid forms a trigonal complex with the diols, which is prone to hydrolysis and exhibits a very short half-life, shifting the equilibrium back to the uncomplexed form of the boronic acid.[163] The resulting polymer network is therefore weakly associated through reversible transient crosslinks with high rates of disassociation.[165] The dominance of G'' over G' at the majority of the frequencies is indicative of a viscous-dominant behavior with transient crosslinks between PBA and SHA. This molecular property of the crosslinks can be characterized by determining the ensemble lifetime or the relaxation time (τ) of the crosslinks. The relaxation time of the crosslinks is defined as the inverse of the crossover frequency which can be computed from the frequency dependent measure of viscous and elastic moduli.[161]

At pH 4.8 the polymer network demonstrates a characteristic relaxation time of 0.9 s and a $G'_{plateau}$ of 11 Pa. The short lifetime of the crosslinks caused by the rapid restructuring of the polymer network in conjunction with the low viscosity may facilitate enhanced flow and coating of the PBA-SHA SMP at acidic pH. In contrast, after the addition of seminal fluid, at neutral pH the equilibrium between the PBA and SHA shifts predominantly to the more stable tetrahedral conformation resulting in an elastic-dominant behavior of the material as shown by $G' > G''$ throughout the frequency sweep in Figure 3.3a. At neutral pH, the SMP demonstrate longer relaxation times (τ > 60 s) and $G'_{plateau}$ of 1800 Pa. The SMP demonstrate two orders of magnitude increase in both crosslink lifetime as well as the overall network strength indicative of increased number of crosslinks. The higher crosslinking density at neutral pH should yield a smaller mesh size, which, if small enough, will act as an impermeable barrier to the transport to free and cell-associated virions from the seminal fluid to the susceptible tissue. Moreover, owing to the higher viscosity of these materials at neutral pH, the PBA-SHA SMP is expected to provide prolonged retention in the vaginal lumen.

To assess the kinetics of increase in network strength on the addition of semen, time sweeps were collected on the SMP at pH 4.8. Less than 3 mins after the addition of seminal fluid, the elastic modulus of the crosslinked polymer increased to almost twice the $G'_{plateau}$ at pH 4.8. As seen in Figure 3.3b, a constant but steep increase in elastic modulus was observed until 30 mins after the addition of seminal fluid. Angular frequency and shear stress applied on the samples were chosen from the linear viscoelastic region

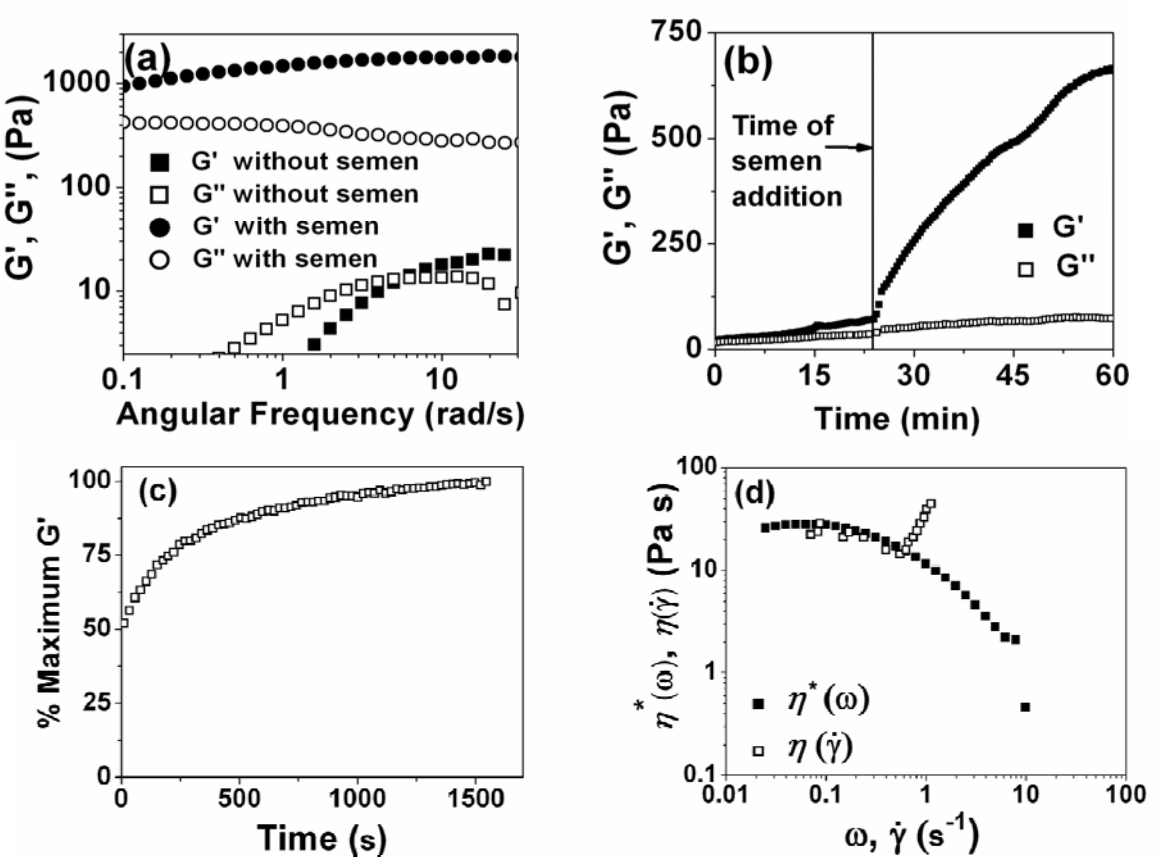

Figure 3.3 Oscillatory frequency sweeps for the assessment of the effect of semen on the network strength and relaxation time of the crosslinks**. (a and b)** Effect of semen on the network strength and relaxation time of the crosslinks at 37°C **(c)** Time dependent dynamic rheology on the SMP at 37°C for the assessment of the gelation kinetics **(d)** Oscillatory frequency sweeps comparing the and of the SMP at 37°C. N=3, Mean.

However, the shear stress experienced *in vivo* during intercourse is expected to be orders of magnitude higher than the shear stress applied in the above investigation. Therefore, the kinetics of mixing of the seminal fluid with the crosslinked polymer can be expected to be quicker merely due to increased shear forces. The novelty of the PBA-SHA SMP lies in its ability to transform from a weakly crosslinked transient network to a covalently crosslinked elastic network in response to seminal fluid as the stimulus.

3.3.3 Assessment of the PBA_5-SHA_5 gelation kinetics

Owing to the *in situ* gelation and the pH-responsive modulation of viscoelastic properties, the SMP could be administered using either a twin-screw applicator or as a premixed viscoelastic fluid. When administering the polymer solutions as a two part system, it is important to quantitatively assess the kinetics of network formation. We characterized the *in situ* gelation kinetics using dynamic rheology. After 60 s, which is the time taken to load the samples, the ratio of the elastic modulus, *G′*, to the viscous modulus, *G″*, was 2.1, suggesting that the crosslinked polymer network had already formed. At this point, the polymer network had also reached 50% of its maximum elastic modulus (Figure 3.3c). The elastic modulus reached equilibrium within 19.2 mins (1154 s) reaching a maximum *G′* of 16.8 Pa and a final ratio of *G′* to *G″* of 2.5. These results suggest that the time taken for the formation of an elastic network is on order of seconds upon mixing of the polymer solutions.

3.3.4 Comparison of simple and complex viscosity

We compared the simple and complex viscosity of the PBA-SHA SMP to evaluate the effect of steady state and dynamic stress on the flow behavior of the SMP. The majority of the current semisolid microbicide systems are formulated with weakly associating polymer networks that exhibit shear thinning behavior above 0.1 s^{-1}.[176] Shear thinning behavior has the potential to improve coverage of vaginal tissue, but may also result in leakage,[92] whereas the less common shear-thickening systems may provide enhanced retention during and after intercourse. Steady state flow viscosity $\eta(\dot{\gamma})$ was compared with complex viscosity, $\eta^*(\omega)$,

determined from dynamic oscillatory frequency sweeps. Complex viscosity displays Newtonian behavior at long time scales, as exhibited by the linear region that decreases at frequencies higher than 0.1 s^{-1} (Figure 3.3d). Acceptable superimposition of $\eta^*(\omega)$ with $\eta(\dot{\gamma})$ occurs until a critical shear rate of 0.6 s^{-1} indicating that the Cox-Merz rule is applicable only at the low shear rates. Above the critical shear, $\eta(\dot{\gamma})$ rises sharply and similar shear thickening behavior has been previously observed for materials produced from boronate-diol crosslinking chemistry. Above 1 s^{-1} the flow became unstable (Figure 3.3d), a phenomenon exhibited by poly(vinyl alcohol))-sodium borate materials,[58, 176] impeding our ability to quantitatively determine behavior at higher shear rates. However, it appears that at high shear rates the PBA-SHA SMP shear thins followed by ability to self-heal upon removal of the shear stress. Shear thickening behavior implies that an increased number of crosslinks is impacted by flow.[177] It has been hypothesized that crosslinking between diol-boronate complexes may be impacted by polymer chain orientation.[177, 178] An increase in the flow potentially allows parallel orientation of the polymer chains, which could create a favorable alignment for increasing association between polymer-bound PBA and SHA on adjacent chains. Altogether, we believe that the shear thickening behavior displayed by the PBA-SHA SMP may improve retention compared to other microbicide formulations.

3.3.5 Effect of mucin on the viscoelastic behavior of the PBA_5-SHA_5 crosslinked polymer network

PBAs are known to bind to cis-diols of sugar residues[179] found in many glycoproteins which may create a dynamic interaction between the PBA-SHA SMP and mucin that could lead to a mucoadhesive effect. Mucoadhesion of a vaginal formulation results in the capacity for long-term delivery and improved patient compliance due to noncoitally dependent application, and non-leaky formulations.[95, 165] Dynamic rheological assessment of mucoadhesion has been used extensively, partly due to its simplicity.[95] The rheological analysis of the PBA-SHA SMP in the presence of 1% (w/w) mucin does indicate that there is interaction, likely between PBA and mucin, that impacts the material's viscoelasticity properties, including the dynamic network strength measured from the $G'_{Plateau}$ and relaxation time of the PBA-SHA crosslink.

At pH 4.8 the oscillatory frequency sweep indicates not only an increase in the overall elastic modulus of the polymer network in the presence of mucin, but also an increase in τ from 0.9 s to 2.1 s. A corresponding increase in the $G'_{plateau}$ from 16.8 Pa to 47.8 Pa was observed, yielding a positive rheological synergy parameter, $\Delta G'$, of 31 Pa (Figure 3.4a&b).

The shift to longer τ in the presence of mucin points to an increased stability of the PBA-SHA crosslink, thereby increasing the number of crosslinks formed at a given time resulting in the increased $G'_{plateau}$. These results indicate that the presence of mucin results in a higher elastic modulus and increase in the lifetime of the PBA-SHA crosslink.

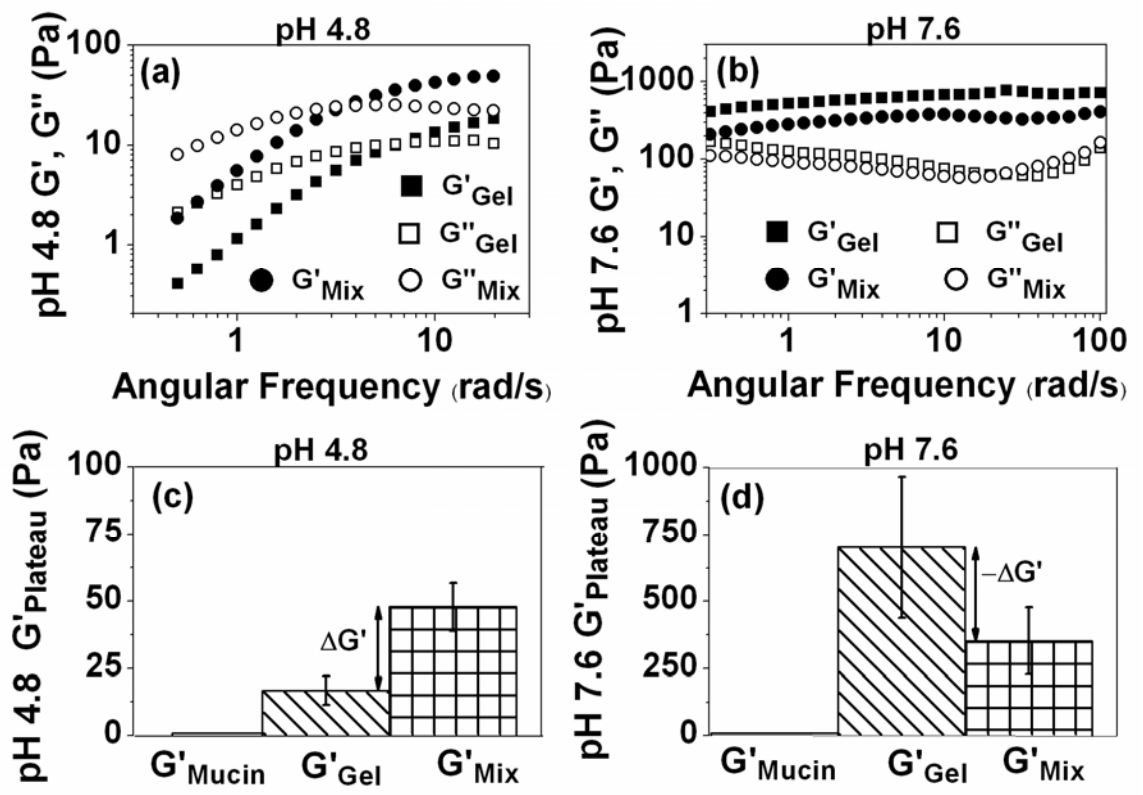

Figure 3.4 Rheological assessment of the interactions between porcine gastric mucin and PBA-SHA SMP. **(a)** Oscillatory frequency sweeps at pH 4.8 with and without mucin. N=3, Mean; **(b)** Oscillatory frequency sweep at pH 7.6 with and without mucin. N=3, Mean; **(c)** $G'_{Plateau}$ at pH 4.8 with and without mucin. N=3, Mean ± SD and **(d)** $G'_{Plateau}$ at pH 7.6 with and without mucin. Study at 37°C.

An opposite effect is observed at pH 7.6. During the oscillatory frequency sweep, both *G′* and *G″* decreased across the frequency range of 0.1-100 rad/s due to the presence of mucin. A shift in the relaxation time to a lower timescale indicates that the presence of mucin creates a more dynamic equilibrium in the PBA-SHA crosslink. We hypothesize that diols present in mucin may be binding to the PBA moieties in the crosslinked polymer, competing with the SHA moiety, resulting in weaker transient network. The overall $G'_{plateau}$ is also lower in the presence of mucin, with a negative rheological synergy, $\Delta G'$ of -349 Pa indicating

formation of a weaker network (Figure 3.4c&d). However, the $G'_{plateau}$ of the formulation at seminal pH in the presence of mucin is still an order of magnitude higher when compared to the formulation at vaginal pH. A similar observation has previously been reported for acrylic acid polymers and mucin.[170] Overall, these results indicate that the PBA-SHA SMP has the capacity to chemically interact with mucin and demonstrate mucoadhesive properties.

3.3.6 Tracking the movement of HIV virions in the PBA-SHA crosslinked polymer network

Single particle tracking using time lapse microscopy was employed for the quantification of the movement of Gag-cherry labeled HIV virions embedded in the PBA-SHA SMP as a function of pH. Rheological assessments on the PBA-SHA crosslinked polymers reveal a pH-responsive viscoelastic behavior. In turn, modulations in the viscoelastic properties and the crosslink lifetime warrant alteration in the network mesh size, and thus the mobility of HIV virions in the PBA-SHA SMP. Tracking the movement of a single particle in the polymer network is illustrative of the local microenvironment.[170, 180] Solid lines in Figure 3.5 show the MSD of the individual virions whereas the open squares show the ensemble average MSD for a given location in the polymer network. At pH 4.3 (Figure 3.5a), the linear dependence between ensemble-averaged MSD and lag time is a classic representation of particle diffusion in a viscoelastic fluid.[181] In contrast, at pH ≥ 4.8 (Figure 3.5c&d), the plateaus observed in the ensemble-averaged MSD vs. lag time is a representation of particle diffusion in an elastic solid-like network.[180]

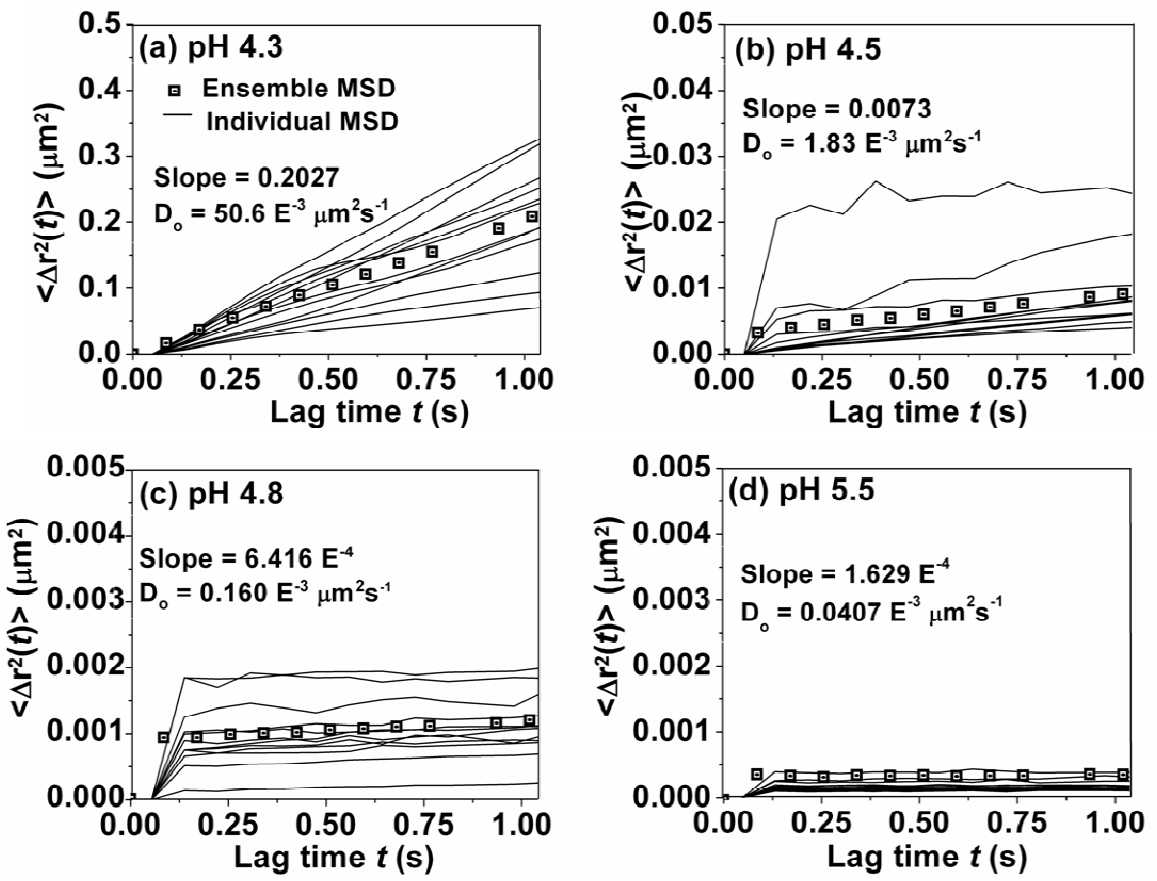

Figure 3.5 Tracking of Gag–Cherry-labeled HIV (BaL strain) movement in PBA-SHA SMP at 37°C as a function of pH. The mean square displacement was determined using IDL and the diffusion coefficients (D_o) for Gag-Cherry-labeled virions were computed as one-fourth of the slope of ensemble-average mean squared displacement versus time for five image stacks with an average of 25 virions/stack. **(a-d)** Representative plots of individual virion movement and the ensemble-average mean squared displacement of virions as a function of the lag time (t, s) at pH 4.3, 4.5, 4.8 and 5.5. No discernable movement of the virions was observed at pH above the vaginal pH (4.5-5.0), indicating that the HIV virions will likely be trapped in these materials. N=3, mean.[120]

The diffusion coefficients of the virions in the polymer network decreased by almost an order of magnitude with the increase in pH suggesting caging effects and impeded movement of virions in the polymer network. At pH 4.8 and 5.5, the plateau measured is marginally above the noise level. At pH 4.8 the diffusion coefficient of the virions in the PBA-SHA crosslinked polymer network was calculated as 0.160 x 10^{-3} $\mu m^2/s$. Based on these results, we expect the HIV virions to move as little as 5 μ before the vaginal environment reacidifies. Once the acidic pH is restored, the innate vaginal defense mechanism presents a hostile environment with the capacity to attenuate HIV infection. Altogether, the PBA-SHA SMP exhibit the ability to impede viral transport at pH > 4.8 through physical entrapment. This unique functionality qualifies the use of the PBA-SHA SMP as a drug delivery vehicle that bears the potential to act as a physical barrier to the transport of virions from semen to the susceptible immune cells in the vaginal tissue. Moreover, the ingenuity of the material to respond to changes in pH would allow the crosslinked polymer to flow and coat at vaginal pH and when in contact with seminal fluid, form a solid-like impermeable physical barrier.

3.3.7 Tracking the migration of macrophages in the PBA_5-SHA_5 SMP

The semen-borne infectious virions prevail as both free-virions as well as virions associated with T-lympocytes and macrophages in the seminal fluid.[38, 54, 181] Therefore, with the goal of attenuating the transport of both cell-free and cell-associated viruses, migration of macrophages in the PBA-SHA SMP was monitored as a function of time and dilution with vaginal fluid simulant. Universal

placebo gel[54] was used as a negative control. In the Universal placebo gel, the cells showed ~250 μ migration into the gel layer (Figure 3.6a).

On dilution of Universal placebo gel, complete migration (> 1000 μ) of macrophages was observed (Figure 3.6b). In case of the PBA-SHA SMP, no discernable movement of macrophages was observed even after 4 h of incubation (Figure 3.6c). Similarly, postdilution the PBA-SHA SMP showed negligible migration of macrophages. Note that the marginal shift in the cell layer seen in Figure 3.6d is an artifact caused by the cell suspension settling as a function of time. Migration of macrophages in the polymer can be distinguished from settling by virtue of the stepped movement of cells as seen in Figure 3.6a&b. Migration of the cells appeared slower and somewhat hindered in the undiluted Universal placebo gel; however, when subjected to dilution, complete migration of macrophages was observed at the end of 4 h. The figure on the right is a quantitative representation of the cell migration as a function of depth and time based on percent fluorescence intensity (Figure 3.6).

3.3.8 Safety evaluation using reconstructed human ectocervical tissue

The toxicity and irritation potential of materials indicated for pharmaceutical application - including those for microbicide delivery - demand meticulous safety assessments.[152, 172] More often than not, toxicological investigations probe an important but specific pathway. Hence, for an integrated realization of the toxicity potential of the formulation, a combination of assays that render complementary information was employed.

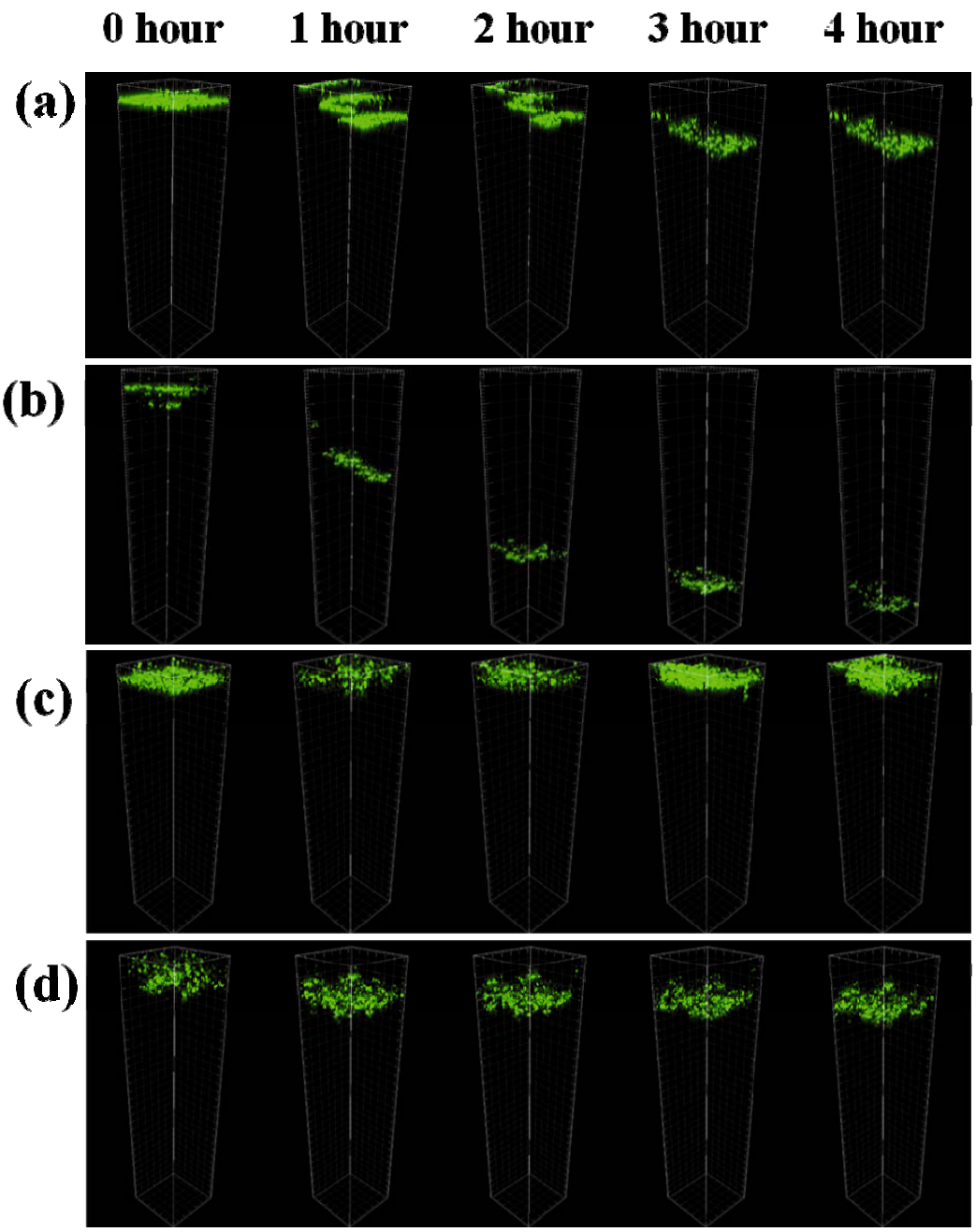

Figure 3.6 Migration of human macrophages through SMP and the Universal placebo gel. **(a & c)** Undiluted and **(b & d)** on dilution with vaginal fluid simulant (VFS) as a function of time. Macrophages were tagged with cell tracker dye and the migration of the macrophages through the polymer network was monitored by collecting z-stacks at 1 h intervals between times 0 to 4 h. Unlike the Universal placebo gel, the PBA-SHA SMP demonstrated complete inhibition of macrophage diffusion through the crosslinked polymer network, independent of dilution with VFS.

Here we report a preliminary *in vitro* toxicological evaluation using a human vaginal cell line,[75] and a detailed safety assessment using a 3D reconstructed ectocervical tissue model ,[171] an *ex vivo* polarized human cervical tissue[172] and an *in vivo* mouse model. MTT assay was performed to quantify cell proliferation and viability, while cytokine and chemokine levels were monitored to identify manifestation of inflammatory responses, Transepithelial electrical resistance (TEER) to ensure integrity of the vaginal epithelium and histological evaluations to monitor emergence of detrimental morphological changes.

From the biocompatibility studies using VEC-100, tissue viability after three repeated exposures was determined to be 98 ± 12% as compared to the naive control. The TEER measurements for the tissue samples exposed to PBA-SHA SMP were 94 ± 15, 98 ± 13 and 94 ± 8% of the no treatment control for days 1, 2 and 3, respectively, suggesting that the formulation caused no significant loss in tissue barrier properties (Figure 3.7a&b). In summary, the PBA-SHA SMP revealed no significant loss of viability or tissue integrity after three repeated doses. Triton® X-100 served as the toxic control, resulting in a near complete loss of viability as well as tissue integrity. The discrepancy in the results between the Vk2/E6E7 and the tissue viability can be attributed to differences between the robustness of the cell monolayer and the multilayer tissue. The 3D reconstructed tissue models retain the complexity and therefore, offer a reasonable representation of the morphological characteristics of the human vaginal tissue.[75]

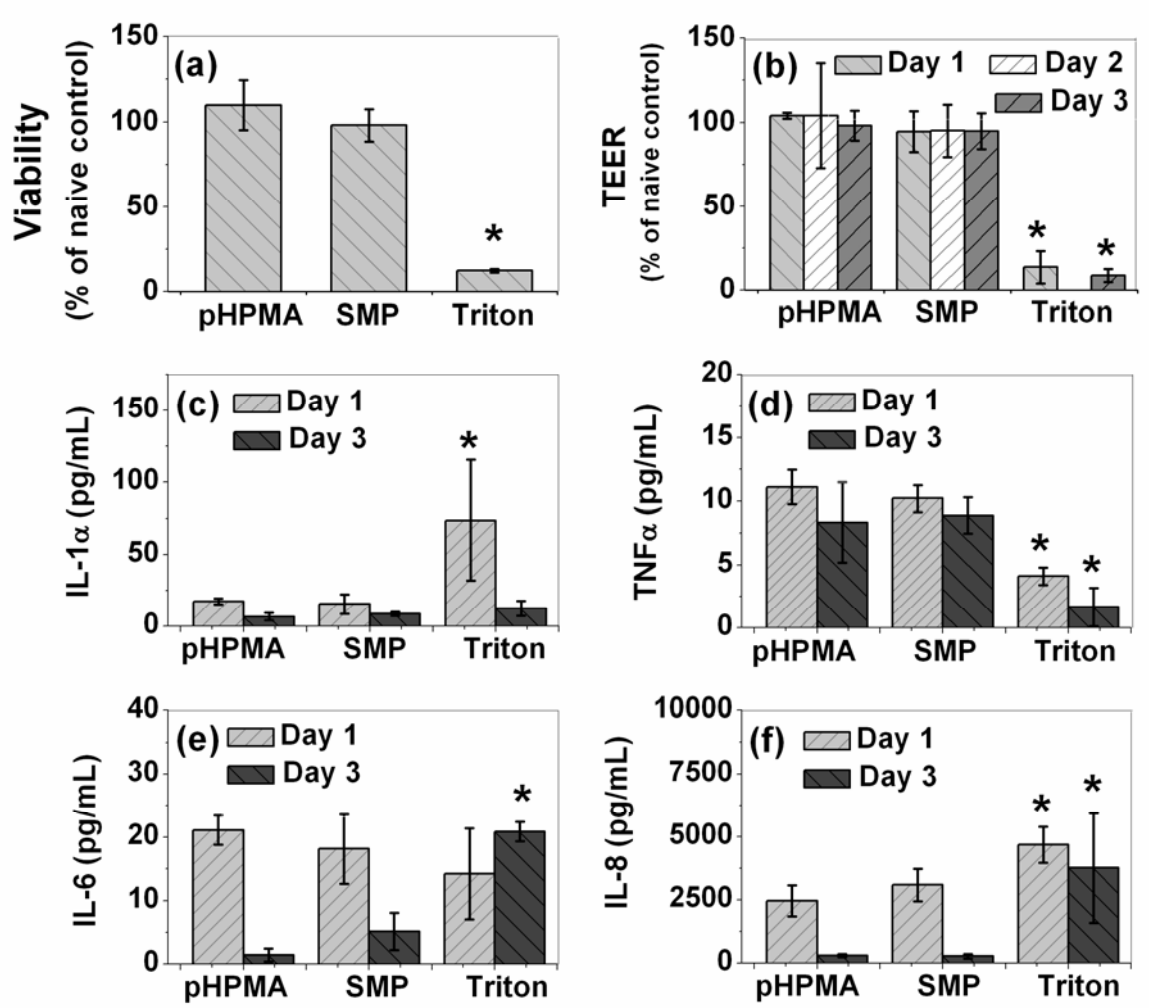

Figure 3.7 Safety evaluation of PBA-SHA SMP on reconstructed human ectocervical tissue model. pHPMA and Triton served as nontoxic and toxic controls, respectively. **(a)** Percentage viability of the tissue determined using MTT assay at the end of day 3, **(b)** TEER measurements graphed as percentage of the naïve control for days 1-3. **(c-f)** Pro-inflammatory cytokine IL-1α, TNFα, IL-6 and IL-8 release for days 1-3. Samples were compared to the nontoxic control pHPMA, for days 1-3.Tissues treated with PBA-SHA SMP showed no major symptoms of toxicity or inflammatory response when compared to pHPMA treated tissue, N=3, Mean ± SD, single-factor ANOVA followed by Bonferroni correction for multiple comparisons (* $p < 0.05$).

Moreover, the tissue model allows repeated exposure to the crosslinked polymers in contrast to the limited assessment of polymer solutions in the cell cytotoxicity evaluation. Additionally, lower toxicity of the polymers in the crosslinked state can be attributed to the fact that polymers, when examined as individual solutions, possess free functional groups in contrast to the crosslinked polymers in which the functional groups remain conjugated. This may contribute to decreased toxicity. IL-1α, IL-6 and IL-8 and TNFα were chosen as biomarkers, as they have been found to play a critical role in predicting mucosal toxicity following administration of microbicides.[172] As shown in Figure 3.7(c-f), when treated with the PBA-SHA SMP, the VEC-100 tissues showed no significant induction of cytokines or chemokines (single-factor ANOVA, $p > 0.05$) as compared to the pHPMA. Triton, used as the toxic control, triggered upregulation of IL-1α, IL-6 and IL-8, but down-regulation of TNFα. Similar results have previously been reported by other researchers.[182]

3.3.9 *Ex vivo* and *in vivo* safety assessment

Ancillary to the viability and cytokine analysis, which measure overall safety of the test product to vaginal tissue, histological examinations were employed to identify site-specific toxicity to the vaginal epithelium or the underlying submucosal tissue. Loss of basal layer and epithelial sloughing and/or necrosis was evaluated as indicators of toxicity.The viability of the tissues exposed to PBA-SHA SMP was 81±0.8%. A comparison of the histology of the tissue exposed to PBA-SHA SMP and DMEM reveal no evidence of significant morphological differences (Figure 3.8, top panel).

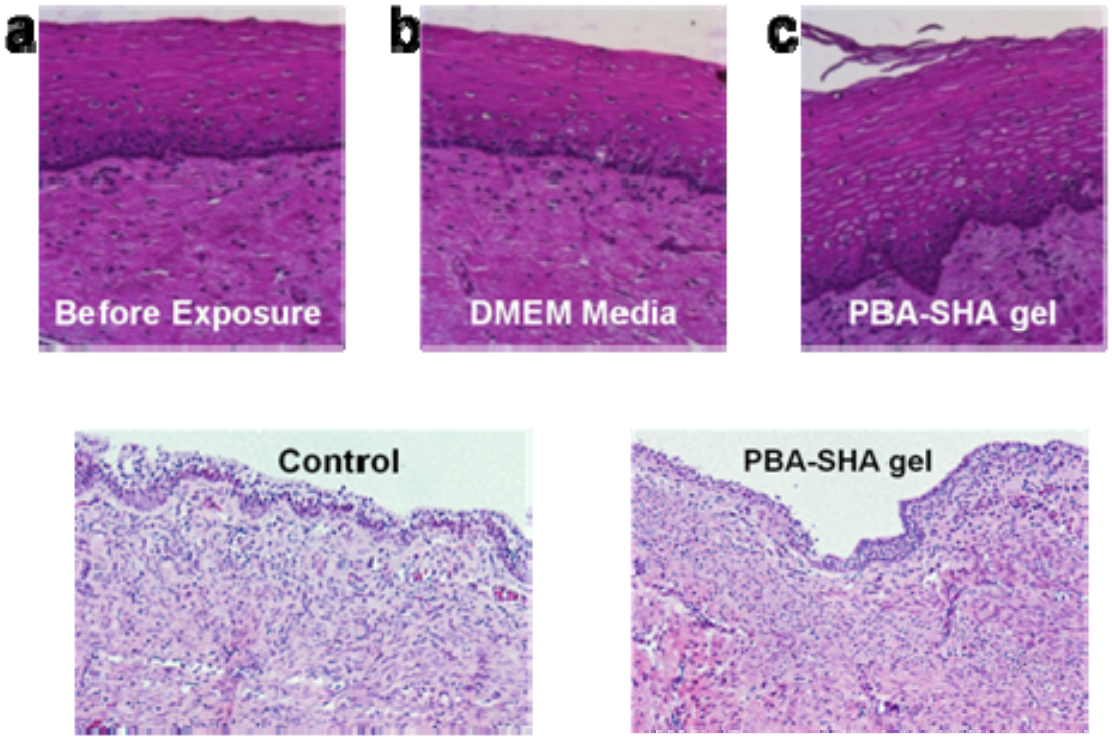

Figure 3.8 Safety of the PBA-SHA SMP evaluated *ex vivo* in the human ectocervical explants and *in vivo* using a mouse model. **Top Panel** - After overnight culture, the explants were washed and processed for histology. Image shown is representative of the three repeats. The images are 5 μ sections of the tissues; stained with Hematoxylin and Eosin. **(a)** Tissue before exposure, **(b)** tissue after 4 h of exposure to DMEM (control) and **(c)** tissue after 4 h of exposure to PBA-SHA SMP. Comparison of the histology of the tissue before and after exposure to the PBA-SHA SMP showed no evidence of significant morphological changes. **Bottom Panel** - Two groups of three animals were exposed to three repeated doses of PBA-SHA SMP or PBS (placebo arm). On day 3, the animals were sacrificed and the vaginal tract was collected, fixed and stained with Hematoxylin and Eosin. The vaginal tissues demonstrated uniform epithelium throughout with vacuolated cells in some locations. The vacuolated cell localization was found to be irregular and was observed in both the PBS and SMP treated animals. No sign of apoptosis was identified.

In conjunction to the *ex vivo* histopathological assessment, *in vivo* safety was evaluated using a mouse model. Vaginal tissues from the animal treated with PBA-SHA SMP appeared normal with intact lamina propia and submucosa. There were some locations in the mucosa from both the control and the PBA-SHA SMP groups, which showed signs of vacuolated and necrotic cells (Figure 3.8, bottom panel). However, no evidence of specific toxicity of any other type was identified.

3.3.10 Transport assay using photoactivateable-GFP-HIV

No photoactivatable signal was detected in the uninfected control tissue, demonstrating specificity of the photoactivated GFP signal for PA-GFP HIV. Without the SMP, we were able to detect HIV penetrating the first couple of cell layers of the ectocervical epithelia and penetrating the endocervical epithelia, at various depths from the mucosal surface (Figure 3.9a&b). We noticed some heterogeneity in the tissue, not just between specimens but even within a single biopsy and as a result we scanned large areas of tissue without detecting any HIV particles. The addition of the SMP to the explant perturbed viral interaction with the epithelium. A photoactivatable GFP signal was observed in the AMCA-labeled polymer, but not in the epithelium of the explants (Figure 3.9c&d). The SMP showed even spreading on the ectocervical epithelium. On the other hand, varying thickness of the SMP was observed on the endocervical epithelium. The endocervical epithelium contains mucus filled crypts which may hinder SMP-epithelium contact explaining the uneven coating properties of the SMP.

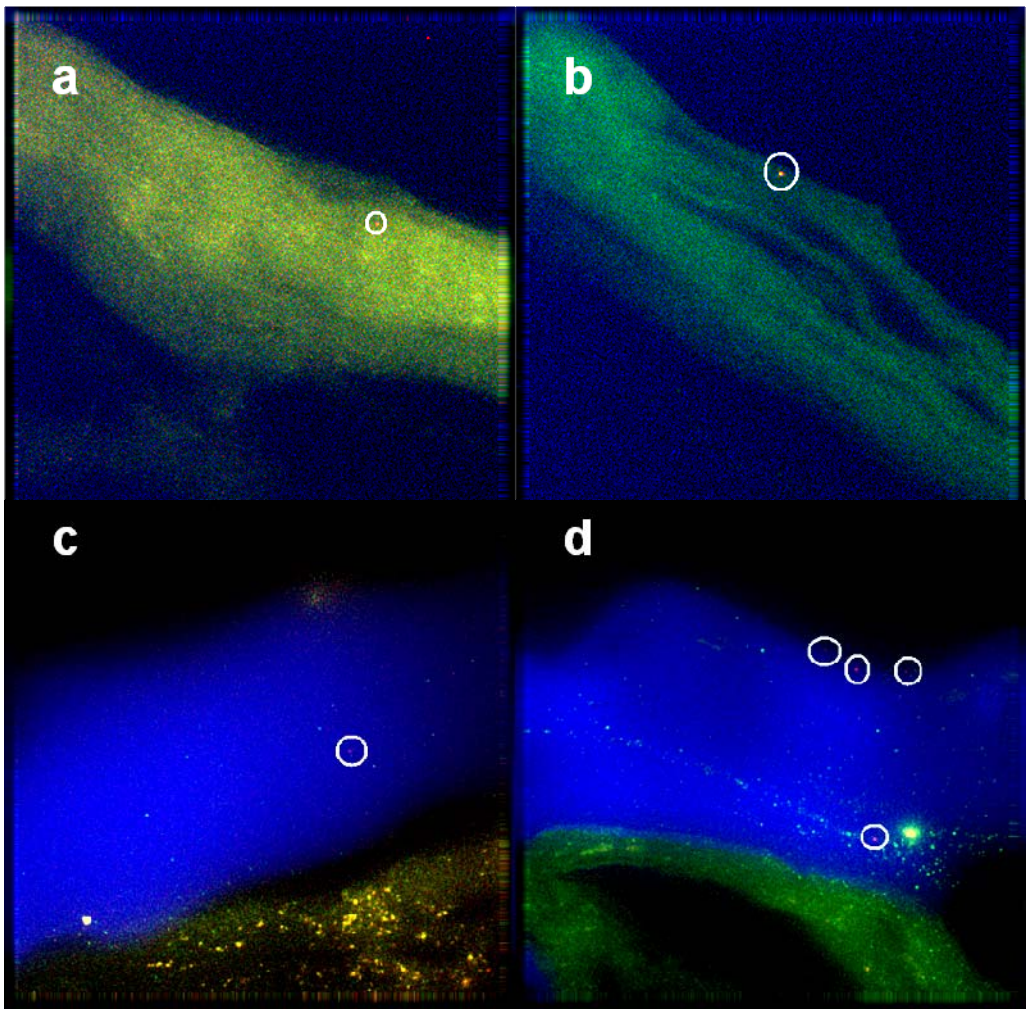

Figure 3.9 *Ex vivo* evaluation of viral transport through the PBA-SHA SMP using human cervical tissue. Cervical tissues were inoculated with 300 µL of photoactivatable-GFP labeled HIV for 4 h. **(a & b)** Z-scan prior to photo-activation for background (green) deletion, **(c)** cervical tissue after 4 h of exposure to PA-GFP-Vpr HIV (red) and photo-activation and **(d)** cervical tissue with PBA-SHA SMP (blue) after 4 h of exposure to PA-GFP-Vpr HIV (red) and photo-activation. The Z-scans reveal localization of the virions in the topmost layer of the SMP, suggesting that the polymer network poses an impermeable barrier to the transport of virions. In contrast, the Z-scan on the tissue with no SMP reveals penetration of the virions into the interstitial space within the columnar epithelium of the cervical tissue.

3.4 Conclusion

Inspired by the ability of cervical mucus to trap HIV virions at acidic pH and its role in transport processes in reproductive health, we designed a SMP that has reversible crosslinking and can impede viral transport. However, one way in which the SMP differ from cervical mucus is in regards to the sensitivity of the PBA-SHA complexation to pH, where the crosslinking density, and thereby the barrier property, increases as pH increases from vaginal pH to seminal pH. Modulation of the viscoelastic behavior of the covalently crosslinked PBA-SHA SMP in response to pH provides a semisolid hydrogel capable of being applied as a viscoelastic fluid which can interact with mucus, and thereby enhance spreading and retention in the vaginal lumen. Furthermore, driven by the change in pH caused by the presence of semen, the PBA-SHA SMP forms a crosslinked network that inhibits the transport of virions and cells. In summary, the pH-responsive PBA-SHA SMP hold promise as a biologically inspired microbicide capable of acting as a safe physical barrier to HIV transport.

3.5 Acknowledgements

The authors would like to thank Prasoona Karra and Shweta Ugaonkar for help with the cytokine analysis, Dr. Lawrence McGill for assisting in H&E analysis, Theodore Segarra for murine studies and Molli Kiser for graphic design of Figure 3.1. This work was supported by the NIH, grant number R21-AI062445 (P.K.), T32-AI060523 (S.S), R33-AI076968 (T.J.H) and grant from the Bill & Melinda Gates Foundation, Grand Challenges Explorations Initiative (P.K.).

CHAPTER 4

VAGINAL MICROBICIDE GEL FOR DELIVERY OF IQP-0528, A PYRIMIDINEDIONE ANALOG WITH DUAL MECHANISM OF ACTION AGAINST HIV[4]

4.1 Introduction

The need for prophylactic strategies to prevent heterosexual transmission of HIV was recognized more than 20 years ago.[172] Since then researchers from various fields have actively been developing technologies to combat the rapid spread of HIV. These strategies include pre-exposure prophylactics[9, 183] and microbicides[184, 185] designed to topically deliver single or combination antiviral agents. Currently, microbicide delivery systems under development include gels, rings, films and suppositories. Of these systems, vaginal gels remain the preferred choice for the first line of microbicide product development. This can be attributed to the ease of vaginal gel development, the extensive work reported in

[4]Adapted from Vaginal microbicide gel for the delivery of IQP-0528, a pyrimidinedione analog with a dual mechanism of action against HIV-1, Antimicrobial Agents and Chemotherapy, Volume 55, 2011, 1650-60, Alamelu Mahalingam, Adam P. Simmons, Shweta R. Ugaonkar, Karen Watson, Charlene S. Dezzutti, Lisa C. Rohan, Robert W. Buckheit Jr. and Patrick F. Kiser.

the literature using this dosage form and the existence of several vaginal semisolid products on the market. Microbicide administration via the vaginal route is advantageous as it allows local, noninvasive delivery of antiviral agents and enhanced biodistribution of drugs facilitated by the rich underlying blood supply.[21, 140] Furthermore, vaginal gels can be self-administered, which is critical in the development of woman-controlled preventive strategies such as vaginal microbicides.[20]

An effective prevention strategy will undoubtedly require a multi-targeted approach that can be achieved by either combining multiple antiviral agents or by employing drugs that possess multiple mechanisms of inhibiting HIV transmission.[21] Pyrimidinedione derivatives constitute a unique class of non-nucleoside reverse transcriptase inhibitors (NNRTIs) that also inhibit HIV entry through an unknown mechanism thought to target a conformational epitope formed prior to the fusion of the viral envelope with the host cellular membrane.[15] The dual mechanisms of action, high potency, minimal toxicity to vaginal cells and natural flora and broad range of activity against wild-type and drug-resistant clinical viruses make these molecules attractive candidates for microbicide development. Previous work by Buckheit et al. reported a detailed exploration of the structure-function relationship of PYD analogs. All of the PYD derivatives demonstrated inhibition of both reverse transcriptase and virus entry; however, the effective concentration for the inhibition of cell entry and reverse transcriptase varied depending on the chemical modifications to the pyrimidinedione ring.[186, 187] In this work, we report a preformulation screen of nine PYDs with reverse

transcriptase inhibition activity in the nanomolar range and therapeutic indices ≥ 10,000.[188]

This work focuses on the development of an inexpensive vaginal gel formulation for the sustained delivery of PYD using GRAS (generally regarded as safe) ingredients - polyacrylic acid (PAA) and a cellulose derivative.[97, 187, 189] In particular, hydroxyl ethyl cellulose (HEC) has been used in several vaginal gel formulations, including the universal placebo gel.[190] Chemical stability of the active compound and mechanical stability of the gel formulation was evaluated under accelerated conditions for three months. The release kinetics of the active compound from the gel matrices were assessed using *in vitro* and *ex vivo* drug release studies.

In addition to careful selection of the drug delivery vehicle and the active ingredient, a detailed exploration of the safety and efficacy of the end formulation is critical to the development of a microbicide. Particularly after the clinical failures of cellulose sulfate, N-9, Savvy and several other first-generation microbicides, *in vitro* safety and efficacy evaluations have become a major component of topical microbicide product development.[72, 152, 191] These studies offer a cost-effective method of evaluating microbicide formulations prior to more complex and expensive *in vivo* studies.[67] We evaluated the safety and efficacy of the PYD gel formulation using reconstructed VEC-100 tissue (MatTek Corp.) and human polarized ectocervical tissue. The VEC-100 tissue recapitulates only the morphological characteristics of the stratified squamous epithelial layer whereas the polarized ectocervical explants contains both the epithelium and relevant

immune cells.[75, 173, 192, 193] In an *in vitro* HIV entry inhibition assay the 3.0% HEC gel with 0.25% IQP-0528 demonstrated an EC_{50} of 0.14 µg/mL of gel in culture media, corresponding to approximately 0.001 µM IQP-0528 and showed complete protection of the human polarized ectocervical tissue against HIV infection.

4.2 Materials and Methods

4.2.1 Materials

The PYD derivatives were provided by ImQuest BioSciences, Inc. (Frederick, MD). HEC 250 HX PHARM was purchased from Ashland, Inc. (Wilmington, DE). Carbopol 974P NF was purchased from Lubrizol (Wickliffe, OH). Glycerin was supplied by Mallinckrodt Baker, Inc. (Phillipsburg, NJ). Hydrogen peroxide (ACS grade), 19-norethindrone (purity > 98%), bovine serum albumin, methylparaben and propylparaben were obtained from Sigma-Aldrich Corp. (St. Louis, MO). Acetonitrile and isopropyl alcohol (HPLC grade) were obtained from Fisher Scientific (Houston, TX). Lecithin and nonoxynol-9 (N-9) were purchased from Spectrum Chemicals (Gardena, CA). Solutol HS-15 was purchased from BASF (Florham Park, NJ). The 3-(4,5-dimethylthiazol-2-yl)-5-(3-carboxymethoxyphenyl)-2-(4-sulfophenyl)-2H-tetrazolium (MTS) kit was obtained from Promega (Madison, WI) and all cell culture media supplies were purchased from Invitrogen Corp. (Carlsbad, CA). VEC-100 tissues were purchased from MatTek Corporation (Ashland, MA).

4.2.2 Selection of lead PYD analog

We investigated the stability of nine PYD analogs to select a lead candidate for formulation development. The stability studies were conducted under various physiologically relevant conditions including pH 7.0 (neutral pH), pH 4.2 (vaginal pH)[97] and pH 4.2 with a 0.1% hydrogen peroxide solution (simulates vaginal environment). All the samples were stored at 40 °C and 75% relative humidity to evaluate the stability of the PYD analogs under accelerated conditions. Stock solutions of PYD were prepared in methanol. Dilutions were made with 100 mM phosphate buffer (pH 7.0) containing 2% Solutol HS-15 to obtain a final concentration of 30 μM. Similarly, solutions were made in pH 4.2 100 mM acetate buffer containing 2% Solutol HS-15 for the pH 4.2 conditions. Solutol HS-15 was added to the buffers to keep the compounds solubilized after dilution. Samples were collected at 0, 1, 2 and 4 weeks and analyzed using high-performance liquid chromatography (HPLC). All samples were run on a Zorbax ODS 5-μm, 4.6 × 150 mm C18 column at 37 °C with a flow rate of 1.0 mL/min. A 12 m isocratic method was run at a 65:35 water: acetonitrile ratio. PYD was detected at 267 nm. PYD quantification was performed on an Agilent 1200 Series HPLC equipped with ChemStation32 software. For each sample, the concentration of analyte was determined from a standard curve relating peak area to analyte concentration. Percentage recovery of the PYD at each time point was calculated by normalizing the recovery to time 0. Samples were run in triplicate.

4.2.3 Preparation of the gel formulation

Appropriate amounts of the gelling agent (Carbopol 0.65%, HEC 3.0 %) were added to 80% 18 MΩ distilled water and stirred for 45 mins. To increase the buffering capacity of the gel, acetate buffer (25 mM, pH 5.2) was used instead of distilled water in the preparation of the HEC gel. A paste of the active compound (0.25%) in glycerin (3.5%) was added to the solution containing the gelling agent. The preservatives methylparaben (0.15%) and propylparaben (0.05%) were weighed and mixed with preheated glycerin (1.5%) until all solids had dissolved. The paste obtained was added to the solution containing the gelling agent, with constant stirring using an overhead stirrer equipped with a paddle-shaped propeller. Lastly, the pH of the gel was adjusted to 5.2 ± 0.2 and the total weight was adjusted to 100%. All gels were allowed to equilibrate overnight and were retested for pH before use.

4.2.4 Chemical stability of the active compound in the gel formulation

Upon identification of the lead PYD molecule, the drug (at a concentration of 0.25%) was incorporated into a gel containing 3.0% HEC gel or a gel containing 0.65% Carbopol 974P. Gel formulations were evaluated for stability under accelerated conditions, which would be predictive of the long-term stability of the formulation at room temperature. Aliquots of the gel formulations were prepared in amber vials with rubber stoppers and aluminum crimps. The vials were stored at 40 °C and 75% relative humidity (RH) (Caron, Marietta, OH) and at 50 °C in a dry convection oven (Thermo Haake, Waltham, MA). Samples were

collected at 0, 1, 2, 4, 8, and 12 weeks, and IQP-0528 was extracted for quantification using HPLC.

IQP-0528 extraction was performed in the presence of an internal standard (19-norethindrone). Required amounts (100 µL) of 19-norethindrone stock in methanol were added to each vial containing the gel. The contents of the vials were transferred into 10-mL volumetric flasks and sonicated for 30 mins. Approximately 1 mL of the supernatant was filtered through a 0.2-µ PTFE filter and analyzed using HPLC. To determine the extraction efficiency of the above-mentioned method, we created controls consisting of placebo gels spiked with known amounts of IQP-0528. The extraction efficiency of the method was determined using percent recovery of the internal control and IQP-0528 from the controls. Samples and controls were run in triplicate.

4.2.5 Mechanical stability of the gel formulation

The viscosity of the gel formulations was measured using a stress-controlled AR 550 rheometer equipped with 20-mm 4° steel cone geometry. A sample of the gel (150 µL) was allowed to equilibrate for 2 mins on a Peltier plate at 37 °C, after which a steady-state shear was applied to the gel to obtain viscosity profiles. Viscosity was measured in triplicate over the range of 1-100 s^{-1} to simulate physiological conditions.[95] The mechanical stability of the gel formulations stored at 40 °C/75% RH and at 50 °C/dry atmosphere was evaluated at 0, 1, 2, 4, 8 and 12 weeks. Viscosity measured at each time point was compared to viscosity at time 0.

4.2.6 *In vitro* release study

A continuous flow in-line Franz cell was used to perform the *in vitro* release study. The gel (200 µL) was placed on the donor compartment using a positive-displacement pipette. The donor and receptor compartments were separated by a 13-mm nylon membrane (Millipore, Billerica, MA) prewetted by soaking in the receptor solution for 1 hr. Three different sink conditions were evaluated: 2% Solutol HS-15 in 100 mM acetate buffer (pH 4.2); liposomes (prepared from soy lecithin)[95] in acetate buffer (pH 4.2); and 50:50 isopropyl alcohol: phosphate buffer (pH 7.0, 100 mM). The receptor solution was circulated at a flow rate of 0.18 mL/m and collected at 2, 4, 6, 8 and 24 h for IQP-0528 content analysis using HPLC (n=5).

4.2.7 IQP-0528 uptake study

Porcine vaginal tracts were collected immediately following sacrifice, placed in Kreb's buffer and transported to the laboratory at ambient temperature within 1 hr.[194] Small sections of the tissue were dissected using surgical scissors, snap-frozen and stored at -80 °C until testing. To confirm the integrity of the porcine vaginal tissue after a single freeze-thaw cycle, permeability studies were performed with the model compound caffeine. As previously reported, results from the permeability measurements indicated no difference between fresh and frozen vaginal tissue.[195] The frozen tissue was thawed prior to use. To obtain consistent tissue thickness, the tissue samples were sliced using a Thomas-Stadie-Riggs tissue slicer. The epithelium was separated using blunt tweezers and gently pulled up to generate a final tissue thickness of approximately 500 µm

(500 ± 200 μm). A biopsy punch was used to obtain tissues with the desired cross-sectional diameter.

IQP-0528 uptake by the porcine vaginal tissue was determined using a continuous flow Franz cell. Gel (20 μL) was placed on the donor compartment using a positive-displacement pipette. Donor and receptor compartments were separated using a 6-mm biopsy of porcine vaginal tissue. Phosphate-buffered saline (PBS) was circulated continuously through the receptor compartment to keep the tissue hydrated. Tissue samples were collected after 2, 4 and 6 h and washed three times with PBS to remove any residual gel on the tissue before IQP-0528 content analysis.

4.2.8 Determination of IQP-0528 content in porcine vaginal tissue

Porcine vaginal tissue was placed in a 2-mL flat-bottom tube with locks. To create a calibration curve, 1-300 μL of a 3 mM IQP-0528 stock in methanol was added to blank tissue to create eight spiked samples of known concentrations. To precipitate proteins, 800 μL of acetonitrile and 200 μL of a 5% trichloroacetic acid (TCA) solution were added to each tube and incubated for 5 mins. Finally, the samples were homogenized using the Qiagen TissueLyser for 5 mins. Samples were centrifuged at 14,000 x g for 10 min, and the supernatant was filtered and analyzed for IQP-0528 content using HPLC. The extraction efficiency for IQP-0528 from tissue samples was determined as 92 ± 4%, with 19-norethindrone as the internal control using the method described above for extraction of the drug from gels. A calibration curve was created using the

theoretical and experimental concentrations of IQP-0528 in the tissue sample after extraction. The actual concentration of IQP-0528 in the tissue was calculated using the calibration curve. All samples were run with n=5.

4.2.9 IQP-0528 permeability studies using human ectocervical tissue

Freshly excised human ectocervical tissue was obtained from the Tissue Procurement Facility at the Magee Women's Hospital, in accordance with institutional review board (IRB) protocol number MWH-98-065. All tissue samples were from premenopausal women undergoing hysterectomy for benign conditions. The tissue was immersed in DMEM medium (Mediatech Cellgro, Fisher Scientific, Pittsburgh, PA) and used within 30 mins of retrieval. Excess stromal tissue from cervical tissue was removed using a Thomas-Sadie slicer (Thomas Scientific, Swedesboro, NJ). The thickness of the tissue was determined by placing the tissue between two premeasured histology slides and it was remeasured using calipers.

Permeability studies were conducted using Franz cells (PermeGear, Nazareth, PA). Cervical tissue was placed between the donor and receptor compartments of the apparatus. The test compound was introduced into the donor compartment of the experimental apparatus. DMEM without phenol red (Hyclone) was used as the receptor solution. Samples were obtained from the receptor compartment at the predetermined time intervals of 0, 15 mins, 30 mins and 1-6 h. The drug permeability of the formulation across the tissue and the antiviral activity of the receptor solution were examined for both the Carbopol and

HEC formulations. Receptor solutions were split; half of each solution was used for quantification of the drug by HPLC and the other half was used for bioactivity testing.

4.2.10 Drug uptake and permeability studies on VEC-100 vaginal tissue

To determine the ability of IQP-0528 to permeate and accumulate in human vaginal tissue, studies were performed on VEC-100 tissue, a stratified, well studied 3D model of human vaginal tissue. Based on the results from the *in vitro* release study and the permeability studies using human ectocervical tissue, the 3.0% HEC gel with higher IQP-0528 release was selected for the VEC-100 permeability studies. The 3.0% HEC gel was applied to the tissue samples in the inserts and cultured as recommended by the suppliers.[196] Tissue samples were washed three times with 100 µl of PBS, and Trans-Epithelial Electrical Resistance (TEER) measurements were recorded to ensure the integrity of the tissue during the study. Following washing, fresh gel was applied to the tissue. This process was repeated for 3 days to study the effect of the gel on tissue after three repeated exposures. Culture medium was collected every 24 h for 3 days for IQP-0528 quantification (n=6). Drug content in the tissue samples after 3 days was extracted and quantified using the same method as used with the porcine vaginal tissue.

4.2.11 *In vitro* safety and HIV antiviral activity

A Vk2/E6E7 human vaginal cell line and the VEC-100 tissue model were used to evaluate the safety of the IQP-0528 gel formulation *in vitro* after a single exposure and three repeated exposures. Diluted gel samples were added to the Vk2/E6E7 cells and incubated for 24 hr. After exposure, cell viability was assessed using an MTS assay. N-9 and the universal placebo gel (at a 1:100 dilution) were used as toxic and nontoxic controls, respectively.

To evaluate the safety of the formulation in the VEC-100 tissue, gel was applied to the tissue samples each day for 3 days. After three repeated exposures, tissue samples were analyzed for viability using 3-(4,5-Dimethylthiazol-2-yl)-2,5-diphenyltetrazolium bromide (MTT). Tissues were also fixed in a 10% formalin solution and processed to evaluate tissue morphology. Following paraffin embedding, sections were cut and stained with hematoxylin and eosin. Toxicity was determined based on observations of loss or damage to the epithelial layer. Culture medium collected every 24 h for 3 days was evaluated for the induction of inflammatory cytokines (IL-8, IL-1α, IL-6 and TNFα) using ELISA kits (R & D Systems, Minneapolis, MN). These cytokines were chosen as they have been reported to be consistent indicators of cumulative mucosal toxicity and inflammatory responses.[172] All samples were evaluated in triplicate except for the samples undergoing cytokine analysis, which were evaluated with six replicates (n=6). N-(2-hydroxypropyl) methacrylamide polymer (pHPMA)[182] and 1% Triton® X-100 were used as the nontoxic and toxic controls, respectively.

We also evaluated the *in vitro* antiviral activity of the 3.0% HEC formulation using a luminescence assay as described previously. The HEC placebo gel was used as a negative control and Chicago sky blue was used as a positive control. Gels were serially diluted to generate solutions that could be directly added to the cells. MAGI cells were seeded in a 96-well microtiter plate at a density of 10,000 cells/well for 24 h prior to the assay. Following the overnight incubation at 37°C in 5% CO_2, diluted test samples were added to the cells in triplicate. HIV-1_{IIIB} was diluted in the assay medium to generate the desired viral titer and was then added to the cells. Cells were incubated with the test sample for 2 h, following which the cell monolayers were washed three times and incubated for an additional 48 h. The inhibitory activity of the gels was evaluated by chemiluminescence detection with the Gal-Screen system, and toxicity was evaluated using the tetrazolium dye 2,3-bis-(2-methoxy-4-nitro-5-sulphenyl)-(2H)-tetrazolium-5-carboxanilide (XTT). We also assayed the activity of the API and the gel formulation in the presence of 25% seminal fluid.

In a separate assay, we preincubated the cells with the gel formulation for 1 h, following which the virus was added to the cells and incubated for an additional 2 h. Additionally, to evaluate the residual activity of the formulation, following the preincubation of the formulation with the cells, we washed the cell monolayer to remove the formulation. The virus was then added and incubated for 2 h. Antiviral activity was assayed after an additional 48 h of incubation by measuring β-galactosidase activity. Antiviral and toxicity results were reported as 50% effective concentration (EC_{50}) and 50% toxic concentration (TC_{50}).

4.2.12 Safety and antiviral activity in polarized ectocervical explants

Evaluations of the safety and antiviral activity of the lead formulation, IQP-0528, were performed as previously described.[75, 197] Briefly, the explant was placed in a transwell. The edges around the explant were sealed with Matrigel™ (BD Biosciences, San Jose, CA). The explants were maintained with the luminal surface at the air-liquid interface. The lamina propria was immersed in culture medium. Cultures were maintained at 37°C in a 5% CO_2 atmosphere.

For the safety evaluation, the explants were prepared in duplicate on the day of surgery. To ensure an even spread of the gels and to allow them to be mixed with HIV for the efficacy evaluation (below), a 1:5 dilution of IQP-0528 or HEC placebo gels was applied to the apical side of the explants for 18 h. Control explants were untreated or treated with an apically-applied 1:5 dilution of 2% N-9 gel (Gynol II; purchased over-the-counter). The following day, the explants were washed and safety was evaluated using an MTT [1-(4,5-dimethylthiazol-2-yl)-3,5-diphenylformazan] assay and histology methods.[75, 173]

For the evaluation of antiviral activity, a 1:5 dilution of IQP-0528 or HEC placebo gel was mixed with HIV-1_{BaL} and added to the apical side of the explants. Eighteen hours after application, the explants were washed and fresh culture medium was added to the basolateral compartment. Every 3 to 4 days over a 3 week period, supernatant was collected and stored at -80 °C for HIV-1 p24 gag analysis, and fresh culture medium was replenished. Immunohistochemistry (IHC) was performed at the study endpoint for HIV-1 infected cells by staining for p24 gag.

4.2.13 Statistical Analysis

Decreases in the drug content and viscosity of the gel were evaluated by comparison to levels at time 0 using a single-factor ANOVA followed by Bonferroni correction. Viability, TEER and cytokine levels were compared to the untreated controls using a single-factor ANOVA followed by Bonferroni correction. p-values<0.05 were considered significant.

4.3 Results

4.3.1 Selection of lead PYD analog

As shown in Figure 4.1(a & b), the majority of compounds stored at pH 4.2 and pH 7.0 and at 40°C/75% RH in the dark showed no significant degradation after four weeks when compared to their concentrations on day 0. However, recovery of IQP-0558, -0410 and -1187 was significantly reduced (single-factor ANOVA, $p < 0.05$) (Figure 4.1a) compared to day 0 concentrations. After 4 weeks at pH 4.2 in the presence of sunlight, all compounds with the exception of IQP-0532 and -0528 showed significant degradation (Figure 4.1c).

Similarly, at pH 4.2 in the presence of 0.1% H_2O_2, all compounds showed significant degradation with the exception of IQP-0528 and -0532 (Figure 4.1d). Owing to its higher therapeutic index and greater stability under all conditions tested, IQP-0528 was chosen as the lead candidate for further formulation development.

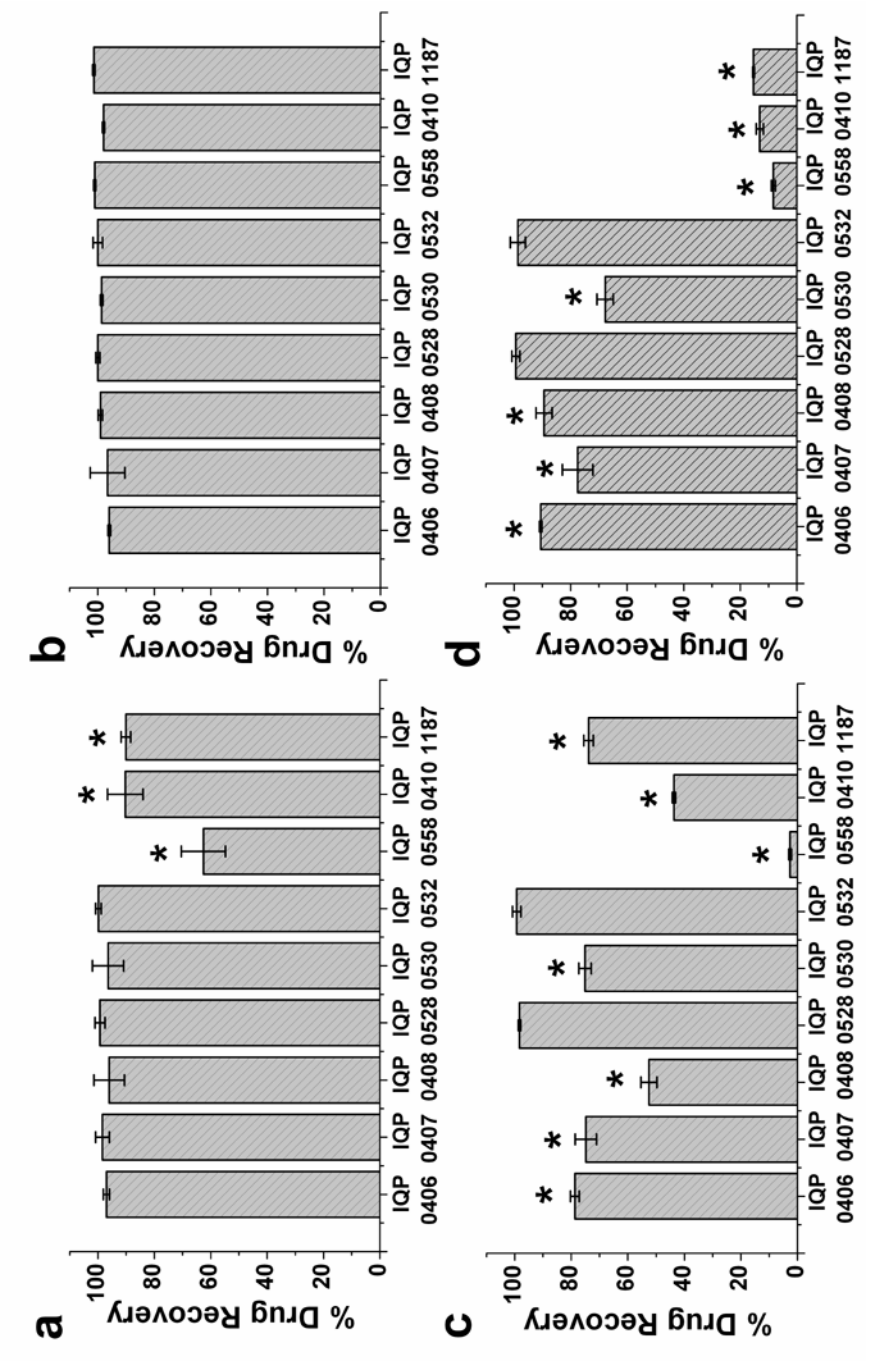

Figure 4.1 Percent recovery of nine PYD analogs after four weeks of storage. **(a)** pH 7.0, 40°C/75% relative humidity (RH), dark; **(b)** pH 4.2, 40°C/75% RH, dark; **(c)** pH 4.2, room temperature, sunlight; and **(d)** pH 4.2 with 0.1% H_2O_2, 40°C/75% RH, dark. All samples were analyzed using HPLC (n=3, Mean ± SD, *$p < 0.05$, single-factor ANOVA).

4.3.2 Chemical and mechanical stability of IQP-0528 and the gel formulation

Percent recovery of IQP-0528 at the end of 12 weeks of storage at 50 °C in the dark was 101.1 ± 4.8% in the HEC gel and 102.4 ± 4.1% in the Carbopol gel (Figure 4.2). These results indicate that there was no significant degradation of IQP-0528 in either the HEC or the Carbopol gel after 12 weeks when compared to levels on day 0 using a two-tailed Student's *t* test ($p > 0.05$). Therefore, it can be concluded that the compound's stability in the formulation was not impacted by the elevated temperature. As shown in Figure 4.3, the flow curves for IQP-0528 formulated in both HEC and Carbopol gels displayed non-Newtonian shear-thinning behavior. The rheological data on gels stored at 40°C/75% RH demonstrated no significant loss in viscosity after 12 weeks of storage.

However, HEC gels stored under accelerated conditions (50°C) showed a statistically significant loss in viscosity at 1 s^{-1} shear rate (Figure 4.3b). This loss in viscosity had no statistically significant effect on the drug release profile. Similar loss of viscosity in HEC gels have been reported previously[173] and is considered to be within the product specifications (<15% variation). Carbopol gels showed no loss in viscosity after 12 weeks under accelerated conditions (Figure 4.3d). Altogether, these results suggest that the Carbopol and HEC formulations would be mechanically stable after long-term storage.

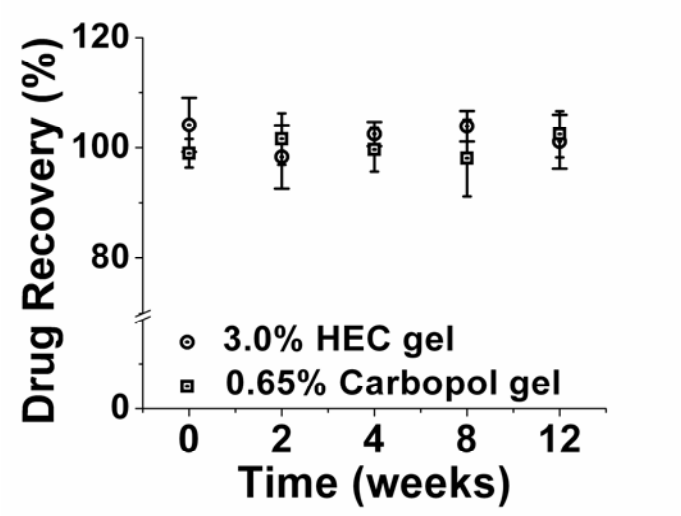

Figure 4.2 Percent IQP-0528 recovery from the 3.0% HEC and 0.65% Carbopol gels after 12 weeks of storage at 50°C (n=3, Mean ± SD).

4.3.3 *In vitro* release study

After 24 h, approximately 90%, 45% and 35% of the IQP-0528 was released in 1:1 IPA:PBS, Solutol, and liposome solutions, respectively (Figure 4.4a). A similar trend was observed with 0.65% Carbopol gels, in which approximately 70%, 24% and 20% of the IQP-0528 was released in 1:1 IPA: PBS, Solutol, and liposome solutions, respectively (data not shown). To describe the release kinetics of IQP-0528 from the gel formulations, the cumulative amount of IQP-0528 released at each time point was fitted to three mathematical models: Ficks's first and second laws of diffusion and Higuchi's equation[126, 152]. Based on the goodness of fit (r^2 > 0.90), the IQP-0528 release was fitted to Higuchi's equation. As described by Higuchi's equation, the cumulative IQP-0528 release when plotted as a function of the square root of time was linear, indicating diffusion-controlled release of IQP-0528.

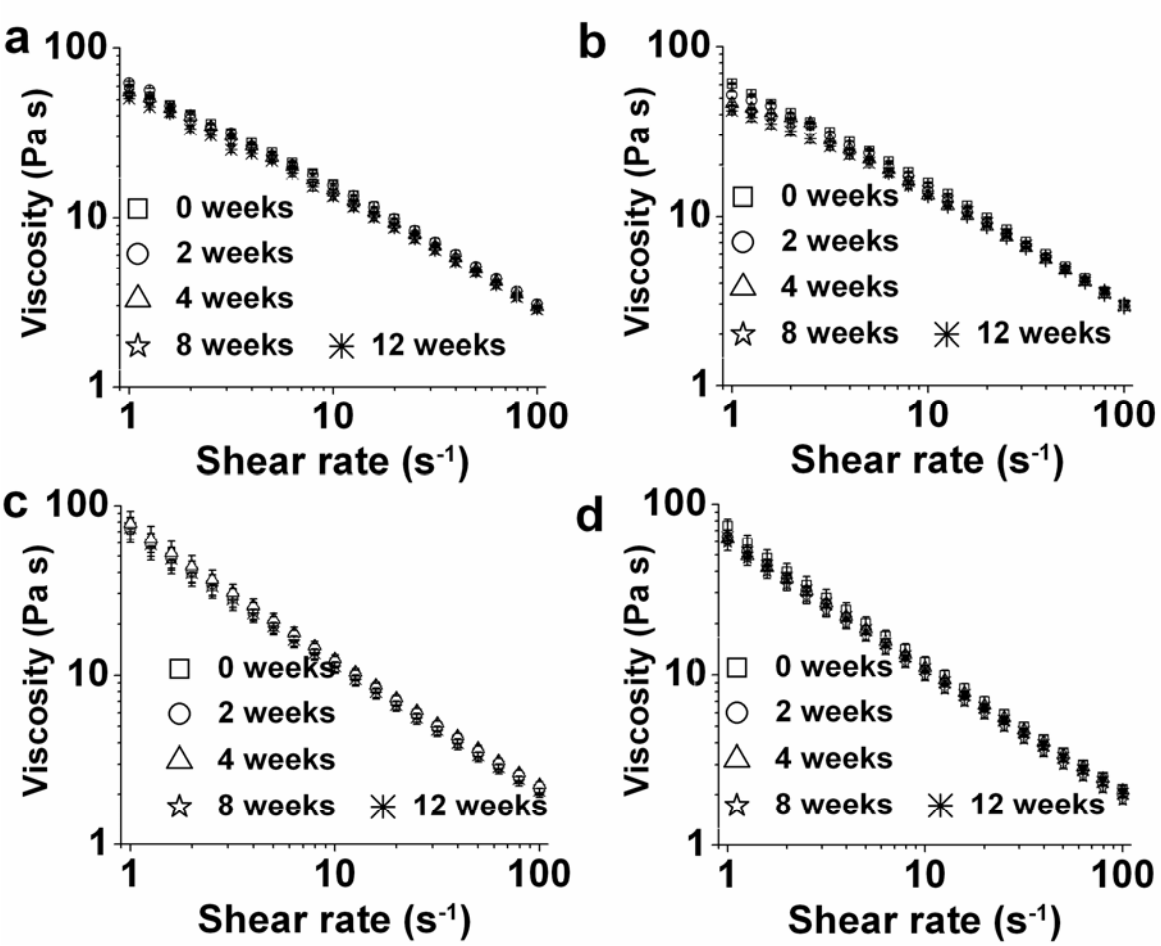

Figure 4.3 Steady-state flow curves of 3.0% HEC gel and 0.65% Carbopol gel. **(a)** 3.0% HEC gel with 0.25% IQP-0528 stored at 40°C/75% RH and **(b)** 50°C. **(c)** 0.65% Carbopol gel with 0.25% IQP-0528 stored at 40°C/75% RH and **(d)** 50°C.

4.3.4 IQP-0528 permeability and uptake studies using porcine vaginal tissue

The amount of IQP-0528 in porcine vaginal tissue samples was quantified after extraction in the presence of an internal standard using HPLC. As shown in Figure 4.4b, after 6 hr, 858 ± 78 nanomoles of IQP-0528 in the HEC gel was released for each gram of tissue, which corresponds to approximately 30% of the IQP-0528 loaded in the HEC gel.

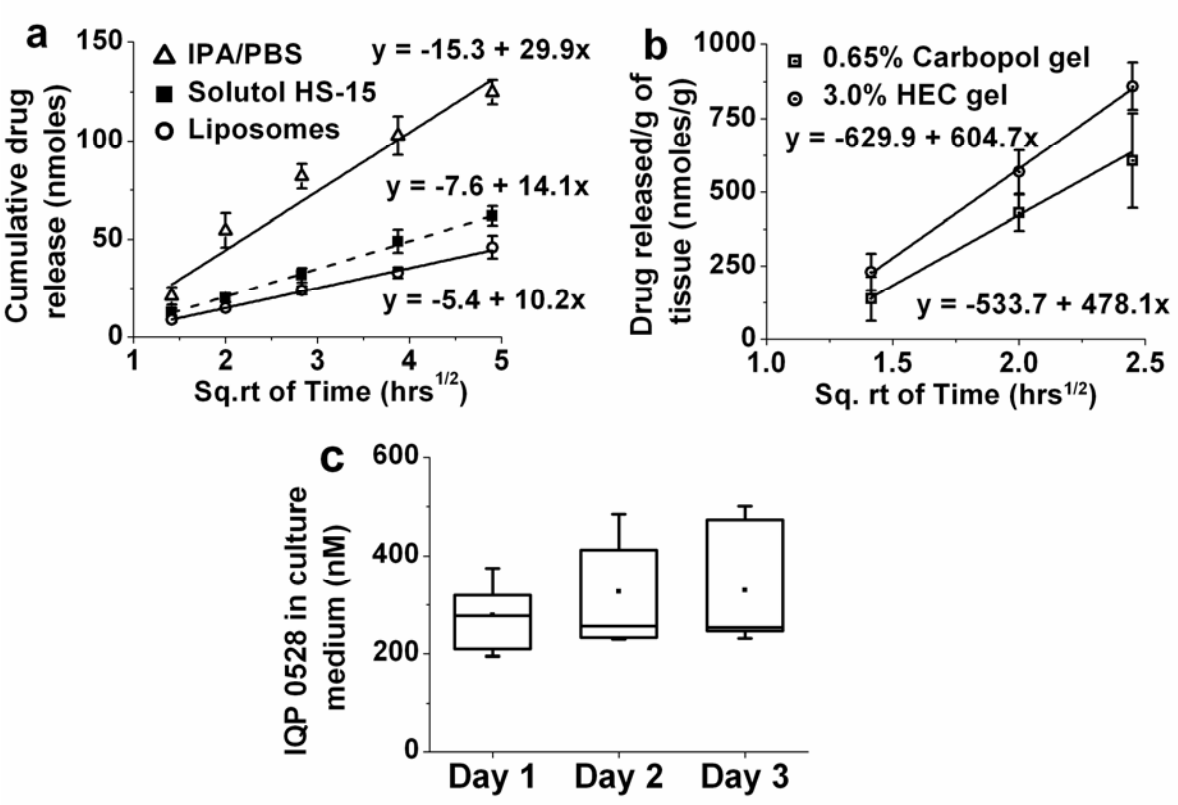

Figure 4.4 *In vitro* and *ex vivo* release studies. **(a)** *In vitro* IQP-0528 release from a 3.0% HEC gel formulation under sink conditions at 37°C (n=3, Mean ± SD). * Indicates percent drug released at the end of 24 h; **(b)** IQP-0528 uptake study using porcine vaginal tissue (n=5, Mean ± SD); **(c)** Boxplot of IQP-0528 concentration each day in the VEC-100 culture medium. (n=6).

In contrast, with the Carbopol gel, 607 ± 160 nanomoles of IQP-0528 was released per gram of tissue, corresponding to approximately 20% of the IQP-0528 loaded in the Carbopol gel. Sustained release of IQP-0528 was observed from both formulations until 6 h after administration. An initial lag time of approximately 1 h was calculated using the linear mathematical fit between the amount of drug released and the square root of time.

4.3.5 IQP-0528 permeability studies using human ectocervical tissue

In the permeability study using human ectocervical tissue, no detectable levels of IQP-0528 were found in any of the receptor compartment samples as analyzed by HPLC. However, upon bioactivity testing, the media in the receptor compartment showed viral inhibition, suggesting the presence of inhibitory concentrations of the drug at 4 h for the HEC formulation and at 6 h for the Carbopol formulation. These data correlate with the observation of increased drug release obtained using the HEC formulation in the *in vitro* and *ex vivo* release studies.

Based on the *in vitro* release results, data on accumulation in porcine vaginal tissue and the results from the permeability studies on human ectocervical tissue, the 3.0% HEC IQP-0528 gel was chosen as the lead formulation for further evaluation of toxicity and antiviral activity studies *in vitro* with cell lines and *ex vivo* with cervical tissue.

4.3.6 Drug uptake and permeability studies using VEC-100 vaginal tissue

As shown in Figure 4.4c, the concentration of IQP-0528 in growth media was measured as 278 ± 67 nM, 329 ± 123 nM and 360 ± 174 nM on day 1, 2 and 3, respectively, following exposure of vaginal tissue to IQP-0528 gel. Additionally, the IQP-0528 that accumulated in the VEC-100 tissue after 3 days was extracted and the concentration was measured as 115 ± 62 μM.

4.3.7 *In vitro* safety evaluation using Vk2/E6E7 cells and VEC-100 vaginal tissue

As shown in Figure 4.5, the IQP-0528 gel showed no significant toxicity to Vk2/E6E7 cells after 24 h of exposure when compared with the untreated control, whereas the toxic control 0.1% N-9 caused a significant (approximately 90%) loss in cell viability (single-factor ANOVA).

As shown in Figure 4.5b, tissue viability after three repeated exposure was determined to be 113 ± 8% compared to the nontoxic control pHPMA. The TEER measurements for the tissue samples exposed to the IQP-0528 3.0% HEC gel formulation were 112 ± 19%, 105 ± 25% and 109 ± 28% compared to the nontoxic control at days 1, 2 and 3, respectively, suggesting that the formulation caused no significant loss in tissue barrier properties (Figure 4.5c). As shown in Figure 4.5d, the IQP-0528 formulation-treated tissues were morphologically similar to the naïve tissue. Samples treated with Triton® X-100 (1%) showed complete disintegration of the epithelium. These results are in agreement with the TEER measurements, which showed no evidence of structural damage from exposure to the IQP-0528 gel.

Among the four cytokines that were evaluated, there were relatively high basal levels of IL-8 in naïve tissues. Similar observations have previously been reported in assays performed using the human vaginal Vk2/E6E7 cell line.[198] When compared to the basal cytokine levels detected in the VEC-100 naïve tissues, the IQP-0528 3.0% HEC gel formulation showed no significant change in IL-1α, IL-6, IL-8 or TNFα levels (Figure 4.6, single-factor ANOVA, $p > 0.05$).

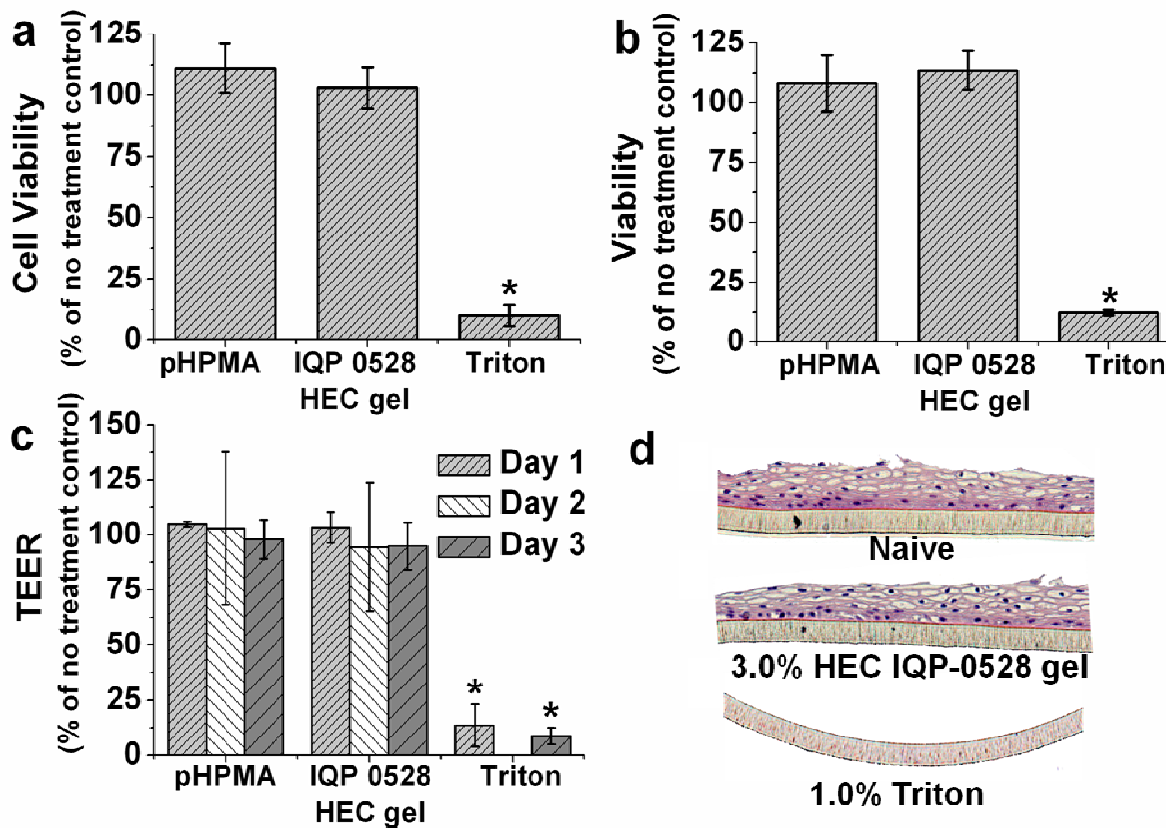

Figure 4.5 Safety of 3.0% HEC IQP-0528 formulation in Vk2/E6E7 and reconstructed human vaginal tissue. **(a)** Vk2/E6E7 cell viability measured by MTS assay after 24 h of exposure (n=5, Mean ± SD). The 3.0% HEC IQP-0528 formulation showed no significant loss in cell viability when compared to the untreated control. Universal placebo and N-9 at 0.1% were used as the nontoxic and toxic controls, respectively; **(b)** VEC-100 tissue viability determined using the MTT assay after three repeated exposures to the 3.0% HEC IQP-0528 formulation (n=3, Mean ± SD). The formulation showed no significant loss in cell viability when compared to the nontoxic control (pHPMA). Triton® X-100 (1% solution) was used as the toxic control; **(c)** TEER measurements on VEC-100 cells at days 1, 2, and 3 following treatment. No statistically significant difference was observed in the tissue samples exposed to the 3.0% HEC IQP-0528 formulation when compared to the pHPMA samples (n=3; Mean ± SD); **(d)** Hematoxylin and eosin-stained sections of VEC-100 tissue after three repeated exposures to test samples (n=3). Single-factor ANOVA followed by Bonferroni correction for multiple comparisons, *p<0.05.

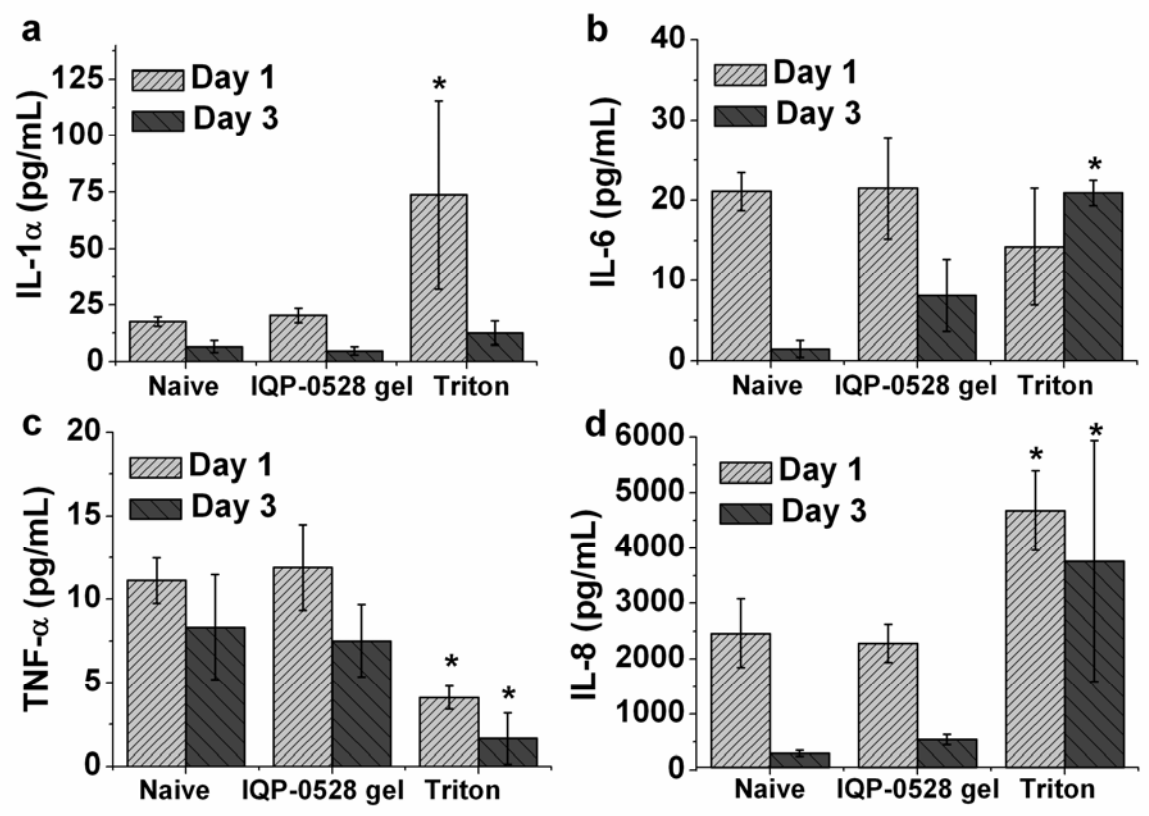

Figure 4.6 Cytokine and chemokine release after exposure to a 3.0% HEC IQP-0528 formulation. Naïve samples were used as negative controls and 1% Triton® X-100-treated samples were used as positive controls. The IQP-0528 formulation showed no significant induction of the cytokines compared to the naive control. **(a)** IL-1α, **(b)** IL-6, and **(c)** TNFα and **(d)** chemokine IL-8. The positive control 1% Triton® X-100 resulted in a significant increase in IL-1α release at day 1 and in IL-6 release on day 3 when compared to the naïve samples. (Single-factor ANOVA followed by Bonferroni correction for multiple comparisons, *$p < 0.05$, n=6, Mean ± SD).

4.3.8 *In vitro* antiviral activity

As shown in Figure 4.7, the HEC gels with IQP-0528 showed no significant toxicity to cells compared to the naïve control (single-factor ANOVA, $p > 0.05$). To evaluate the effect of the drug delivery vehicle alone, placebo gels were prepared using a composition similar to the IQP-0528 HEC gel formulation, but without the API.

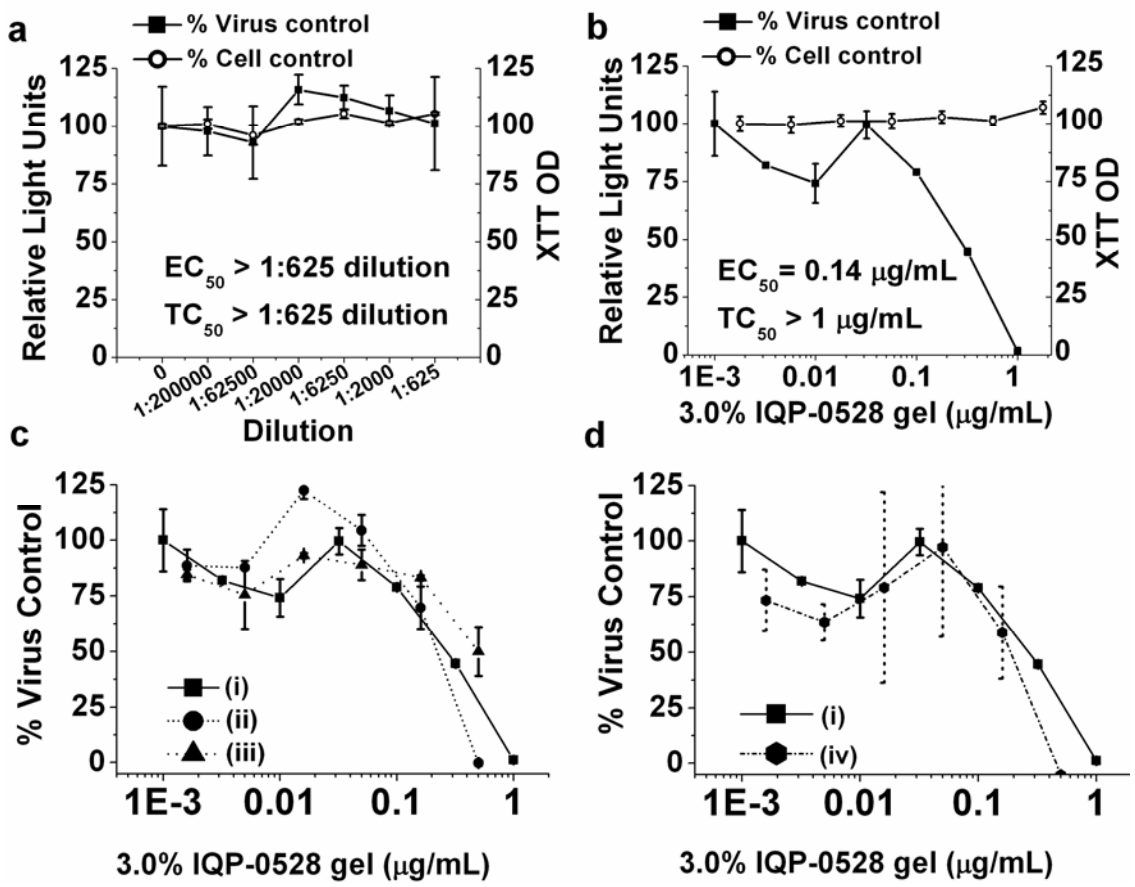

Figure 4.7 Assessment of the antiviral activity of the 3.0% HEC gel formulation. **(a)** Gel without IQP-0528 and **(b)** with 0.25% IQP-0528. **(c)** Antiviral activity of when (i) formulation was added to cells for 15 m followed by addition of virus, (ii) formulation was preincubated with cells for 1 h followed by the addition of virus, (iii) formulation was added to cells for 1 h and then removed by washing, followed by addition of virus and incubation for an additional 2 h. **(d)** Comparative antiviral activity of the formulations (iv) in the presence of 25% seminal fluid.

The placebo gels did not show any antiviral activity, as indicated by the nearly 100% relative luminescence units (RLU) (Figure 4.7a). The 3.0% HEC gel with 0.25% IQP-0528 demonstrated significantly higher antiviral activity when compared to the HEC placebo gel (Figure 4.7b). The EC_{50} for the IQP-0528 formulation was calculated using dose-response plots and was found to be 0.14 μg/mL for the gel in the culture medium, corresponding to approximately 0.001

μM IQP-0528. No significant loss in antiviral activity was observed following preincubation of the 3.0% HEC gel containing 0.25% IQP-0528 (Figure 4.7c).

In the assay designed to evaluate the residual antiviral activity of the IQP-0528 HEC gel formulation we observed a significant reduction (> 2 log scale) in the antiviral activity of IQP-0528 when administered alone. However, the IQP-0528 HEC gel showed only a marginal loss in antiviral activity. Following simultaneous exposure to 25% seminal fluid and virus, the API showed severely compromised activity, whereas the IQP-0528 gel showed no significant loss in antiviral activity (Figure 4.7d). Taken together, these results reveal enhanced activity of IQP-0528 when formulated in a 3.0% HEC gel, with nanomolar antiviral activity that was retained following preincubation, removal of the formulation and in the presence of seminal fluid. Table 4.1 summarizes the antiviral activities of the IQP-0528 (API alone), the placebo and the IQP-0528 HEC gel formulation.

4.3.9 Safety evaluation using a polarized ectocervical explant model

To confirm the results obtained with the VEC-100 tissue, human ectocervical tissue was obtained after surgery and placed in culture using a polarized system.[75, 199] The HEC IQP-0528 gel and HEC placebo gel preserved tissue viability similarly to control (untreated) explants, as measured by the MTT. The gel formulations also preserved epithelial/tissue integrity as shown by histology (Figure 4.8b). The results with human ectocervical tissue confirmed the findings obtained using the reconstructed VEC-100 tissue.

Table 4.1 Inhibitory activity of IQP-0528 and in the 3.0% HEC gel formulation

Assay conditions	Inhibition of HIV-1_{IIIB}			
	Simultaneous addition of virus and test substance		**Pre-incubation	+Test substance removed prior to virus addition
	*Without Seminal Fluid	*With 25% Seminal Fluid		
	EC_{50} (mg/mL)	EC_{50} (mg/mL)	EC_{50} (mg/mL)	EC_{50} (mg/mL)
IQP-0528 (API alone)	< 0.0001	0.05	0.05	> 0.17
IQP-0528 HEC gel formulation/ IQP-0528 when formulated$	0.14/0.0003	0.21/0.0005	0.26/0.0006	0.5/0.0012
HEC Placebo (dilution)	> 1:625	> 1:625	>1:625	> 1:625

*The test substance (API or gel formulation) was added to cells for 15 m before adding virus. Cells were incubated with virus and the test substance for 2 h. Following the incubation, the monolayer was washed and activity was assayed after an additional 48 h of incubation by measuring β-galactosidase activity.

** The test substance was preincubated with cells for 1 h before adding virus.

+ The test substance was added to cells for 1 h and then removed by washing. Virus was added and incubated for 2 h.

$$EC_{50}$ for IQP-0528 was back-calculated from the EC_{50} for the complete gel formulation, which consists of 0.25% IQP-0528 with the assumption that the drug was homogenously dispersed in the polymer matrix.

4.3.10 Antiviral activity using a polarized ectocervical explant model

The efficacy of the HEC IQP-0528 gel was evaluated by mixing a 1:5 dilution of the formulation with HIV-1_{BaL} and applying this mixture to the apical surface of the polarized explants. After an overnight exposure, the explants were washed and the cultures were observed for 21 days. Unformulated IQP-0528 did not confer any protection in the polarized ectocervical tissue model. Unformulated IQP-0528 did not confer any protection in the polarized ectocervical tissue model.

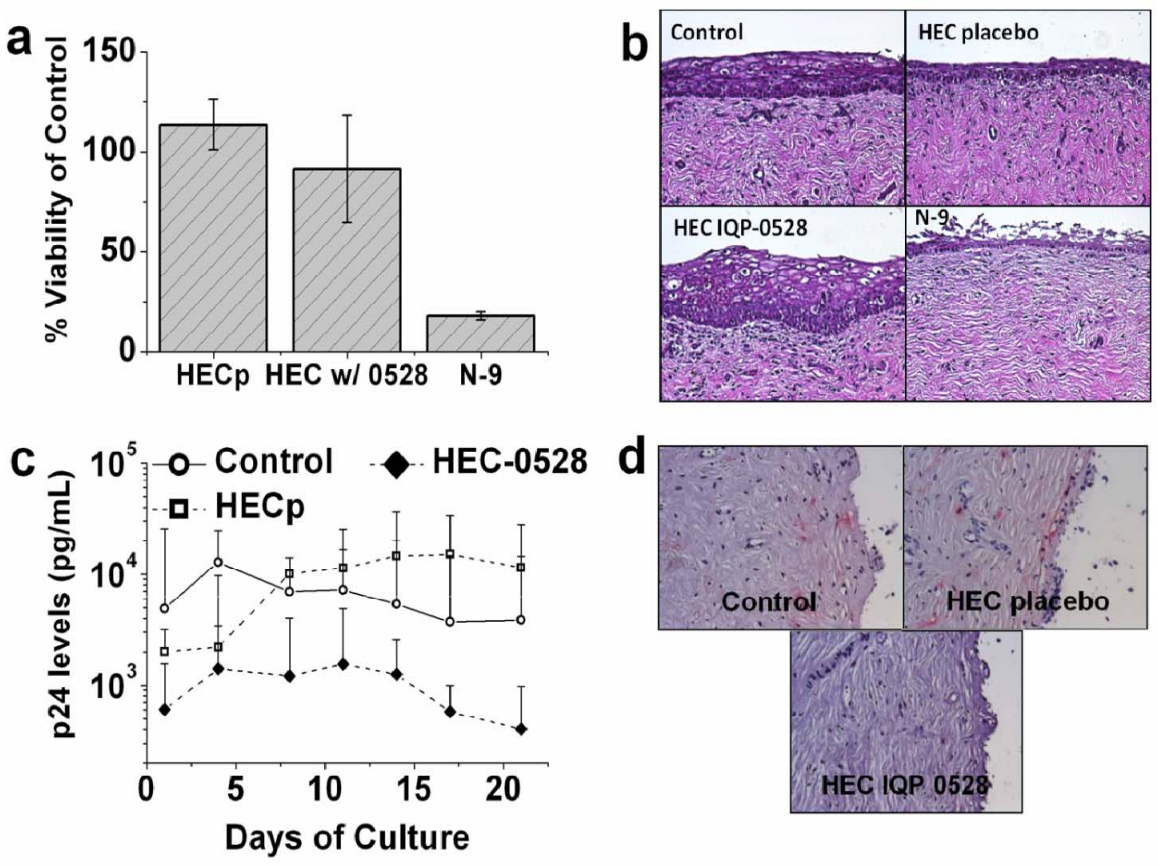

Figure 4.8 Evaluation of the safety and efficacy of the 3.0% HEC gel using ectocervical explant cultures. **(a)** The safety of the gels was evaluated in duplicate in polarized explants treated with the gels or in untreated controls. After overnight culture, the explants were washed and one of the duplicates was processed for the MTT assay and the other was processed for histology. The MTT assay data are based on three independent tissue samples and the **(b)** histology image is representative of one of those samples. Tissues were harvested after overnight exposure to the gel. **(c)** To evaluate the effectiveness of the gel, polarized ectocervical explants were treated with the gels along with HIV-1. After overnight culture, the explants were washed and then observed for 21 days. Culture medium on the basolateral side was harvested to test for viral replication by p24 gag ELISA. The HEC gel with IQP-0528 showed a significant decrease in p24 levels when compared to the placebo gel and the untreated control, **(d)** Tissues were exposed to the formulation overnight, followed by washing and 21 days of incubation. After incubation, the tissues were stained using p24 monoclonal antibody. Representative tissue samples are shown. The red cells in the untreated control and the tissues treated with placebo gels indicate p24-positive cells, reflecting the presence of HIV-1 infected cells. No HIV infected cells were found in the 3.0% HEC IQP-0528 formulation-treated tissue samples (n=3).

However, when formulated in a 3.0 % HEC gel, IQP-0528 conferred protection against HIV-1 infection as indicated by a greater than 1 log reduction in HIV-1 p24 antigen levels by day 21 (Figure 4.8c). This significant reduction in HIV-1 p24 ($p<0.05$, single-factor ANOVA) following treatment with the gel formulation emphasizes the role of adequate formulation in enhancing the efficacy of water-insoluble and poorly permeable active pharmaceutical ingredients. The absence of HIV-1 infection in these samples was confirmed by endpoint immunohistochemistry (IHC) of the explants; the control and HEC placebo-treated explants harbored HIV-1 infected cells, whereas no infected cells were detected in the HEC IQP-0528 treated explants (Figure 4.8d).

4.4 Discussion

The field of rectal and vaginal microbicides is a new therapeutic area with several candidates in clinical trials and no registered products. Many of these candidates, with the exception of a 1% Tenofovir gel evaluated in the recent CAPRISA 004 trial, have failed to demonstrate safety or efficacy.[173] Despite these setbacks, the field is still progressing rapidly due to the pressing need for prophylactic technologies and the advantages of a vaginal route of delivery for antiretroviral drugs.[55, 66] Typically, drugs delivered through the vaginal route encounter an acidic environment with pH ranging from 4.0 – 5.0.[21, 67] However, soon after intercourse, the vaginal pH increases to a neutral pH due to the introduction of semen. The vaginal environment also hosts several *Lactobacillus* strains that constantly generate lactic acid and hydrogen peroxide, maintaining an acidic pH in the vaginal cavity.[20, 21] Therefore, successful development of a

vaginal microbicide product requires an active ingredient that can withstand both neutral and acidic pH in the presence of hydrogen peroxide. For this reason, we chose to evaluate the stability of our drug candidates at pH 4.2, pH 4.2 with 0.1% H_2O_2 and pH 7.0. Results from our stability study on the nine active PYD congeners suggested that substitutions at the N-1 site play a critical role in determining the stability of the compounds in solution. Cyclopropyl (IQP-0406, -0407, -0408, -0528) and cyclobutyl (IQP-0530, -0532) substitutions demonstrated better stability compared to the 1- or 3-cyclopenten-1-yl substitutions (IQP-0558, -0410, -1187) at the N-1 site. Furthermore, isopropyl substitutions in the heterocyclic ring (IQP-0528, -1187) resulted in compounds with greater stability compared to drugs with ethyl substitutions (IQP-0408, -0410). As seen in Figure 4.1, the most potent PYD congeners failed to show the desired stability profile and thus were eliminated from consideration for formulation development. The combination of the antiviral activity, the therapeutic index, and, most importantly, the stability of the molecules under the physiologically relevant conditions tested (shown in Figure 4.1) made IQP-0528 a promising candidate to be explored further down the formulation development pipeline.

In addition to the stability and activity of the antiviral agent, the effectiveness of a vaginally-applied microbicide gel also depends on the ability of the gel to coat the vaginal epithelium and be retained at the target site for the desired duration of action.[95] Formulations with high viscosity and yield stress would most likely result in gels that provide poor coating and, consequently, suboptimal release of the active ingredient, since flux is proportional to contact

surface area. On the other hand, low-viscosity gels often lead to excessive coating and leakage, resulting in poor user compliance and partial dose delivery. We have previously optimized semisolid vaginal gel compositions based on a detailed exploration of the composition, properties, and performance of vaginal gels.[95] Our results indicated the 3.0% HEC gel, followed by the 0.65% Carbopol gel, as the near-ideal microbicide gel candidates at a 3.5 mL volume of administration because of their spreadability and coating properties.[200]

To design a sustained-release formulation for vaginal microbicide delivery, a thorough understanding of the vaginal anatomy and the barrier properties of the vaginal epithelium is imperative.[201] Transport across the vaginal epithelium is largely driven by diffusion, which is governed by the physicochemical properties of the active ingredient and the barrier through which the drug diffuses. The drug entrapped in the gel network diffuses to the boundary layer and partitions into the lipid and protein domains of the vaginal epithelium. The drug diffuses through the lipid and protein domains to repartition into the microcirculation provided by the local capillary network, which offers an infinite sink. This repeated diffusion-partition process drives the diffusion of the drug into and out of the vaginal tissue.[202] The rate at which each of these steps occurs depends on several factors such as the partition coefficient (Log P), solubility (melting point), polarity (hydrogen bond-forming functional groups), degree of ionization (pK_a/pK_b) and molecular weight of the drug. IQP-0528 has a molecular weight of 340.42 g/mole and is practically insoluble in water, with a cLog P = 4.1. Of all these factors, the one with perhaps the greatest influence on drug transport is the ability of the drug

to partition into host tissues.[201] Typically, drugs with log P values in the range of 2-3 show optimal permeability across the stratum cornea (SC), as well as moderate partitioning out of the SC. On the contrary, drugs with log P > 3 are expected to exhibit high partitioning into the SC but poor partitioning into the systemic circulation.[20] It is known that lipophilic compounds have higher tissue residence times and therefore lower systemic exposure.[203] The lipophilicity of IQP-0528 could similarly limit its systemic exposure when administered vaginally, and therefore could be advantageous for a prophylactic antiretroviral strategy where there is concern over generating resistant viral mutants in infected individuals exposed to the gel.[204]

In vitro release studies are an important precursor to *ex vivo* or *in vivo* studies as they permit the determination of release kinetics and serve to evaluate the mechanism of drug release.[77] *In vitro* release studies on gels typically employ synthetic membranes chosen to provide minimal resistance to drug diffusion.[198] Flux in the three sink solutions in our study varied dramatically. We believe that the high flux in 1:1 IPA:PBS solution can be attributed to the observation that IPA causes the polymer in the gel to swell, resulting in rapid depletion of drug from the polymer matrix. Ideally, release studies should be conducted under sink conditions that do not interfere with or swell the release matrix;[198] therefore, liposomes and Solutol offered suitable sink conditions.

Porcine vaginal tissue is a convenient alternative to human vaginal tissue[198, 201] since human vaginal tissue is difficult to obtain in sufficient quantities to conduct drug transport studies with multiple replicates. There is significant

similarity between the architecture of human and porcine vaginal tissue and for studies investigating drug-release kinetics excised porcine tissues have provided good correlation with human tissue studies. This is because the permeability of the SC has been shown to be unaltered in an nonviable tissue sample after removal from the body.[192] IQP-0528 could not be detected in the receptor fluid from the *ex vivo* release studies using HPLC. However, the receptor fluid showed complete inhibition of viral replication and therefore inhibitory concentrations of drug. The concentration of IQP-0528 permeated across the tissue was estimated by comparing the extent of viral inhibition by the receptor fluid with a standard viral inhibition curve for IQP-0528. Using the above method for the HEC formulation, we estimate approximately 0.005 μM and 0.01 μM IQP-0528 to have permeated the ectocervical tissue after 4 h and 6 h, respectively. For the Carbopol formulation, we estimate approximately 0.003 μM IQP-0528 to have permeated the ectocervical tissue after 6 h. Following comparison of the drug release profiles of IQP-0528 from the HEC and the Carbopol gels, we observed that the HEC gel demonstrated a shorter lag time (4 h) and greater permeation across the tissue. However, for the IQP-0528 HEC formulation, the lag time, which is the time needed to attain inhibitory concentrations of drug in the basal compartment, was eight times longer than that of the 1% Tenofovir gel (lag time < 30 min). This delay can be attributed to the low permeability of IQP-0528.

Thorough investigation of the toxicity and irritation potential of microbicide formulations is critical, as in the past some microbicides that have caused irritation to genital tissue also led to higher infection rates in women when

compared to placebos.[172, 201] VEC-100 tissue treated with an IQP-0528 HEC gel formulation showed no significant induction of cytokines or chemokines (single-factor ANOVA, $p > 0.05$), suggesting absence of any significant inflammatory response. Triton®X-100 (1% solution), which was used as the toxic control, induced a significant increase in the release of IL-1α, IL-6 and IL-8 and a decrease in the levels of TNFα (Figure 4.6). Similar results have been reported previously.[72] To further support these *in vitro* results, we evaluated the safety and efficacy of the 3.0% HEC gel on ectocervical tissue explants. The 3.0% HEC gel was chosen over the 0.65% Carbopol gel as the lead formulation based on our previous study that optimized gels based on their coating and retention properties[172] and higher release of IQP-0528 from the HEC gel.

Tissues exposed to the IQP-0528 HEC formulation showed no significant loss in viability or change in tissue morphology. A similar study evaluating the safety of a 1% Tenofovir gel showed an initial loss in TEER of the tissue, likely due to the hyperosmolarity of the formulation (approximately 3000 mOsm). The formulation developed in our study was designed to have an osmolarity of < 1000 mOsm (~850 mOsm). As a result, although the composition of the 3.0% HEC IQP-0528 gel was similar to that of the Tenofovir gel, the IQP-0528 formulation showed no signs of loss in tissue viability or barrier functions after 4 h of exposure. We have observed that IQP-0528, when unformulated, does not show any protection in a polarized ectocervical tissue model. However, when formulated in a semisolid gel formulation as described in this work, IQP-0528 showed complete protection of the tissue against HIV-1 infection. This

emphasizes the role of formulation in enhancing the efficacy of APIs with poor aqueous solubility and low tissue permeability. The formulation developed in this work is composed of GRAS polymers HEC and Carbopol for the delivery of IQP-0528. These polymers are acceptable drug delivery vehicles, because of their cost-effectiveness, bioadhesivity and biocompatibility. The estimated cost of a single dose of this gel is 30 cents/dose, similar to the 1% Tenofovir gel (M. Schoofs and P. Wonacott, presented at the 18th International AIDS Conference (IAC), Vienna, Austria, 18 to 23 July 2010). Based on our *in vitro* and *ex vivo* evaluations, we conclude that our gels provide diffusion-controlled release of the active ingredient. Additionally, this formulation is expected to provide complete protection against infection with no significant toxicity or irritation to vaginal tissue. The findings of the present study indicate that the formulation developed in this work provides a simple, inexpensive, stable and efficacious microbicide gel for the prevention of heterosexual transmission of HIV-1.

4.5 Acknowledgments

We thank Prasoona Karra at the University of Utah, Salt Lake City, UT for assistance with the cytokine analysis. We also thank Nicole Billitto, who performed the ectocervical explant work, and Marilyn Cost, who performed the explant histology at Magee-Womens Research Institute, Pittsburgh, PA. This work was supported by SBIR grant number 2-R44-AI067047-02 and NIH grant number 5U19AI077289-03.

CHAPTER 5

ACTIVITY AND SAFETY OF SYNTHETIC LECTIN - BENZOBOROXOLE FUNCTIONALIZED POLYMERS FOR INHIBITION OF HIV-1 ENTRY[5]

5.1 Introduction

From a therapeutic perspective, each step in the HIV lifecycle provides an opportunity for pharmaceutical intervention. Amongst the initial steps in HIV infection is the binding event that occurs between the gp120 receptor on the viral envelope and surface proteins on the target cell. The HIV envelope is among the most heavily glycosylated proteins known to mankind.[205, 206] The gp120 of HIV_{IIIB} has 24 potential N-linked glycosylation sites, of which 13 sites contain complex-type oligosaccharides, and the remaining 11 sites contain hybrid and/or high mannose-type structures.[207, 208] Reports on the antiviral activity of lectin-based

[5]Adapted from Activity and Safety of Synthetic Lectin Based on Benzoboroxole Functionalized Polymers for Inhibition of HIV-1 Entry, Molecular Pharmaceutics (in press), Alamelu Mahalingam, Anthony R. Geonnotti, Jan Balzarini, Patrick F. Kiser.

entry inhibitors suggest that targeting the oligomannose regions of gp120 can potentially produce broad spectrum entry inhibitors capable of inactivating HIV independent of tropism and strains. Prolonged exposure of these agents to virus-infected cells causes deglycosylations on the viral envelope, creating virions that are highly susceptible to neutralization by immunogenic responses. Such mutated virions also lack resistance to other small molecule entry inhibitors.[209-212] Therefore, lectin-based gp120 targeted entry inhibitors represent an interesting class of antiretroviral agents that potenatially can inactivate HIV in the vaginal lumen even before they reach susceptible CD4+ cells, preventing male-to-female heterosexual HIV transmission.[211, 213]

All the entry inhibitors - with the exception of Maraviroc[214] and Fuzeon[215] - that have been tested in clinical trials have failed, most likely due to nonspecific interactions with the cell surface and/or suboptimal efficacy.[216-218] Consequently, there are a limited number of clinical candidates that target HIV entry in comparison to agents that target the enzymatic machinery involved in the viral replication.[219] Carbohydrate binding proteins (CBP), such as the nonhuman naturally occurring lectin protein (MBL),[220] cyanovirin-N (CV-N)[221] and griffithsin[222] that bind to the high-mannose oligosaccharides found on gp120, demonstrate the ability to inhibit HIV infection *in vitro* and *ex vivo*, irrespective of the cell type, or the coreceptor tropism of the viral strain.[223] However, the unacceptably high cost of large scale production and purification of these protein-based lectins, added to their low-stability and plausible immunogenic response,[224] may limit their use as a microbicide.[225]

Polyvalency - a mechanism capitalized by CBPs - pertains to simultaneous interactions between multiple-linked ligands and receptors with repeating epitopes, such as those found on the HIV envelope.[226] Due to translational entropic advantage[227] and steric stabilization, polyvalent interactions may enhance binding affinity of weak ligands.[226, 228] Inspired by nature's adaptation to harness polyvalent interactions as a mechanism to enhance weak binding affinity between ligand-receptor pairs,[226] we aimed to develop a synthetic polyvalent inhibitor of the HIV entry by targeting the high-density glycosylation sites on the viral envelope (Figure 5.1A&B).

Phenylboronic acids (PBA) form reversible covalent complexes with cis-diols - a common chemical entity found on glycoproteins - e.g., mannose, galactose, N-acetylneuraminic acid, and fucose residues.[229] The presence of end standing multiple mannose residues on each of the hybrid and/or complex-type N-linked glycans of gp120 suggests multiple binding sites for PBA-containing ligands. While PBA-containing polymers have demonstrated the ability to bind to glycosylated proteins, interactions of boronic acids with glycans have yet not been exploited as a mechanism to attenuate HIV entry. This is because the PBA and cis-diol form hydrolytically stable complexes only when the boronic acid exists in its tetrahedral form, mostly prevalent at a pH value greater than the pKa of PBA.[230] PBA without any substitutions on the aromatic ring have a pKa of 8.8 and therefore, is found to bind strongly to diols only at alkaline pH's.[231]

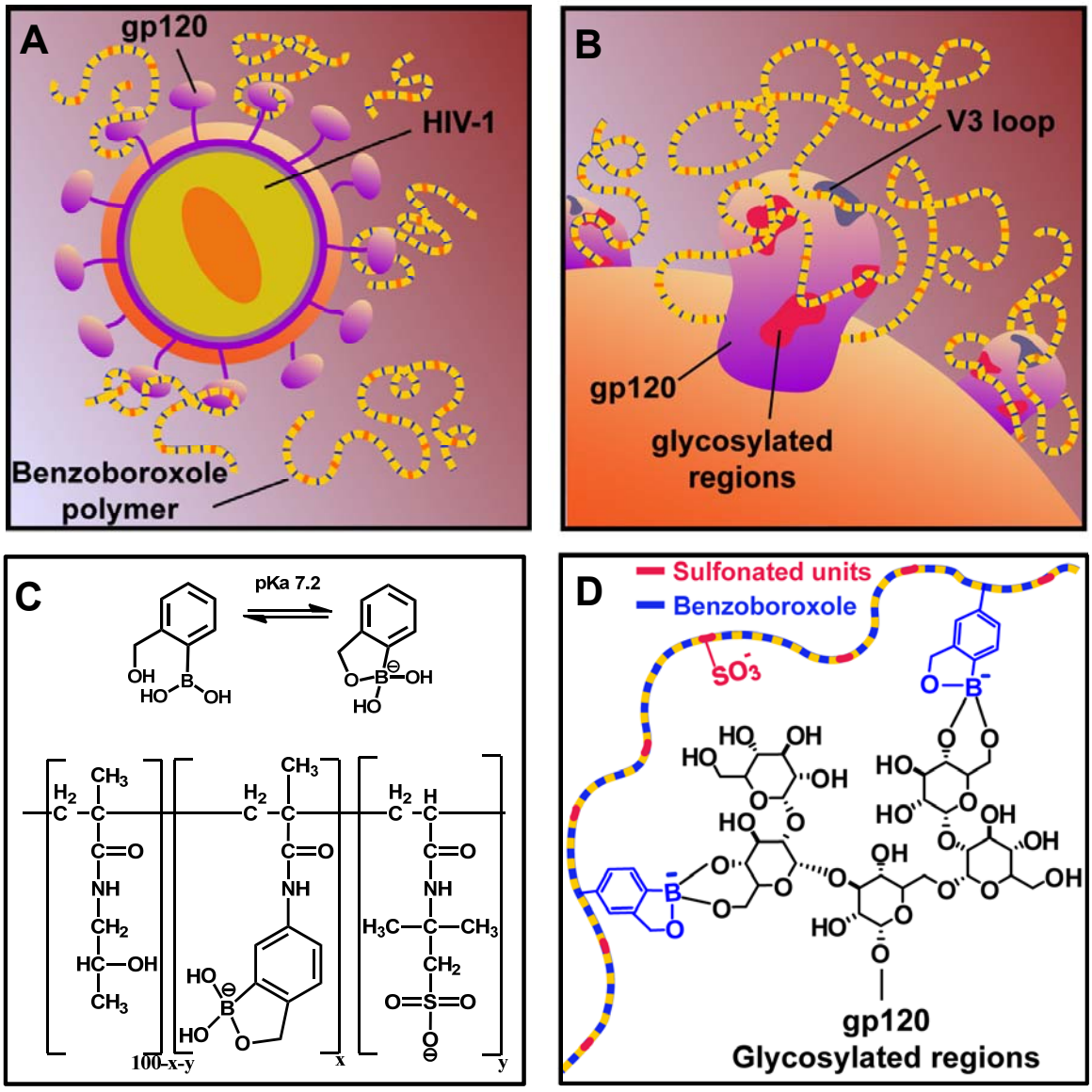

Figure 5.1 Graphical depiction of the multivalent benzoboroxole-functionalized polymer interacting with the gp120 complex of HIV-1. **(A and B)** Schematic illustration of the binding between the polymers (shown in panel **C**) and the gp120 through interactions between benzoboroxole groups and the gp120 and/or through interactions between the anionic polysulfonate polymer and the cationic peptide fragments in the V3 loop of the gp120. **(C)** Chemical structure of benzoboroxole and the linear water-soluble polymers containing benzoboroxole and 2-acrylamido-2-methyl-1-propanesulfonic synthesized using a HPMA polymer backbone. **(D)** Hypothetical scheme of the binding chemistry between the multivalent polymers and the glycosylated regions on the gp120 heterotrimer.

In order to improve binding at physiological pH researchers have investigated various methods to facilitate the formation of stable tetrahedral boronate species at neutral pH by lowering the pKa,[231] through dative bonds formed with boron,[232, 233] and multivalency.[234] The addition of electron-withdrawing groups such as hydroxymethyl, fluoro and nitro to the phenyl ring of the PBA has been found to improve binding to diols at physiological pH compared to unsubstituted PBA.[230, 231, 234, 235] Benzoboroxole (*ortho*-hydroxymethyl phenylboronic acid; BzB; Figure 5.1c) demonstrates strong binding to reducing sugars like fructose and is also capable of binding to glycopyranosides, like galactopyranose, a nonreducing sugar structurally similar to those found in the terminal glycan residues on gp120 at neutral pH.[236] Owing to the ease of synthesis, stability and improved affinity to terminal sugar residues at neutral pH, this work focused on investigating BzB as an gp120-targeted HIV entry inhibitors.

In the past, our laboratory has shown that BzB ligands are capable of binding to the terminal sugar residues on the N-linked glycans of the gp120 and that multivalent polymers of BzB copolymerized with the water-soluble nontoxic 2-hydroxypropyl methacrylamide (HPMAm) monomer show cross-clade antiviral activity at nanomolar to low micromolar concentrations.[237] Based on our investigations to evaluate the effect of mole functionalization of BzB on antiviral activity of the synthetic lectins,[237] we chose the 50 mol% BzB polymers for further assessment. However, our previous system involved problems regarding solubility and activity, in addition to the need for biocompatibility evaluations. We

hypothesized that incorporation of negatively-charged moieties would improve affinity to gp120 through electrostatic interactions with the positively charged V3 loop, while improving solubility and steric availability of the reactive boronic moieties. This work therefore pertains to modulating the multiplicity, ligand density and charge of ligand presenting a polymer backbone to augment the entry inhibition activity of the synthetic lectins. In the current work, we investigate the effect of - (a) ligand density (BzB mole % incorporation), (b) molecular weight of the BzB_{50} polymers and (c) activity of the polyvalent synthetic lectins with a sulfonated polymer backbone to inhibit HIV entry. Additionally, we also assayed the influence of fructose and the role of binding kinetics on the antiviral activity of the BzB_{50} polymers.

5.2 Materials and Methods

Alizarin Red S., phenylboronic acid, 2-hydroxymethyl phenylboronic acid and all the diols were purchased from Acros and were used as received. Water was double distilled with a Milli-Q filtration system. 2-Acrylamido-2-methyl- 1-propanesulfonic acid (AMPS) and AIBN was recrystallized from chloroform (dissolved at 60 °C, recrystallized at -80 °C) prior to use in free radical polymerizations. All other chemicals and reagents were purchased from Aldrich (St. Louis, MO) or Acros (Morris Plains, NJ) and used without further purification unless otherwise noted.

5.2.1 Colorimetric assay to determine binding constants for boronic acid–diol complexes

An ARS-based binding assay was performed as described by Wang et al.[230, 238] Briefly, 10 μM solution of ARS dye was freshly prepared in 100 mM pH 7.4 phosphate buffer. A 2 mM stock solution of BzB was prepared in 10 μM solution of ARS. The pH of both solutions was readjusted to 7.4. Using a 96-well plate, varying amounts of BzB solution were added to ARS solution to obtain a range of concentrations of BzB maintaining the concentration of ARS constantly at 10 μM. The plate was allowed to shake for 60 s prior to measurements. Fluorescence was measured at an excitation wavelength of 485 nm and emission at 620 nM. The experiments were carried out in triplicate. Absorbance spectra were collected over 300-600 nm.

The association constant of PBA or BzB for ARS was determined by plotting the inverse of change in fluorescence vs. the inverse of the concentration of boronic acid. The quotient of the y-intercept and the slope of line were used to compute K_a for the boronic acid-ARS complex. To validate the assay we first determined the effect of varying concentrations of PBA on the absorbance and fluorescence intensity of ARS. ARS showed a color change, from red to yellow and an 80-fold increase in fluorescence intensity at pH 7.4. The association constant for the PBA-ARS complex was determined to be 1260 M^{-1}, which is consistent with the values reported in literature.[230, 238] Following this, solutions with varying concentrations of the diol (D-fructose, glucose, sialic acid, methyl-β-D-galactopyranoside and methyl-α-D-mannopyranoside) were prepared in 100 mM pH 7.4 phosphate buffers containing 10 μM ARS and 2 mM PBA or BzB.

Solutions containing excess of the diol were titrated against the boronic acid-ARS complex. As the diol replaces the ARS to form a boronic acid-diol complex, the concentration of free ARS in the solution increased, thereby showing a marked decrease in fluorescence. This shift in fluorescence was used to compute the association constant for the boronic acid-diol complex.[238]

5.2.2 Polymer Synthesis and characterization

BzB monomers and polymers were synthesized using methods similar to those described previously[238]. Briefly, polymers were prepared by free radical polymerization at 25 mol%, 50 mol% , 75 mol% and 90 mol% BzB feed ratio, in the presence of 5 mol% 2,2'-azobisisobutyronitrile (AIBN) (Figure 5.1). The reaction mixture was purged with nitrogen and degassed for 1 h in ice. Following this, the reaction was moved to a 65 ºC oil bath for 24 h. Polymers were precipitated in anhydrous ether using fractional precipitation technique. Polymers were centrifuged and purified using dialysis across a 10,000 MWCO membrane using VivaFlow dialysis system. Polymers with varying molecular weights were synthesized as described above, with 50 mol% feed ratio of BzB and varying feed ratio's of AIBN (1 mol% - 5 mol%). Polymers with sulfonic acid were also synthesized using conditions described above. The degree of substitution was determined by ^{1}H NMR (Mercury 400 MHz spectrometer, Varian). Molecular weight was determined by GPC (GPC 1100, Agilent Technologies, Santa Clara, CA) equipped with an organic column (PLgel mixed bed, Polymer Laboratories, Amherst, MA), a differential refractive index detector (BI-DNDC, Brookhaven

Instruments, Holtsville, NY) and a multiangle light scattering detector (BI-MwA, Brookhaven Instruments, Holtsville, NY).

5.2.3 Neutralization assay to evaluate the activity of the synthetic lectins against clinical HIV-1 isolates

Anti-HIV activity of the synthetic lectin polymers was evaluated using a single-cycle HIV-1 infectivity inhibition assay in TZM-bl cells.[237] A well characterized R5 tropic DU156 (Clade C) virus isolated from a sexually transmitted virus infection and cultured in PBMC was used in the neutralization assay. A well characterized R5 tropic DU156 (Clade C) virus isolated from a sexually transmitted virus infection and cultured in PBMC was used in the neutralization assay. Additionally, R5 TRO (Clade C) and the pseudotyped X4 WEAU (Clade B) viral strains were assayed to investigate cross-clade and cross-tropism activity. Polymer solutions were prepared at 10 mg/mL in DMEM (4.5 g/ L D-glucose, 110 mg/mL sodium pyruvate and L-glutamine, Invitrogen, Carlsbad, CA), with the pH adjusted to 7.5 as necessary, and pasteurized for 5 m at 70°C. After pasteurization, the stock solution was diluted 1:1 with DMEM containing 2X nutrients (DMEM supplemented with 20% fetal bovine serum (Hyclone, Logan, UT), 50 mM HEPES (Gibco/Invitrogen, Carlsbad, CA) and 100 µg/mL gentamicin (Sigma, St. Louis, MO) under sterile conditions. Preparation was designed to pasteurize the polymers without proteins being present in the media. The final media composition after 1:1 dilution was 10% FBS, 25 mM HEPES, and 50 µg/mL gentamicin. The assay was conducted in a 96-well plate such that the polymer solution at the highest concentration was added to the bottom row. From

the bottom row of the plate 20 µL of the test sample was added to the prior row with 100 µL of growth media to create a 6-fold dilution. This scheme of serial dilution was repeated five times to obtain a dose-response curve. Appropriate cell controls and virus controls were included in each plate. Following the serial dilutions, 50 µL of cell-free virus (200 $TCID_{50}$) was added to each well, with the exception of the wells that served as cell control. The plate was then incubated for 1 h in a 37 °C, 5% CO_2 incubator.

After the preincubation, 100 µL of TZM-bl cell suspension prepared at a density of 1 x 10^5 cells/mL in growth media containing DEAE dextran (37.5 µg/mL) were added to each well and incubated for an additional 48 h. Luminescence was measured after 2 m incubation with Britelite Reagent (PerkinElmer, Waltham, MA). Toxicity of the samples was simultaneously analyzed using an identical plate layout in the absence of virus. To determine loss in cell viability, luminescence from the sample-treated wells was compared to that of the cell controls. EC_{50} is reported as the concentration of the sample which reduced the relative luminescence units (RLUs) by 50% compared to the virus control. Dose response curves were fit to the percent neutralization data using GraphPad Prism software (Graph Pad, LaJolla, CA).

In the assay evaluating the effect of preincubation time on the antiviral activity of the synthetic lectins, the assay was conducted using a procedure similar to the one above described, with the exception of the preincubation time. The polymer solutions were incubated for 0, 15, 30 and 60 mins with the virus prior to addition of TZM-bl cells. For the assay evaluating the effect of fructose,

30 mg/mL fructose solution was prepared in DMEM media. To the polymer solution, 10 µL of the fructose solution was added along with the virus to create a fructose concentration of 3 mg/mL. The remaining of the steps were performed as described above.

5.2.4 Broad-spectrum antiviral assays and activity against laboratory HIV-1 strains

The anti-HIV activity and cytotoxicity were also evaluated against the laboratory HIV-1 strain IIIB and HIV-2 strain ROD in human T-lymphocyte CEM cell cultures. Briefly, virus stocks were titrated in human T-lymphocyte CEM cells and expressed as the 50% cell culture infective dose ($CCID_{50}$, 1 $CCID_{50}$ being the virus dose to infect 50% of the cell cultures). CEM cells were suspended in culture medium at ~ 3 x 10^5 cells/ml and infected with HIV at ~ 100 $CCID_{50}$. Immediately after viral exposure, 100 µl of the cell suspension was placed in each well of a flat-bottomed microtiter tray containing various concentrations of the test compounds. After a 4-d incubation period at 37 °C, the giant cell formation was microscopically determined. Compounds were tested in parallel for their potential cytostatic effects in uninfected CEM cell cultures.

In a cultivation assay, 5 × 10^4 persistently HIV-1 infected HUT-78 cells (designated HUT-78/HIV-1) were mixed with 5 × 10^4 SupT1 cells, along with appropriate concentrations of the test compound. After 20 h, marked syncytium formation was noted in the control cell cultures, and the number of syncytia was determined under the microscope. The EC_{50} was defined as the compound concentration required to prevent syncytium formation by 50%.

The other antiviral assays were based on inhibition of virus-induced cytopathicity in HEL [herpes simplex virus type 1 (HSV-1), HSV-2 (G), vaccinia virus, and vesicular stomatitis virus], Vero (parainfluenza-3, reovirus-1, Coxsackie B4, and Punta Toro virus), HeLa (vesicular stomatitis virus, Coxsackie virus B4, and respiratory syncytial virus) and CrFK (feline corona virus (FIPV) and feline herpes virus) cell cultures. Confluent cell cultures in microtiter 96-well plates were inoculated with 100 $CCID_{50}$ of virus in the presence of varying concentrations (5,000, 1,000, 200 nM) of the test compounds. Viral cytopathicity was recorded as soon as it reached completion in the control virus-infected cell cultures that were not treated with the test compounds.

5.2.5 Biocompatibility evaluation in MatTek VEC-100 reconstructed human vaginal tissue

Triplicate solutions of BzB_{50}-$AMPS_{10}$-$HPMA_{40}$ at 1 mg/mL were prepared in serum containing media. Polymer solutions were pasteurized at 70 °C for 5 mins. Media containing the polymers were applied to the apical surface of tissues cultured in 24-well plate inserts. Three repeated exposures to the test sample were performed in intervals of 24 h. After 72 h of exposure, tissue viability was determined using MTT assay and change in tissue morphology was evaluated through histological examination of the epithelium. On days 1-3, cytokine levels were assayed using ELISA. Levels for IL-1α, IL- 8, IL-6 and TNF-α were measured in tissue culture supernatant by utilizing human cytokine kits (R&D System). Tissue integrity was monitored through measurements of Transepithelium Electrical Resistance (TEER).

5.3 Results and Discussion

5.3.1 Comparative evaluation of the binding affinity of PBA and BzB

To measure the affinity of the boronic acid ligands for reducing and nonreducing sugar residues, we used the ARS-based three-component colorimetric binding assay.[238] Affinity for glucose, fructose, sialic acid, methyl-β-D-galactopyranoside and methyl-α-D-mannopyranoside was assayed. To ensure the viability of the assay, the association constant of PBA-ARS was compared to values reported in the literature by Wang and coworkers.[238] Table 5.1 summarizes the association constants of PBA and BzB for various diols. Comparison between PBA and BzB affinities for simple reducing sugars revealed four-fold stronger affinity of BzB for fructose (~600 M^{-1}) when compared to PBA (160 M^{-1}); however, the affinity of BzB and PBA for glucose was comparable. Unsubstituted PBA demonstrated minimal affinity for nonreducing sugars such as methyl-β-D-galactopyranoside or methyl-α-D-mannopyranoside at neutral pH. In contrast, BzB revealed higher, but still weak, affinity (~25 M^{-1}) for nonreducing complex sugars. To develop a boronic acid based synthetic entry inhibitor for HIV, we have exploited the ability of the BzB to bind to nonreducing sugars,[236] which are structurally similar to the terminal sugar moieties found on the high mannose and complex-type N-linked glycans of gp120. We have previously confirmed this observation also using surface plasmon resonance (SPR), in which BzB showed a K_d of ~180 mM for HIV_{BaL} gp120, whereas no measurable binding was observed with PBA.[237]

Table 5.1 Association constants of phenylboronic acid and benzoboroxole determined using ARS assay at pH 7.4.

Diol	Association Constant (M^{-1})	
	Phenylboronic acid	**Benzoboroxole**
ARS	1260	1307
D-fructose	160	664
N-Acetylneuraminic acid	21	160
Glucose	6	21
Methyl-β-D-galactopyranoside	[a]	24
Methyl-α-D-mannopyranoside	[a]	21

[a]Not measurable. Likely below 5 M^{-1} based on quantitative ARS assay

Unsubstituted PBA-containing polymers have demonstrated the ability to bind to glycosylated proteins only at alkaline pH; whereas BzB binds to glycosides at neutral pH.[233] This difference has been ascribed to the presence of oxygen from the *ortho* substituent that stabilizes the boronate ester towards hydrolysis[232] and decreases the energy barrier for tetrahedral formation.[239]

While the BzB shows superior binding affinity for sugar residues, when compared to the unsubstituted PBA, the binding is fairly weak for practical applications. In this regard, polyvalency has commonly been exploited to improve binding affinity of weak ligands. This effect is well known in natural protein-ligand interactions as well as for other synthetic protein mimics.[226, 227] Kaur *et al.* demonstrated almost a double increase of affinity for glucose for a tweezer-like bis-boronic acid molecule compared to a monovalent boronic acid.[234] Incorporating ligands into polymer backbones provides a synthetically accessible mechanism for increasing the affinity of ligands for glycoproteins.

5.3.2 Polymer synthesis and characterization

Table 5.2 summarizes the molecular weight of the polymers synthesized by free-radical polymerization, determined using size exclusion chromatography (Agilent Technologies, Santa Clara, CA) equipped with a PLgel mixed-B column (Polymer Labs, Amherst, MA), a differential refractive index detector (BI-DNDC, Brookhaven Instruments, Holtsville, NY) and a multiangle light scattering detector (BI-MwA, Brookhaven Instruments, Holstville, NY). Mole functionalization of BzB in the polymer was determined using ^{1}H NMR.

5.3.3 Effect of BzB mole functionalization (ligand density) on the entry inhibition activity of the synthetic lectins

While the binding affinity of BzB for nonreducing sugars determined by the ARS-based colorimetric assay and for gp120 from SPR revealed weak affinity (Table 5.1), high molecular weight polymers with polyvalent presentation of BzB showed ≥ 4 log scale increase in activity (EC_{50} in low micromolar to nanomolar range). As seen in Figure 5.2, ~2 log scale increase in antiviral activity was observed with an increase in BzB mole functionalization from 25 mol% to 50 mol% in the polymer (single-factor ANOVA, $p < 0.001$) and further increase in BzB functionalization from 50 mol% to 75 mol% showed only a marginal increase in activity (single-factor ANOVA, $p = 0.01$). On the contrary, an increase in ligand density from 75 mol% to 90 mol% showed a reduction in the ability of the polymers to neutralize HIV entry (single-factor ANOVA, $p = 0.01$), with an anti-HIV activity that was comparable to the 50 mol% BzB-functionalized polymers.

Table 5.2 Polymer composition and molecular weight distribution.

Polymer	Mole Functionalization[a]			Molecular Weight[b] (kDa)		PDI
	BzB	AMPS	HPMA	M_w	M_n	
BzB_{25}-$HPMA_{75}$	29	-	71	103	88	1.17
BzB_{75}-$HPMA_{25}$	70	-	30	74	50	1.48
BzB_{90}-$HPMA_{10}$	91	-	8	98	76	1.30
BzB_{50}-$HPMA_{50}$	48	-	52	110	91	1.21
	54	-	54	226	159	1.42
	51		51	382	285	1.34
$AMPS_{10}$-$HPMA_{90}$	-	-	-	153	111	1.38
BzB_{50}-$AMPS_{10}$-$HPMA_{40}$	45	10	55	131	109	1.20

[a]Degree of substitution was determined by ^{1}H NMR and found to correlate with the feed ratios.
[b]Molecular weight was determined by GPC attached to a light scattering and a refractive index detector.

We believe that the increase in antiviral activity with increasing mole functionalization can be explained by at least two distinct mechanisms described by Mammen and coworkers[226, 228] – polyvalency and steric stabilization. The combined effect of the increase in the number and density of ligands likely improves the probability of binding, thereby enhancing binding and antiviral activity through avidity and polyvalency. As a secondary mechanism, we suspect that, when the BzB presenting polymers bind to gp120, they escort along a large water-swollen polymer drape which possibly makes the viral envelope physically inaccessible for fusion and entry into the host cell.[228, 240] If we assume that it is these two mechanisms that collectively determine the activity of synthetic lectins, the gradual increase in activity from 50 to 75 mol% and the decrease in activity from 75 to 90 mol% can be explained through loss in the steric stabilization effect of these polymers.

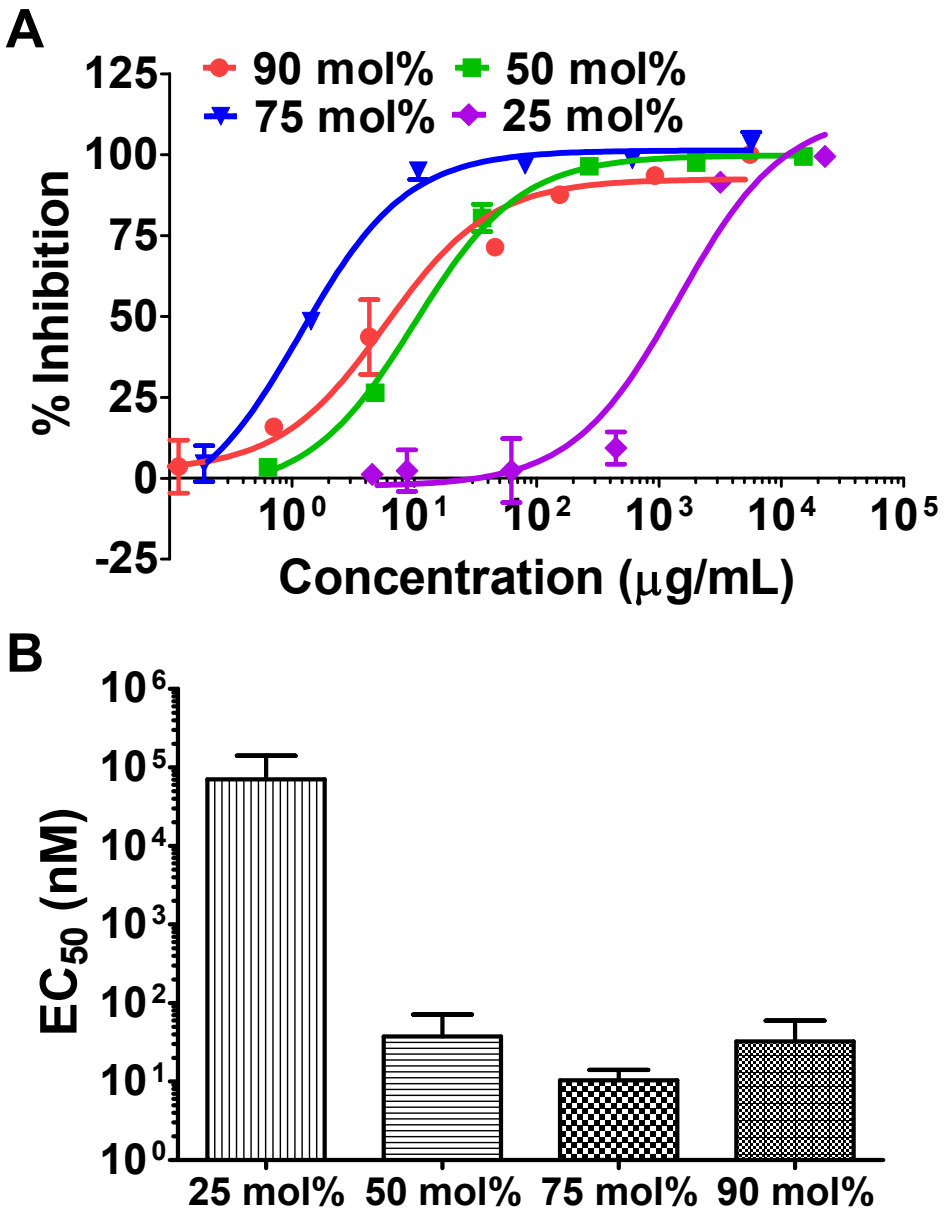

Figure 5.2 Effect of BzB mole functionalization on the entry inhibition activity of BzB_{50} polymers. Results from the single-cycle HIV-1 infectivity inhibition in TZM-bl cells against R5 DU156 (Clade B) isolated from acute STIs. **(A)** Dose response curve of BzB functionalized HPMA polymers at varying mole incorporation. **(B)** EC_{50} was determined by fitting a sigmoidal dose-response curve with variable Hill's slope. Single-factor ANOVA followed by Bonferroni correction showed significant differences between groups ($p<0.05$). Significant increase in activity from 25 to 50 and 75 mol% was observed. Further increase from 75 to 90 mol% showed reduction in activity; EC_{50} of BzB_{90}-$HPMA_{10}$ was comparable to EC_{50} of BzB_{50}-$HPMA_{50}$ (N = 3, mean ± SD; *$p<0.05$; **$p<0.01$).

As we increase the ligand density in the polymers, the negatively charged borons could repel each other, thereby distorting the polymer conformation from an effective random coil structure to a less effective rigid elongated structure.[228] On the other hand, increasing the number of available ligands and therefore, points of attachment between the polymer and the gp120 could result in a collapsed polymer structure; compromising the ability of the polymer to sterically stabilize the binding surface.[228] Although the relative contribution of the abovementioned two mechanisms towards antiviral activity is yet to be elucidated, it is reasonable to assume that steric stabilization plays a critical role[228] in governing the ability of BzB-functionalized polymer to block HIV entry. Based on these results, further assessments were performed on 50 mol% functionalized BzB polymers.

Depending on the coreceptor tropism and clades, HIV displays significant variations in the different areas on the viral envelope,[241, 242] making it important to evaluate cross-clade and –tropism activity of new therapeutic agent.[83, 243] For example, agents targeting the positively charged V3 loop of the gp120, such as the nonspecific sulfated polymers, show severely compromised activity against R5 tropic strains.[244] This is because, the coreceptor tropism of the virus impacts the extent of the positive charge on the gp120 V3 loop, with the CXCR4 coreceptor-tropic HIV-1 strains (X4) exhibiting more positive charges than the CCR5-tropic HIV-1 strains (R5). We have previously reported the antiviral activity of the BzB-HPMA copolymers at 25, 50 and 75 mol% BzB mole incorporation, against HIV strains across clades and tropism.[237]

The assays were performed using Clade B - R5 DU156 and Clade C - R5 TRO, isolated from acute sexually transmitted infections, and the pseudotyped Clade B - X4 WEAU. Independent of the ligand density BzB polymers showed comparable antiviral activity across the clades and tropisms of HIV.[237] Although, the HIV envelope exhibits domains of heterogeneity across viral strains, many N-linked glycans are believed to be fairly conserved, providing a potential mechanism for the observed broad-spectrum activity of lectins.

5.3.4 Effect of molecular weight of the BzB_{50} polymers on the entry inhibition activity of the synthetic lectins

Having an understanding of how ligand density affects activity of the BzB functionalized polymers; we were next interested in exploring the influence of the molecular weight of the polymer at a fixed BzB functionalization on antiviral activity of the synthetic lectins. BzB functionalized polymers at 50 mol% were synthesized using varying concentrations of the initiator, yielding polymers with a range of molecular weights. As shown in Figure 5.3, EC_{50}'s of the polymers decreased (thus, higher activity) from 68 nM for 132 kDa BzB_{50} to 12 nM for 382 kDa BzB_{50} (single-factor ANOVA, $p = 0.01$). Owing to the increased number of ligands available for binding per polymer chain, increase in molecular weight of the polymers at a fixed percent BzB incorporation showed improved activity. However, the improvement in activity found with molecular weight variations was less dramatic than that seen with variation in percent BzB functionalization.

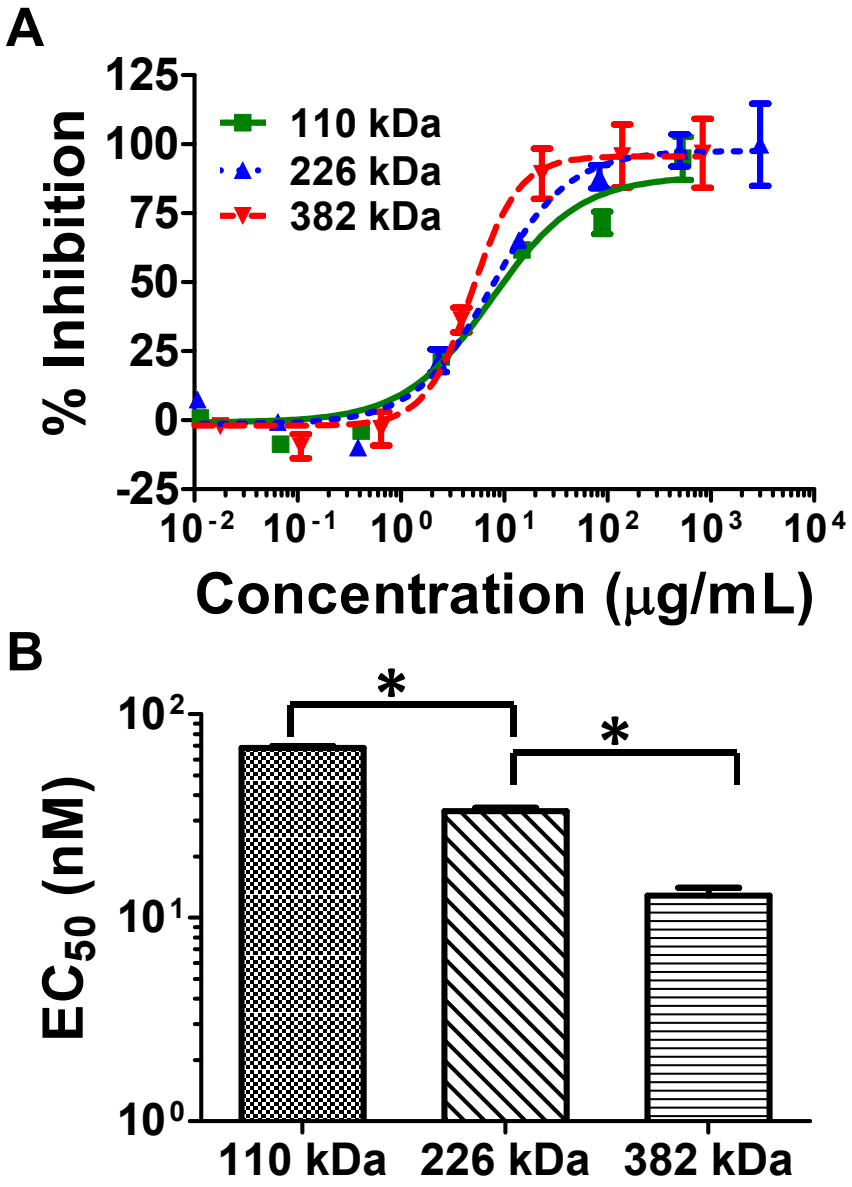

Figure 5.3 Effect of molecular weight on the entry inhibition activity of BzB_{50} polymers. Results from the single-cycle HIV-1 infectivity inhibition in TZM-bl cells against R5 DU156 (Clade B) isolated from acute STIs. **(A)** Dose response curve of BzB_{50}-$HPMA_{50}$ polymers at varying molecular weights and **(B)** EC_{50} determined by fitting a sigmoidal dose-response curve with variable Hill's slope. Single-factor ANOVA followed by Bonferroni correction was used (N = 3, mean ± SD; *$p < 0.05$). Significant increase in activity was observed with increase in MW of the polymer from 110 to 226 kDa and further to 382 kDa ($p = 0.03$ and 0.01, respectively). Highest activity was observed with 382 kDa MW polymer (11.3 ± 2.9 nM).

5.3.5 Antiviral activity of BzB_{50} polymers against viruses bearing glycosylated envelopes

Entry inhibition activity of lectins originates from their ability to bind to glycans spiked on the viral surface. Several of the enveloped viruses bear carbohydrate shields on the envelope,[245] which could be effectively targeted using lectins that nonspecifically bind to carbohydrates. Therefore, we and others in the field have tested the activity of plant, bacterial and/or synthetic lectins against lentiviruses[246] (HIV-1, HIV-2, SIV, MSV), RNA viruses[247] (VSV, Coxsackie virus B4, and respiratory syncytial virus; and parainfluenza type 3 virus, reovirus type 1, Sindbis virus, and Punta Toro virus, Ebola, Coronaviruses, Influenza viruses), DNA viruses[246] (herpesvirus such as cytomegalovirus) with glycosylated envelopes. Table 5.3 summarizes the inhibitory concentration of $BzB_{50,382\ kDa}$ against the viruses we tested.

We notably observed activity solely against HIV. Except for HIV, none of the other viruses were inhibited by the BzB polymers even at concentration 100-fold higher than the EC_{50} for HIV. These results are in contrast with UDA that inhibit viruses such as HIV-1, HIV-2, RSV, Influenza, CMV, SIV and FIV. CV-N an extensively reviewed CBP which is derived from the cyanobacterium *Nostoc ellipsosporum* demonstrated marked inhibition of viruses such as HIV-1,[83, 248] SIV, Ebola,[247] HCV,[249] Influenza A virus[250] and HSV. The HIV-specific activity we observed with the synthetic lectins can be attributed to the fact that no other virus that was tested in this assay exhibited comparable extent of glycosylation sites and/or a similar nature of the glycans (i.e., high-mannose-type) as HIV.

Table 5.3 Antiviral activity of BzB_{50}-$HPMA_{50}$ (382 kDa) against viruses with glycosylated envelope

Virus	EC_{50} (nM)[+]	Virus	EC_{50} (nM)[+]
HIV-1	1.1	Herpes simplex virus-1 (KOS)[c]	> 1000
Feline Corona Virus[a]	1000	Herpes simplex virus-2 (G)[c]	> 1000
Feline Herpes Virus[a]	5000	Herpes simplex virus-1TK[c]	> 1000
Punta Toro virus[b]	> 40	Vesicular stomatitis virus[c,d]	> 1000
Parainfluenza-3 virus[b]	> 40	Respiratory syncytial virus[d]	> 1000
Reovirus-1[b]	> 40	Coxsackie virus B4[d]	> 1000
Vaccinia virus[c]	> 1000		

[+]50% Effective concentration or compound concentration producing 50%inhibition of virus-induced cytopathic effect; [a]Crandell-Rees Feline Kidney cells (CRFK cells), [b]Vero cells, [c]HEL cells, [d]HeLa cells

Since, the interactions between a polyvalent construct such as the BzB-based synthetic lectin and the viral envelope depends on a multitude of factors such as the density of glycosides on the viral surface, degree of oligomerization of the glycoprotein, spatial arrangement of saccharides and flexibility or both, it is conceivable that the synthetic lectins selectively inhibit viruses, in this particular case HIV and not just all types of viruses that bear a glycosylated envelope.

5.3.6 Incorporation of sulfonic acid in the polymer backbone affords a synergistic increase in viral entry inhibition activity of BzB_{50} polymers

Lead polymers from the above studies with an antiviral activity of ~ 10 nM ($BzB_{75,\ 75kDa}$ and $BzB_{50,\ 382kDa}$) showed poor-aqueous solubility (< 5 mg/mL). Considering that the activity of the BzB polymers could be compromised in the presence of proteins and other components in the vaginal environment, improving aqueous solubility of the polymers may be required in order to deliver the required drug concentrations. Kataoka *et al.* and others have demonstrated

that the incorporation of amines into a PBA-containing polymer could lower the pKa of the boronic acid to around 7, thereby enhancing solubility.[251, 252] Incorporation of amines was also utilized by Winblade *et al.*, who reductively aminated 4-formylphenylboronic acid to a poly-lysine-PEG backbone. The pKa of this polymer was below 6.[240, 253] To address the poor aqueous solubility of the polymers at high benzoboroxole functionalization (≥ 50 mol%) and/or high molecular weight polymers (≥ 125 kDa), we have synthesized polymers with 10 mole% 2-Acrylamido-2-methylpropane sulfonic acid (AMPS), which is an anionic monomer. Incorporation of AMPS into the copolymer adds charge to the otherwise neutral HPMA backbone, increasing the aqueous solubility of the polymer at neutral pHs by Nearly 100-fold.

Since both AMPS and BzB bind to gp120, we tested both polymers individually, as a physical mixture and a copolymer of AMPS and BzB. The physical mixture of the two polymers - BzB_{50} and $AMPS_{10}$ - did not demonstrate any significant increase in activity (single-factor ANOVA, p=0.21) (Figure 5.4). This data suggests that the presence of $AMPS_{10}$ only in the polymer solution has no influence on the binding of BzB to gp120. In contrast, when the AMPS and BzB were copolymerized, the resulting polymer showed a more than two log scale decrease in EC_{50} (single-factor ANOVA, p=0.012). We believe that the presence of (a) simultaneous ionic and covalent interactions; (b) steric stabilization; and (c) entropic advantage with multiple binding events - may contribute to the observed synergistic improvement in antiviral activity of the copolymers over the physical mixture.

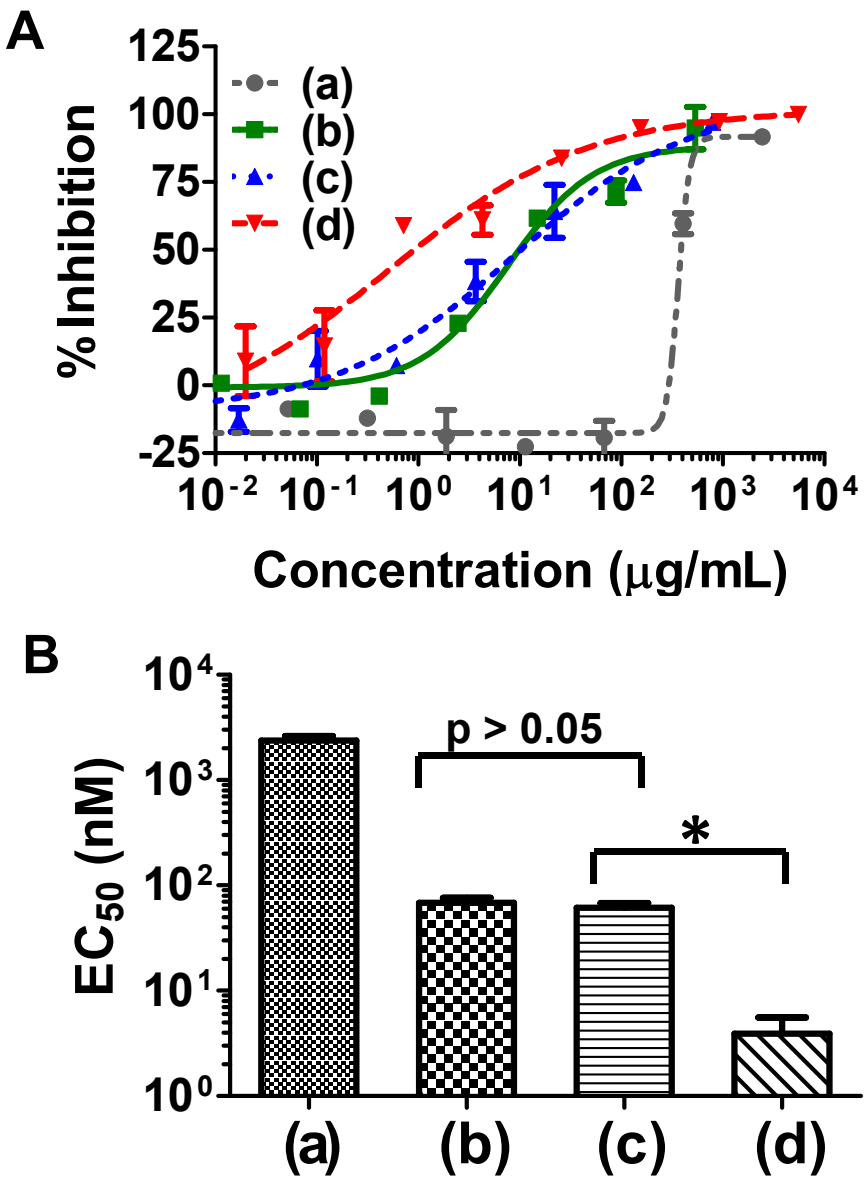

Figure 5.4 Effect of incorporation of sulfonic acid on the entry inhibition activity of BzB_{50} polymers. Results from the single-cycle HIV-1 infectivity inhibition in TZM-bl cells on (a) $AMPS_{10}$-$HPMA_{90}$, (b) BzB_{50}-$HPMA_{50}$, (c) physical mixture of $AMPS_{10}$-$HPMA_{90}$ and BzB_{50}-$HPMA_{50}$ and (d) copolymer BzB_{50}-$AMPS_{10}$-$HPMA_{40}$ against R5 DU156 (Clade B) isolated from acute STIs. **(A)** Dose response curve of the polymers and **(B)** EC_{50} determined by fitting a sigmoidal dose-response curve with variable Hill's slope. Single-factor ANOVA followed by Bonferroni correction was used (N = 3, mean ± SD; $p < 0.05$). $AMPS_{10}$ showed an EC_{50} of 2361 nM ± 60 (~350 μg/mL). Physical mixture of BzB_{50}-$HPMA_{50}$ and $AMPS_{10}$-$HPMA_{90}$ showed no significant increase in antiviral activity over BzB_{50}-$HPMA_{50}$ ($p=0.21$). However, copolymers of HMPBA and AMPS at 50 and 10 mol% functionalization, respectively, showed a dramatic increase in antiviral activity with EC_{50} of 4.0 nM ± 1.6 (~1 μg/mL) (*$p = 0.012$).

The charged sulfonated polymer backbone likely facilitates initial ionic interactions with the V3 loop on gp120; thereby sterically facilitating covalent interactions between the BzB on the polymer and the glycans on gp120. This implies that, irrespective of the binding affinity, the binding event would bring along a large polymer drape to the viral surface, thus inhibiting interactions with the host cell. The BzB-AMPS copolymers show activity at concentrations (~ 1 to 4 nM) comparable to CV-N (~ 0.6 nM). BzB polymers displayed an EC_{50} of 50 ± 2.6 nM in preventing syncytium formation in cultures of persistently HIV-1_{IIIB} infected HUT-78 and uninfected Sup T1 cells.

Sulfated anionic polymers have previously been evaluated as a microbicide that targets the V3 loop on gp120.[254] We are aware of the issues associated with the sulfonated polymers for microbicide applications which include toxicity due to nonspecific binding, tropism-specific activity[244] and loss of antiviral activity in the presence of semen.[254] In an attempt to address the above issues, we synthesized polymers with small amounts of AMPS copolymerized with the biocompatible HPMAm; most likely reducing potential toxicity. Furthermore, the primary mechanism of action of the synthetic lectins is through the ability of BzB to covalently bind to gp120, which demonstrates clade and tropism independent activity.[237] The ionic interaction between AMPS and the V3 loop is an auxiliary mechanism of action that augments the overall activity of the BzB-based synthetic lectins. In summary, incorporation of AMPS in BzB_{50} yields a polymer with enhanced aqueous-solubility and generates a heteromeric polyvalent presentation of ligands with superior binding to gp120.

5.3.7 Effect of binding kinetics on the activity of the synthetic lectins

We were next interested in asking whether the activity of these polymers is governed by thermodynamics alone or whether binding kinetics also influences the entry inhibition activity of the BzB. To evaluate the effect of binding kinetics, the BzB-APMS copolymer samples were preincubated with the virions for 0, 15, 30 and 60 mins. As shown in Figure 5.5, irrespective of the incubation time, the copolymer samples showed 50% inhibition of HIV at ~ 4.5 ± 2.0 nM (single-factor ANOVA, $p>0.05$). Unlike the α-(1-3)- and α-(1-6)-D-mannose oligomer-specific plant lectins, whose antiviral activity is up to 20-fold more pronounced upon a 1 h preincubation time with the virus,[246] the BzB-based synthetic lectins show superior and rapid inhibition of HIV entry, irrespective of preincubation with the virus particles.

5.3.8 Effect of seminal concentrations of fructose on the activity of the synthetic lectins

Several antiviral agents such as sulfated polymers,[254] intended to be delivered vaginally show compromised or complete loss of antiviral activity in the presence of seminal fluid. Seminal fluid is a rich source of proteins, enzymes, salts, immune cells and sugars.[52] Of these, the presence of high concentrations of simple sugars such as fructose especially may raise concerns for lectin-based therapeutics. As seen by our results from the ARS assay, BzB show exceptionally high affinity for fructose.

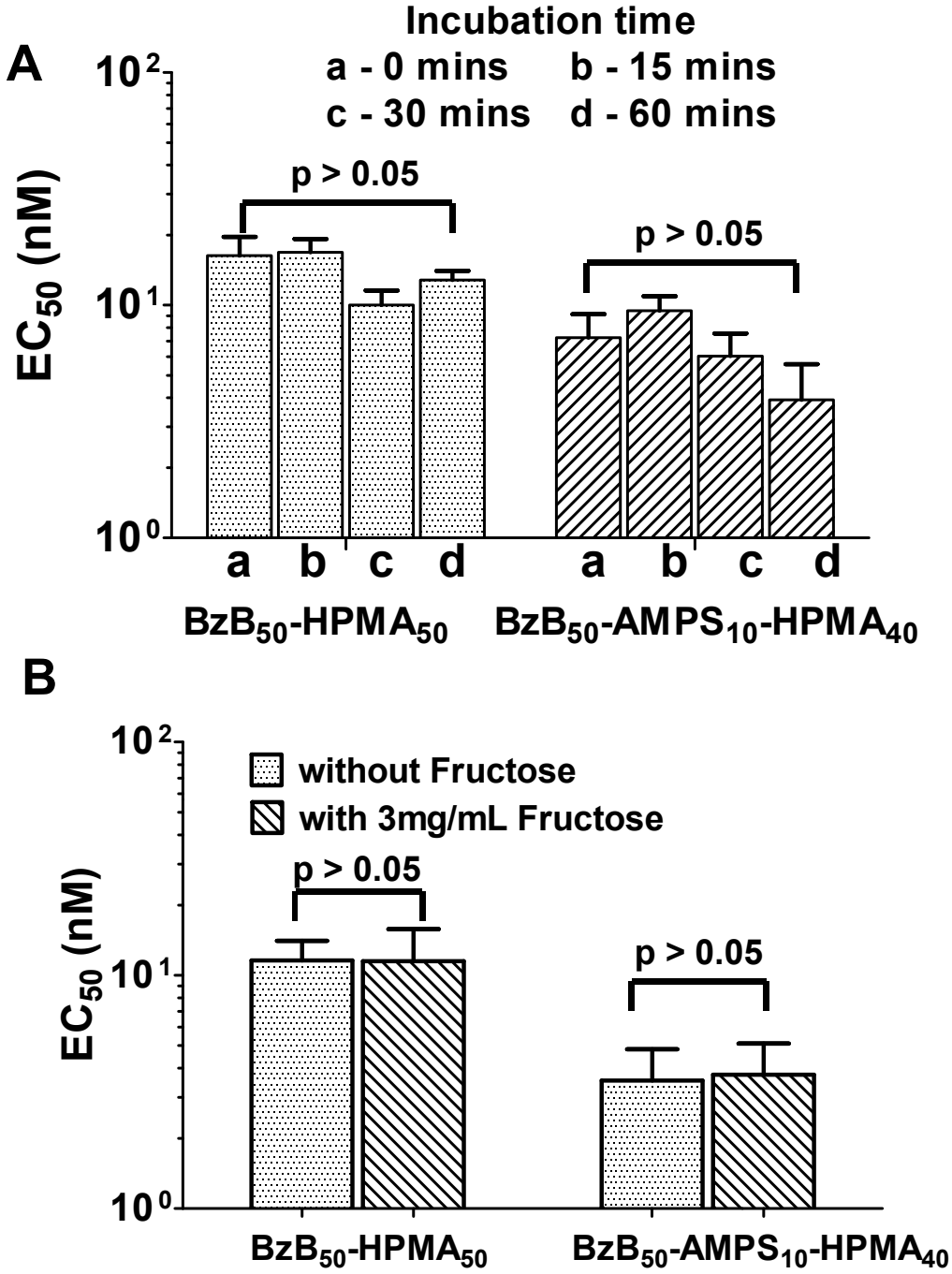

Figure 5.5 Effect of incubation time and fructose on the entry inhibition activity of BzB_{50} polymers. Dose response curves of **(A)** BzB_{50}-$HPMA_{50}$ (382 kDa) and BzB_{50}-$AMPS_{10}$-$HPMA_{40}$ against R5 DU156 as a function of preincubation time. Using single factor ANOVA, independent of the incubation time, no significant difference in EC_{50} was observed ($p = 0.72$ and 0.55). **(B)** EC_{50} of BzB_{50}-$HPMA_{50}$ and BzB_{50}-$AMPS_{10}$-$HPMA_{40}$ in the presence of seminal concentration of fructose. Both polymers showed no significant loss in antiviral activity in the presence of fructose. Using 2-tailed, Student's t-test $p = 0.44$ and 0.53 for BzB_{50}-$HPMA_{50}$ and BzB_{50}-$AMPS_{10}$-$HPMA_{40}$, respectively.

Therefore, we tested the ability of the BzB_{50}-$AMPS_{10}$-$HPMA_{40}$ copolymers and BzB_{50}-$HPMA_{50}$ (383 kDa) to neutralize HIV entry in the presence of average seminal fructose concentration (3 mg/mL) of fructose. As shown in Figure 5.5d, activity of the synthetic lectins was fully preserved in the presence of fructose, suggesting that fructose from seminal fluid would not compromise the antiviral activity of the synthetic lectins (2-tailed student's t-test $p>0.05$).

5.3.9 Biocompatibility evaluation in MatTek VEC-100 reconstructed human vaginal tissue

Enabling this research for microbicide development requires careful determination of how interactions of BzB polymers with the epithelial cells of cervicovaginal tissue may impact their viability and cytokine production. Owing to the ability of the BzB to bind to glycoproteins and the ability of sulfonic acid to nonspecifically bind to positively charged surfaces; it is critical to assess the safety of the BzB-AMPS copolymers in vaginal tissue. The VEC-100 tissue purchased from MatTek Corporation for evaluating the tissue-level toxicity of topical microbicides.[255] As can be seen in Figure 5.6, BzB-AMPS copolymers showed no significant loss in tissue viability when compared to the nontoxic control even at concentrations ~ 1000-fold the *in vitro* EC_{50}, after 72 h of exposure. The irritation potential of test polymers were evaluated by ELISA for inflammatory cytokines associated with mucosal toxicity (i.e., IL-8, IL-1, IL-6, TNFα) using human cytokine kits (R&D System). Our investigations on biocompatibility revealed no significant alterations in tissue viability, cytokine levels, tissue morphology or the barrier properties of the epithelium.

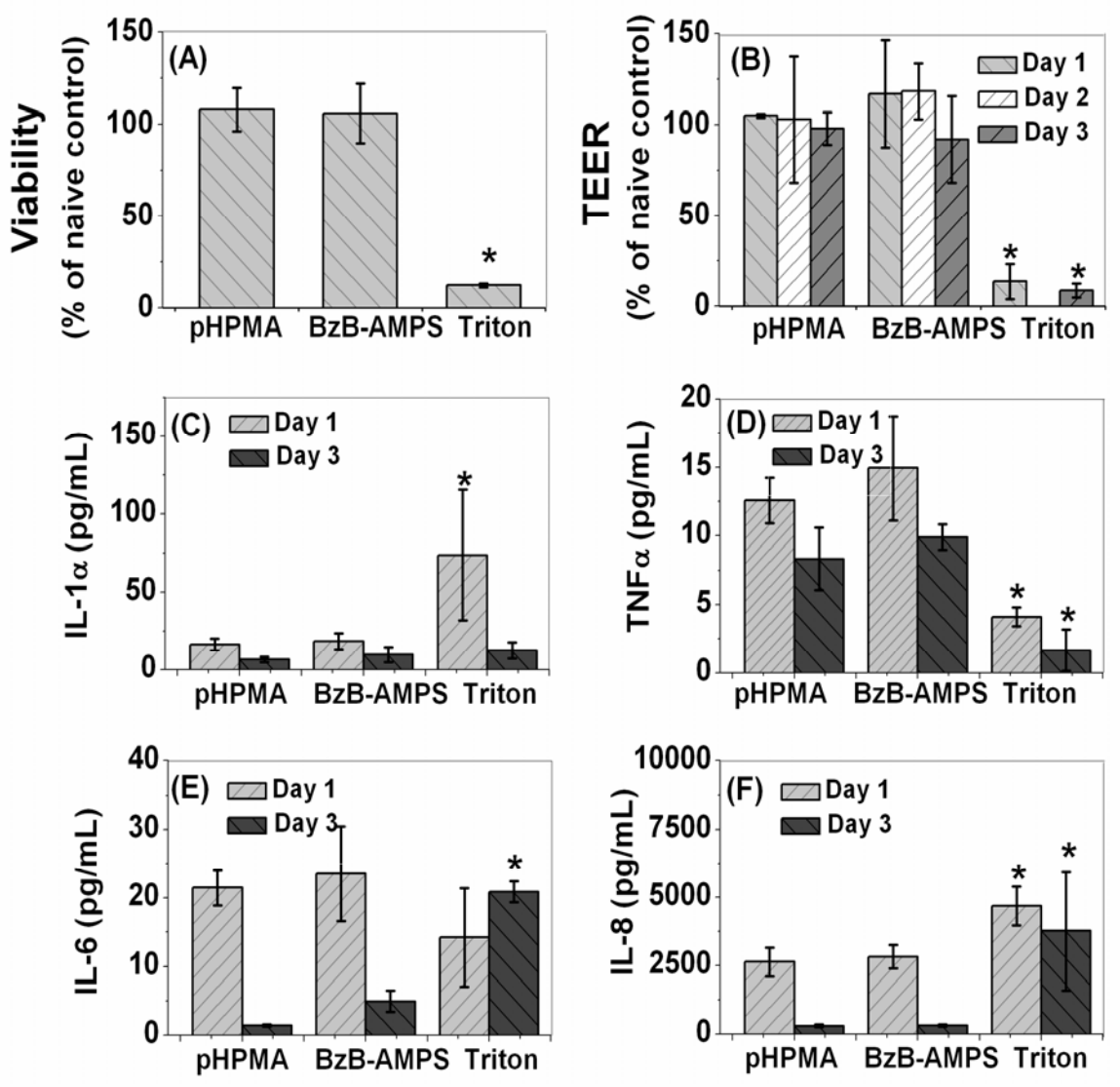

Figure 5.6 Safety evaluation of BzB_{50}-$AMPS_{10}$-$HPMA_{40}$ on reconstructed human ectocervical tissue after three repeated exposures. pHPMA and Triton served as nontoxic and toxic controls, respectively. **(A)** Percentage viability of the tissue determined using MTT assay at the end of day 3, **(B)** TEER measurements graphed as percentage of the no treatment control for days 1-3. **(C-F)** Cytokine IL-1α, TNFα, IL-6 and IL-8 release for days 1-3. Tissues treated with BzB_{50}-$AMPS_{10}$-$HPMA_{40}$ showed no symptoms of loss in tissue viability or elevation in cytokine levels when compared to pHPMA treated nontoxic control. (Mean ± SD, single-factor ANOVA followed by Bonferroni correction; *$p < 0.05$).

In summary, these results suggest that polymers functionalized with BzB moieties, are likely to be nontoxic and are likely to have a high therapeutic index; allowing higher concentrations of the polymer to be dosed safely, thereby minimizing the impact of competing binding sites that may be present in the vaginal environment.

5.4 Conclusion

This work is relevant to the development of new agents capable of rendering the virus inactive during female-to-male heterosexual transmission. An ideal microbicide candidate must exhibit potency, cross-clade broad spectrum activity, selective inhibition of the pathogen, mass producible and biocompatible. While current research on CBPs suggests that they possess several of the above favorable properties to qualify as potential microbicide candidates, their success is largely impeded by the potential mitogenic properties, cost of production and isolation and purification in mass quantities. In this regard, our approach of developing synthetic lectins using the BzB moieties meet all of the above criteria of an ideal microbicide. The BzB can readily be incorporated into a variety of biocompatible polymer backbones and polymeric constructs which can be synthetically modified to enhance activity and specificity. Additionally, the BzB-based synthetic lectins also present an affordable and scalable product that could be delivered to the pandemic regions.

5.5 Acknowledgements

We thank David Montefiori (Duke University) for providing lab space, viral strains, assay reagents and the TZM-bl cell line for the neutralization studies. We thank Julie I. Jay for polymer samples (BzB_{25} and BzB_{75}). This work was supported by the NIH, grant number R21-AI062445, and The Bill & Melinda Gates Foundation Grand Challenge Exploration awarded to Dr. Patrick F. Kiser, the K.U.Leuven Program Financing (PF/10/018) and the “Fonds voor Wetenschappelijk Onderzoek” (no. G.0485.08) to Dr. Jan Balzarini.

CHAPTER 6

SUMMARY OF RESEARCH AND SUGGESTED FUTURE WORK

The purpose of this final chapter is to present a summary of the motivation for the work, major findings and recommendation for future studies.

6.1 Chapter 2 - Design of a Semisolid Vaginal Microbicide Gel by Relating Composition to Properties and Performance

6.1.1 Motivation to the Work

In the development of a semisolid microbicide gel, there has long been the need for a methodology that would help researchers who seek to develop new drug delivery vehicles (DDVs), or even improve some aspects of a current formulation. These tools may also prove useful in optimization exercises or simply in comparing multiple formulations. In this regard, research described in Chapter 2 of this dissertation involved the design of a semi-empirical approach to guide application-specific selection of a DDV, in this case for microbicide delivery. In doing so, a composition-property-performance relationship between polymer concentrations, rheological properties of the resulting gel and predicted

deployment characteristics of the DDV was established. This work helped identify tools, that when used in combination, provides insight into how composition of a DDV can be tailored to meet a predefined set of performance criteria.

6.1.2 Summary of the Research

A preclinical *in vitro* algorithm that allows *de novo* design of vaginal gels, by empirically relating gel composition to gel properties was developed. Gel performance was defined through a multivariate objective function constructed from gel's mechanical properties and selected performance criteria for spreading within the vaginal canal. Mixture design of experiment was used to establish a semiempirical relationship linking composition-property and property-performance relationships for gels with varying concentrations of hydroxyethylcellulose (HEC) and Carbopol 974P. This permits definition of a local optimum for gel composition and volume of administration, within a defined composition space. Rheological behavior and, consequently, the value of the objective function varied broadly with composition. In the composition space consisting of HEC (0-3% w/w) and Carbopol (0-2.5% w/w), the algorithm indicated a 3.0 wt% HEC gel as the near optimal composition for a 3.5 mL applied volume for gels, designed to spread throughout the vagina.

6.1.3 Critical Assessment and Suggested Future Work

The algorithm reported in this work represents the first attempt to develop methods that empirically relate the composition of commonly used gel excipients

to their performance using deterministic squeezing flow calculations. Therefore, the first generation squeezing flow model is simplistic.

6.1.3.1 Consideration of intermolecular interactions. Some of the factors that the future generation squeezing flow models need to incorporate include interactions between the DDV and the vaginal epithelium. These interactions may depend on the surface properties of the vaginal epithelium such as wetability, cell turnover, variations in epithelium with menstrual cycle and presence of cervical mucus.[256, 257] Incorporating intermolecular interactions into the equation for the score, could prove critical in assessing the ability of the gel to spread over the vaginal tissue and adhere to the surface to minimize leakage.[257]

6.1.3.2 Assumption of a constant force of squeezing. The model as it stands, assumes a constant force of squeezing which is an idealistic representation of the *in vivo* condition.[56] To address this shortcoming, tools that would enable measuring of the squeezing forces between the anterior and posterior walls of the vaginal lumen are required. Values of squeezing force when fed into a dynamic stress device would apply force that varies with time, providing a physiologically relevant measure of the area coated by the gel.

6.1.3.3 Kinetics of dilution of the gel. A major advancement required of the squeezing flow model is the need for a time-dependent function that may account for gradual dilution of the formulation with vaginal fluid.[56, 57] The approach employed in this study, involved physical mixing of the gel with vaginal fluid simulant (VFS) at 4:1 weight ratio. The dilution and physical agitation was an exaggeration of dilution and mixing observed *in vivo*. Therefore, it would be

necessary to develop a rheological method that, in real time, would assess the implication of gradual dilution of the gel with biological fluids.

6.1.3.4 Augmenting the scoring function with factors beyond deployment that contribute to the overall effectiveness of a semisolid microbicide gel. This study evaluated the algorithm for its use in predicting deployment characteristics of several PAA and cellulose-based commercially available formulations. It will be valuable to assess the applicability of the algorithm for gels composed of gelling agents such as carageenan, chitosan and others. Moreover, incorporating terms that account for drug release and toxicity profiles of the DDV would provide a more complete numerical equation and a collective score that may allow researchers to rank order formulations during preclinical optimization process. Finally, to enable this research as a preclinical tool to guide selection of DDV and to evaluate performance of a microbicide gel, the predictions of the model would need to be confirmed and correlated with *in vivo* observations of deployment.

6.2 Chapter 3 - Inhibition of the Transport of HIV-1 *In vitro* Using a pH-Responsive Synthetic Mucin-Like Polymer System

6.2.1 Motivation to the Work

Polymeric materials based on entangled polymer networks or weak noncovalent interactions, offer little control over the mechanical properties and performance of the delivery vehicle.[117] Moreover, these gels are nonresponsive and may be rapidly eroded in the presence of genital secretions; requiring

application immediately prior to intercourse.[258] Advancements in the development of formulations capable of longer retention, along with the properties for acceptable application and complete distribution may require *in situ* crosslinking materials.[259] Inspired by the ability of the cervicovaginal mucus to impede the movement of HIV-1 at acidic pH,[30] we have engineered a pH-responsive polymer system that shows improved barrier properties over the naturally occurring cervicovaginal mucus, such that it inhibits viral transport at both acidic and neutral pH. The pH-responsive synthetic mucin-like polymer (SMP) is constructed with phenylboronic acid (PBA) and salicylhydroxamic acid (SHA), each individually copolymerized with a 2-hydroxypropylmethacrylamide (pHPMA) polymer backbone. This research is amongst the first to apply contemporary capabilities for designing a platform of a bioresponsive polymer to the specific physiological and biomechanical requirements for a vaginal microbicide product, along with liberation from immediate precoital product use.

6.2.2 Summary of Research

At pH 4.8, the crosslinked polymers form a transient network with a characteristic relaxation time of 0.9 s and elastic modulus of 11 Pa. On addition of semen, the polymers form a densely crosslinked elastic network with a characteristic relaxation time greater than 60 s and elastic modulus of 1800 Pa. Interactions between the PBA-SHA crosslinked polymers and mucin at acidic pH showed a significant increase in elastic modulus and crosslink lifetime ($p < 0.05$). A transport assay revealed that migration of HIV-1 and cells was significantly

impeded by the polymer network at pH ≥ 4.8 with a diffusion coefficient of 0.160 x 10^{-3} $\mu m^2/s$ for HIV-1. SMP did not induce symptoms of toxicity or irritation in either human vaginal explants or a mouse model. In summary the, pH-responsive crosslinked polymer system reported in Chapter 3 of this dissertation holds promise as a new class of bioinspired environmentally responsive material that could inhibit the transport of virions from semen to the target tissue and, thereby, contribute to the overall activity of the microbicide drug delivery system.

6.2.3 Critical Assessment and Suggested Future Work

Influence of biofluids on the transport of virions through the SMP - Through our study on gelation kinetics, we have shown that the SMP forms a viscoelastic fluid almost instantaneously on mixing and on contact with semen forms an elastic solid. However, it is important to reassess these results in the presence of biological fluids such as cervical mucus and vaginal fluid. Thus far, we have only examined the influence of semen and simulants of mucus and vaginal fluid, individually on the viscoelastic properties of the SMP. Conducting viral tracking in samples diluted with cervical mucus, vaginal fluid and semen would answer important questions in regards to the ability of the SMP to inhibit viral transport *in vivo*. To further, validate SMP's applicability as a microbicide, inhibition of viral transport will need to be assayed in an *in vivo* infectivity study, in the presence of the abovementioned factors, simultaneously.

6.2.3.1 Consideration for an infectivity study in an in vivo model. For an *in vivo* study, the first step is the selection of an appropriate animal model.[31, 91, 260]

Of the various animal models such as mouse, rabbit, sheep and macaque used for microbicide testing, mouse or a macaque would be a suitable model for assaying infectivity.[261, 262] However in the case of a mouse model, the variations in the temperature of the vaginal lumen with respect to food intake and higher pH in a mouse vagina when compared to human vagina need careful consideration. Additionally, the virus stock is usually suspended in PBS which bears lower buffering capacity than semen. These differences together, have the ability to alter the behavior of the SMP and the resulting outcome of the study.

6.2.3.2 Influence of gelation kinetics and biodistribution on the ability of SMP to inhibit viral transport. Examining the effect of gelation kinetics on inhibiting viral transport may involve introducing the virus stock at varying time intervals after application of the SMP. On sacrifice, sectioning the mouse vaginal tract would provide a depth profile, revealing the extent of viral penetration into the gel and the tissue.[263] These studies will also be illustrative of epithelial damage, if any, on exposure to the SMP.[264] Future studies also need to examine the ability of the SMP to coat vaginal tissue and retain at the site of application. While our investigations reveal that the SMP can be applied as an *in situ* gelling system, effectiveness of SMP compels the need for complete coating over the vaginal tissue. Therefore, assessing the deployment characteristics of the SMP becomes imperative. Deployment of SMP can be evaluated using MRI studies in mouse, similar to those conducted by others in human subjects[128, 265, 266] or by using an approach similar to the one discussed in Chapter 2 of this dissertation. If either of the above two studies fail to demonstrate desired performance,

composition of the polymers can be altered to accommodate necessary changes in gelation and mechanical properties of the crosslinked polymer system. In our lab, we have demonstrated the ability to control properties of crosslinked polymer systems by varying the polymer backbone, concentration of the polymers and/or mole functionalization in the polymers.[258, 267]

6.2.3.3 SMP formulated with antiretroviral agents to provide dual level of protection against HIV-1 infection. Development of a microbicide delivery vehicle that physically inhibits viral transport, combined with agents that cause chemical inactivation of virus will create an effectual barrier to infectivity. Based on our preliminary data, we anticipate that SMP engineered with pH-responsive, reversible PBA-SHA crosslinks combined with BzB polymers may provide both chemical inhibition, through the activity of BzB as gp120 targeted entry inhibitors (detailed discussion in Chapter 5), and physical inhibition, through reduced movement of virions in the crosslinked polymer network. Studies required to characterize the drug delivery potential of the SMP would be parallel to those conducted in Chapter 4 of this dissertation. Looking forward, the PBA-SHA crosslinking technology can be formulated to deliver a hydrophilic drug such as tenofovir[66, 268] or hydrophobic candidates such as IQP-0528.[269] A system of this nature would benefit from dual mechanism of inhibition, provided by the semen-triggered impermeability and chemical inhibition of viral multiplicity.

6.2.3.4 Other suggested future studies. While the SMP demonstrates the ability to impede transport of macrophages, motility of sperms in the SMP still needs to be investigated.[270] All the assays conducted so far employed SMP at

100 mM buffering capacity. Examining the effect of lower buffering capacity of the formulation on erosion and barrier properties of SMP would be valuable. Based on our observation, SMP do reheal at pH above 5.5, however the timescale of rehealing demands further improvement of the formulation for instantaneous rehealing. This characteristic is essential, as the SMP layer could be ruptured during intercourse which, if fails to reheal may allow free passage for the migration of HIV-1. The HIV-1 transport study we conducted using human vaginal tissue showed complete protection; however, additional studies are required to determine the minimum thickness of the SMP required to completely inhibit transport of HIV-1 over a period of 6 to 8 h.

6.3 Chapter 4 - Vaginal microbicide gel for the delivery of IQP-0528, a pyrimidinedione analog with a dual mechanism of action against HIV-1

6.3.1 Summary of Research

Chapter 4 discusses the work on identification of a lead pyrimidinedione analog based on preformulation stability evaluation, followed by development of a vaginal gel formulation for the delivery of the lead pyrimidinedione analog. Detailed *in vitro* and *ex vivo* release, safety and antiviral activity evaluation of the vaginal gel formulation for its application as a microbicide was conducted. With the increasing number of hydrophobic and poorly permeable drugs being evaluated as microbicide candidates, it is critical to develop a robust, biocompatible drug delivery system that is stable and capable of delivering the

molecules to vaginal tissue at a concentration high enough to prevent viral replication. Results in Chapter 4 reveal that although many of the PYD congeners exhibit potent antiviral activity with dual-mechanism of action[271], their physicochemical properties render them nonfunctional from the perspective of drug delivery. The composition of the formulations used in this study, were selected based on the outcome from the studies conducted in Chapter 2 of this dissertation. Amount of glycerin in the formulation was chosen such that a homogenous dispersion of the solid API could be achieved, but at the same time maintains the osmolarity of the final formulation < 1000 mOsm to avoid toxicity to the tissue induced by hyperosmolarity of the formulation.[270]

Chapter 4 reports the development of two vaginal gels - 3.0% hydroxyethyl cellulose (HEC) formulation and a 0.65% carbopol formulation, for the delivery of IQP-0528. Stability studies under accelerated conditions confirmed the chemical stability of IQP-0528 and mechanical stability of the gel formulation for three months. *In vitro* release studies revealed that diffusion-controlled release of IQP-0528 occurred over 6 h, with an initial lag time of approximately 1 h. Based on the drug release profile, the 3.0% HEC gel was selected as the lead formulation for safety and activity evaluations. The *in vitro* and *ex vivo* safety evaluations showed no significant loss in cell viability or inflammatory response following treatment with a 3.0% HEC gel containing 0.25% IQP-0528. In an *in vitro* HIV-1 entry inhibition assay, the lead formulation showed an EC_{50} of 0.14 µg/mL of gel in culture media, which corresponds to approximately 0.001 µM IQP-0528. The antiviral activity was further confirmed

using polarized cervical explants, in which the formulation showed complete protection against HIV-1 infection.

IQP-0528 when unformulated did not show protection in a polarized ectocervical tissue model. However, when formulated in a semisolid gel formulation as described in Chapter 4, IQP-0528 showed protection against HIV-1 infection as indicated by >1 $\log_{10}$ reduction in HIV-1 p24 antigen levels. IQP-0528 (when unformulated) suffered from severe loss in antiviral activity in the presence of seminal fluid, which was circumvented when formulated in a 3.0% HEC gel formulation. This evidence emphasizes the role of formulation in retaining the efficacy of API with poor aqueous solubility and low tissue permeability. These results are encouraging and warrant further evaluation of IQP-0528 gel formulations in an *in vivo* model as well as the development of alternative formulations for the delivery of IQP-0528 as a microbicide.

6.4 Chapter 5 - Activity and Safety of Synthetic Lectin Based on Benzoboroxole Functionalized Polymers for Inhibition of HIV-1 Entry

6.4.1 Summary of Research

Lectins derived from plant and microbial sources constitute a vital class of entry inhibitors that target the oligomannose residues on the HIV envelope gp120. Despite their potency and specificity, success of lectin-based entry inhibitors may be impeded by issues in regards to economical production, formulation and potential mitogenicity. Therefore, there exists a gap in the HIV

therapeutics pipeline that underscores the need for mass producible, synthetic, broad-spectrum, and biocomptabile inhibitors of HIV entry. Research in Chapter 5, presents the development of a polymeric synthetic lectin, based on benzoboroxole (BzB), which exhibits weak affinity (~25 M^{-1}) for nonreducing sugars, similar to those found on the HIV envelope. High molecular weight BzB-functionalized polymers demonstrated antiviral activity that increased with an increase in ligand density and molecular weight of the polymer construct, revealing that polyvalency improves activity. Polymers showed significant increase in activity from 25 to 75 mol% BzB functionalization with EC_{50} of 15 μM and 15 nM, respectively. A further increase in mole functionalization to 90% resulted in an increase of the EC_{50} (59 ± 5 nM), likely due to the elongated rigid structure of the polymer chain compelled by electrostatic repulsion between the boronic acid groups. An increase in molecular weight of the polymer at 50 mol% BzB functionalization showed a gradual but significant increase in antiviral activity, with the highest activity seen with the 382 kDa polymer (EC_{50} of 1.1 ± 0.5 nM in CEM cells and 11 ± 3 nM in TZM-bl cells).

Supplementing the polymer backbone with 10 mol% sulfonic acid not only increased the aqueous solubility of the polymers by at least 50-fold, but also demonstrated a synergistic increase in anti-HIV activity (4.0 ± 1.5 nM in TZM-bl cells), possibly due to electrostatic interactions between the negatively charged polymer backbone and the positively charged V3-loop in the gp120. The benzoboroxole-sulfonic acid copolymers showed no decrease in activity in the presence of a seminal concentration of fructose ($p > 0.05$). Additionally, the

copolymers exhibit minimal, if any effect on the cellular viability, barrier properties, or cytokine levels in human reconstructed ectocervical tissue after 3 days of repeated exposure and did not show pronounced activity against a variety of other RNA and DNA viruses.

6.4.2 Critical Assessment and Suggested Future Work

While Chapter 5 of this dissertation describes the examination of safety and efficacy of BzB-functionalized polymers as gp120 targeted HIV-1 entry inhibitor, further work is required to enhance the activity and affinity of the synthetic lectin platform for glycans on the HIV-1 viral envelope. This would require identification of the exact mechanism of binding between BzB polymers and the sugars on the viral envelope.

6.4.2.1 Elucidate the mechanism of binding between BzB and gp120. The first step in attempt to develop polymers with improved activity involves bracketing the type of sugar moieties that are required for high affinity binding of BzB-functionalized polymers. These mechanistic studies may involve competitive binding studies, frontal affinity chromatography or X-ray crystal analysis.[272]

Impact of various concentrations of mannose derivatives on the binding affinity of BzB polymers to gp120 can be analyzed by preincubating the polymers with the sugars, prior to assaying antiviral activity of the BzB polymers. Mannose derivatives of interest include Manα(1-2)Man, Manα(1-3)Man, Manα (1-6)Man, Manα(1-2)Manα(1-2)Man, and Manα(1-3)Manα(1-6)Manα(1-6)Manα(1-3)Man.[273] In attempt to clarify, the terminal residues that are required to enhance entry

inhibition activity of BzB polymers, gp120 consisting of N-linked glycans (complex, hybrid, and high-mannose types) will require a haircut using site-specific enzymes. For example, endoglycosidase treatment of gp120 would digest both hybrid and high-mannose residues, whereas sialidase and β-galactosidase, would digest hybrid and complex-type sugars leaving only the high-mannose sugar chains on gp120.[273] Additionally, it is critical to examine if BzB-functionalized polymers are capable of discriminating between low and high-density mannose residues - an important feature that may enhance gp120-specific activity, and reduce nonspecific interactions between cellular glycoproteins and BzB polymers.[273]

6.4.2.2 Strategies to enhance activity and specificity of BzB constructs for gp120. Designing BzB constructs with enhanced affinity for gp120 can be achieved by creating a small library of constructs with varying architectures and conducting a screen using surface plasmon response (SPR). Constructs with varying chain lengths, spacing between ligands, chain flexibility and architecture constructed using solid phase peptide synthesis (SPPS) would allow precisely controlled synthesis.[234, 274-277] Similar approach employed by others showed ~50 fold increase in affinity of the ligands over the monovalent presentation of the ligand.[278]

An alternative approach includes a structure-guided identification of the lead. In this approach, on elucidating the crystal structure of the ligands, computer-aided tools can facilitate identification of ligands and multivalent constructs with high affinity for glycan on the gp120.[234, 279, 280] Similar approach

has found application in elucidating the binding domain and affinity of several protein-based lectins such as cyanovirin and griffithin for gp120.[279-281]

Polymer architectures studied in our lab thus far involve only linear architecture. It will be interesting to evaluate the effect of branched or dendritic architectures along with variations in chain flexibility and chain length around the ligand.[281] Creating nanoparticles and dendritic structures decorated with multiple ligands for inhibition of influenza have shown promising results.[282] Similar approach could prove useful in enhancing the activity of BzB-functionalized systems.

6.4.2.3 HIV-1 specific activity of BzB. Our results from the virus screen indicate that the activity of BzB polymers is specific to HIV-1. Although, it is conceivable that the high glycosylation density on the HIV-1 envelope could be responsible for this aberrant result; however further experiments are necessary to test this hypothesis.

6.4.2.4 Activity and safety of BzB functionalized polymers in vivo. Preliminary studies evaluating the effect of physiological concentrations of fructose showed no impact on the antiviral activity of the BzB polymers. These results require reassessment in an *in vivo* model in the presence of semen.

6.4.2.5 Activity against cell-associated viruses. Antiviral studies need to evaluate if BzB polymers show uncompromised activity against cell-associated viruses. This is critical as semen consists of both free and cell-associated viruses. Assays that evaluate the inhibition of cell-cell transmission of HIV-1 use a culture of target cells and a chronically infected cell-line in the presence of the

inhibitory agent.[283, 284] Inhibition of infection can be quantified by measuring cell-associated p24 antigen levels.

6.4.2.6 Applicability of BzB-polymers as self-therapeutic vaccine. Some recent studies support the hypothesis that mannose-targeted therapeutics against HIV-1 entry, may trigger deletion of glycosylation sites of gp120, exposing previously hidden epiptopes.[285, 286] This in turn may make the virus susceptible to immunological neutralization, initiating subsequent production of neutralizing antibodies against HIV-1. To test if this hypothesis of self-therapeutic vaccine applies to the BzB-polymers, investigation would involve three steps. Firstly, the genetic barrier to BzB-polymers as gp120 targeted therapeutics need to be evaluated, followed by identification of points of mutation and its impact on the N-glycosylation sites of the gp120.[287, 288] Finally, evaluate if point mutations in gp120 result in progressive increase in levels of neutralizing antibodies. Assays to evaluate the above hypothesis may involve dose escalating studies in a macaque model until the emergence of mutations in the glycosylation sequence is observed.[288, 289] Viral isolates will need to be sequenced to identify plausible mutations or deletions in the conserved glycosylation amino-acid sequence.[287, 289] Monitoring the levels of neutralizing antibodies throughout the study would serve as a direct measure of the ability of the BzB polymers as a therapeutic vaccine technology. The assumption that the gp120 does not evolve through an alternative mechanism to escape the pressure from these agents will require thorough investigation.

REFERENCES

1. Reeves, J. D.; Piefer, A. J. *Drugs* **2005,** 65, (13), 1747-66.

2. *Report on the global AIDS epidemic*; UNAIDS: 2010.

3. Quinn, T. C.; Overbaugh, J. *Science* **2005,** 308, (5728), 1582-83.

4. Lawn, S. D. *J Infect* **2004,** 48, (1), 1-12.

5. Mantell, J. E.; Needham, S. L.; Smit, J. A.; Hoffman, S.; Cebekhulu, Q.; Adams-Skinner, J.; Exner, T. M.; Mabude, Z.; Beksinska, M.; Stein, Z. A.; Milford, C. *Cult Health Sex* **2009,** 11, (2), 139-57.

6. Myer, L.; Kuhn, L.; Stein, Z. A.; Wright, T. C., Jr.; Denny, L. *Lancet Infect Dis* **2005,** 5, (12), 786-94.

7. Glynn, J. R.; Carael, M.; Auvert, B.; Kahindo, M.; Chege, J.; Musonda, R.; Kaona, F.; Buve, A. *AIDS* **2001,** 15, (Supp 4), S51-S60.

8. Madkan, V. K.; Giancola, A. A.; Sra, K. K.; Tyring, S. K. *Arch Dermatol* **2006,** 142, (3), 365-70.

9. Stein, Z. A. *Am J Pub Health* **1990,** 80, (4), 460-62.

10. Hendrix, C. W.; Cao, Y. J.; Fuchs, E. J. *Annu Rev Pharmacol Toxicol* **2009,** 49, 349-75.

11. Cutler, B.; Justman, J. *Lancet Infect Dis* **2008,** 8, (11), 685-97.

12. Stone, A. *Nat Rev Drug Discov* **2002,** 1, (12), 977-85.

13. Nuttall, J. *Drugs* **2010,** 70, (10), 1231-43.

14. Garg, A. B.; Nuttall, J.; Romano, J. *Antiviral Chem Chemother* **2009,** 19, (4), 143-50.

15. Klasse, P. J.; Shattock, R.; Moore, J. P. *Annu Rev Med* **2008,** 59, 455-71.

16. Kelvin, E. A.; Smith, R. A.; Mantell, J. E.; Stein, Z. A. *Am J Public Health* **2009,** 99, (6), 985-87.

17. Bowman, M.-C.; Archin, N. M.; Margolis, D. M. *Exp Rev Mol Med* **2009,** 11, (1).

18. D'Cruz, O. J.; Uckun, F. M. *Curr Opin Invest Drug* **2008,** 9, (2), 152-69.

19. Cohen, J. *Science* **2010,** 329, (5990), 374-75.

20. Woolfson, A. D.; Malcolm, R. K.; Gallagher, R. *Crit Rev Ther Drug Carrier Syst* **2000,** 17, (5), 509-55.

21. Vermani, K.; Garg, S. *Pharm Sci Technol Today* **2000,** 3, (10), 359-64.

22. Barnhart Kurt, T.; Izquierdo, A.; Pretorius, E. S.; Shera David, M.; Shabbout, M.; Shaunik, A. *Hum Reprod* **2006,** 21, (6), 1618-22.

23. Kieweg, S. L.; Geonnotti, A. R.; Katz, D. F. *J Pharm Sci* **2004,** 93, (12), 2941-52.

24. Okano, A.; Ogawa, H.; Takahashi, H.; Geshi, M. *J Reprod Dev* **2007,** 53, (4), 923-30.

25. Poonia, B.; Walter, L.; Dufour, J.; Harrison, R.; Marx, P. A.; Veazey, R. S. *J Endocrinol* **2006,** 190, (3), 829-35.

26. Sato, T.; Fukazawa, Y.; Kojima, H.; Enari, M.; Iguchi, T.; Ohta, Y. *Anat Rec* **1997,** 248, (1), 76-83.

27. Hsu, C. C.; Park, J. Y.; Ho, N. F.; Higuchi, W. I.; Fox, J. L. *J Pharm Sci* **1983,** 72, (6), 674-80.

28. Wira, C. R.; Fahey, J. V.; Sentman, C. L.; Pioli, P. A.; Shen, L. *Immunol Rev* **2005,** 206, (1), 306-35.

29. Firoz Mian, M.; Ashkar, A. A. *Am J Reprod Immunol* **2011,** 65, (3), 344-51.

30. Cone, R. A. *Adv Drug Deliv Rev* **2009,** 61, (2), 75-85.

31. Lai, S. K.; Hida, K.; Shukair, S.; Wang, Y. Y.; Figueiredo, A.; Cone, R.; Hope, T. J.; Hanes, J. *J Virol* **2009,** 83, (21), 11196-200.

32. Iqbal, S. M.; Kaul, R. *Am J Reprod Immunol* **2008,** 59, (1), 44-54.

33. Iwasaki, A. *Nat Rev Immunol* **2010,** 10, (10), 699-711.

34. Kaul, R.; Pettengell, C.; Sheth, P. M.; Sunderji, S.; Biringer, A.; MacDonald, K.; Walmsley, S.; Rebbapragada, A. *J Reprod Immunol* **2008,** 77, (1), 32-40.

35. Clarke, J. G.; Peipert, J. F.; Hillier, S. L.; Heber, W.; Boardman, L.; Moench, T. R.; Mayer, K. *Sex Transm Dis* **2002,** 29, (5), 288-93.

36. Sobel, J. D. *Curr Infect Dis Rep* **1999,** 1, (4), 379-83.

37. Hladik, F.; McElrath, M. J. *Nat Rev Immunol* **2008,** 8, (6), 447-57.

38. Hladik, F.; Sakchalathorn, P.; Ballweber, L.; Lentz, G.; Fialkow, M.; Eschenbach, D.; McElrath, M. J. *Immunity* **2007,** 26, (2), 257-70.

39. Hladik, F.; Doncel, G. F. *Antiviral Res* **2010,** 88, (Supp 1), S3-S9.

40. Permanyer, M.; Ballana, E.; Esté, J. A. *Trends Microbiol* **2010,** 18, (12), 543-51.

41. Haase, A. T. *Nature* **2010,** 464, (7286), 217-23.

42. Miyauchi, K.; Kim, Y.; Latinovic, O.; Morozov, V.; Melikyan, G. B. *Cell* **2009,** 137, (3), 433-44.

43. Shattock, R. J.; Moore, J. P. *Nat Rev Microbiol* **2003,** 1, (1), 25-34.

44. Kaushic, C.; Ferreira, V. H.; Kafka, J. K.; Nazli, A. *Am J Reprod Immunol* **2010,** 63, (6), 566-75.

45. Hladik, F.; Hope, T. J. *Curr HIV/AIDS Rep* **2009,** 6, (1), 20-28.

46. Roth, S.; Monsour, M.; Dowland, A.; Guenthner, P. C.; Hancock, K.; Ou, C. Y.; Dezzutti, C. S. *Antimicrob Agents Chemother* **2007,** 51, (6), 1972-78.

47. Fox, J.; Fidler, S. *Antiviral Res* **2010,** 85, (1), 276-85.

48. Maher, D.; Wu, X.; Schacker, T.; Horbul, J.; Southern, P. *Proc Natl Acad Sci* **2005,** 102, (32), 11504-09.

49. Caffrey, M. *Trends Microbiol* **2011,** 19, (4), 191-97.

50. Balzarini, J. *Antiviral Res* **2006,** 71, (2-3), 237-47.

51. Doncel, G. F.; Joseph, T.; Thurman, A. R. *Am J Reprod Immunol* **2011,** 65, (3), 292-301.

52. Owen, D. H.; Katz, D. F. *J Androl* **2005,** 26, (4), 459-69.

53. Tevi-Benissan, C.; Belec, L.; Levy, M.; Schneider-Fauveau, V.; Si Mohamed, A.; Hallouin, M. C.; Matta, M.; Gresenguet, G. *Clin Diagn Lab Immunol* **1997,** 4, (3), 367-74.

54. Quayle, A. J.; Xu, C.; Mayer, K. H.; Anderson, D. J. *J Infect Dis* **1997,** 176, (4), 960-68.

55. das Neves, J.; Bahia, M. F. *Int J Pharm* **2006,** 318, (1-2), 1-14.

56. Kieweg Sarah, L.; Katz David, F. *J Biomech Eng* **2006,** 128, (4), 540-53.

57. Lai Bonnie, E.; Xie Yao, Q.; Lavine Michael, L.; Szeri Andrew, J.; Owen Derek, H.; Katz David, F. *J Pharm Sci* **2008,** 97, (2), 1030-38.

58. Mahalingam, A.; Smith, E.; Fabian, J.; Damian, F. R.; Peters, J. J.; Clark, M. R.; Friend, D. R.; Katz, D. F.; Kiser, P. F. *Pharm Res* **2010,** 27, (11), 2478-91.

59. Olmsted, S. S.; Meyn, L. A.; Rohan, L. C.; Hillier, S. L. *Sex Transm Dis* **2003,** 30, (3), 257-61.

60. Van Damme, L.; Niruthisard, S.; Atisook, R.; Boer, K.; Dally, L.; Laga, M.; Lange, J. M.; Karam, M.; Perriens, J. H. *AIDS* **1998,** 12, (4), 433-37.

61. Tabet, S. R.; Surawicz, C.; Horton, S.; Paradise, M.; Coletti, A. S.; Gross, M.; Fleming, T. R.; Buchbinder, S.; Haggitt, R. C.; Levine, H.; Kelly, C. W.; Celum, C. L. *Sex Transm Dis* **1999,** 26, (10), 564-71.

62. Mayer, K. H.; Peipert, J.; Fleming, T.; Fullem, A.; Moench, T.; Cu-Uvin, S.; Bentley, M.; Chesney, M.; Rosenberg, Z. *Clin Infect Dis* **2001,** 32, (3), 476-82.

63. Garg, S.; Anderson, R. A.; Chany, C. J., 2nd; Waller, D. P.; Diao, X. H.; Vermani, K.; Zaneveld, L. J. *Contraception* **2001,** 64, (1), 67-75.

64. Morrow, K.; Rosen, R.; Richter, L.; Emans, A.; Forbes, A.; Day, J.; Morar, N.; Maslankowski, L.; Profy, A. T.; Kelly, C.; Abdool Karim, S. S.; Mayer, K. H. *J Womens Health* **2003,** 12, (7), 655-66.

65. Ramjee, G.; Morar, N. S.; Braunstein, S.; Friedland, B.; Jones, H.; van de Wijgert, J. *AIDS Res Ther* **2007,** 4, 20.

66. Abdool Karim, Q.; Abdool Karim, S. S.; Frohlich, J. A.; Grobler, A. C.; Baxter, C.; Mansoor, L. E.; Kharsany, A. B.; Sibeko, S.; Mlisana, K. P.; Omar, Z.; Gengiah, T. N.; Maarschalk, S.; Arulappan, N.; Mlotshwa, M.; Morris, L.; Taylor, D. *Science* **2010,** 329, (5996), 1168-74.

67. Grant, R. M.; Hamer, D.; Hope, T.; Johnston, R.; Lange, J.; Lederman, M. M.; Lieberman, J.; Miller, C. J.; Moore, J. P.; Mosier, D. E.; Richman, D. D.; Schooley, R. T.; Springer, M. S.; Veazey, R. S.; Wainberg, M. A. *Science* **2008,** 321, (5888), 532-34.

68. Harrison, P. F.; Rosenberg, Z.; Bowcut, J. *Clin Infect Dis* **2003,** 36, (10), 1290-94.

69. Cohen, J. *Science* **2008,** 319, (5866), 1026-27.

70. van de Wijgert, J. H.; Shattock, R. J. *AIDS* **2007,** 21, (18), 2369-76.

71. Moscicki, A. B. *J Infect Chemother* **2008,** 14, (5), 337-41.

72. Cone, R. A.; Hoen, T.; Wong, X.; Abusuwwa, R.; Anderson, D. J.; Moench, T. R. *BMC Infect Dis* **2006,** 6, 90.

73. Weiss, R. A. *Clin Exp Immunol* **2008,** 152, (2), 201-10.

74. Lackman-Smith, C.; Osterling, C.; Luckenbaugh, K.; Mankowski, M.; Snyder, B.; Lewis, G.; Paull, J.; Profy, A.; Ptak, R. G.; Buckheit, R. W., Jr.; Watson, K. M.; Cummins, J. E., Jr.; Sanders-Beer, B. E. *Antimicrob Agents Chemother* **2008,** 52, (5), 1768-81.

75. Cummins, J. E., Jr.; Guarner, J.; Flowers, L.; Guenthner, P. C.; Bartlett, J.; Morken, T.; Grohskopf, L. A.; Paxton, L.; Dezzutti, C. S. *Antimicrob Agents Chemother* **2007,** 51, (5), 1770-79.

76. Brayden, D. J.; Martinez, M. N. *Adv Drug Deliv Rev* **2007,** 59, (11), 1071-72.

77. Wilson, D. P.; Coplan, P. M.; Wainberg, M. A.; Blower, S. M. *Proc Natl Acad Sci* **2008,** 105, (28), 9835-40.

78. D'Cruz, O. J.; Uckun, F. M. *J Antimicrob Chemother* **2006,** 57, (3), 411-23.

79. Mahalingam, A.; Simmons, A. P.; Ugaonkar, S. R.; Watson, K. M.; Dezzutti, C. S.; Rohan, L. C.; Buckheit, R. W., Jr.; Kiser, P. F. *Antimicrob Agents Chemother* **2011,** 55, (4), 1650-60.

80. Nel, A. M.; Coplan, P.; van, d. W. J. H.; Kapiga, S. H.; von, M. C.; Geubbels, E.; Vyankandondera, J.; Rees, H. V.; Masenga, G.; Kiwelu, I.; Moyes, J.; Smythe, S. C. *AIDS* **2009,** 23, (12), 1531-38.

81. Fletcher, P. S.; Elliott, J.; Grivel, J. C.; Margolis, L.; Anton, P.; McGowan, I.; Shattock, R. J. *AIDS* **2006,** 20, (9), 1237-45.

82. Liu, S.; Lu, H.; Niu, J.; Xu, Y.; Wu, S.; Jiang, S. *J Biol Chem* **2005,** 280, (12), 11259-73.

83. Buffa, V.; Stieh, D.; Mamhood, N.; Hu, Q.; Fletcher, P.; Shattock, R. J. *J Gen Virol* **2009,** 90, (1), 234-43.

84. Tiwari, V.; Shukla, S. Y.; Shukla, D. *Antiviral Res* **2009,** 84, (1), 67-75.

85. Westby, M.; van der Ryst, E. *Antiviral Chem Chemother* **2010,** 20, (5), 179-92.

86. Balzarini, J.; Van Damme, L. *Lancet* **2007,** 369, (9563), 787-97.

87. Sluis-Cremer, N.; Tachedjian, G. *Virus Res* **2008,** 134, (1-2), 147-56.

88. *Microbicides: ways forward*; Alliance for microbicide development: 2010.

89. Minces, L. R.; McGowan, I. *Curr Infect Dis Rep* **2010,** 12, (1), 56-62.

90. Esté, J. A.; Cihlar, T. *Antiviral Res* **2010,** 85, (1), 25-33.

91. Coutsinos, D.; Sloan, R.; Wainberg, M. A. *Future Virol* **2008,** 3, (6), 529-32.

92. das Neves, J.; da Silva, M. V.; Goncalves, M. P.; Amaral, M. H.; Bahia, M. F. *Curr Drug Deliv* **2009,** 6, (1), 83-92.

93. Pirillo, M.; Palmisano, L.; Pellegrini, M.; Galluzzo, C.; Weimer, L.; Bucciardini, R.; Fragola, V.; Andreotti, M.; Marchei, E.; Pichini, S.; Vella, S.; Giuliano, M. *AIDS Res Hum Retrovir* **2010,** 26, (5), 541-45.

94. Este, J. A.; Telenti, A. *Lancet* **2007,** 370, (9581), 81-88.

95. Owen, D. H.; Peters, J. J.; Katz, D. F. *Contraception* **2000,** 62, (6), 321-26.

96. Sanso, G. Vaginal gel formulation. 2000-1414, 2001.

97. Valenta, C. *Adv Drug Deliv Rev* **2005,** 57, (11), 1692-712.

98. Russo Paul, S., A perspective on reversible gels and related systems. In *Reversible polymeric gels and related systems*, American Chemical Society: 1987; Vol. 350, pp 1-21.

99. Almdal, K.; Dyre, J.; Hvidt, S.; Kramer, O. *Polym Gels Netw* **1993,** 1, (1), 5-17.

100. Edwards, S. F. *Farad Disc Chem Soc* **1974,** 57, 47-55.

101. Flory, P. J. *Farad Disc Chem Soc* **1974,** 57, 7-18.

102. Ferry, J. D. *J Res Natl Bur Stand* **1948,** 41, (1), 53-62.

103. Bhattarai, N.; Gunn, J.; Zhang, M. *Adv Drug Deliv Rev* **2010,** 62, (1), 83-99.

104. Hoffman, A. S. *Adv Drug Deliv Rev* **2002,** 54, (1), 3-12.

105. Peppas, N. A.; Huang, Y.; Torres-Lugo, M.; Ward, J. H.; Zhang, J. *Annu Rev Biomed Eng* **2000,** 2, (1), 9-29.

106. Salamat-Miller, N.; Chittchang, M.; Johnston, T. P. *Adv Drug Deliv Rev* **2005,** 57, (11), 1666-91.

107. Peppas, N. A.; Khare, A. R. *Adv Drug Deliv Rev* **1993,** 11, (1-2), 1-35.

108. Vasile, C.; Dumitriu, R. P.; Cheaburu, C. N.; Oprea, A. M. *App Surf Sci* **2009,** 256, (3, Supp 1), S65-S71.

109. Nisato, G.; Schosseler, F.; Candau, S. J. *Polym Gels Netw* **1996,** 4, (5-6), 481-98.

110. Flory, P. J. *Science* **1975,** 188, (4195), 1268-76.

111. Kolb, M. *Polym Gels Netw* **1996,** 4, (5-6), 375-82.

112. Barton, A. F. M., *Handbook of solubility parameters and other cohesion parameters*. 2nd ed.; CRC Press: 1991.

113. Flory, P. J., *Principles of polymer chemistry*. 2nd ed.; Cornell Univ Press: 2000; p 640.

114. Coleman, M. M.; Painter, P. C., *Fundamentals of polymer science: An introductory text*. 2nd ed.; CRC Press: 1998; p 496.

115. Ross-Murphy, S. B. *Polym Gels Netw* **1994,** 2, (3-4), 229-37.

116. Knuth, K.; Amiji, M.; Robinson, J. R. *Adv Drug Deliv Rev* **1993,** 11, (1-2), 137-67.

117. Kieweg, S. L. Mechanical analysis of vaginal gels intended for microbicide application. 2005.

118. Kieweg, S. L.; Katz, D. F. *J Pharm Sci* **2007,** 96, (4), 835-50.

119. Kiser, P. F.; Katz, D. F.; Stewart, R. J. Bioresponsive polymer system for delivery of microbicides. 2005-US10285, 2005.

120. Jay, J. I.; Shukair, S.; Langheinrich, K.; Hanson, M. C.; Cianci, G. C.; Johnson, T. J.; Clark, M. R.; Hope, T. J.; Kiser, P. F. *Adv Func Mat* **2009,** 19, (18), 2969-77.

121. Wei, G.; Lu, W. Temperature-sensitive in situ vaginal gel preparations for treating infection. 1002-5582, 2005.

122. Zhang, D. Pharmaceutical compositions of new vaginal-use in-situ gel preparation and its production process. 1007-2312, 2006.

123. Lai, B. E.; Geonnotti, A. R.; DeSoto, M. G.; Montefiori, D. C.; Katz, D. F. *Antiviral Res* **2010,** 88, (2), 143-51.

124. Mathiowitz, E., *Encyclopedia of controlled drug delivery*. 1st ed.; Wiley-Interscience: 1991; Vol. 2, p 1061.

125. Amsden, B. *Macromolecules* **1998,** 31, (23), 8382-95.

126. Higuchi, W. I. *J Pharm Sci* **1962,** 51, 802-04.

127. Smart, J. D. *Adv Drug Deliv Rev* **2005,** 57, (11), 1556-68.

128. Barnhart, K.; Kulp, J. L.; Rosen, M.; Shera, D. M. *Contraception* **2009,** 79, (4), 297-303.

129. Barnhart, K. T.; Pretorius, E. S.; Shera, D. M.; Shabbout, M.; Shaunik, A. *Contraception* **2006,** 73, (1), 82-87.

130. Justin-Temu, M.; Damian, F.; Kinget, R.; Van Den Mooter, G. *J Womens Health* **2004,** 13, (7), 834-44.

131. Owen, D. H.; Peters, J. J.; Kieweg, S. L.; Geonnotti, A. R.; Schnaare, R. L.; Katz, D. F. *J Pharm Sci* **2007,** 96, (3), 661-69.

132. Barnhart, K. T.; Pretorius, E. S.; Shaunik, A.; Timbers, K.; Nasution, M.; Mauck, C. *Contraception* **2005,** 72, (1), 65.

133. Szeri, A. J.; Park, S. C.; Verguet, S.; Weiss, A.; Katz, D. F. *Phys Fluids* **2008,** 20, (8), 83101.

134. Nicolaou, C. A.; Brown, N.; Pattichis, C. S. *Curr Opin Drug Discov Devel* **2007,** 10, (3), 316-24.

135. Handl, J.; Kell, D. B.; Knowles, J. *IEEE/ACM Trans Comput Biol Bioinform* **2007,** 4, (2), 279-92.

136. Rajamani, R.; Good, A. C. *Curr Opin Drug Discov Devel* **2007,** 10, (3), 308-15.

137. Chopra, S.; Motwani, S. K.; Iqbal, Z.; Talegaonkar, S.; Ahmad, F. J.; Khar, R. K. *Eur J Pharm Biopharm* **2007,** 67, (1), 120-31.

138. Furlanetto, S.; Cirri, M.; Maestrelli, F.; Corti, G.; Mura, P. *Eur J Pharm Biopharm* **2006,** 62, (1), 77-84.

139. Patton, D. L.; Sweeney, Y. T.; Balkus, J. E.; Rohan, L. C.; Moncla, B. J.; Parniak, M. A.; Hillier, S. L. *Antimicrob Agents Chemother* **2007,** 51, (5), 1608-15.

140. Terrazas-Aranda, K.; Van Herrewege, Y.; Lewi, P. J.; Van Roey, J.; Vanham, G. *Antiviral Chem Chemother* **2007,** 18, (3), 141-51.

141. Barditch-Crovo, P.; Deeks, S. G.; Collier, A.; Safrin, S.; Coakley, D. F.; Miller, M.; Kearney, B. P.; Coleman, R. L.; Lamy, P. D.; Kahn, J. O.; McGowan, I.; Lietman, P. S. *Antimicrob Agents Chemother* **2001,** 45, (10), 2733-39.

142. Bateman, C. *S Afr Med J* **2007,** 97, (7), 496.

143. Mayer, K. H.; Maslankowski, L. A.; Gai, F.; El-Sadr, W. M.; Justman, J.; Kwiecien, A.; Masse, B.; Eshleman, S. H.; Hendrix, C.; Morrow, K.; Rooney, J. F.; Soto-Torres, L. *AIDS* **2006,** 20, (4), 543-51.

144. Cornell, J. A., *Experiments with mixtures*. 3rd ed.; John Wiley & Sons Inc.: New York, 2002.

145. Chu, J. S.; Amidon, G. L.; Weiner, N. D.; Goldberg, A. H. *Pharm Res* **1991,** 8, (11), 1401-07.

146. Owen, D. H.; Katz, D. F. *Contraception* **1999,** 59, (2), 91-95.

147. Henderson, M. H.; Couchman, G. M.; Walmer, D. K.; Peters, J. J.; Owen, D. H.; Brown, M. A.; Lavine, M. L.; Katz, D. F. *Contraception* **2007,** 75, (2), 142-51.

148. Mauck Christine, K.; Katz, D.; Sandefer Erik, P.; Nasution Marlina, D.; Henderson, M.; Digenis George, A.; Su, I.; Page, R.; Barnhart, K. *Contraception* **2008,** 77, (3), 195-204.

149. Kilmarx, P. H.; Blanchard, K.; Chaikummao, S.; Friedland, B. A.; Srivirojana, N.; Connolly, C.; Witwatwongwana, P.; Supawitkul, S.; Mock, P. A.; Chaowanachan, T.; Tappero, J. *Sex Transm Dis* **2008,** 35, (3), 226-32.

150. Wang, Y.; Lee, C. H. *Contraception* **2002,** 66, (4), 281-87.

151. Szeri AJ, P. S., Tasoglu S and Katz DF, Effects of dilution on coating flow of an anti-HIV microbicide vehicle. In *Am Phys Soc*, Minneapolis, MN, 2009.

152. Tien, D.; Schnaare, R. L.; Kang, F.; Cohl, G.; McCormick, T. J.; Moench, T. R.; Doncel, G.; Watson, K.; Buckheit, R. W.; Lewis, M. G.; Schwartz, J.; Douville, K.; Romano, J. W. *AIDS Res Hum Retroviruses* **2005,** 21, (10), 845-53.

153. Lai, B. E.; Xie, Y. Q.; Lavine, M. L.; Szeri, A. J.; Owen, D. H.; Katz, D. F. *J Pharm Sci* **2008,** 97, (2), 1030-38.

154. Sassi, A. B.; Isaacs, C. E.; Moncla, B. J.; Gupta, P.; Hillier, S. L.; Rohan, L. C. *J Pharm Sci* **2008,** 97, (8), 3123-39.

155. Alvarez-Lorenzo, C.; Concheiro, A. *Mini Rev Med Chem* **2008,** 8, (11), 1065-74.

156. Bawa, P.; Pillay, V.; Choonara, Y. E.; du Toit, L. C. *Biomed Mater* **2009,** 4, (2).

157. Saeed, A. O.; Magnússon, J. P.; Twaites, B.; Alexander, C., *Stimuli-responsive and 'active' polymers in drug delivery*. John Wiley & Sons, Ltd: 2009; p 61-88.

158. Soyez, H.; Schacht, E. *Pharm Technol Eur* **1997,** 9, (10), 50-56.

159. Traitel, T.; Goldbart, R.; Kost, J. *J Biomater Sci Polym Ed* **2008,** 19, (6), 755-67.

160. Owen, D. H.; Peters, J. J.; Katz, D. F. In *Rheological properties of microbicidal formulations governing spreading and retention in the vagina and rectum*, Microbicides, Antwerp, Belgium, 2002; Antwerp, Belgium, 2002.

161. Stolowitz, M. L.; Ahlem, C.; Hughes, K. A.; Kaiser, R. J.; Kesicki, E. A.; Li, G.; Lund, K. P.; Torkelson, S. M.; Wiley, J. P. *Bioconjug Chem* **2001,** 12, (2), 229-39.

162. Wiley, J. P.; Hughes, K. A.; Kaiser, R. J.; Kesicki, E. A.; Lund, K. P.; Stolowitz, M. L. *Bioconjug Chem* **2001,** 12, (2), 240-50.

163. Roberts, M. C.; Hanson, M. C.; Massey, A. P.; Karren, E. A.; Kiser, P. F. *Adv Mater* **2007,** 19, (18), 2503-07.

164. Roberts, M. C.; Mahalingam, A.; Hanson, M. C.; Kiser, P. F. *Macromolecules* **2008,** 41, (22), 8832-40.

165. Springsteen, G.; Wang, B. *Tetrahedron* **2002,** 58, (26), 5291-300

166. Rihova, B.; Bilej, M.; Vetvicka, V.; Ulbrich, K.; Strohalm, J.; Kopecek, J.; Duncan, R. *Biomaterials* **1989,** 10, (5), 335-42.

167. Carlstedt, I.; Lindgren, H.; Sheehan, J. K.; Ulmsten, U.; Wingerup, L. *Biochem J* **1983,** 211, (1), 13-22.

168. Jay, J. I.; Shukair, S.; Langheinrich, K.; Hanson, M. C.; Cianci, G. C.; Johnson, T. J.; Clark, M. R.; Hope, T. J.; Kiser, P. F. *Adv Funct Mater* **2009,** 19, (18), 2969-77.

169. Madsen, F.; Eberth, K.; Smart, J. D. *J Control Release* **1998,** 50, (1-3), 167-78.

170. Hagerstrom, H.; Edsman, K. *Eur J Pharm Sci* **2003,** 18, (5), 349-57.

171. Fichorova, R. N.; Rheinwald, J. G.; Anderson, D. J. *Biol Reprod* **1997,** 57, (4), 847-55.

172. Ayehunie, S.; Cannon, C.; Lamore, S.; Kubilus, J.; Anderson, D. J.; Pudney, J.; Klausner, M. *Toxicol In Vitro* **2006,** 20, (5), 689-98.

173. Rohan, L. C.; Moncla, B. J.; Kunjara Na Ayudhya, R. P.; Cost, M.; Huang, Y.; Gai, F.; Billitto, N.; Lynam, J. D.; Pryke, K.; Graebing, P.; Hopkins, N.; Rooney, J. F.; Friend, D.; Dezzutti, C. S. *PLoS One* **2010,** 5, (2), e9310.

174. Hermanson, G. T., *Bioconjugate techniques*. 2nd ed.; Academic Press: 2008; p 785.

175. McDonald, D.; Vodicka, M. A.; Lucero, G.; Svitkina, T. M.; Borisy, G. G.; Emerman, M.; Hope, T. J. *J Cell Biol* **2002,** 159, (3), 441-52.

176. Robb, I. D.; Smeulders, J. B. A. F. *Polymer* **1997,** 38, (9), 2165-69

177. Ide, N.; Sato, T.; Miyamoto, T.; Fukuda, T. *Macromolecules* **1998,** 31, (25), 8878-85.

178. Choplin, L.; Sabatié, J. *Rheol Acta* **1986,** 25, (6), 570-79.

179. Inoue, T.; Osaki, K. *Rheol Acta* **1993,** 32, 550-55.

180. Valentine, M. T.; Kaplan, P. D.; Thota, D.; Crocker, J. C.; Gisler, T.; Prud'homme, R. K.; Beck, M.; Weitz, D. A. *Phys Rev E* **2001,** 64, (6).

181. Wirtz, D. *Annu Rev Biophys* **2009,** 38, 301-26.

182. Fichorova, R. N.; Bajpai, M.; Chandra, N.; Hsiu, J. G.; Spangler, M.; Ratnam, V.; Doncel, G. F. *Biol Reprod* **2004,** 71, (3), 761-69.

183. Youle, M.; Wainberg, M. A. *J Int Assoc Physicians AIDS Care* **2003,** 2, (3), 102-05.

184. Smith, S. M. *Retrovirology* **2004,** 1, 16.

185. Garg, A. B.; Nuttall, J.; Romano, J. *Antiviral Chem Chemother* **2008,** 19, (4), 143-50.

186. Buckheit, R. W., Jr.; Watson, K.; Fliakas-Boltz, V.; Russell, J.; Loftus, T. L.; Osterling, M. C.; Turpin, J. A.; Pallansch, L. A.; White, E. L.; Lee, J. W.; Lee, S. H.; Oh, J. W.; Kwon, H. S.; Chung, S. G.; Cho, E. H. *Antimicrob Agents Chemother* **2001,** 45, (2), 393-400.

187. Buckheit Robert, W., Jr.; Hartman Tracy, L.; Watson Karen, M.; Kwon Ho, S.; Lee Sun, H.; Lee Jae, W.; Kang Dong, W.; Chung Sun, G.; Cho Eui, H. *Antiviral Chem Chemother* **2007,** 18, (5), 259-75.

188. Buckheit Robert, W., Jr.; Hartman Tracy, L.; Watson Karen, M.; Chung, S.-G.; Cho, E.-H. *Antimicrob Agents Chemother* **2008,** 52, (1), 225-36.

189. Singla, A. K.; Chawla, M.; Singh, A. *Drug Dev Ind Pharm* **2000,** 26, (9), 913-24.

190. Walters, K. A., *Dermatological and transdermal formulations*. 1st ed.; Informa Healthcare: 2002; p 592.

191. Milligan, G. N.; Dudley, K. L.; Bourne, N.; Reece, A.; Stanberry, L. R. *Sex Transm Dis* **2002,** 29, (10), 597-605.

192. van Eyk, A. D.; van der Bijl, P. *Int J Pharm* **2005,** 305, (1-2), 105-11.

193. Dezzutti, C. S.; James, V. N.; Ramos, A.; Sullivan, S. T.; Siddig, A.; Bush, T. J.; Grohskopf, L. A.; Paxton, L.; Subbarao, S.; Hart, C. E. *Antimicrob Agents Chemother* **2004,** 48, (10), 3834-44.

194. Gupta, K. M.; Pearce, S. M.; Poursaid, A. E.; Aliyar, H. A.; Tresco, P. A.; Mitchnik, M. A.; Kiser, P. F. *J Pharm Sci* **2008,** 97, (10), 4228-39.

195. Kulkarni, U.; Mahalingam, R.; Pather, I.; Li, X.; Jasti, B. *J Pharm Sci* **2010,** 99, (3), 1265-77.

196. van Eyk, A. D.; van der Biijl, P. *SADJ* **2006,** 61, (5), 200-03.

197. Ijeoma F. Uchegbu, A. G. S., *Polymers in drug delivery*. CRC Press: 2006.

198. Flynn, G. L.; Shah, V. P.; Tenjarla, S. N.; Corbo, M.; DeMagistris, D.; Feldman, T. G.; Franz, T. J.; Miran, D. R.; Pearce, D. M.; Sequeira, J. A.; Swarbrick, J.; Wang, J. C.; Yacobi, A.; Zatz, J. L. *Pharm Res* **1999,** 16, (9), 1325-30.

199. Fichorova, R. N.; Anderson, D. J. *Biol Reprod* **1999,** 60, (2), 508-14.

200. Mahalingam, A.; Smith, E.; Fabian, J.; Damian, F. R.; Peters, J. J.; Clark, M. R.; Friend, D. R.; Katz, D. F.; Kiser, P. F. *Pharm Res* **2010**, 27, (11), 2478-91.

201. Squier, C. A.; Mantz, M. J.; Schlievert, P. M.; Davis, C. C. *J Pharm Sci* **2008,** 97, (1), 9-21.

202. Hadgraft, J.; Lane, M. E. *Int J Pharm* **2005,** 305, (1-2), 2-12.

203. Lewi, P.; Arnold, E.; Andries, K.; Bohets, H.; Borghys, H.; Clark, A.; Daeyaert, F.; Das, K.; de Bethune, M. P.; de Jonge, M.; Heeres, J.; Koymans, L.; Leempoels, J.; Peeters, J.; Timmerman, P.; Van den Broeck, W.; Vanhoutte, F.; Van't Klooster, G.; Vinkers, M.; Volovik, Y.; Janssen, P. A. *Drugs R D* **2004,** 5, (5), 245-57.

204. Desai, A.; Lee, M. D., *Gibaldi's drug delivery systems*. ASHP: 2007; p 505.

205. Wyatt, R.; Kwong, P. D.; Desjardins, E.; Sweet, R. W.; Robinson, J.; Hendrickson, W. A.; Sodroski, J. G. *Nature* **1998,** 393, (6686), 705-11.

206. Poignard, P.; Saphire, E. O.; Parren, P. W.; Burton, D. R. *Annu Rev Immunol* **2001,** 19, 253-74.

207. Gallaher, W. R.; Ball, J. M.; Garry, R. F.; Martin-Amedee, A. M.; Montelaro, R. C. *AIDS Res Hum Retrovir* **1995,** 11, (2), 191-202.

208. Leonard, C. K.; Spellman, M. W.; Riddle, L.; Harris, R. J.; Thomas, J. N.; Gregory, T. J. *J Biol Chem* **1990,** 265, (18), 10373-82.

209. Balzarini, J.; Van Laethem, K.; Hatse, S.; Vermeire, K.; De Clercq, E.; Peumans, W.; Van Damme, E.; Vandamme, A. M.; Bolmstedt, A.; Schols, D. *J Virol* **2004,** 78, (19), 10617-27.

210. Balzarini, J.; Van Laethem, K.; Hatse, S.; Froeyen, M.; Van Damme, E.; Bolmstedt, A.; Peumans, W.; De Clercq, E.; Schols, D. *Mol Pharmacol* **2005,** 67, (5), 1556-65.

211. Balzarini, J.; Van Laethem, K.; Hatse, S.; Froeyen, M.; Peumans, W.; Van Damme, E.; Schols, D. *J Biol Chem* **2005,** 280, (49), 41005-14.

212. Balzarini, J.; Van Laethem, K.; Peumans, W. J.; Van Damme, E. J. M.; Bolmstedt, A.; Gago, F.; Schols, D. *J Virol* **2006,** 80, (17), 8411-21.

213. Balzarini, J. *Curr Opin HIV AIDS* **2006,** 1, (5), 355-60.

214. Vandekerckhove, L.; Verhofstede, C.; Vogelaers, D. *J Antimicrob Chemother* **2008,** 61, (6), 1187-90.

215. Makinson, A.; Reynes, J. *Curr Opin HIV AIDS* **2009,** 4, (2), 150-58.

216. Pirrone, V.; Wigdahl, B.; Krebs, F. C. *Antiviral Res* **2011,** 90, (3), 168-82.

217. Van Damme, L.; Govinden, R.; Mirembe, F. M.; Guedou, F.; Solomon, S.; Becker, M. L.; Pradeep, B. S.; Krishnan, A. K.; Alary, M.; Pande, B.;

Ramjee, G.; Deese, J.; Crucitti, T.; Taylor, D. *N Engl J Med* **2008,** 359, (5), 463-72.

218. McCormack, S.; Ramjee, G.; Kamali, A.; Rees, H.; Crook, A. M.; Gafos, M.; Jentsch, U.; Pool, R.; Chisembele, M.; Kapiga, S.; Mutemwa, R.; Vallely, A.; Palanee, T.; Sookrajh, Y.; Lacey, C. J.; Darbyshire, J.; Grosskurth, H.; Profy, A.; Nunn, A.; Hayes, R.; Weber, J. *Lancet* **2010,** 376, (9749), 1329-37.

219. Greene, W. C. *Nat Immunol* **2004,** 5, (9), 867-71.

220. Sato, Y.; Hirayama, M.; Morimoto, K.; Yamamoto, N.; Okuyama, S.; Hori, K. *J Biol Chem* **2011,** 286, (22), 19446-58.

221. Boyd, M.; Gustafson, K.; McMahon, J.; Shoemaker, R.; O'Keefe, B.; Mori, T.; Gulakowski, R.; Wu, L.; Rivera, M.; Laurencot, C.; Currens, M.; Cardellina, J., 2nd; Buckheit, R., Jr; Nara, P.; Pannell, L.; Sowder, R., 2nd; Henderson, L. *Antimicrob Agents Chemother* **1997,** 41, (7), 1521-30.

222. Mori, T.; O'Keefe, B. R.; Sowder, R. C., 2nd; Bringans, S.; Gardella, R.; Berg, S.; Cochran, P.; Turpin, J. A.; Buckheit, R. W., Jr.; McMahon, J. B.; Boyd, M. R. *J Biol Chem* **2005,** 280, (10), 9345-53.

223. Dey, B.; Lerner, D. L.; Lusso, P.; Boyd, M. R.; Elder, J. H.; Berger, E. A. *J Virol* **2000,** 74, (10), 4562-69.

224. Micewicz, E. D.; Cole, A. L.; Jung, C. L.; Luong, H.; Phillips, M. L.; Pratikhya, P.; Sharma, S.; Waring, A. J.; Cole, A. M.; Ruchala, P. *PLoS One* **2010,** 5, (12), e14360.

225. Balzarini, J.; Van Laethem, K.; Daelemans, D.; Hatse, S.; Bugatti, A.; Rusnati, M.; Igarashi, Y.; Oki, T.; Schols, D. *J Virol* **2007,** 81, (1), 362-73.

226. Mammen, M.; Choi, S.-K.; Whitesides, G. M. *Angew Chem Int Ed* **1998,** 37, (20), 2754-94.

227. Kitov, P. I.; Bundle, D. R. *J Am Chem Soc* **2003,** 125, (52), 16271-84.

228. Mammen, M.; Dahmann, G.; Whitesides, G. M. *J Med Chem* **1995,** 38, (21), 4179-90.

229. Taylor, M. E.; Drickamer, K., *Introduction to glycobiology*. 2nd ed.; Oxford University Press: 2006.

230. Springsteen, G.; Wang, B. H. *Tetrahedron* **2002,** 58, (26), 5291-300.

231. Yan, J.; Springsteen, G.; Deeter, S.; Wang, B. *Tetrahedron* **2004,** 60, (49), 11205-09.

232. Cai, S. X.; Keana, J. F. W. *Bioconj Chem* **1991,** 2, 317-22.

233. Dowlut, M.; Hall, D. G. *J Am Chem Soc* **2006,** 128, (13), 4226-27.

234. Kaur, G.; Fang, H.; Gao, X.; Li, H.; Wang, B. *Tetrahedron* **2006,** 62, (11), 2583-89.

235. Mulla, H. R.; Agard, N. J.; Basu, A. *Bioorg Med Chem Lett* **2004,** 14, (1), 25-27.

236. Bérubé, M.; Dowlut, M.; Hall, D. G. *J Org Chem* **2008,** 73, (17), 6471-79.

237. Jay, J. I.; Lai, B. E.; Myszka, D. G.; Mahalingam, A.; Langheinrich, K.; Katz, D. F.; Kiser, P. F. *Mol Pharm* **2010,** 7, (1), 116-29.

238. Springsteen, G.; Wang, B. *Chem Commun* **2001**, (17), 1608-09.

239. Bhat, K. L.; Howard, N. J.; Rostami, H.; Lai, J. H.; Bock, C. W. *J Mol Struc* **2005,** 723, (1-3), 147-57.

240. Winblade, N. D.; Schmökel, H.; Baumann, M.; Hoffman, A. S.; Hubbell, J. A. *J Biomed Mat Res* **2002,** 59, (4), 618-31.

241. Cutalo, J. M.; Deterding, L. J.; Tomer, K. B. *J Am Soc Mass Spectrom* **2004,** 15, (11), 1545-55.

242. Zhu, X.; Borchers, C.; Bienstock, R. J.; Tomer, K. B. *Biochemistry* **2000,** 39, (37), 11194-204.

243. Rogers, K. M.; Heise, M. *J Innate Immun* **2009,** 1, (5), 405-12.

244. Moulard, M.; Lortat-Jacob, H.; Mondor, I.; Roca, G.; Wyatt, R.; Sodroski, J.; Zhao, L.; Olson, W.; Kwong, P. D.; Sattentau, Q. J. *J Virol* **2000,** 74, (4), 1948-60.

245. Vigerust, D. J.; Shepherd, V. L. *Trends Microbiol* **2007,** 15, (5), 211-18.

246. Balzarini, J.; Schols, D.; Neyts, J.; Van Damme, E.; Peumans, W.; De Clercq, E. *Antimicrob Agents Chemother* **1991,** 35, (3), 410-16.

247. Barrientos, L. G.; O'Keefe, B. R.; Bray, M.; Sanchez, A.; Gronenborn, A. M.; Boyd, M. R. *Antiviral Res* **2003,** 58, (1), 47-56.

248. Tsai, C. C.; Emau, P.; Jiang, Y.; Agy, M. B.; Shattock, R. J.; Schmidt, A.; Morton, W. R.; Gustafson, K. R.; Boyd, M. R. *AIDS Res Hum Retroviruses* **2004,** 20, (1), 11-18.

249. Helle, F.; Wychowski, C.; Vu-Dac, N.; Gustafson, K. R.; Voisset, C.; Dubuisson, J. *J Biol Chem* **2006,** 281, (35), 25177-83.

250. O'Keefe, B. R.; Smee, D. F.; Turpin, J. A.; Saucedo, C. J.; Gustafson, K. R.; Mori, T.; Blakeslee, D.; Buckheit, R.; Boyd, M. R. *Antimicrob Agents Chemother* **2003,** 47, (8), 2518-25.

251. Kataoka, K.; Miyazaki, H.; Okano, T.; Sakurai, Y. *Macromolecules* **1994,** 27, (4), 1061-62.

252. Morokoshi, S.; Ohhori, K.; Mizukami, K.; Kitano, H. *Langmuir* **2004,** 20, (20), 8897-902.

253. Winblade, N. D.; Nikolic, I. D.; Hoffman, A. S.; Hubbell, J. A. *Biomacromolecules* **2000,** 1, (4), 523-33.

254. Patel, S.; Hazrati, E.; Cheshenko, N.; Galen, B.; Yang, H.; Guzman, E.; Wang, R.; Herold, B. C.; Keller, M. J. *J Infect Dis* **2007,** 196, (9), 1394-402.

255. Ayehunie, S.; Cannon, C.; Lamore, S.; Kubilus, J.; Anderson, D. J.; Pudney, J.; Klausner, M. *Toxicol in Vitro* **2006,** 20, (5), 689-98.

256. Kieweg, S. L. Mechanical analysis of vaginal gels intended for microbicide application. Duke University, Durham, 2005.

257. Hu, B. The effect of surface tension on the epithelial spreading of non-Newtonian drug delivery vehicles: Numerical simulations. University of Kansas, 2009.

258. Roberts, M. C. New in situ crosslinking chemistries for hydrogelation. University of Utah, 2008.

259. Geonnotti, A. R.; Peters, J. J.; Katz, D. F. *J Pharm Sci* **2005,** 94, (8), 1705-12.

260. Ambrose, Z.; KewalRamani, V. N.; Bieniasz, P. D.; Hatziioannou, T. *Trends Biotech* **2007,** 25, (8), 333-37.

261. Haigwood, N. L. *Eur J Immunol* **2009,** 39, (8), 1994-99.

262. Shacklett, B. L. *PLoS Med* **2008,** 5, (1), e13.

263. Mudd, P. A.; Watkins, D. I. *Curr Opin HIVAIDS* **2011,** 6, (3), 197-201.

264. Wilson, S. S.; Cheshenko, N.; Fakioglu, E.; Mesquita, P. M.; Keller, M. J.; Herold, B. C. *Antiviral Ther* **2009,** 14, (8), 1113-24.

265. Galen, B. T.; Martin, A. P.; Hazrati, E.; Garin, A.; Guzman, E.; Wilson, S. S.; Porter, D. D.; Lira, S. A.; Keller, M. J.; Herold, B. C. *J Infect Dis* **2007,** 195, (9), 1332-39.

266. Barnhart, K.; Pretorius, E. S.; Stolpen, A.; Malamud, D. *Fertil Steril* **2001,** 76, (1), 189.

267. Brown Michele, A.; Mattrey Robert, F.; Stamato, S.; Sirlin Claude, B. *AJR Am J Roentgenol* **2005,** 185, (5), 1221-27.

268. Jay, J. I. Modification of phenyboronate-diol crosslink: applications in pH-responsive vehicles and synthetic lectin for women controlled HIV prevention University of Utah, Salt Lake City, 2009.

269. Fung, H. B.; Stone, E. A.; Piacenti, F. J. *Clin Ther* **2002,** 24, (10), 1515-48.

270. Buckheit, C. E., Pyrimidinediones: molecules with dual mechanism of action. In *International Microbicides Conference*, 2008.

271. Friend, D. R.; Doncel, G. F. *Antiviral Res* **2010,** 88, (Supp1), S47-S54.

272. Lacey, C. J.; Woodhall, S.; Qi, Z.; Sawant, S.; Cowen, M.; McCormack, S.; Jiang, S. *Int J STD AIDS* **2010,** 21, (10), 714-17.

273. Tanaka, H.; Chiba, H.; Inokoshi, J.; Kuno, A.; Sugai, T.; Takahashi, A.; Ito, Y.; Tsunoda, M.; Suzuki, K.; Takénaka, A.; Sekiguchi, T.; Umeyama, H.; Hirabayashi, J.; Ōmura, S. *Proc Nat Acad Sci* **2009,** 106, (37), 15633-38.

274. Doores, K. J.; Bonomelli, C.; Harvey, D. J.; Vasiljevic, S.; Dwek, R. A.; Burton, D. R.; Crispin, M.; Scanlan, C. N. *Proc Natl Acad Sci* **2010,** 107, (31), 13800-05.

275. Duggan, P. J.; Offermann, D. A. *Tetrahedron* **2009,** 65, (1), 109-14.

276. Li, M.; Lin, N.; Huang, Z.; Du, L.; Altier, C.; Fang, H.; Wang, B. *J Am Chem Soc* **2008,** 130, (38), 12636-38.

277. Yang, W.; Fan, H.; Gao, X.; Gao, S.; Karnati, V. V. R.; Ni, W.; Hooks, W. B.; Carson, J.; Weston, B.; Wang, B. *Chem Biol* **2004,** 11, (4), 439-48.

278. Zou, Y.; Broughton, D. L.; Bicker, K. L.; Thompson, P. R.; Lavigne, J. J. *ChemBioChem* **2007,** 8, (17), 2048-51.

279. Moulaei, T.; Shenoy, S. R.; Giomarelli, B.; Thomas, C.; McMahon, J. B.; Dauter, Z.; O'Keefe, B. R.; Wlodawer, A. *Structure* **2010,** 18, (9), 1104-15.

280. Rini, J. M. *Annu Rev Biophys Biomol Struc* **1995,** 24, (1), 551-77.

281. Vorontsov, I. I.; Miyashita, O. *Biophys J* **2009,** 97, (9), 2532-40.

282. Perumal, O.; Khandare, J.; Kolhe, P.; Kannan, S.; Lieh-Lai, M.; Kannan, R. M. *Bioconjug Chem* **2009,** 20, (5), 842-46.

283. Papp, I.; Sieben, C.; Ludwig, K.; Roskamp, M.; Böttcher, C.; Schlecht, S.; Herrmann, A.; Haag, R. *Small* **2010,** 6, (24), 2900-06.

284. Inouye, Y.; Kanamori, T.; Fujimoto, Y.; Sugiyama, M.; Yoshida, T. *Biol Pharm Bull* **1995,** 18, (6), 920-22.

285. Hossain, M. M.; Parniak, M. A. *J Virol* **2006,** 80, (9), 4440-46.

286. Balzarini, J. *Lancet Infect Dis* **2005,** 5, (11), 726-31.

287. Balzarini, J.; Van Laethem, K.; Hatse, S.; Froeyen, M.; Peumans, W.; Van Damme, E.; Schols, D. *J Biol Chem* **2005,** 280, (49), 41005-14.

288. Balzarini, J.; Van Laethem, K.; Hatse, S.; Vermeire, K.; De Clercq, E.; Peumans, W.; Van Damme, E.; Vandamme, A. M.; Bohlmstedt, A.; Schols, D. *J Virol* **2004,** 78, (19), 10617-27.

289. Balzarini, J.; Van Laethem, K.; Peumans, W. J.; Van Damme, E. J. M.; Bolmstedt, A.; Gago, F.; Schols, D. *J Virol* **2006,** 80, (17), 8411-21.